

Cardiff University

ANTI-EPIDERMAL GROWTH FACTOR
RECEPTOR (EGFR) THERAPY MODELLED
IN THE MOUSE

PhD Thesis

Paul HS Shaw
2010

UMI Number: U584458

All rights reserved

INFORMATION TO ALL USERS

The quality of this reproduction is dependent upon the quality of the copy submitted.

In the unlikely event that the author did not send a complete manuscript and there are missing pages, these will be noted. Also, if material had to be removed, a note will indicate the deletion.



UMI U584458

Published by ProQuest LLC 2013. Copyright in the Dissertation held by the Author.
Microform Edition © ProQuest LLC.

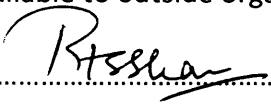
All rights reserved. This work is protected against
unauthorized copying under Title 17, United States Code.



ProQuest LLC
789 East Eisenhower Parkway
P.O. Box 1346
Ann Arbor, MI 48106-1346

DECLARATION

This work has not previously been accepted in substance for any degree and is not concurrently submitted in candidature for any degree. This thesis is being submitted in partial fulfillment of the requirements for the degree of PhD, and is the result of my own independent work/investigation, except where otherwise stated. Other sources are acknowledged by explicit references. I hereby give consent for my thesis, if accepted, to be available for photocopying and for inter-library loan, and for the title and summary to be made available to outside organisations.

Signed  Date 27/5/10

Anti-Epidermal Growth Factor Receptor (EGFR) Therapy Modelled In The Mouse.

Student ID No. 0163081344

Abstract

Despite advances in response prediction to epidermal growth factor receptor (EGFR) targeted therapy in colorectal cancer there remain unknown factors determining the clinical outcome in patients with *K-RAS* wild type tumours in the absence of mutations activating *B-RAF* or *PIK3CA/PTEN* signalling. In addition, therapeutic agents for *K-RAS* mutant colorectal cancer and advances in the treatment of *K-RAS* wild type tumours are needed. Here the *Apc^{min/+}* mouse has been used to define mRNA transcripts altered in response to Egfr receptor inhibition based upon the hypothesis that early gene expression changes will predict response to EGFR targeted therapy in *K-RAS* wild type colon cancer and thus identify novel biomarkers of response. In addition, the *Apc^{min/+}* mouse and a model including endogenous *K-ras* activated colon tumourigenesis have been used to examine the consequences of dual Egfr/Igf1r signalling inhibition, short term interruption of the Ras/Raf/Mek/Erk pathway with Mek inhibition and Egfr signalling inhibition combined with the induction of apoptosis.

Gene expression microarray analysis and qRT-PCR validated 3 genes (*IKBKG*, *CXCL9* and *CCNE2*) which, upon probing of transcript datasets from patients with *K-RAS* wild type colorectal cancer, identified their discriminatory value in terms of clinical responses to cetuximab monotherapy. *Apc^{min/+}* intestinal adenomas acutely exposed to a small molecular inhibitor of Egfr (gefitinib) showed concurrent suppression of downstream signalling and induction of Igf signalling. To test the hypothesis that blockade of Egfr signalling was tempered by compensatory activation of the Igf pathway, the effect of chronic suppression of Igf1r using AZD12253801, a small molecular tyrosine kinase inhibitor of IGF1R, was examined alone and in combination with gefitinib. Compared to either drug alone, combined dosing with gefitinib and AZ12253801 suppressed small intestinal tumourigenesis more effectively, but this failed to translate into a survival advantage possibly due to an increased incidence of intra-abdominal abscess formation. Nonetheless, this data provides preliminary evidence in support of combinatorial therapy. Examination of Mek inhibition using AZD6244 revealed induction of immediate cell death and perturbation of the cell cycle

in intestinal tumours. These changes were not limited to *K-ras* mutant tumours suggesting a potential application to *K-ras* wild type intestinal cancer. Finally the addition of a BH3 mimetic, ABT737, to gefitinib induced a 3-fold increase in cell death indicating that short term pathway inhibition combined with induction of apoptosis is a rational treatment strategy for malignancy, and should also be extended in future experiments with Mek inhibition. This work has demonstrated the value of these mouse models in relation to target validation, biomarker prediction, resistance mechanisms and therapeutic utility.

Acknowledgements.

I would like to thank my supervisors, Prof Alan Clarke and Prof Tim Maughan for their support, wisdom and guidance over the last 4 years. My appreciation and thanks also go to Cancer Research UK for funding this period of research over 4 years. Valerie Meniel and Karen Reed have demonstrated great kindness and selfless support throughout my PhD studies and I thank you both for sharing your scientific knowledge and skills. James Matthews, Trevor Hay, Lee Parry and Kirsty Greenow have also shared valuable lab experience and time which is very much appreciated. I would also like to thank Mark Bishop and Lucie Pietzka for their help genotyping animals and all the animal technicians based in T1. I am also grateful to Orosia Asby, Bridgette Allen, Luke Bradshaw and Lee Austin for contributing towards excellent animal welfare. Derek Scarborough was instrumental in providing excellent histological specimens for further analysis. Yvonne Hey (Patterson Institute of Cancer Research) kindly processed RNA samples prior to microarray hybridisation/scanning. Richard Adams provided rectal cancer specimens from the Xerxes study, in addition to a listening ear and moral support which was much appreciated. I am also very grateful to Katja Seigpel and Meera Raja (PhD student) for help with Mek inhibitor related immuno-staining and phenotypic scoring. Thanks are also extended to Astrazeneca and Abbott Laboratories for access to their drug compounds. A final very big thank you to my wife Alison, and children Joseph, Emily and Reuben, for your continued love and patience; I dedicate this work to you and thank God for the joy and blessings you have each brought into my life.

Contents

Declaration	1
Abstract	2
Acknowledgments	4
Contents	5
Abbreviations and definitions	21
Chapter 1	
1. Introduction	26
1.1 Advanced colorectal cancer	26
1.1.1 Cytotoxic chemotherapy	26
1.1.2 EGFR targeted therapy	26
1.2 Personalised medicine	27
1.3 Predictive biomarkers	28
1.3.1 Gene expression microarray technology	28
1.3.2 Gene expression microarray studies in colorectal cancer and treatment response prediction	29
1.3.3 Predictive biomarkers in metastatic colorectal cancer	30
1.3.4 Mutations in downstream EGFR signalling pathways and response to EGFR targeted therapy in metastatic colon cancer	32
1.3.5 Xerxes clinical trial	33
1.4 Epidermal growth factor receptor (EGFR)	34
1.4.1 Signal transduction	34
1.4.2 Deregulated function	35
1.4.3 Therapeutic targeting	36
1.4.4 Resistance to EGFR targeted agents	37
1.5 Insulin-like growth factor 1 receptor (IGF-1R)	38
1.6 Genetically engineered mouse models of colon tumourigenesis	40
1.6.1 <i>Apc^{min/+}</i> mouse	40

1.6.2 <i>AhCre</i> ^{T/+} <i>Apc</i> ^{fl/+} <i>K-ras</i> ^{v12/+} conditional transgenic mouse model	42
1.7 Mitogen activated protein kinase (MAPK) signalling and colorectal cancer	43
1.7.1 Pharmacological manipulation by inhibition of MEK1/2	43
1.8 Apoptotic cell death	45
1.8.1 BH3 mimetics	46
1.9 Aims and Objectives	48

Chapter 2

2. Materials and methods	52
2.1 Animal experiments and reagents	52
2.1.1 Animals	52
2.1.2 Animal genotyping	52
2.1.3 Animal experiments	53
2.1.3.1 Materials for injection	53
2.1.3.1.1 Gefitinib	53
2.1.3.1.2 AZ12253801	54
2.1.3.1.3 ME1	54
2.1.3.1.4 AZD 6244	55
2.1.3.1.5 ABT 737	55
2.1.3.1.6 Vehicle injections	55
2.1.3.1.7 β -naphthoflavone	55
2.1.3.2 Acute drug exposure	56
2.1.3.2.1 Gefitinib and ME1	56
2.1.3.2.2 ABT-737	56
2.1.3.2.3 AZD 6244	56
2.1.3.3 Chronic drug exposure	56
2.1.3.4 Animal dissection and tissue preparation	58
2.2 Patients' tumour specimens	58

2.2.1 Xerxes trial	58
2.3 RNA handling and processing	59
2.3.1 Extraction of RNA	59
2.3.1.1 RNA quantification and quality	60
2.3.2 Pooling RNA samples	61
2.3.2.1 Microarray	61
2.3.2.2 Biological replicates for qRT-PCR	61
2.3.2.3 Chronic gefitinib induced transcripts	62
2.3.2.4 Transcripts from autochthonous mouse models	62
2.3.2.5 Human rectal cancer specimen transcripts	62
2.3.3 Reverse transcription	63
2.3.4 Target preparation, hybridisation and scanning of Affymetrix GeneChips	64
2.4 Real-Time Quantitative Reverse Transcription Polymerase Chain Reaction (qRT-PCR)	64
2.4.1 Primer design for qRT-PCR	65
2.4.2 Human primers for qRT-PCR	66
2.5 TriplePrep extraction (extraction of gDNA, RNA and protein)	67
2.5.1 TriplePrep working solutions	67
2.5.2 Sample homogenisation and lysis	67
2.5.3 Genomic DNA (gDNA) isolation	67
2.5.4 Isolation of RNA	68
2.5.5 Precipitation of protein	68
2.5.6 Determination of protein concentration (2-D Quant Kit)	69
2.5.6.1 Protocol	69
2.5.6.2 Colon polyp protein pooling	70
2.6 Western blotting	71
2.6.1 Sodium dodecyl sulphate polyacrylamide gel electrophoresis	71
2.6.2 Protein transfer	73
2.6.3 Membrane probing	73

2.6.3.1 Membrane incubation	74
2.6.3.2 Chemi-luminescent signal and protein identification	74
2.6.3.3 Densitometric measurements	74
2.7 Histology	75
2.7.1 Preparation of tissue for light microscopy	75
2.7.2 Immuno-histochemical staining	75
2.7.3 Scoring apoptosis and cell proliferation	77
2.8 Detection of <i>K-ras</i> and <i>B-raf</i> mutations in <i>Apc</i> ^{min/+} colon polyps	77
2.8.1 Pyrosequencing for <i>K-ras</i> mutations	77
2.8.2 Allelic discrimination assay for <i>B-raf</i> V600E mutation	78
2.9 Statistical analysis	78
2.10 Microarray analysis	79
2.10.1 AffymGUI	79
2.10.2 Time series regression analysis	80
2.10.3 Fold change and ranked products analysis	80
2.10.4 Significance analysis of microarrays (SAM)	81
2.10.5 Analysis of the GSE5851 dataset	81
2.11 Working solutions, materials and reagents	82
2.11.1 TBE/Agarose gels for DNA electrophoresis	82
2.11.1.1 Orange G loading dye	82
2.11.2 TAE/Agarose gels for RNA electrophoresis	83
2.11.2.1 RNA loading buffer	83
2.11.3 Solutions for drug suspensions	84
2.11.3.1 Vehicle solutions	84
2.11.3.2 Drug suspensions	85
2.11.4 TriplePrep kit reagents and working solutions	86
2.11.5 SDS PAGE	86
2.11.5.1 Upper buffer	86

2.11.5.2 Lower buffer	87
2.11.5.3 Running buffer (10X Stock)	87
2.11.5.4 Laemmli buffer	87
2.11.6 Protein transfer buffer	88
2.11.7 PVDF Membrane incubation buffers	88
2.11.8 Immuno-histochemistry	89
2.11.8.1 Antigen retrieval	89
2.11.8.2 Wash buffers	89
2.11.8.3 Blocking buffers	90
2.11.8.4 Endogenous peroxidase block	90
2.11.8.5 Signal amplification and DAB staining	90

Chapter 3

3. Gene expression changes in *Apc^{min/+}* *K-ras* wild type colon polyps in response to Egfr blockade: Identification of novel putative biomarkers or response to anti-EGFR therapy.

3.1 Introduction	92
3.2 Results	93
3.2.1 Colon polyp <i>K-ras</i> and <i>B-raf</i> mutation status	93
3.3 Pharmacodynamic effects of Egfr blockade in <i>Apc^{min/+}</i> intestinal tumours	93
3.3.1 Small intestine and colon tumours	93
3.3.1.1 Gefitinib	93
3.3.1.2 ME1	94
3.3.2 Apoptotic and cell cycle transcript changes in colon polyps	95
3.3.2.1 Gefitinib	95
3.3.2.2 ME1	95
3.3.3. Downstream signalling changes in colon polyps	95
3.3.3.1 Gefitinib	96
3.3.3.2 ME1	96

3.4 Microarray analysis	96
3.4.1 Fold change and ranked product computations	96
3.4.2 Time series regression analysis	97
3.4.3 AffyImGui and SAM analysis	99
3.5 qRT-PCR validation of microarray candidate genes	100
3.6 Colon polyp transcript expression following chronic gefitinib exposure	100
3.7 Protein validation of candidate transcripts of response to Egfr blockade	101
3.8 Probing human transcriptome data (GSE5851) for mouse candidate genes which dichotomise patient outcome	101
3.9 Affymetrix expression values for genes discriminating patient outcome (GSE5851 dataset)	102
3.10 Probing Xerxes trial rectal cancer specimens for the expression of putative candidates of response to anti-EGFR therapy identified by the <i>Apc^{min/+}</i> mouse	103
3.11 Discussion	104
3.11.1 Acute pharmacodynamic effects of Egfr inhibition in <i>Apc^{min/+}</i> intestinal tumours	104
3.11.1.1 Apoptosis and cell proliferation	104
3.11.1.2 Egfr signalling	105
3.11.2 Transcript expression changes in <i>Apc^{min/+}</i> colon polyps induced by Egfr antagonism	106
3.11.2.1 Microarray	106
3.11.2.1.1 Comparison of microarray and qRT-PCR results for gefitinib	107
3.11.2.1.2 Comparison of qRT-PCR transcript changes for gefitinib and ME1	108
3.11.2.1.3 Contextualization of identified transcripts	108
3.11.2.1.4 Protein validation of transcripts induced by Egfr blockade	109
3.11.3 Probing human rectal cancer transcriptome data (GSE5851) for 'mouse' candidate genes	109
3.11.3.1 <i>IKBK</i>	110

3.11.3.2 <i>CCNE2</i>	110
3.11.3.3 <i>CXCL9</i>	111
3.11.4 Exploring the potential biological significance of mouse candidate genes proposed to indicate putative response to EGFR targeted therapy	112
3.11.4.1 <i>Bmf</i>	112
3.11.4.2 <i>Cbl</i>	113
3.11.4.3 <i>Epha3</i>	113
3.11.4.4 <i>Ubd</i>	114
3.11.4.5 <i>Hip1</i>	115
3.11.4.6 <i>Plcd4</i>	115
3.11.4.7 <i>ErbB3</i>	115
3.11.4.8 <i>Ereg</i>	116
3.11.5 Transcript expression after chronic gefitinib exposure	117
3.11.5.1 Chronic transcripts affirming gefitinib induced 4 hour transcript changes	117
3.11.5.2 Chronic transcripts opposing gefitinib induced 4 hour transcript changes	118
3.11.6 Transcripts identified in patients' rectal cancer specimens	118
3.11.7 Summary	119

Chapter 4

4. Verification of *K-ras* wild type specific transcript changes in colon polyps using a conditional transgenic mouse model of colon tumourigenesis.

4.1 Introduction	121
4.2 Results	122
4.2.1 Gefitinib induced transcript changes in the context of <i>K-ras</i> mutation status	122
4.3 Discussion	124

Chapter 5

5. Investigating Igf-1r pathway activation in *Apc^{min/+}* *K-ras* wild type colon polyps in response to Egfr blockade

5.1 Introduction	126
5.2 Results	127
5.2.1 AZ12253801 test doses	127
5.2.2 Gefitinib test doses	127
5.3 Consequences of chronic treatments in <i>Apc^{min/+}</i> mice upon survival, tumour volume and tumour counts	128
5.3.1 Gefitinib (Egfr inhibition)	128
5.3.2 AZ12253801 (Igf-1r inhibition)	129
5.3.3 Combined Gefitinib with AZ12253801 (Dual Egfr and Igf-1r inhibition)	130
5.3.4 Adverse effects of chronic treatment	131
5.4 Acute effects of drug exposure in tumours from <i>Apc^{min/+}</i> mice	132
5.4.1 Tumour phenotypic change	132
5.4.2 Molecular effects of acute drug exposure	133
5.4.2.1 AZ12253801	133
5.4.2.2 Combined Gefitinib with AZ12253801	133
5.5 Molecular signalling changes in tumours chronically exposed to drugs	133
5.5.1 Chronic Gefitinib	134
5.5.2 Chronic AZ12253801	134
5.5.3 Chronic combined Gefitinib with AZ12253801	135
5.6 Discussion	137
5.6.1 Igf-1r up-regulation and activation in response to chronic gefitinib treatment	137
5.6.2 Treatment outcome in <i>Apc^{min/+}</i> mice following chronic drug exposures	138
5.6.2.1 Chronic Gefitinib	139
5.6.2.2 Chronic AZ12253801	139
5.6.2.3 Chronic combined Gefitinib with AZ12253801	140
5.6.2.4 Adverse effects	141
5.6.3 Acute downstream molecular effects of drug treatments	142
5.6.4 Molecular effects of chronic treatment against Igf-1r and Egfr/Igf-1r inhibition	144

5.7 Summary	145
Chapter 6	
6. Enhancing the therapeutic effect of gefitinib in the <i>Apc^{min/+}</i> mouse	148
6.1 Introduction	148
6.2 Results	149
6.2.1 Probing <i>Apc^{min/+}</i> microarray data for <i>Bim</i> transcript levels	149
6.2.2 Acute effects of drug exposure in tumours from <i>Apc^{min/+}</i> mice	150
6.2.2.2 Colon tumours	150
6.2.2.3 Small intestinal microadenomas	150
6.3 Discussion	151
Chapter 7	
7. Investigating the immediate effect of Mek inhibition in a genetically defined and clinically relevant autochthonous model of human colorectal cancer.	
7.1 Introduction	154
7.2 Results	156
7.2.1 Phosphorylated Erk levels in <i>AhCre^{T/+}Apc^{fl/+}Kras^{+/+}</i> and <i>AhCre^{T/+}Apc^{fl/+}Kras^{v12/+}</i> intestinal tumours	156
7.2.2 Acute pharmacodynamic effects of Mek inhibition using AZD6244 delivered by intraperitoneal injection	156
7.2.2.1 <i>AhCre^{T/+}Apc^{fl/+}Kras^{v12/+}</i> derived intestinal tumours	156
7.2.2.2 <i>Apc^{min/+}</i> intestinal tumours (<i>K-ras</i> and <i>B-raf</i> wild type)	157
7.2.3 Acute pharmacodynamic effects of Mek inhibition using AZD6244 by oral gavage	157
7.2.4 Phosphorylated Erk immuno-staining of intestinal tumours in response to Mek inhibition	158
7.2.5 Phosphorylated Erk immuno-staining of epidermal tissue	159
7.3 Discussion	160
7.3.1 Future direction	163

Chapter 8

8. Conclusion

168

References

172

Publications

197

Figures

1. EGF receptor signalling.

1.1 Insulin-like growth factor (IGF) signalling.

1.2 Central role of MEK-ERK signalling and BCL-2 homology domain 3 (BH3)-only protein BIM mediating the efficacy of gefitinib and MEK inhibition in the presence of ABT-737.

2.1 Chronic dosing strategy to examine antagonism of the *Igf-1r* in the context of *Apc^{min/+}* gefitinib resistant intestinal tumourigenesis.

2.2 Expected and calculated fold changes ($\Delta\Delta CT$ method) for *Cbl* product using appropriate qRT-PCR primer pairs and serial dilutions of template cDNA.

2.3 A typical standard curve.

3.1 Pyrogram result from a colon polyp (sample 28D) demonstrating wild type status (GGT and GGC) of *K-ras* gene codons 12/13.

3.2 Phenotypic consequences of acute (4 hour) gefitinib exposure on *Apc^{min/+}* small and large intestinal tumours.

3.3 Consequences of acute (4 hour) ME1 exposure on *Apc^{min/+}* small and large intestinal tumours.

3.4 Apoptotic and cell cycle transcript changes induced in *Apc^{min/+}* colon polyps by 4 hour exposure to gefitinib or ME.

3.5 Signalling changes in *Apc^{min/+}* colon polyps following 4 hour Egfr antagonism with gefitinib or ME1.

3.6 Transcript changes in *Apc^{min/+}* colon polyps induced by gefitinib over 24 hours.

3.7 Validation of microarray transcript changes (time series regression model) by qRT-PCR using microarray mRNA.

3.8 Protein validation of *Apc^{min/+}* colon polyp transcript changes induced by ME1 (4 hours).

3.9 Protein validation of *Apc^{min/+}* colon polyp transcript changes induced by gefitinib (8 hours).

3.10 Affymetrix expression values for genes discriminating patient outcome in response to cetuximab monotherapy.

5.1 qRT-PCR determined transcript expression of *Igf-1r* in colon polyps from *Apc^{min/+}* mice treated with long term vehicle (1% Tween80) or gefitinib (75mg/kg).

5.2 Box plots showing the age range of mice at the start of each treatment.

5.3. Survival and intestinal tumour metrics of *Apc^{min/+}* mice treated with once daily gefitinib 75mg/kg, AZ12253801 12.5mg/kg or combination gefitinib 75mg/kg+AZ12253801 12.5mg/kg.

5.4 Adverse effects of chronic administration of drugs in mice.

5.5 Phenotypic changes in *Apc^{min/+}* small intestinal tumours post 4 hour drug exposure.

5.6 Acute downstream signalling changes in *Apc^{min/+}* colon tumours post 4 hour drug exposure.

5.7 Signalling pathways in *Apc^{min/+}* tumours following chronic treatment.

5.8 Phospho-Erk immuno-reactivity in colon polyps from *Apc^{min/+}* mice treated with long term vehicle, Egfr, Igf-1r or Egfr/Igf-1r combined antagonists.

5.9 Igf-1r β immuno-reactivity in colon polyps from *Apc^{min/+}* mice treated with long term vehicle, Egfr, Igf-1r or Egfr/Igf-1r combined antagonists.

5.10 Igf-1r β immuno-reactivity in small intestinal adenomas from *Apc^{min/+}* mice treated with long term vehicle, Egfr, Igf-1r or Egfr/Igf-1r combined antagonists.

5.11 Phospho-Erk immuno-reactivity in small intestinal adenomas from *Apc^{min/+}* mice treated with long term vehicle, Egfr, Igf-1r or Egfr/Igf-1r combined antagonists.

5.12 Phospho-Akt immuno-reactivity in small intestinal adenomas from *Apc^{min/+}* mice treated with long term vehicle, Egfr, Igf-1r or Egfr/Igf-1r combined antagonists.

5.13 Phospho-Akt immuno-reactivity in colon polyps from *Apc^{min/+}* mice treated with long term vehicle, Egfr, Igf-1r or Egfr/Igf-1r combined antagonists.

5.14 Resistance mechanisms postulated as a consequence of chronic Egfr or Igf-1r inhibition in *Apc^{min/+}* mice.

5.15. Rebound activation of Igf-1r signalling following Igf-1r inhibition through reduced PTP1B activity.

5.16. Hypothetical clinical trial stratifying patients according to drug induced tumour molecular profile.

6.1 Caspase3 immuno-staining in *Apc^{min/+}* colon tumours at a 4 hour time point following ABT-737 administration with and without gefitinib and gefitinib alone.

6.2 Apoptosis in *Apc^{min/+}* small intestinal microadenomas at a 4 hour time point following ABT-737 administration with and without gefitinib and gefitinib alone.

- 7.1 *AhCre^{T/+}Apc^{fl/+}Kras^{+/+}* and *AhCre^{T/+}Apc^{fl/+}Kras^{v12/+}* derived colon polyps immuno-stained for Erk phosphorylation.
- 7.2 *AhCre^{T/+}Apc^{fl/+}Kras^{+/+}* and *AhCre^{T/+}Apc^{fl/+}Kras^{v12/+}* derived small intestinal microadenomas immuno-stained for Erk phosphorylation.
- 7.3 Acute effect of AZD6244 in *AhCre^{T/+}Apc^{fl/+}Kras^{v12/+}* colon and small intestinal tumours.
- 7.4 Acute effect of AZD6244 in *Apc^{min/+}* colon and small intestinal tumours at 24 hours.
- 7.5 Acute effects of AZD6244 administered by oral gavage in *Apc^{min/+}* colon tumour.s
- 7.6 Phospho-Erk immuno-reactive staining of colon tumours from *AhCre^{T/+}Apc^{fl/+}Kras^{v12/+}* mice exposed to Mek inhibitor (AZD6244) and Vehicle for 4 hours.
- 7.7 Phospho-Erk immuno-staining of small intestinal microadenomas from *AhCre^{T/+}Apc^{fl/+}Kras^{v12/+}* mice exposed to acute AZD6244 and Vehicle.
- 7.8 Phospho-Erk immuno-staining of *K-ras* wild type *Apc^{min/+}* colon polyps from mice treated with acute AZD6244 or Vehicle treatments.
- 7.9 Phospho-Erk immuno-staining of epidermis from *Apc^{min/+}* mice exposed to acute AZD6244 or Vehicle.
- 7.10 Theoretical survival curves for long term treatment with AZD6244 in *AhCre^{T/+}Apc^{fl/+}Kras^{+/+}* and *AhCre^{T/+}Apc^{fl/+}Kras^{v12/+}* mouse models.
- 7.11 Interval therapy in colorectal cancer using AZD624.

Tables

- 2.1 Reagents included in each PCR genotyping reaction.
- 2.2 Primers used to genotype experimental mice, PCR conditions and expected products.
- 2.3 Reverse transcription reagents.
- 2.4 Murine primer sequences for qRT-PCR.
- 2.5 Primers for human qRT-PCR.
- 2.6 Numbers of mice and colon polyps retrieved for each drug exposure time.
- 2.7 Gel formulations for SDS-PAGE.
- 2.8 Primary antibodies used to probe protein blot membranes.
- 2.9 Primary antibodies and summary protocols for immuno-histochemistry.
- 2.10 Primary antibodies for IHC and overview of protocols highlighting endogenous peroxidase blocks, washes and ABC signal amplifications.

- 3.1 Top 50 up-and down-regulated genes (fold change ≤ 5 or ≥ 2 ; $P \leq .05$) based on microarray fold changes in *Apc^{min/+}* colon polyps in response to gefitinib at 4 hours.
- 3.2a Top 50 ranked genes in *Apc^{min/+}* colon polyps in response to gefitinib.
- 3.2b Bottom 50 ranked genes in *Apc^{min/+}* colon polyps in response to gefitinib.
- 3.3 *Apc^{min/+}* colon polyp genes changes in response to gefitinib identified by SAM analysis.
- 3.4 Microarray detected gene expression fold changes in *K-ras* wild type *Apc^{min/+}* colon polyps in response to gefitinib at 4 hours: Candidates for qRT-PCR validation.
- 3.5 qRT-PCR validation of targets identified by microarray using biological replicate experiments of 4 hour gefitinib and ME1 exposure.
- 3.6 Acute and chronic transcript changes in *Apc^{min/+}* colon polyps following short term gefitinib or ME1 and long term gefitinib.
- 3.7 Human rectal cancer transcriptome (GSE5851) probing by novel mouse candidate genes.
- 3.8 *Apc^{min/+}* mouse directed transcript expression levels in rectal cancer specimens from the Xerxes trial.

- 4.1 Altered gene expression patterns (qRT-PCR) in *K-ras* mutant colon polyps relative to *K-ras* wild type colon polyps in response to gefitinib at 4 hours.

6.1. Mouse GeneChip 430 2.0 array probe ID's linked to *Bim* (*Bcl2l11*) and associated transcript fold changes in *Apc*^{min/+} colon polyps relative to normal adjacent colon tissue.

6.2. *Mcl-1* microarray probe transcript changes in *Apc*^{min/+} colon tumours relative to adjacent normal colon.

Appendix

2.1 Colon polyp RNA pooling for specific *Apc*^{min/+} treatment times.

2.2 Colon polyp RNA pools for biological replicate experiments of *Apc*^{min/+} mice treated with 0.5% tween80, gefitinib, 1x PBS or ME1 for 4 hours.

2.3 Colon polyp RNA pools for *Apc*^{min/+} mice exposed to chronic vehicle or gefitinib until survival endpoint reached.

2.4 Colon polyp RNA pool from *AhCre*^{T/+} *Apc*^{+/-} *Kras*^{+/+} and *AhCre*^{T/+} *Apc*^{+/-} *Kras*^{V12/+} polyps exposed to a single dose of gefitinib.

2.5 RNA extraction from human rectal cancer specimens.

2.6 Colon polyp protein quantification using the 2D Quant Kit.

2.7 Protocol for Haematoxylin and Eosin staining.

Abbreviations and definitions

A1	Bcl-2 family member, A1
<i>AhCre^{T/+}</i>	aryl hydrocarbon promoter of <i>Cre</i> transgene
Abs	absorption
Akt	Akt 1 kinase/ protein kinase B
Apc	adenomatous polyposis coli
<i>Apc^{min/+}</i>	germline <i>Apc</i> mutation giving rise to multiple intestinal neoplasia
APS	ammonium persulphate
<i>Aqp4</i>	aquaporin 4
<i>Arid3b</i>	AT-rich interactive domain-containing protein 3B
<i>Arhgef9</i>	Cdc42 guanine exchange factor 9
AZD6244	small molecule kinase inhibitor of Mek
AZ12253801	small molecule kinase inhibitor of Igf-1r
<i>Bad</i>	Bcl-2 associated agonist of cell death
<i>Bak</i>	Bcl-2 antagonist killer
<i>Bax</i>	Bcl-2 associated protein
<i>Bcl-2</i>	B-cell lymphoma protein 2
<i>Bcl-xl</i>	apoptosis regulator Bcl-X
<i>Bcl-w</i>	apoptosis regulator Bcl-W
<i>Bcr/Abl</i>	breakpoint cluster region/ Abelson murine leukemia viral oncogene homolog 1
<i>Bid</i>	BH3 interacting domain death agonist
<i>BH3</i>	Bcl-2 homology domain 3
<i>Bim</i>	Bcl-2-like11 apoptosis facilitator
<i>Bmp10</i>	bone morphogenetic protein 10
<i>Bmf</i>	Bcl-2 modifying factor
<i>Boo</i>	apoptosis regulator Bcl-B
Bp	base pairs
<i>B-raf</i>	v-raf murine sarcoma viral oncogene
Brdu	Bromodeoxyuridine
BSA	bovine serum albumin
<i>Cbl</i>	casitas b-lineage lymphomas

<i>Ccne2</i>	cyclin E2
cDNA	complimentary deoxyribonucleic acid
°C	degrees Celsius
cm	centimetre
<i>Cre</i>	causes recombination
CT	cycle time
<i>Cxcl9</i>	chemokine receptor ligand 9
<i>Cxcl10</i>	chemokine receptor ligand 10
DAB	diaminobenzidine
DEPC	diethylpyrocarbonate
dNTP	deoxyribonucleotide triphosphate
DNase	deoxyribonuclease
DSW	5% dextrose water
ECL	chemi-luminescent reagent
Egf	epidermal growth factor
<i>Egfr</i>	epidermal growth factor receptor
<i>Epha3</i>	Eph receptor A3
<i>ErbB3</i>	v-erb-b2 erythroblastic leukaemia viral oncogene homolog 3
<i>Ereg</i>	epiregulin
Erk	extracellular signal-regulated kinase
<i>Fabp2</i>	fatty acid binding protein 2
FDR	false discovery rate
FFPE	formalin fixed and paraffin embedded
FISH	fluorescent in situ hybridisation
5-FU	5- fluorouracil
g	gram
Gapdh	glyceraldehyde 3-phosphate dehydrogenase
gDNA	genomic deoxyribonucleic acid
Gefitinib	small molecule kinase inhibitor of Egfr
GEMMs	genetically engineered mouse models

<i>Gng4</i>	guanine nucleotide binding protein (G protein), gamma 4
x g	gravitation force
Gprc5a	G protein- coupled receptor family C type 5A
H&E	Haematoxylin and Eosin
HER2	epidermal growth factor receptor -2
<i>Hip1</i>	huntingtin interacting protein-1
hr	hour
HRP	horseradish peroxidise
IC ₅₀	half maximal inhibitory concentration
<i>Igf1r</i>	insulin-like growth factor 1 receptor
Igf 1or 2	insulin like growth factor -1 or -2
IHC	immuno-histochemistry
<i>Iigp1</i>	interferon inducible GTPase 1
<i>Ikbkg</i>	inhibitor of kappa light polypeptide gene enhancer in B-cells, kinase gamma
ip	intra-peritoneal
Irs1	insulin receptor substrate-1
kg	kilogram
KDa	Kilodalton
<i>K-ras</i>	Kirsten ras
mAB	monoclonal antibody
Mapk	mitogen activated protein kinase
Mcl-1	myeloid cell leukemia sequence 1
mCRC	metastatic colorectal cancer
ME1	rat monoclonal antibody raised against murine Egfr
Mek	mitogen activated protein kinase kinase
mg	microgram
ml	millilitre
mM	millimolar
Myc	myelocytomatosis viral oncogene homolog (avian)
NICE	National institute for health and clinical excellence

nM	nanomolar
<i>Nov</i>	nephroblastoma over-expressed
<i>Noxa</i>	PMA-induced protein
NSCLC	non-small cell lung cancer
Oxtr	oxytocin receptor
PBS	phosphate buffered saline
pCR	pathological complete response
PCR	polymerase chain reaction
<i>Phox2b</i>	paired-like homeobox 2b
<i>Pi4kb</i>	phosphatidylinositol 4-kinase, catalytic, beta
<i>Plcd4</i>	phospholipase C, delta 4
<i>Plcy/pkc</i>	phospholipase C, gamma/protein kinase C
PLK-1	polo-like kinase 1
PIK3CA	PI3-kinase p110 α subunit
<i>Prss22</i>	protease, serine, 22
<i>PTEN</i>	phosphatase and tensin homologue
PTPB1	protein tyrosine phosphatase 1B
PUMA	p53 up-regulated modulator of apoptosis
PVDF	polyvinylidene fluoride
qRT-PCR	real-time quantitative reverse transcription polymerase chain reaction
<i>Rassf2</i>	Ras association (RalGDS/AF-6) domain family member 2
<i>Retnlb</i>	resistin like beta
RNA	ribonucleic acid
RNAi	RNA interference
RNase	ribonuclease
rpm	revolutions per minute
<i>Rps4y2</i>	ribosomal protein S4Y
rRNA	ribosomal RNA
s	second
SDS PAGE	sodium dodecyl sulphate polyacrylamide gel electrophoresis

Slc26a3	solute carrier family 26, member 3
SN38	7-ethyl-10-hydroxycamptothecin
Src/fak	sarcoma/focal adhesion kinase
TAE	tris-acetate-EDTA
TBE	tris-borate-EDTA
TEMED	N,N,N',N'-tetramethylethylenediamine
Tgtp	T cell-specific GTPase
Topo1	topoisomerase-1
Ubd	ubiquitin D
μ l	microlitre
μ M	micromolar
W	watts
ypTNM	Tumour, node, metastasis staging based on pathological samples

Chapter 1

1 Introduction

1.1 Advanced colorectal cancer

Bowel cancer is the 2nd most common cause of cancer death in the UK, with 16,000 deaths pa. Approximately 9% of patients present with Dukes stage D disease at diagnosis with a 5 year survival figure of only 7%¹. Furthermore 50% of patients who have undergone potentially curative surgery for early stage disease will relapse with metastatic disease making it a significant burden of disease².

1.1.1 Cytotoxic chemotherapy

Standard chemotherapy for metastatic colorectal cancer includes three active drugs – fluoropyrimidines, irinotecan and oxaliplatin. With current evidence, patients with unresectable metastasis may be treated with fluoropyrimidine monotherapy to maintain quality of life provided close therapeutic monitoring is possible to avoid missing a therapeutic window of combination treatment³. For patients with resectable metastases, and possibly those with a heavy tumour burden or significant symptoms, first line combination therapy is most appropriate to achieve higher response rates and durable treatment responses³.

1.1.2 Epidermal growth factor receptor (EGFR) targeted therapy

Evidence is emerging to show the clinical benefit of EGFR targeted monoclonal antibody therapy using cetuximab in advanced colorectal. In the first line setting of advanced colorectal cancer adding cetuximab to the FOLFIRI (Irinotecan-infused 5-FU/LV) regimen demonstrates a small improvement in median progression free survival, but not overall survival⁴. In the second line setting, treatment with cetuximab and irinotecan improves progression free survival and response rates without an improvement in overall survival, most probably due to control arm subjects receiving cetuximab at a later time⁵. Finally in refractory metastatic colorectal cancer, cetuximab monotherapy demonstrates an improvement in overall survival compared with best supportive care⁶. In August 2009,

cetuximab was subsequently sanctioned by NICE for the first line therapy of advanced colorectal cancer under certain conditions⁷.

Interestingly, two randomised controlled trials of small molecule tyrosine kinase inhibitors against the EGF receptor have shown little clinical benefit in advanced colorectal cancer³. This is thought to be due to the absence of activating mutations in the EGF receptor³ which have been shown to confer sensitivity to tyrosine kinase inhibition in the setting of NSCLC⁸.

1.2 Personalised medicine

Paul Ehrlich coined the term 'magic bullet' back in the late 1800's for targeted microbial therapy⁹. Contemporary science has adopted this concept and applied it to cancer therapy built on the hypothesis that cancer cells are 'addicted' to a particular oncogene or pathway¹⁰. Targeting of such aberrant pathways, it is argued, will lead to therapeutic responses. Clinical evidence for this concept has been demonstrated based upon the success of antibodies or small molecules targeting specific oncogenes in human cancers, for example trastuzumab which targets the HER2 receptor in breast cancer, and imatinib which targets the oncogenic BCR/ABL fusion protein and the product of the oncogene c-kit, in gastrointestinal stromal tumours¹¹. Such examples raise expectations that greater understanding of deregulated molecular pathways driving malignant phenotypes will increase the prospects of new targeted drugs.

Patients with malignancy are traditionally treated with standardised regimens which have proven efficacy in population-based randomised controlled clinical trials for a given stage and primary cancer site¹². As a result, conventional approaches to treatment development are effective in only identifying therapy that works 'on average' for a population of patients similar to those in whom it was tested¹³. The low success rate of phase III trials is complicated by such a 'blanket' treatment approach for patients with heterogenous tumours, without the identification of individuals most likely to respond. This results in outcomes which are too small to be detected in the sample sizes used and an increased likelihood of false negative outcomes¹³. Unfortunately, in the absence of predictive markers of response to therapy, this approach exposes patients to potentially toxic treatment effects, with the risk of no benefit. However, given the recent identification

of molecular drug targets in cancer and developments in targeted therapy, there is an increasing desire to practice personalised medicine, facilitated by the identification of markers of response to therapy. There is a clear need to develop predictive markers that are specific for a particular therapy, that will save unnecessary exposure to toxic drugs and inconvenience to patients, and facilitate the receipt of effective drugs to patients most likely to gain benefit.

1.3 Predictive biomarkers

Biomarkers can relate to toxicity, biological effect and efficacy. A pharmacodynamic biomarker is associated with the biological effect of a compound¹⁴. A predictive marker predicts the clinical benefit of a particular treatment approach based on marker status and can therefore be used to guide the choice of therapy. This differs from a prognostic marker which classically identifies patients at risk of a particular outcome such as relapse or death and can be used to guide whether treatment is appropriate but not the choice of therapy¹⁵.

1.3.1 Gene expression microarray technology

Hybridization to high density arrays of oligonucleotides to access genetic variation has become possible since the mid-nineties¹⁶ and such microarray technology has become widely applied to medicine and oncology in particular. With the advent of microarray technology, multi-gene expression signature classifiers are now able to classify tumours based on the expression level of its component genes¹⁷. Genomic classifiers require internal validation in developmental studies using data independent from that used to develop the model and external validation using independent data in a prospective planned study¹⁷.

The microarray technique uses gene-specific probes representing thousands of different genes, which are arrayed on inert substrates. Levels of gene expression from target tissue are then assayed. RNA is extracted from the tissue of interest, labelled and then hybridised to the arrays by associating with complimentary gene-specific probes. Labelled RNA is detected by confocal laser scanning and images are produced which show the intensity of each gene-specific probe. A greater degree of hybridisation results in a more intense signal, implying a higher relative level of gene expression¹⁸.

Genomic signatures can be developed by measuring features on a body of training data, and then selecting features (gene expression levels) which are most significantly correlated with outcome (clinical response). Then having selected the features most correlated with outcome, those features can be combined into a multivariate signature classifier which is reproducible and accurate in predicting outcome¹³.

1.3.2 Gene expression microarray studies in colorectal cancer and treatment response prediction

Microarray technology has been applied to colorectal cancer to exploit transcriptome changes related to carcinogenesis and the prediction of prognosis and treatment responses¹⁹. Basal gene expression profiles of colorectal cell lines showing correlation with apoptosis induced by 5-FU and camptothecin have been determined in a panel of 30 colon cancer cell lines²⁰ as have expression profiles for the prediction of response to oxaliplatin²¹. Pertinently, clinical samples obtained from primary colon tumours have been used to define genes which discriminate response to leucovorin, fluorouracil and irinotecan (FOLFIRI)²² and pre-treatment rectal cancer biopsies have been used to define transcripts associated with response to preoperative chemo-radiotherapy in rectal adenocarcinomas²³. Transcriptional profiling of pre-treatment metastatic colorectal cancer biopsies have also allowed the identification of genes whose expression is correlated with clinical responses to cetuximab monotherapy. From this work increased expression of epiregulin and amphiregulin mRNA was first described to be associated with disease control in response to a monoclonal antibody, cetuximab, targeting the EGF receptor²⁴.

Most recently the transcriptional profile of baseline rectal cancer biopsies have been compared to profiles after cetuximab monotherapy (Day 6-8) leading to the identification of 16 genes that were differentially expressed²⁵. Although microarray analysis did not identify simple predictive signatures for pathological response, the authors noted that tumoural EGFR up-regulation after the initial dose of cetuximab was associated with improved disease free survival²⁵. This research is similar in design to the Xerxes study (1.3.5) however the time at which rectal cancer transcriptomes are explored differ, being examined 4 hours following cetuximab, on the basis that detected gene changes will reflect the primary influence of the drug alone.

The current status of microarray –based testing in cancer patients, regardless of site, does not extend to selection of treatments guided by microarray platform data. Progress is being made however as AmpliChip CYP450 and MammaPrint are the first FDA approved microarray-based tests for assessments of drug metabolising enzymes and prognosis of node negative invasive breast cancer respectively²⁶.

1.3.3 Predictive biomarkers in metastatic colorectal cancer

Already, a number of studies including conventional cytotoxics have probed the relationship between genes and their association with drug metabolism, treatment outcomes and toxicity³. For example, translational research emerging from the FOCUS trial has led to the discovery that moderate or high levels of Topo1, a molecular target of SN38, is a predictive biomarker associated with benefit from either oxaliplatin or irinotecan²⁷. Thus in due course, independent validation and prospective randomised trials, such as FOCUS-3, which plans incorporation of molecular-guided therapy decisions, will continue to push forward biomarkers for personalised therapy of colorectal cancer²⁷.

During the last 4 years research efforts have been directed towards the discovery of predictive markers with a particular emphasis on treatments targeting the EGF receptor in metastatic colorectal cancer. The pivotal studies in bowel cancer introducing cetuximab, a chimeric monoclonal antibody against the epidermal growth factor receptor (EGFR), revealed response rates ranging from 9-23%, but no correlation was found between response and degree of EGFR immuno-histochemical (IHC) staining^{28, 29}. This was somewhat surprising in view of HER2 over-expression in breast cancer and responses to trastuzumab³⁰. Colon cancers seemingly negative for EGFR IHC evidently still responded to EGFR monoclonal antibodies presumably through high affinity binding sites (10-1000 per cell³¹) below the threshold of IHC detection^{32, 33}.

In light of data establishing the relationship between NSCLC EGFR tyrosine kinase mutations and response to EGFR targeted therapy with tyrosine kinase inhibitors⁸, a search for similar mutations in colorectal cancer was undertaken as a means establishing molecular criteria for response prediction. A screen for DNA alterations in the EGFR kinase domain (exons 17-24) from 293 colorectal tumours only found one single mutation identical to an activating mutation previously reported in lung cancer, showing that EGFR mutations occur

at a very low frequency in colon cancer³⁴. Other reports corroborated this finding^{35, 36} leading to the conclusion that EGFR kinase domain mutations were not the basis of response to monoclonal antibodies targeting EGFR in colorectal cancer. The observation that mutant EGFR kinases significantly increase the binding affinity of gefitinib³⁷ has been suggested to explain the improved sensitivity to EGFR kinase inhibition in a subset of lung cancers. This is of relevance in terms of a drug's therapeutic index given that the balance of anti-tumour effects relative to normal tissue toxicity will be more favourable. This is also emphasised by EGFR/HER2 genomic amplification in breast cancer³⁸ and response to trastuzumab therapy (monoclonal antibody targeting HER2).

Simultaneous reports were made of the association between EGFR induced skin rash and clinical responses in colon cancer patients treated with EGFR antagonists, suggesting that rash may be a surrogate marker for treatment response³⁹. From a molecular biology standpoint, interest was growing in the relevance of increased *EGFR* copy number and its association with treatment responses, following the publication of data showing that more than 3 copies of *EGFR* per nucleus identified by Fluorescent In-Situ Hybridisation (FISH), was more likely to indicate response to anti-EGFR monoclonal therapy³⁵. However this story was by no means clear cut given reports that *EGFR* gene copy assessed by qRT-PCR did not share the same relationship with response³⁶. Increasingly however, it appears that *EGFR* copy number, analysed by FISH or chromogenic in situ hybridization, is a promising biomarker for response to EGFR targeted therapy. Patients with <3 copies of *EGFR* per nucleus have a relatively low level of response to anti-EGFR therapy, but increased *EGFR* copy number is associated with higher response rates and longer progression free survival⁴⁰.

Finally, there is a limited relationship between EGFR IHC protein expression and gene copy number, as only a small proportion of colon cancers expressing EGFR protein detected by IHC were associated with gene amplifications⁴¹. Similarly, a poor correlation between different methods of measuring EGFR status at DNA, RNA and protein level, has been described in colon cancer⁴². This contrasts with the situation in breast cancer where over-expression of HER2 detected by IHC in carefully fixed, processed and embedded samples correlates well with gene copy status⁴³, and goes some way towards explaining why a simple

relationship between target expression and treatment response (c.f. trastuzumab in breast cancer), is not evident for colorectal cancer and EGFR targeted therapy.

1.3.4 Mutations in downstream EGFR signalling pathways and response to EGFR targeted therapy in metastatic colon cancer

An emerging story of great importance unfolded during 2006 with the first full report that *Kirsten rat sarcoma viral oncogene homolog (K-RAS)* mutation was significantly associated with the absence of response to cetuximab in the setting of metastatic colorectal cancer⁴⁴. Subsequent retrospective evaluation of *K-RAS* mutations in metastatic colorectal cancer confirmed its presence in approximately 40% of cases and a negative outcome in terms of response prediction in monotherapy trials^{24, 45, 46}. Others extended these findings to combination studies of cytotoxics and cetuximab in first line therapy^{4, 47}. It became clear that antagonism of EGF receptor signalling with monoclonal antibodies, in the presence of *K-RAS* mutations constitutively activating the RAS/RAF/MEK/ERK pathway, was futile. Indeed there is emerging evidence that EGFR-targeted agents in this setting is detrimental, impairing the efficacy of the cytotoxic components of combination treatment reducing progression free survival⁴⁷.

K-RAS mutation status however is not the whole story as only 40% of *K-RAS* wild type metastatic colorectal cancer patients receiving treatment with cetuximab obtain objective responses⁴⁸. Autocrine loops involving ligands for EGFR such as epiregulin and amphiregulin have been suggested to promote tumour growth in colorectal cancer²⁴. Moreover it is now known that high tumoural epiregulin expression in *K-RAS* wild type colorectal tumours is associated with improved outcome to cetuximab treatment (vs. best supportive care)⁴⁹. Therefore monoclonal antibodies targeting EGFR appear to inhibit ligand-dependent tumour growth, potentially explaining their association with monoclonal antibody induced tumour responses²⁴.

The finding that *K-RAS* wild type status does not guarantee sensitivity to anti-EGFR targeted therapy led the search for other oncogenic mutations associated within downstream EGFR signalling cascades. As a consequence activating mutations in the *v-raf murine sarcoma viral oncogene homolog b (B-RAF)* (10% colorectal cancer⁵⁰), *PI3-kinase p110 α subunit (PIK3CA)*; (20% colorectal cancer⁵¹) or loss of function in *phosphatase and*

tensin homologue (PTEN; 30% colorectal cancer⁵¹) have been incriminated in the lack of response to EGFR targeted therapy⁵⁰⁻⁵⁴. Recent estimates report that 70% of patients' likelihood of response to EGFR targeted monoclonal antibodies can be predicted based on the mutational status of *K-RAS* and *PIK3CA/PTEN* pathways⁵¹. This still however leaves a large gap where our understanding of response mechanism to EGFR targeted therapy is unknown. In light of this the *Apc^{min/+}* mouse model has been used to explore and identify novel putative biomarkers capable of predicting response to EGFR targeted therapy (Chapter 3).

1.3.5 Xerxes clinical trial

The Xerxes study was designed to examine the role of early neo-adjuvant and synchronous cetuximab therapy in pre-operative chemo-radiotherapy using capecitabine (5FU prodrug) followed by excisional surgery. This translational study intended to provide rectal cancer specimens at baseline and 4 hours following the first infusion of cetuximab to enable probing of transcript changes induced by EGFR targeted therapy, to generate hypotheses regarding biomarkers of response prediction guided by data obtained from the *Apc^{min/+}* model of colon cancer.

The Xerxes trial postulated the addition of cetuximab to radiotherapy would improve pathological response and clinical outcomes as demonstrated in the setting of locally advanced head and neck cancer⁵⁵. Subsequent studies have found that complete pathological response (pCR) rates to pre-operative radiotherapy combined with capecitabine and cetuximab (\pm oxaliplatin), in locally advanced rectal cancer, were poor (5-9%)^{56, 57}, compared to pathological responses seen without cetuximab (pCR 16% in pre-operative radiotherapy plus capecitabine and oxaliplatin)⁵⁸. It has been suggested that cetuximab compromises the efficacy of capecitabine/radiotherapy, through a reduced tumour cell turnover, which is required for the uptake of capecitabine to enable its cytotoxic and radiosensitising effects²⁵.

As a consequence of these findings, trial recruitment to XERXES was halted and clearly impacted the availability of rectal cancer samples for assessment of gene expression changes in tumour specimens. This has made planned comparisons between transcript

changes induced by anti-EGFR therapy in *Apc^{min/+}* mouse colon tumours and human rectal cancers, very limited, highlighting the difficult nature of translational research.

1.4 Epidermal growth factor receptor (EGFR)

In the 1950's extracts of sub-maxillary glands from mice were directly injected into newborn animals inducing early opening of eyelids and eruption of incisors^{59, 60}. The same extract was later found to stimulate epidermal growth and keratinisation⁶¹. This 'epidermal growth factor' was isolated and a homologous polypeptide, human EGF was detected shortly thereafter⁶⁰. The receptor for EGF was subsequently detected using crude membrane fractions prepared from different animal tissues⁶², however it was not until 1984 that Ullrich et al isolated and characterised the cDNA sequence of EGFR⁶³.

1.4.1 Signal transduction

EGFR (ERBB or HER-1) is a 170-kDa membrane protein⁶⁴ and a member of the subclass I receptor tyrosine kinase (RTK) super family along with v-erb-b2 erythroblastic leukaemia viral oncogene homolog 2, ERBB2 (HER-2), v-erb-b2 erythroblastic leukaemia viral oncogene homolog 3, ERBB3 (HER-3), and v-erb-a erythroblastic leukaemia viral oncogene homolog 4, ERBB4 (HER4)⁶⁵. Each member has an extracellular ligand binding region, a short membrane spanning region and intracellular protein-tyrosine kinase containing domain⁶⁵. Ligand binding results in the formation of homo-and hetero receptor dimers and activation of the cytoplasmic tyrosine kinase domain resulting in auto-phosphorylation of specific tyrosine sites, which subsequently act as docking sites for downstream intracellular signalling pathways⁶⁶. The two main signal transduction pathways stimulated are the mitogen-activated protein kinase (MAPK) and phosphatidylinositol 3-kinase (PI3K)-AKT pathways (fig 1). Other pathways involved in transmitting ErbB signals include phospholipase C⁶⁷, signal transducer and activator of transcription (STAT); SRC tyrosine kinase, which is stimulated in response to EGFR and ERBB2, and mammalian target of rapamycin (mTOR), a serine/threonine protein kinase activated beyond PI3K-AKT⁶⁶. Different ERBBs preferentially modulate certain downstream signalling pathways owing to receptor binding to specific effector proteins. As a result cells harbouring EGFR tyrosine kinase mutations tend to activate PI3K-AKT and STAT pathways, whereas ERBB2 couples to

Figure 1. EGF receptor signalling

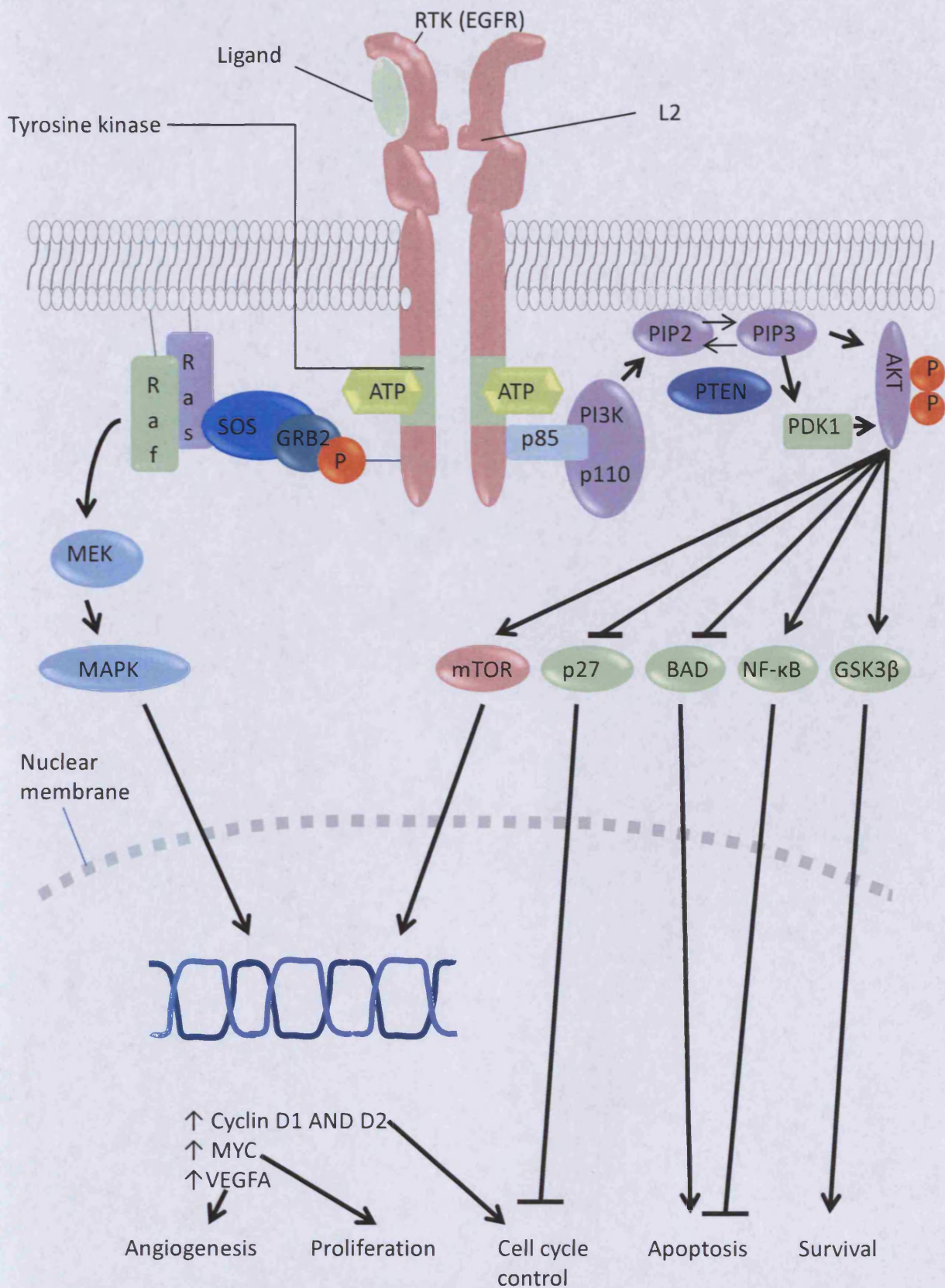


Fig 1. Signalling downstream of EGFR showing the two key pathways activated. The MAPK pathway stimulates proliferation and the PI3K/AKT pathway promotes cell survival. Gefitinib is an ATP analogue and competes with ATP binding within the catalytic kinase domain of RTKs. Cetuximab binds to the L2 domain of EGFR. GSK3 β , glycogen synthase kinase 3 β ; NF-KB, nuclear factor-KB; PDK1, pyruvate dehydrogenase kinase 1; PIP2, phosphatidylinositol biphosphate; PIP3, phosphatidylinositol triphosphosphate; RTK, Receptor tyrosine kinase. Adapted from Baselga and Swain *Nature Reviews Cancer* (2009) and Imai and Takaoka *Nature Reviews Cancer* (2006)

the MAPK pathway, and ERBB3 associates with the p85 adapter subunit of PI3K through its numerous p85 docking sites to signal through PI3K-AKT cascades⁶⁶.

It is interesting to note that no ligand binds ERBB2, but it is the preferred dimerisation partner for all other ERBB members and, that ERBB3 has no functioning tyrosine kinase activity and only transmits a signal when it pairs with another ERBB receptor⁶⁶. ERBB2 is normally only activated following hetero-dimerisation with another ligand bound ERBB receptor or when over-expressed due to constitutive activation presumably as a result of increased membrane receptor concentration^{66, 68}. Conventional wisdom has recently been challenged based on the finding that ERBB2 shows striking similarity to a tightly ligand-regulated invertebrate EGF receptor, suggesting that ERBB2 has activating ligands⁶⁹. Alvarado and colleagues conclude that identifying these possible membrane associated ligands and understanding their role in human cancers may provide new therapeutic directions for targeting ERBB receptor signalling.

1.4.2 Deregulated function

In vivo functions of the ERBB family are crucial for embryogenesis and development of epithelial organs such as the skin, lung and gastrointestinal tract. *Egfr* gene knock out studies in mice have shown embryonic lethality or impaired development of skin, heart, lungs and gastrointestinal tract, whereas knock out of *ErbB2*, *ErbB3* or *ErbB4* causes defects in cardiac and neural development⁷⁰. Given their central role in development, it is of no surprise that deregulation of the ERBB receptor family occurs in cancer, evidenced by over-expression and mutation in the various family members. Pertinently EGFR was the first tyrosine kinase receptor directly linked to tumour development in humans^{66, 70}. EGFR is over-expressed in head and neck, NSCLC, breast, bladder, kidney, prostate and colon cancer^{71, 72}. Over-expression of EGFR also occurs in gliomas and is often associated with structural rearrangements that produce in-frame deletions in the extracellular domain of the receptor; the most frequent being the EGFR variant III⁶⁶. The remaining family members ERBB2, ERBB3 and ERBB4 are implicated in a range of other cancers such as breast, lung, pancreas, oesophagus, endometrium, cervix and stomach cancer⁷¹.

Deregulated ERBB signalling activates key processes involved in tumour growth and progression, including proliferation and survival. The main effector pathway mediating cell

survival is the PI3K-AKT pathway since several AKT substrates control various apoptotic processes⁶⁸. Signalling through the MEK/ERK pathway is linked to cell growth, survival and invasion in cancer and its pattern determines whether activation favours mitogenesis (short duration) or differentiation (long duration)⁷³. By disturbing ERBB2 signalling activity, using a variety of methods such as antagonistic antibodies, small molecule kinase inhibitors and antibodies causing functional inactivation of the receptor in endoplasmic reticulum, ERBB2 has been shown to be important in promoting proliferation of malignant cells. The nuclear effectors of such proliferative activity include G1 regulators Myc, D-type cyclins, cyclin E2/cdk2 complexes and the cyclin dependent kinase inhibitor p27 (KIP1)⁶⁸.

1.4.3 Therapeutic targeting

The main approaches in the clinic to counter aberrant signalling through EGF receptor tyrosine kinases include monoclonal antibodies (mABs) and small molecule tyrosine kinase inhibitors. mABs have been created against the extracellular domain of the EGF receptor (fig 1) and have their effect by recruiting cytotoxic lymphocytes as well as interfering with cancer cell signalling (see below). Such drugs include Cetuximab (Erbix[™]; Bristol Myers Squibb/Imclone) or Panitumumab (Vectibix; Amgen)⁷¹. Small molecule tyrosine kinase inhibitors (ATP mimetics) block ERBB function by competing for the ATP-binding pocket⁹ located on the intracellular portion of its receptor⁷¹ (fig 1) thereby disrupting mitotic signalling downstream. Two examples include Gefitinib (Iressa; AstraZeneca) and Erlotinib (Tarceva; Genentech/OSI) which are active in NSCLC expressing catalytically active EGFR. Drugs with activity against both EGFR and ERBB2 have been developed and may represent a more attractive strategy (Lapatinib, GlaxoSmithKline; CI-1033, Pfizer and EKB-569, Wyeth-Ayerst Research)⁷¹.

The putative mechanisms of monoclonal antibody based cancer therapies are mediated through direct or indirect actions⁹. Direct effects include blockade of ligand receptor binding, increased receptor internalisation, inhibition of cell cycle progression or DNA repair, regression of angiogenesis and pro-apoptotic effects. Indirect effects of monoclonal antibodies mediated by the immune system include eradication of tumour cells by Ig-mediated complement-dependent cytotoxicity and antibody-dependent cellular cytotoxicity.

Small molecule tyrosine kinase inhibitors by contrast do not have indirect effects on the immune system. Gefitinib targets EGFR selectively and unlike mABs is able to translocate cell membranes to interact with the cytoplasmic domain of the receptor tyrosine kinase⁹(fig 1). Gefitinib has been shown to inhibit growth mainly through cytostatic effects, but also through increased programmed cell death⁷⁴. Recent studies have shown that gefitinib induced apoptosis, at least in gefitinib sensitive NSCLC cell lines, is dependent upon the transcription and post-translational modification of BIM, a BH3-only pro-apoptotic protein⁷⁵.

1.4.4 Resistance to EGFR targeted agents

Understanding the mechanisms of drug resistance in tumours is a crucial component of treating any cancer. Primary drug resistance may occur in patients who have not achieved stable disease or who progress within 6 months of therapy after an initial response, whereas resistance after prolonged treatment is termed secondary resistance, for which several molecular mechanisms may be responsible⁷⁶.

In terms of understanding resistance to small molecule therapy a number of mechanisms have been proposed⁷⁶. These include structural alteration of the kinase domain resulting in an inability of the inhibitor to bind to the intracellular catalytic domain, secondary activating mutations in the kinase domain, or the development of a 'kinase switch' activating a kinase other than the primary targeted kinase, in cancer cells. Other possible mechanisms include gene amplifications leading to higher expression levels of receptor and a higher required dose of inhibitor to produce a sustained effect.

A further mechanism accounting for resistance to tyrosine kinase inhibition is up-regulated expression of ERBB3 and consequent enhanced PI3K-AKT signalling⁷⁷ through the ability of ERBB3 to dock with the p85 alpha regulatory subunit of PI3K⁷⁸. This highlights the ability of tumour cells to enhance signalling pathways to circumvent drug effects. Additional mechanisms which have yet to be defined, but are potentially important in determining resistance to small molecular tyrosine kinase inhibitors include extracellular sequestration of drug by plasma proteins, and increased drug efflux by trans-membrane pump proteins.

When considering targeted treatments relating to metastatic colorectal cancer it is possible some of the mechanisms accounting for resistance to tyrosine kinase inhibition

may have a role in mediating resistance to mABs against EGFR. Several primary mechanisms of resistance have already been mentioned including mutations in *K-RAS*, *B-RAF*, *PIK3CA* and *PTEN* loss (1.3.4). However it is likely that these signalling molecules will be targeted in the future. Genome wide RNAi screens have already identified synthetic lethal interactions with the RAS oncogene which can be targeted. For example, inhibition of PLK1 (using BI-2536) which has a role in mitosis, has shown profound G2/M accumulation in RAS mutant cells⁷⁹.

Signalling through another member of the receptor tyrosine kinase family, IGF1R has also been shown to confer resistance to EGF family blockade⁸⁰⁻⁸² and is activated in response to chemotherapy for treatment of colorectal cancer⁸³. Hence cross-communication between members of receptor tyrosine kinases is likely to be a route exploited by cancer cells to overcome targeted drugs against EGFR.

Finally, parallel signalling pathways can become activated as a means of inducing tumour growth to counter anti-tumour drug effects, as exemplified by increased AKT activity in cancer cells resistant to the MEK inhibitor, AZD6244⁸⁴. Tumours are therefore poised to exploit established circuitry links between RAS and PI3K/AKT, evidenced by GTP-bound RAS interacting directly with PI3K to create an effector pathway for RAS signalling⁸⁵, thus enabling parallel pathway activation.

1.5 Insulin-like growth factor 1 receptor (IGF1R)

IGF1R and insulin receptors have tetrameric structures and are composed of two half receptors, comprising a predominantly extracellular α -chain, involved with ligand binding, and, a principally intracellular β -chain including the tyrosine kinase domain. Hybrid receptors can form between insulin and IGF-1 receptors expressed in cells that possess both receptors⁸⁶(Fig 1.1) and given this, the specificity of IGF1R targeting is biologically challenging. As a consequence of receptor activity, AKT and MAPK transmit mitogenic signals downstream. Interestingly the IGF-2 receptor is not implicated in signal transduction but sequesters IGF-2 and in doing so regulates ligand bioavailability⁸⁶. The bioavailability of IGF-1 and IGF-2 is also modulated by the binding affinities of various IGFbps and in general limit the access of IGFs to IGF1R suppressing biological activity⁸⁶. IGF-1 and IGF-2 are both manufactured in the liver but are also produced in tumours allowing them to act locally and influence tumour dynamics at this level⁸⁶.

Fig 1.1 Insulin-like growth factor (IGF) signalling

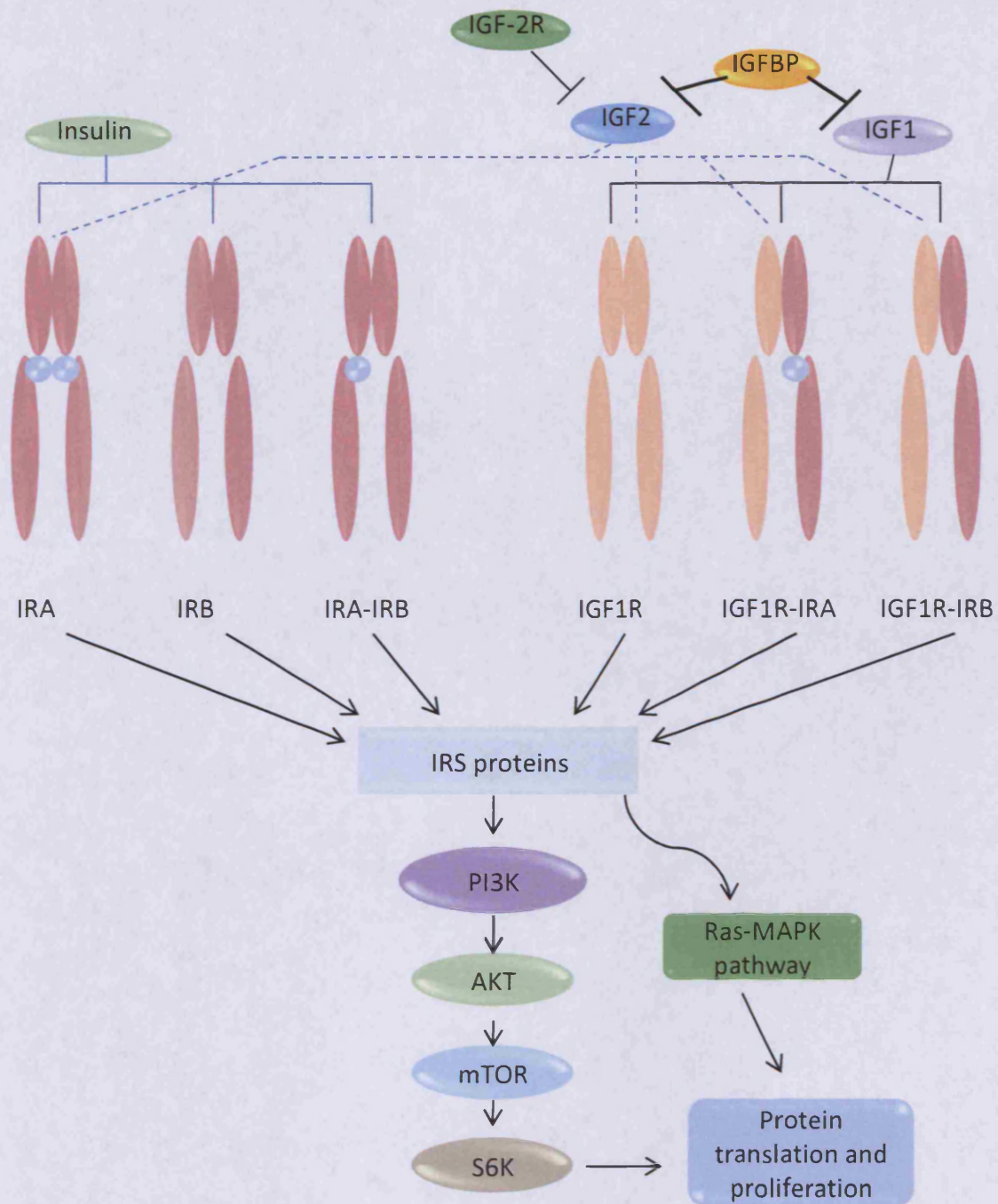


Fig 1.1 The ligands IGF-1, IGF-2 and insulin bind to various members of the insulin receptor (IR)-IGF1R family. IGF2 binds with a greater affinity to IRA than IRB. The bioavailability of IGF-1 is limited by IGF binding proteins (IGFBP) and that of IGF-2 is governed by IGFBPs and the IGF-2R. The IR and IGF-1R receptors are tetrameric and composed of 'half receptors'. The intracellular domain of each receptor has tyrosine kinase activity regulated by ligand binding. Receptors may form into pure insulin receptors, pure IGF-1 receptors or hybrids. Downstream signalling is mediated by PI3K/AKT and MAPK. Adapted from Pollak, Nature Reviews Cancer (2008).

The type 1 insulin-like growth factor receptor has been implicated in various aspects of tumour development and metastasis^{86, 87}. Expression of IGF1R has been demonstrated in cancer cell lines and human malignancies and mitogenic responses have been observed in cell lines at physiological levels of IGF-1 ligand⁸⁶. Specifically increased levels of IGF1R at transcript and protein level have been documented in colon cancers relative to adjacent normal colonic mucosa⁸⁸ suggesting its relevance in the pathogenesis of colon cancer. Indeed IGF-2 was found to be the uppermost differentially regulated transcript in colon tumour tissue compared with normal colonic epithelium⁸⁹.

The IGF system has also been shown to be important and relevant to intestinal physiology and tumourigenesis in the *Apc^{min/+}* mouse which models familial adenomatous polyposis. Expression of *Igf-2* and *Igf1r* has been demonstrated in *Apc^{min/+}* intestinal adenomas and genetic manipulation of *Igf-2* availability modifies their growth⁹⁰. Furthermore expression of a soluble *Igf2r* transgene has been shown to rescue *Igf-2* dependent normal intestinal and intestinal adenoma phenotypes in *Apc^{min/+}* mice⁹¹.

A very recent publication has demonstrated increased expression of *Igf1r* in a mouse model of mammary cancer driven by over-expression of a constitutively active oncogenic *K-ras* allele. Interestingly, ablation of *Igf1r* expression increased tumour latency in this model, suggesting *Igf1r* had a causal role in mammary tumourigenesis⁹². This may be a context dependent effect, restricted to subtypes of mammary cancer, but it could imply IGF1R has a role in the genesis of colorectal cancer carrying *K-RAS* mutations, and that therapeutic manipulation of IGF1R signalling in this setting may be advantageous.

IGF1R drug targeting has emerged over the last two decades using monoclonal antibodies and small molecule inhibitors in a range of malignancies⁹³. Reliable biomarkers for the prediction of sensitivity to IGF1R targeted agents however appear biologically complicated. So far, evidence suggests that receptor and ligand levels together with differentiation markers may be required to help define tumours predisposed to IGF1R inhibition⁹³. Clinical evidence supporting IGF1R as a treatment target for Ewing's sarcoma, adrenocortical cancer and non-small cell lung cancer⁹⁴ highlights the need to understand the resistance pathways which will emerge in response to antagonism of the IGF1R receptor. Interestingly, resistance to IGF1R targeted therapies has been demonstrated in a reciprocal

fashion, with up-regulation of EGFR and its ligands, suggesting EGFR pathway activation may be an alternative route for growth signals to be transmitted in the presence of inhibition of IGF1R signalling^{95, 96}. Given the possible bidirectional cross communication between EGFR and IGF1R pathways, it is not surprising that research, in response, has been directed towards combined targeted therapy against both these pathways⁹⁷.

1.6 Genetically engineered mouse models of colon tumourigenesis

Murine models of cancer have expanded our understanding of basic cancer biology and many genetically engineered mouse models (GEMMs) have been created to explore intestinal tumourigenesis in detail⁹⁸. GEMMs have desirable qualities allowing tumour development in the presence of an intact immune system and also permit tumour-stromal interactions that influence tumour progression (angiogenesis/matrix degradation)⁹⁹. Furthermore GEMMs attempt to faithfully mirror the genetic events occurring in human malignancies making them pertinent to the study of the cancers they model. The two models used in this work include the *Apc*^{min/+} mouse and *AhCre*^{T/+} *Apc*^{fl/+} *K-ras*^{V12/+} and *AhCre*^{T/+} *Apc*^{fl/+} *K-ras*^{+/+} conditional transgenic models.

1.6.1 *Apc*^{min/+} mouse

Apc^{min/+} mice were established from ethylnitrosurea-treated C57BL/6 male mice, whose offspring were noted to develop adult onset anaemia, transmitted as an autosomal dominant trait. Further enquiry established chronic blood loss due to multiple small and large intestinal adenomas and consequently the mutant gene responsible was named multiple intestinal neoplasia (Min)¹⁰⁰. Further work in William Dove's laboratory determined that the *Min* phenotype was a result of a germ-line nonsense mutation in the murine homologue of the *APC* gene¹⁰¹ which gives rise to familial adenomatous polyposis, an inherited colorectal cancer syndrome characterised by multiple colorectal tumours¹⁰². Extensive loss of *Apc* was subsequently shown in adenomas from *Apc*^{min/+} mice¹⁰³ and furthermore, deregulation of Wnt signalling has been found to be pivotal in intestinal tumourigenesis as truncating mutations in *APC* lead to constitutive nuclear β catenin/TCF complexes driving a proliferative genetic programme^{104, 105}. The *Apc*^{min/+} mouse is considered a relevant model of human colon cancer as more than 80% of adenomas and colorectal cancers have at least one mutation in the *APC* gene associated with the

development of the majority of colorectal cancers¹⁰⁶. Despite this the *Apc^{min/+}* mouse is limited in its ability to mirror genetic events that follow mutations in *Apc* and has given an impetus to the development of better models of colon cancer.

The number of intestinal tumours in *Apc^{min/+}* mice is strongly influenced by genetic background and genetic mapping identified the *Mom-1* (Modifier of Min-1) locus as a dominant modifier of the intestinal phenotype, accounting for 50% of the genetic variance in tumour number¹⁰⁷. A *phospholipase A2*, *Pla2g2a* transgene, derived from within the *Mom-1* region, has been shown to act as a resistance modifier in *Apc^{min/+}* intestinal phenotypes and closely reproduced the quantitative reduction in tumour numbers seen in *Mom-1* heterozygotes, suggesting that the *Mom-1* locus is in fact *Pla2g2a*¹⁰⁸. It is worth noting that the gene expression experiments, using *Apc^{min/+}* mice to identify putative genes indicative of response to anti-EGFR targeted therapy, were performed using in-bred C57BL/6 mice homozygous for *Mom-1*. This enabled the identification of gene changes in genetically similar tumours, thus removing a source of genetic variation which could obscure any induced transcript changes (Chapter 3).

Of relevance to this project, studies have shown evidence of *Egfr* activity in *Apc^{min/+}* intestinal tumours. Increased total *Egfr* protein expression in *Apc^{min/+}* adenomas relative to wild type enterocytes has been demonstrated, as has the level of phospho-*Egfr* from membrane preparations of intestinal adenomas relative to the same fraction from normal *Apc^{min/+}* colon¹⁰⁹. Further work supporting *Egfr* in adenoma pathogenesis comes from work showing *Apc^{min/+}* mice carrying a homozygous *Egfr^{wa2}* hypomorphic allele demonstrate a marked reduction in intestinal polyp number¹¹⁰. Pharmacological inhibition of the *Egf* receptor using the *Egfr* tyrosine kinase inhibitor EKI-785 also produced similar results in *Apc^{min/+}* mice¹¹⁰. Less dramatic reductions in tumour multiplicity following exposure to EKI-785 have however been reported¹¹¹ and controversially, an alternative *Egfr* inhibitor, *N*-[4-(3-chloro-4-fluoro-phenylamino)-quinazolin-6-yl]-acrylamide (CFPQA), failed to demonstrate suppression of intestinal adenomas at levels sufficient to abolish phospho-*Egfr*, leading the authors to conclude that *Egfr* mediated signalling was not critical for early stages of intestinal carcinogenesis¹¹². The role of *Egfr* signalling in *Apc^{min/+}* intestinal tumourigenesis is examined in detail in acute and chronic dosing studies of gefitinib described in Chapter 5.

1.6.2 $AhCre^{T/+} Apc^{fl/+} K-ras^{v12/+}$ conditional transgenic mouse model

The limitation of the $Apc^{min/+}$ mouse to recapitulate the genetic changes following mutation in Apc has driven investigators to develop and characterise mouse models which include the common mutations seen in human colorectal cancer beyond Apc . Work to develop genetically engineered mouse models of colorectal cancer displaying the full features of human colorectal cancers is progressing and invasive models are now available^{113, 114}. However, models displaying the full metastatic phenotype of colorectal cancer continue to remain elusive. This is important to tackle if we aim to use *in-vivo* platforms closely resembling metastatic cancers as a preclinical test bed for therapeutic manipulation.

The presence of $K-RAS$, and other mutations which predict lack of response to EGFR targeted agents in metastatic colorectal cancer, represent areas of unmet clinical need. To address this therapeutic challenge, a conditional transgenic mouse model of accelerated and invasive colon tumourigenesis has been used, in this project, as an *in vivo* platform, by inducing intestinal expression of an oncogenic $K-ras^{v12}$ allele in the context of Apc deficiency ($AhCre^{T/+} Apc^{fl/+} K-ras^{v12/+}$)¹¹⁴.

This model of $K-ras$ mutant colorectal cancer was made possible by conditional gene targeting using Cre-loxP recombination¹¹⁵ which permits cell-type specific and inducible mutagenesis. By crossing mice bearing the targeted allele (Apc^{580S})¹¹⁶ onto mice carrying the transgenic line $AhCre$, cre expression was inducible from a cytochrome P450 promoter element which is transcriptionally up-regulated in response to β -naphthoflavone¹¹⁷, resulting in loss of Apc exon 14 throughout the intestine¹¹⁴. Simultaneously the intestinal expression of the oncogenic $K-ras^{v12/+}$ allele was achieved by cre due to the loss of a STOP transcriptional cassette¹¹⁸. The loss of this STOP cassette also permitted expression of a reporter stain, LacZ, to confirm recombination¹¹⁴.

This clinically relevant model of $K-ras$ mutant intestinal cancer has been subject to investigation using novel therapy targeting the constitutively activated MAPK pathway, via inhibition of MEK using AZD6244 (Chapter 7). It is hoped this *in vivo* platform will have pre-clinical utility, overcoming some of the disappointments xenograft studies present, and thus demonstrate an improved correlation between therapeutic activity of compounds tested

and efficacy in humans. To date, little drug evaluation has been carried out in well designed GEMMs of cancer that faithfully mimic the genetic and biological evolution of their counterpart diseases⁹⁹.

1.7 Mitogen activated protein kinase (MAPK) signalling and colorectal cancer

Human tumours frequently possess activating mutations in one of the *RAS* genes¹¹⁹ and downstream effector signalling pathways include Raf kinases, type I phosphoinositide 3-kinases, Ral-guanine nucleotide exchange factors, Rac exchange factor Tiam 1 and phospholipase C ϵ ¹²⁰. The most intensively studied effector is the protein serine/threonine kinase RAF, which is activated by GTP-bound RAS and consequently phosphorylates and activates mitogen-activated protein kinase kinases 1 and 2 (MEK1 and MEK2). Activated MEK1/2 subsequently activates the mitogen-activated protein kinases (MAPKs) ERK1 and ERK2 (extracellular signal-regulated kinases 1 and 2) which interact with transcription factors regulating cell cycle proteins¹²⁰.

The MAPK pathway is activated in colorectal cancer and is involved in the regulation of apoptosis, cell proliferation, tumour invasion and metastasis⁷³. In keeping with this, human primary colorectal cancers demonstrate increased expression of phosphorylated MEK in 76% of cases, highlighting the potential importance of the RAF-MEK-ERK signalling in colorectal tumour development¹²¹. As *K-RAS* mutations are frequently observed in colorectal cancer (approx. 40%⁴⁶) strategies to counter constitutive signalling activity are under development, including drugs which target MEK1/2.

1.7.1 Pharmacological manipulation by inhibition of MEK1/2

AZD6244, previously known as ARRY-142886, is a potent, selective and ATP uncompetitive inhibitor of mitogen-activated protein kinase/extracellular signal-regulated kinase kinase 1/2 kinases (MEK1/2)¹²². MEK inhibition has been shown to produce cell cycle arrest and BCL-2 regulated apoptosis in *B-RAF* mutant tumour cells. In addition MEK inhibitor-induced apoptosis has been found to be dependent upon BIM (BH3 only pro-apoptotic protein) expression, in B-RAF mutant colorectal cancer cells¹²³. Other studies have also demonstrated that MEK inhibition induces down-regulation of cyclin D1 with induction of G1 arrest¹²⁴.

In vitro cell viability inhibition screening studies have shown that tumour cells harbouring *B-RAF* and *K-RAS* mutations are likely to be sensitive to AZD6244¹²². Furthermore, chronic dosing with AZD6244 results in growth suppression of tumour bearing xenografts which harbour Colo-205, Calu-6 and SW-620 transplants possessing either *K-RAS* or *B-RAF* mutations. This contrasts with previously published work showing that mutant *B-RAF* cell lines are associated with heightened sensitivity to MEK inhibition using CI 1040, compared to cell lines carrying wild type or *K-RAS* mutations, which were resistant¹²⁴. These data may arise due to differences between the MEK inhibitors AZD6244 and CI 1040, however it does raise the possibility that MEK inhibition is perhaps a more appropriate therapy for *B-RAF* rather than *K-RAS* mutant colorectal cancer.

Pharmacodynamic studies have confirmed that the unique substrate of MEK, ERK, and its subsequent phosphorylation, is inhibited by AZD6244 and is therefore a potential biomarker for target inhibition¹²². However defining the molecular determinants that identify patient tumours responsive to MEK inhibition appears more complicated than at first thought. A recent report has shown that the majority of colorectal cancers carrying *B-RAF* or *K-RAS* (but not wild-type) cancer cell lines show growth inhibition with MEK inhibition (using U0126 and CI-1040)¹²⁵. However, despite there being a correlation between ERK activation and *B-RAF* mutation status in colorectal cell lines and patient colorectal tumour samples, there was no correlation with *K-RAS* mutations¹²⁵. In addition MEK inhibitor suppression of soft agar colony formation was not correlated with ERK activity¹²⁵. As a consequence ERK activity appears to be an unreliable biomarker of therapeutic response to MEK inhibition. However, *K-RAS* and *B-RAF* mutation status may be useful to reliably predict patient response to MEK inhibition¹²⁵.

It will be of interest to observe how these findings relate to *in vivo* dosing studies of AZD6244 in *AhCre^{T/+} Apc^{fl/+} K-ras^{v12/+}* GEMMs (Chapter 7). Crucially, and in light of the poor correlation between *K-RAS* mutation status and ERK activity¹²⁵, *K-RAS* can clearly influence distal mitogenic signalling independent of ERK activity through alternative pathways¹²⁰ (e.g. PI3K/AKT). As a result these pathways may need to be targeted alone or in combination with MEK inhibition if therapy in *K-RAS* mutant colorectal cancer is to be effective in.

Interestingly, recent work in the context of *B-RAF* melanoma has shown on-target resistance to MEK inhibition arising through reduced drug binding affinity, or enhanced MEK1 kinase activity (e.g. *MEK1^{P124L}*)¹²⁶, which could also have implications for any future therapeutic role of MEK inhibition in colorectal cancer.

1.8 Apoptotic cell death

There are three major pathways of cell death - apoptosis, necrosis and autophagy, with the predominant mode of cell death being dependent upon cell type and injury¹²⁷. In contrast to swelling of the cell and its organelles that defines necrosis, the primary morphological feature of apoptosis is shrinkage of the cell and its nucleus (condensation of chromatin and nuclear fragmentation). In addition the integrity of the plasma membrane is lost early in the course of necrosis, whereas with apoptosis, the plasma membrane remains intact until late in the process¹²⁷.

Two major pathways of cellular apoptosis are present in cells: the extrinsic death receptor pathway mediated through activation of death receptors, and the BCL-2 regulated mitochondrial pathway. The intrinsic (mitochondrial) pathway is activated by intracellular reactive oxygen species, DNA damage and loss of growth factors, which leads to activation of pro-apoptotic BH3 proteins which interact with and inhibit anti-apoptotic BCL-2 and BCL-XL proteins. As a result BAX and BAK are free to increase mitochondrial permeability resulting in the release of cytochrome c, which activates caspase 9 and subsequently caspase 3, 6 and 7 proteases that herald destruction of the cell by cleaving proteins and activating DNases¹²⁷.

The balance between pro-apoptotic and pro-survival proteins ultimately dictates cell fate. The intrinsic pathway is controlled by three subgroups of BCL-2 family members. The pro-survival members include B-cell CLL/lymphoma 2 (BCL-2), BCL2-like 1 (BCL-XL), BCL2-like 2 (BCL-W), myeloid cell leukemia sequence 1 (MCL-1), A1 and BCL2-like 10 (BOO/DIVA). Members of this subgroup have up to four BCL-2 homology regions¹²⁷. The pro-apoptotic BCL-2 family members BCL2-associated X protein (BAX) and BCL2-antagonist/killer 1 (BAK) have three BCL-2 homology domains¹²⁷. The final pro-apoptotic family members have only the BCL-2 homology 3 (BH3) domain. These BH3 only proteins including BCL2-like 11 (BIM), BCL2 binding component 3 (BBC3/PUMA), BCL2-associated agonist of cell death (BAD),

phorbol-12-myristate-13-acetate-induced protein (NOXA) and BH3 interacting domain death agonist BID¹²⁸, bind to pro-survival BCL-2 family members and inhibit their function, liberating pro-apoptotic BAX and BAK proteins¹²⁷. BIM and PUMA can sequester all anti-apoptotic proteins with high affinity and are therefore powerful killers¹²⁸. Interestingly, different apoptotic stimuli preferentially stimulate certain BH3 only proteins; BIM is necessary for apoptosis induced by deprivation of growth factors, whereas PUMA is essential for apoptosis induced by DNA damage¹²⁷.

1.8.1 BH3 mimetics

BH3 mimetics are small molecules that mimic the effects of pro-apoptotic BH3 only proteins by binding to and inhibiting pro-survival proteins included in the BCL-2 family¹²⁹. ABT-737 is the best characterised BH3 mimetic and has a similar binding profile to BAD¹²⁸ and crucially is unable to kill cells which lack both BAK and BAX, showing that it mediates cell death through the intrinsic apoptotic pathway¹²⁸.

The anti-tumour effects of ABT-737 and its ability to induce apoptosis is dependent upon tumour cell type. It has efficacy against certain small cell lung cancers and various haematological malignancies as a single agent, all of which are dependent upon BCL-2 expression, however it is less effective in other tumours¹²⁸. It has been discovered that sensitivity of a tumour to ABT-737 is dependent upon the levels of apoptotic family members. Increased expression of BCL-2, BCL-XL, NOXA and BIM indicates sensitivity, whereas increased MCL-1 indicates resistance¹³⁰.

Combination studies of ABT-737 with targeted agents have given rise to encouraging results. For example experiments have demonstrated enhanced apoptotic cell killing of NSCLC cell lines when ABT-737 is combined with gefitinib⁷⁵ and similar effects when ABT-737 is combined with MEK inhibition in the setting of Colo205 cell lines¹²³. This documented synergy in cell killing between oncogenic kinase inhibitors and ABT-737 is associated with loss of ERK1/2 activity resulting in inhibition of BIM phosphorylation¹²⁸. As a consequence BIM accumulation is thought to exert pro-apoptotic effects by enhanced association with BCL-2 family members, rather than being targeted for proteosomal degradation. As a result, ABT-737 is available to bind and saturate BCL-2, BCL-XL and BCL-W anti-apoptotic proteins, freeing up induced BIM to bind MCL-1 and A1¹²⁸. The combination therefore effectively

Fig 1.2 Central role of MEK-ERK signalling and BCL-2 homology domain 3 (BH3) –only protein BIM in mediating the efficacy of gefitinib and MEK inhibition in the presence of ABT-737

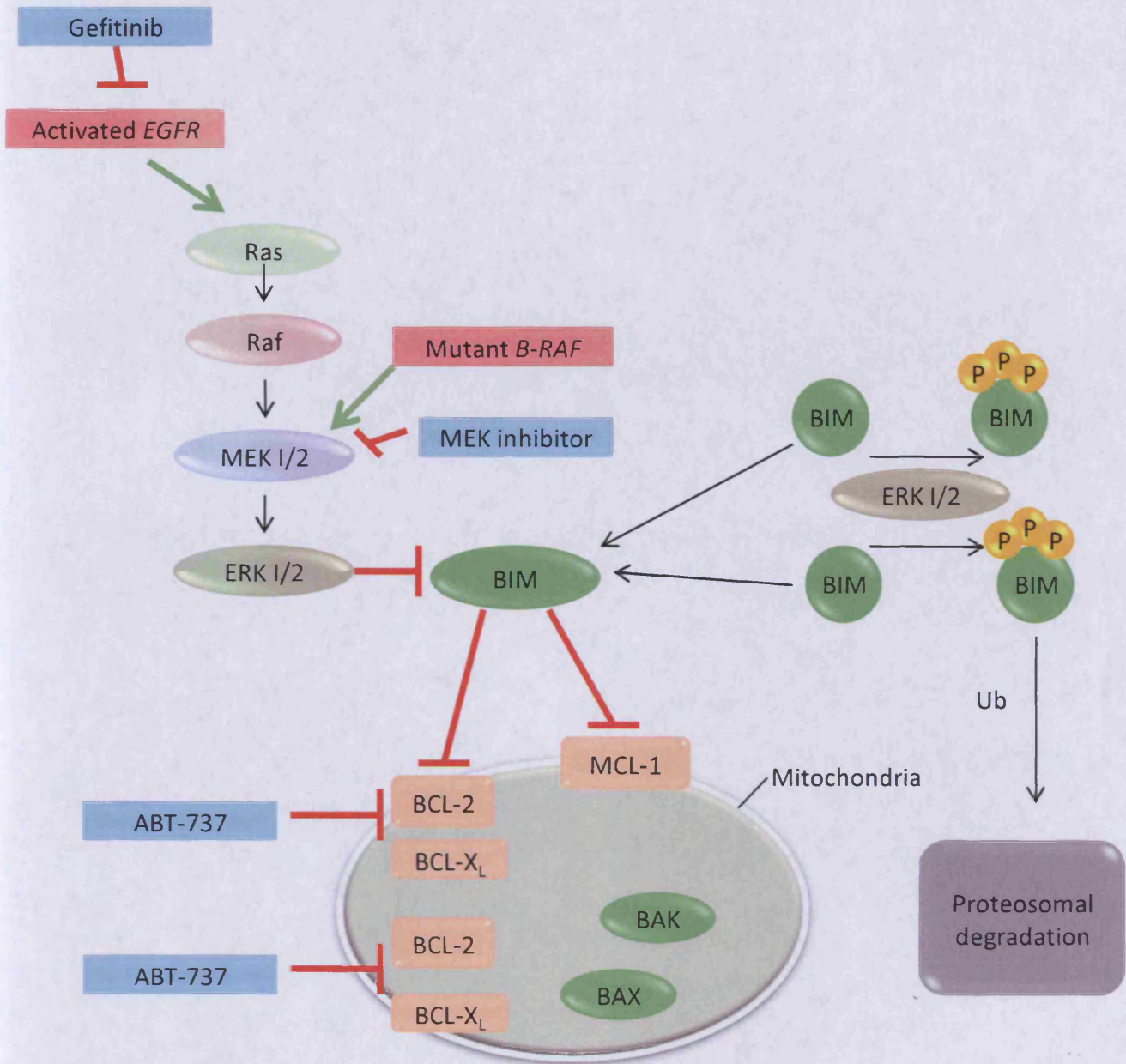


Fig 1.2 The pink boxes represent oncogenic kinases that are targeted with kinase inhibitors and demonstrate synergy in cell killing with ABT-737. The kinase inhibitors reduce ERK 1/2 activity suppressing BIM phosphorylation. The loss of ERK 1/2 mediated phosphorylation of BIM results in increased apoptotic activity of BIM due to reduced targeted destruction by ubiquitylation (Ub) and proteosomal degradation. ABT-737 binds to and saturates the available BCL-2, BCL-X_L and BCL-W pro-survival proteins freeing up accumulated BIM to promote apoptosis by saturating available BCL-2 and MCL-1. Combined treatment results in blockade of all pro-survival proteins and efficient apoptosis. Adapted from Cragg et al Nature Reviews Cancer (2009).

blocks all of the pro-survival family members in tumours resulting in enhanced apoptosis¹²⁸ (fig 1.2). This data precipitated investigation of combined dosing with ABT-737 and gefitinib in *Apc^{min/+}* mice to document its effects *in vivo* (Chapter 6).

1.9 Aims and Objectives

Interest in personalised medicine, targeted oncological therapy and an inherent need for predictive biomarkers in routine oncological practice, has acted as a catalyst for the expansion of translational research in cancer medicine. Furthermore, with developments in targeted therapies, the sceptre of drug resistance continues to emerge, requiring focused research efforts to increase our understanding of tumoural molecular pathways which overcome anti-tumour drug activity. In addition, an increasing number of novel molecularly targeted agents, developed by pharmaceutical industries, need a research driven approach to define how best to combine drugs, especially in relation to the avoidance of tumour drug resistance.

These issues are at the forefront of this project which focuses on translational research in colorectal cancer and has incorporated genetically modified mouse models of colon tumourigenesis in an attempt to address some of the difficulties facing oncologists and their patients with metastatic colorectal cancer. In particular, and as discussed (1.3.4), recent estimates report that 70% of patients' likelihood of response to EGFR targeted therapy can be predicted based on the mutational status of known mutations in *K-RAS*, *B-RAF*, *PIK3CA/PTEN* pathways, leaving a gap in our understanding of the response mechanisms determining outcome to EGFR targeted therapy. Here it is hoped data from *Apc^{min/+}* mouse colon tumours will be useful in expanding our understanding and identification of new putative biomarkers capable of predicting treatment responses to EGFR targeted therapy in *K-RAS* wild type colorectal cancer.

Patients with metastatic colorectal cancer in the absence of *K-RAS* mutations receive EGFR targeted therapy, but will inevitably develop drug resistance. In order to model tumour resistance *in vivo*, the *Apc^{min/+}* mouse has been exposed to Egfr blockade to explore activated pathways of potential importance. The Igf-1 receptor pathway is specifically investigated as a potential resistance mediator of EGFR targeted therapy. In addition, the timing of molecular responses to acute Egfr blockade is examined to assess whether drug induced changes can be identified early in a treatment schedule, which would have clear benefits for personalised drug targeting. I have also explored the effect of Egfr blockade

(using gefitinib) in the *Apc^{min/+}* mouse, with and without additional antagonism of Igf1r signalling using another small molecular tyrosine kinase inhibitor, AZ12253801.

As patients with *K-RAS* mutant metastatic colorectal cancer are at a disadvantage in terms of EGFR monoclonal antibody treatment (1.3.4), novel targeted therapy is explored *in vivo*, using conditional transgenic mouse models of colon cancer (*AhCre^{T/+} Apc^{fl/+} K-ras^{v12/+}*) harbouring the same mutations seen in human colorectal cancer. Given that tumours carrying mutant *K-ras* alleles will have constitutive pathway activation of Raf/Mek/Erk signalling, AZD6244, an inhibitor of Mek, is explored as a new therapeutic option.

Finally, in order to investigate new options of therapy which build upon the benefits of targeted EGFR monotherapy, *Apc^{min/+}* mice have been exposed to Egfr inhibition combined with a BH-3 mimetic, ABT-737. The acute anti-tumour phenotypic changes in response to the drug combination may support longer term studies in mice, which if positive may guide future early phase clinical trials and could build upon the success of EGFR target monoclonal antibody therapy in patient with *K-RAS* wild type advanced colorectal cancer.

The aims of this research can therefore be summarised as follows:

- To validate the *Apc^{min/+}* mouse as a useful model of *K-ras* wild type colon cancer.
- To define putative predictive biomarkers of response to Egfr targeted therapy in *K-ras* wild type colon tumours from *Apc^{min/+}* mice.
- To relate the identified mouse transcripts to human rectal cancer transcriptome data to validate their significance in terms of patient outcomes to EGFR targeted therapy.
- To generate hypotheses regarding the biological significance of mouse transcript changes and inferences regarding their expression patterns in patients' colorectal cancer specimens in response to EGFR blockade.
- To propose novel or reinforce previously identified mechanisms of resistance to EGFR targeted therapy using the *Apc^{min/+}* mouse.
- To specifically investigate Igf1r pathway activity in *Apc^{min/+} K-ras* wild type colon polyps as a resistance mechanism to Egfr blockade.
- To test the *in vivo* proof of concept that early molecular pathway changes may be useful biomarkers for response/resistance prediction.

- To investigate inhibition of Egf and Igf-1 receptors in the *Apc^{min/+}* mouse.
- To explore the acute therapeutic potential of BH3 mimetics combined with Egfr blockade in the *Apc^{min/+}* mouse.
- To explore the immediate effect of Mek inhibition in intestinal tumours from *Apc^{min/+}* and conditional transgenic mice harbouring an endogenously activated *K-ras* mutant allele.

In summary this project uses genetically modified mouse models of colon tumourigenesis and describes their broad application in terms of biomarker discovery, target validation, therapeutic trials and modelling resistance to targeted agents.

Chapter 2

2. Materials and Methods

2.1 Animal experiments and reagents

2.1.1 Animals

Apc^{min/+} mice were in-bred on a C57BL/6 background whereas the *AhCre^{T/+}* *Apc^{fl/+}* *Kras^{+/+}* and *AhCre^{T/+}* *Apc^{fl/+}* *Kras^{V12/+}* mouse models were maintained on an out-bred background. The Min pedigree was maintained by crossing Min/+ males with B6 wild type females whereas *AhCre^{T/+}* *Apc^{fl/+}* *Kras^{+/+}* and *AhCre^{T/+}* *Apc^{fl/+}* *Kras^{V12/+}* mice were produced by mating male *AhCre^{+/+}* *Apc^{fl/fl}* *Kras^{V12/+}* with *AhCre^{T/+}* *Apc^{+/+}* *Kras^{V12/+}* females. All experimental mice were housed in colony specific cages (max 3/cage) with a 12 hr day/light cycle. Mice received expanded RM(3) diet (Special Diet Services) and tap water *ad libitum*. Weaning took place at approximately 4 weeks of age at which time ear marking was also performed. All procedures that involved animals and their welfare were conducted in accordance with the institutional guidelines complying with United Kingdom national policies [Animals (Scientific Procedures) Act 1986].

2.1.2 Animal genotyping

Mice were genotyped at 6-8 weeks of age using tail tip material and re-genotyped at death to corroborate the initial genotyping. Genomic DNA was extracted using Puregene™ cell lysis solution containing 2% proteinase K (Qiagen, UK). Samples were incubated overnight at 37°C or at 55°C for three hr. Puregene™ protein precipitating solution (Gentra systems, UK) was added to the tube and inverted 3-4 times and centrifuged at full speed for 10 min. Supernatants were subsequently placed in 500µl of Isopropanol (Sigma, UK) and inverted 3-4 times followed by centrifugation at full speed for 15 min. Supernatant was removed leaving each DNA pellet to air dry for 1 hr prior to the addition of 500µl of nuclease free water. Extracted genomic DNA was used for subsequent PCR and the reagents for a single reaction are detailed in table 2.1.

Reagent	Quantity
5x GoTaq Reaction buffer	10 μ l
MgCl ₂ (25mM)	5 μ l
dNTPs (25mM)	0.4 μ l
Primer (100 μ M)	0.1 μ l (of each)
GoTaq DNA polymerase (5u/ μ l)	0.2 μ l
Template DNA	2.5 μ l
Nuclease-free water	To total 50 μ l

Table 2.1 Reagents included in each PCR genotyping reaction (reagents supplied by Promega except primers [Sigma-Genosys] and water [Sigma-Aldrich])

The primer sequences used to genotype animals were designed using primer 3 software (<http://frodo.wi.mit.edu/primer3/>) or from previous publications. The primer sequences, genotyping PCR conditions and expected PCR products for each reaction are detailed in table 2.2.

Each PCR product (20 μ l) was loaded into either 2% or 4% TBE/agarose gels (2.11.1) immersed in 1X TBE running buffer and electrophoresed at 120 volts for approximately 30 min. The addition of safe-view nucleic acid stain (NBS biological, UK) to gels made it possible to view bands using a contained UV light source (BioRad GelDoc 2000). Bands were identified based on size with reference to a 100bp DNA ladder (Promega).

2.1.3 Animal experiments

2.1.3.1 Materials for injection

2.1.3.1.1 Gefitinib

Gefitinib (AstraZeneca, Alderley Edge, UK) is a synthetic anilinoquinazoline compound (4-[3-chloro-4-fluoroanilino]-7-methoxy-6-[3-morpholinopropoxy]quinazoline) that displays selective reversible inhibition of the EGF receptor by competitive inhibition of the tyrosine kinase domain ATP binding site¹³¹. The drug was suspended in purite water containing either 0.5% or 1% Tween⁸⁰ (Sigma Chemical Co., St. Louis. MO.) and dosed at 75mg/kg via the intra peritoneal route¹³². Gefitinib is a potent sub-micromolar inhibitor of

Table 2.2 Primers used to genotype experimental mice, PCR conditions and expected products

Allele detected	Primer sequences (5'-3')	PCR program	Product size
<i>Apc</i> floxed	(1) GTT CTG TAT CAT GGA AAG ATA GGT GGT C	94°C, 2min (94°C, 1min; 55°C, 1min; 72°C 2min) ³⁵ 72°C, 10min	wt 226bp
	(2) CAC TCA AAA CGC TTT TGA GGG TTG ATT C		targeted (<i>Apc</i> ^{580s}) allele 314bp
<i>AhCre/LacZ</i>	CRE (1) TGA CCG TAC ACC AAA ATT TG	95°C, 3 min (95°C, 30s; 55°C, 30s; 72°C 1min) ³⁰ 72°C, 5min	CRE 1000bp
	CRE (2) ATT GCC CCT GTT TCA CTA TC LACZ (1) CTG GCG TTA CCC AAC TTA AT LACZ (2) ATA ACT GCC GTC ACT CCA AC		LacZ 500bp
<i>Kras</i> ^{v12}	(F1) AGG GTA GGT GTT GGG ATA GC	94°C, 5min (94°C, 1min; 60°C, 1min; 72°C, 1min 25s) ³⁰ 72°C, 10min	wt 403bp
	(Rmt) CTG CTC TTT ACT GAA GGC TC (Rwt) CTC AGT CAT TTT CAG CAG GC		targeted <i>Kras</i> allele 621bp
<i>Apc</i> ^{min}	(1) TCT CGT TCT GAG AAA GAC AGA AGC T	94°C, 2min (94°C, 1min; 60°C, 1min; 72°C, 1min) ³⁰ 72°C, 10min	HindIII digest of PCR product Min allele 144bp, wt 123bp
	(2) TGA TAC TTC TTC CAA AGC TTT GGC TAT		(4% Gel)
<i>Mom</i>	(1) GCT TGC TTT AGG AGT GTG CC	94°C, 2min (94°C, 45s; 60°C, 45s; 72°C, 1min) ³⁰ 72°C, 5min	B6 194bp
	(2) TAT TTG CTC TCC ATT TCC CC		C3H 164bp
<i>Responder</i>	(1) AGG TTC CCT GGG ACT TGT TT	94°C, 5min (94°C, 20s; 57°C, 20s; 72°C, 30s) ³⁰ 72°C, 5min	Responder 196bp
	(2) TCA CCA AAC CCT CCA TCA GT		Non responder 178bp (4% Gel)

References for primer sequences (i) Shibata, H *et al.* Science Vol 278 pp. 120-3, 1997. (ii) Guerra, C *et al.* Cancer Cell Vol 4 pp. 111-20, 2003. (iii) Ireland, H *et al.* Gastroenterology Vol 126 pp1236-46, 2004. (iv) Luongo, C *et al.* Cancer Res Vol 54 pp5947-52, 1994. wt, wild type.

EGFR tyrosine kinase in vitro (IC_{50} 0.033 μ M) with activity against ErbB2 tyrosine kinase 100 fold less (IC_{50} >3.7 μ M)¹³³ than that against EGFR. It does not inhibit the activity of Raf, MEK-1 and ERK-2. C_{max} for a single 100mg/kg oral dose of gefitinib in LoVo xenographs was 2.5 (μ g/ml)¹³³ whereas the half-life of gefitinib has been calculated as 3.1-3.3 hr in plasma, in a range of tumour xenografts following oral gefitinib at a dose level of 50mg/kg¹³⁴. The fraction of the total amount of gefitinib eliminated per unit of time (elimination rate constant, Kd) using a mouse glioblastoma xenograft was estimated at 0.85 per hr¹³⁵. In mouse studies doses extending to 200mg/kg/day have been well tolerated for up to 42 days (Investigators brochure). In a human LoVo xenograft model oral gavage of gefitinib 100mg/kg once daily resulted in a 40% inhibition of tumour growth¹³³.

2.1.3.1.2 AZ12253801

AZ12253801 (AstraZeneca, Alderley Edge, UK) is a potent and selective small molecule inhibitor of the kinase domain of IGF-1R and was suspended in 1% Tween⁸⁰ and dosed at 12.5mg/kg via the intra-peritoneal route. *In vitro* activity of AZ12253801 has demonstrated inhibition of IGF-1R: IC_{50} 2nM; inhibition of IR phosphorylation: IC_{50} 45nM; inhibition of IGF-driven proliferation: IC_{50} 20nM; inhibition of EGF-driven proliferation: IC_{50} 250nM. *In vivo* anti-tumour activity has been demonstrated at oral doses ranging from 6.25mg/kg/day to 25mg/kg/day. A dose of 25mg/day generates significant anti-tumour activity and also begins to effect blood glucose levels; 12.5mg/kg administered twice daily (12 hr apart) maintains glucose homeostasis (Investigators brochure). A single oral dose of AZD12253801 dose at 12.5mg/kg has a peak plasma concentration (C_{max}) at 2 hr of 6.13 μ M (Personal communication, Roger Ferguson, Astra Zeneca). The conserved nature of the ATP-binding cleft of IGF-1R and the IR has made development of small molecule inhibitors specific for the IGF-1R over the IR a significant challenge¹³⁶.

2.1.3.1.3 ME1

ME1, a rat monoclonal antibody targeting mouse Egfr (ImClone systems, New York) was administered at a dose of 1mg (in 100 μ l of 1xPBS) by the intra-peritoneal route¹³⁷. This dose has been shown to suppress phosphorylation of Egfr in regenerating murine hepatocytes¹³⁷.

2.1.3.1.4 AZD 6244

6-(4-Bromo-2-chloro-phenylamino)-7-fluoro-3-methyl-3H-benzimidazole-5-carboxylic acid (2-hydroxy-ethoxy)-amide or AZD 6244¹²⁵, is a potent selective ATP uncompetitive inhibitor of MAPK/ERK kinase 1/2 and demonstrates increased sensitivity against tumour cells harbouring mutations in *B-RAF* or *K-RAS*¹²². AZD 6244 was dosed at 30mg/kg in 0.5% hydroxypropyl methyl cellulose (Sigma) plus 0.1% Tween⁸⁰ vehicle¹³⁸ via intra-peritoneal injection or oral gavage. Pharmacokinetic data from a phase I study¹³⁹ demonstrates a C_{max} value of 528ng/ml and $t_{1/2}$ range of between 6.6-8.7 hr following oral dosing (50mg/kg).

2.1.3.1.5 ABT-737

ABT-737 (Abbott Laboratories) is a BH-3 mimetic capable of inhibiting anti-apoptotic proteins¹²⁹. Based on *in vivo* experiments showing SCLC xenograft anti-tumour activity, a dose of 75mg/kg was chosen for acute experiments to assess pharmacodynamic effects. The drug was suspended in a mixture of 30% propylene glycol, 5% Tween80 and 65% D5W (5% dextrose in water) (Personal communication, Alex Shoemaker). ABT-737 binds with high affinity to ($K_i \leq 1nM$) to Bcl-X_L, Bcl-2 and Bcl-w, but not to the less homologous proteins Bcl-B, Mcl-1 and A1 ($K_i = 0.46 \pm 0.11\mu M$, $> 1\mu M$ and $> 1\mu M$ respectively)¹²⁹. The median inhibitory concentration $IC_{50} = 35 \pm 1 nM$ and $103 \pm 2 nM$ for Bcl-X_L and Bcl-2 respectively¹²⁹. A single 10mg/kg i.p dose of ABT-737 has a half life of 2.9 hr and C_{max} of 0.52 $\mu g/ml$ (Emma Arriola, Abbott Laboratories)

2.1.3.1.6 Vehicle injections

Control (vehicle) injections 0.5% Tween⁸⁰, 1% Tween⁸⁰, 0.5% Hydroxypropyl methyl cellulose in 0.1% Tween⁸⁰ and 30% propylene glycol/5%Tween80/65%D5W were dosed according to the volume administered for the active drug counterpart. 1x PBS was dosed at a fixed volume of 100 μl .

2.1.3.1.7 β -naphthoflavone

Induction of the *Ah* promoter (and *Cre* activity) was initiated by 3 intra-peritoneal injections of 80mg/kg β -naphthoflavone (Sigma, UK) dissolved in corn oil (Sigma, UK) over 24

hr¹¹⁴ between 10-12 weeks of age. All drugs were administered using 1ml x 29G insulin needles (B&D insulin needles, Medisave, UK). Bromodeoxyuridine (BrdU, GE Healthcare) S phase cell labelling experiments were undertaken using a single i.p. dose of 200µl 2 hr before death.

2.1.3.2 Acute drug exposure

2.1.3.2.1 Gefitinib and ME1

Single test doses of the drugs and vehicle used were administered by intra-peritoneal injection in *Apc*^{min/+} mice to check for adverse effects and safety prior to conducting study experiments. Subsequently *Apc*^{min/+} mice with an intestinal tumour burden indicated by pale feet with or without rectal bleeding, piloerection or hunching were chosen for drug exposure. In acute gene expression experiments *Apc*^{min/+} mice were exposed to gefitinib 75mg/kg or 0.5% Tween⁸⁰ and culled after a series of time points (0, 4, 8, 12 and 24 hr; further detail see 2.3.2.1). Similarly to probe gene expression and/or protein changes, *Apc*^{min/+} mice with an intestinal tumour burden were exposed to either ME1 1mg (or 1x PBS control) for 4 hr or gefitinib 75mg/kg (or 0.5% Tween⁸⁰) for 8 hr prior to cull (2.3.2.2 and 2.5.6.2). To probe gene expression changes in *AhCre*^{T/+} *Apc*^{fl/+} *Kras*^{+/+} and *AhCre*^{T/+} *Apc*^{fl/+} *Kras*^{v12/+}, mice with an intestinal tumour burden were exposed to an intra-peritoneal dose of gefitinib (75mg/kg) and culled after 4 hr.

2.1.3.2.2 ABT-737

To examine the effects of ABT-737, *Apc*^{min/+} mice with an intestinal burden were administered either a single intra-peritoneal 75mg/kg dose of ABT-737, ABT-737 vehicle (30% propylene glycol/5% Tween80/65%D5W, dosed as for active drug), gefitinib 75mg/kg in 0.5% Tween80 or ABT-737 75mg/kg in combination with gefitinib 75mg/kg in 0.5% Tween80. Mice were culled after a four hr drug exposure period. Gefitinib in these experiments was purchased commercially in keeping with material transfer agreements.

2.1.3.2.3 AZD 6244

In AZD 6244 experiments *Apc*^{min/+} or *AhCre*^{T/+} *Apc*^{fl/+} *Kras*^{+/+} and *AhCre*^{T/+} *Apc*^{fl/+} *Kras*^{v12/+} mice with a tumour burden were dosed at 30mg/kg in 0.5% Hydroxypropyl

methyl cellulose in 0.1% Tween⁸⁰ or administered vehicle (0.5% Hydroxypropyl methyl cellulose in 0.1% Tween⁸⁰) at an equivalent volume and culled following 4 or 24 hr exposure.

To assess the early pharmaco-dynamic effects of respective drugs on tumour cell death, cell proliferation, immune-reactive staining and signalling pathway protein changes, at least 3 mice (unless otherwise stated) were used to obtain appropriate tumour tissue.

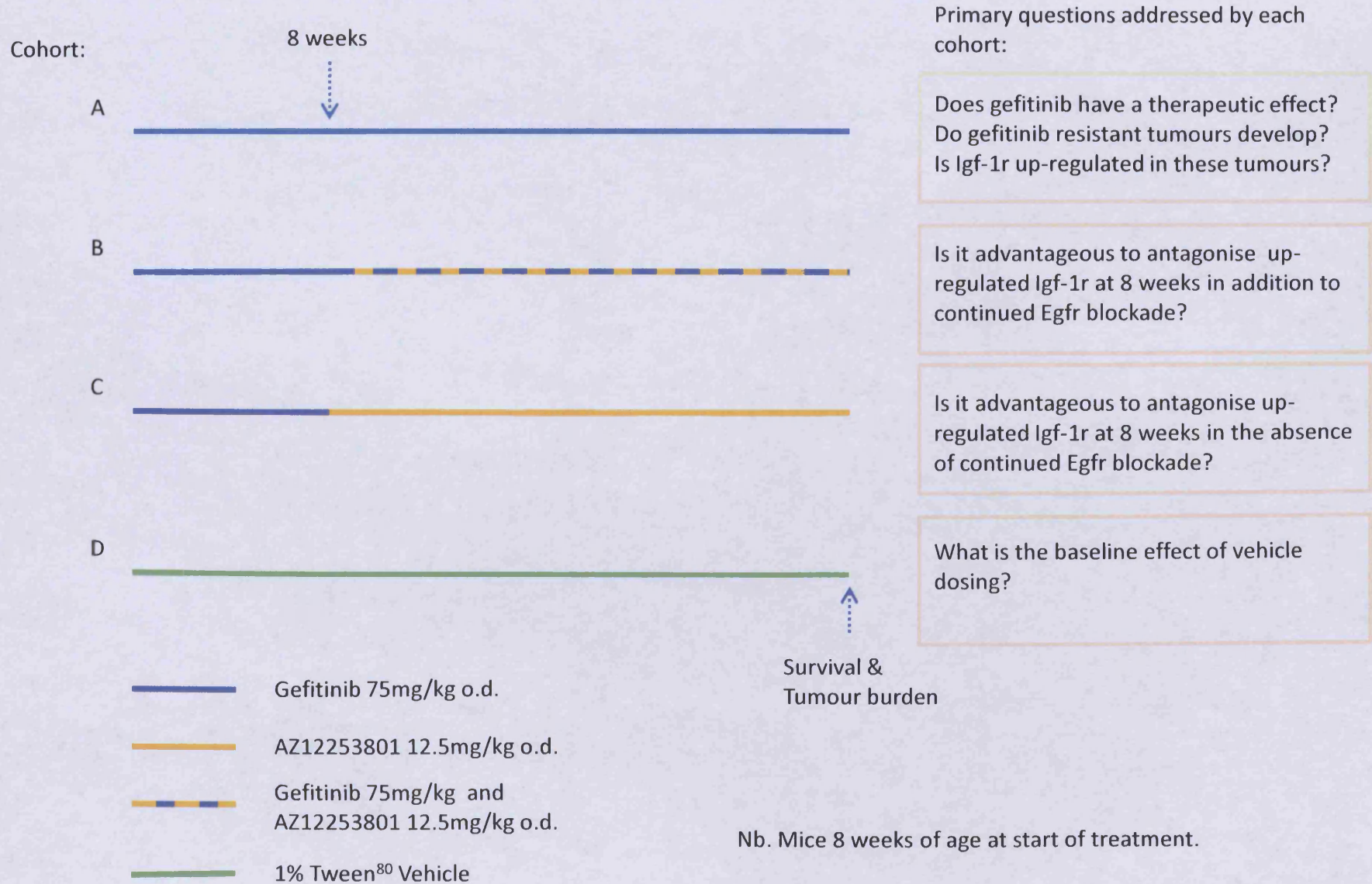
2.1.3.3 Chronic drug exposure

Initial pilot studies were performed to examine:

- 1) Long term tolerance and effect of once daily intra-peritoneal injections of gefitinib 75mg/kg and 0.5% Tween⁸⁰ vehicle in 7 *Apc^{min/+}* mice.
- 2) Acute tolerance of a single 25mg/kg intra-peritoneal injection of AZ12253801 in 3 *Apc^{min/+}* mice (for blood sugar levels).
- 3) Long term tolerance of twice daily intra-peritoneal injections of AZ12253801 12.5mg/kg (8 hr apart) in 3 further *Apc^{min/+}* mice.

This data was used to help determine the chronic dosing schedules for experimental mouse cohorts exposed to vehicle, gefitinib, AZ12253801 and combined gefitinib/AZ12253801. Each cohort included 15 *Apc^{min/+}* mice (range 15-17) to assess long term once daily intra-peritoneal administration of gefitinib 75mg/kg, 1% Tween⁸⁰, AZ12253801 12.5mg/kg and combination gefitinib 75mg/kg with AZ12253801 12.5mg/kg. Each mouse cohort (except vehicle controls, cohort D) was exposed to once daily i.p. gefitinib (75mg/kg) for eight weeks to allow the development of gefitinib resistant intestinal tumour clones. Cohort (A) continued once daily gefitinib thereafter dosed at 75mg/kg; Cohort (B) continued once daily gefitinib 75mg/kg after 8 weeks treatment with the addition of once daily i.p. AZ12553801 dosed at 12.5mg/kg (combination); Cohort (C) stopped gefitinib following 8 weeks treatment and started once daily AZ12553801 as a single agent dosed at 12.5mg/kg and finally Cohort (D) received continuous once daily i.p. injections of vehicle 1% tween⁸⁰ from the outset, dosed according to body weight (fig 2.1). Body weights were recorded weekly (or daily if concern over welfare) and drug doses adjusted accordingly. The primary endpoint of the study was the development of tumour burden as

Figure 2.1 Chronic dosing strategy to examine antagonism of the Igf-1r in the context of *Apc^{min/+}* gefitinib resistant intestinal tumourigenesis



evidence by pale feet. However mice which developed a hunched posture or loss of $\geq 10\%$ of their starting body weight were also culled immediately and included in the final analysis.

2.1.3.4 Animal dissection and tissue preparation

Mice with an intestinal tumour burden indicated by pale feet with or without rectal bleeding, piloerection or hunching were culled by cervical dislocation following drug administration (2.1.3.2 and 2.1.3.3). Following midline excision, small and large intestines were identified, removed and flushed using cold tap water. The large bowel was incised along the mesenteric border to open the luminal surface to permit resection of colon polyps proximal to any polyps related to rectal prolapse. Colon polyps were immediately placed into a 5ml tube containing RNAlater™ (Sigma-Aldrich, UK) or a 1.5ml eppendorf tube and snap frozen in liquid nitrogen for storage at -80°C . The small intestine was sectioned in the transverse plane at three 1 cm intervals, 10cms distal to the gastro-duodenal junction and placed in a fixing parcel of 3M surgical tape prior to overnight fixation in 10% formalin along with any organs of interest (e.g. colon polyps or skin samples). The remaining small intestine and large intestine was placed on Whatman paper and sectioned along the mesenteric border to open the luminal surface to facilitate fixation using methacarn solution overnight (Methanol: Chloroform: Acetic acid; 4:2:1, Fisher Scientific). Small and large intestine tumour counts, size measurements and location were recorded prior to rolling gut tissue into a Swiss roll, securing and placing in 96% ethanol prior to paraffin embedding (2.7.1).

Experiments exposing $Apc^{min/+}$ or $AhCre^{T/+}$ $Apc^{fl/+}Kras^{+/+}$ and $AhCre^{T/+}$ $Apc^{fl/+}Kras^{v12/+}$ with an intestinal tumour burden to short term ABT-737 or AZD 6244 or appropriate vehicle were similarly dissected and included skin samples (AZD 6244 experiments) fixed overnight in 10% formalin

2.2 Patients' tumour specimens

2.2.1 Xerxes trial

The Xerxes study is examining the role of early neo-adjuvant and synchronous cetuximab therapy in pre-operative chemo-radiotherapy using Xeloda followed by excisional

surgery (<http://public.ukcrn.org.uk/search/StudyDetail.aspx?StudyID=1680>). This study provided rectal cancer biopsies at baseline and 4 hr following the first intravenous infusion of cetuximab (400mg/m²) for triplePrep extraction of gDNA and RNA (2.5.3 and 2.5.4) and histological assessment by a consultant histopathologist to estimate the percentage of tumour contributing to each rectal biopsy specimen. Given the availability of tumour tissue 4 hr after cetuximab exposure, mouse experiments were designed to incorporate a similar exposure time to Egfr blockade to maximise the translational relevance. Tumour sample gDNA was screened for *K-RAS* and *B-RAF* mutations (2.8) and RNA processed as described (2.3.2.5) to search for transcripts of interest.

2.3 RNA handling and processing

Extreme care was taken when handling RNA to minimise the risk of RNase contamination and degradation of samples. Disposable powder-free gloves were used when handling samples, and changed frequently. RNase-free sample tubes, filter tip pipettes and reagents were used. All laboratory surfaces were regularly wiped with RNaseZap decontamination solution (Ambion) to decontaminate work areas. RNA samples were stored at -80°C. Samples were prepared in parallel whenever possible and master mixes made to minimise variability.

2.3.1 Extraction of RNA

RNA from colon polyps was obtained using standardised phenol-chloroform extraction facilitated by Precellys (Bertin technologies, Fr) homogenisation. Individual polyps were retrieved from RNAlater™ and washed in DEPC treated water prior to being placed in 2ml homogenisation tubes containing ceramic beads and 1ml Trizol™ reagent (Invitrogen, UK). Samples were homogenized for 45 sec (x2) and then immediately placed on ice prior to being centrifuged for 10 min at 13000 x g. Supernatants from each sample were then placed on ice in new 1.5ml eppendorf tubes and incubated for 15 min with 200µl chloroform and gently agitated occasionally. Following this, samples were centrifuged for a further 10 min at 13000 x g to permit separation of the supernatant which was removed and placed into fresh 1.5ml eppendorf tubes. 500µl of absolute Propanol-2-ol was added, mixed

and left to incubate overnight at 4°C. Samples were then centrifuged at 13000 x g for 15 min and supernatant removed to leave an RNA pellet which was re-suspended in 100% ethanol and centrifuged at 13000 x g for a further 8 min. Finally, the supernatant was removed and discarded and each pellet allowed to air dry for 5 min at room temperature prior to the addition of 50µl of molecular biology grade water (Sigma). Samples were heated to 65°C for 5 min to ensure RNA was in solution.

Qiagen RNeasy™ Kits were used to purify each RNA sample and also permit on column DNAase (DNase set, Qiagen, UK). The purification protocol required each sample to be adjusted to a total volume of 100µl using molecular grade water (Sigma). 350µl of RLT buffer was added to each sample and mixed by inverting the tube. 250µl of molecular grade ethanol (96%) was next mixed gently into each sample and the contents transferred to an RNeasy Mini spin column and centrifuged for 15 sec at 8000 x g. The flow through was discarded. On-column DNase required the preparation of DNase I stock by dissolving 1500 Kunitz units in 550µl of RNase-free water. 350µl of Buffer RW1 was added to the spin column of each sample and centrifuged for 15s at 8000 x g to wash the column. Following discarding the flow through 10µl of DNase stock solution was added to 70µl of Buffer RDD and then mixed gently prior to adding 80µl directly to each spin column and left to incubate on the bench top for 15 min. 350µl of Buffer RW was added to each spin column and again centrifuged for 15 sec at 8000 x g. Having discarded the flow through 500µl of buffer RPE was added to each spin column and centrifuged for 15 sec to wash the column. A further 500µl of buffer RPE was added to each spin column and centrifuged for 2 min at 8000 x g to ensure drying of the membrane and to avoid ethanol being carried over during RNA elution. Finally 30µl of RNase free water was added directly to each spin column before centrifugation for 1 min at 8000 x g to elute RNA. This final step was repeated using the eluate from the previous step to increase RNA concentrations.

RNA extraction from *AhCre^{T/+}Apc^{+/-}Kras^{+/+}* and *AhCre^{T/+}Apc^{+/-}Kras^{v12/+}* autochthonous mouse colon polyps and human rectal cancer specimens was done using the illustra triplePrep kit (GE Healthcare, UK).

2.3.1.1 RNA quantification and quality

Spectrophotometric analysis (NanoDrop ND-3300 Fluorospectrometer) at 260nm and 280nm was used for quantification and purity assessment of the eluted RNA. High quality RNA was judged to have an $A_{260/280nm}$ ratio between 1.9 and 2.1. The integrity of RNA was also assessed by electrophoresis using a non-denaturing 1% Tris-acetate-EDTA (TAE)/Agarose gel stained with ethidium bromide to visualise 28S and 18S ribosomal RNA (rRNA). Intact RNA had sharp and clear 28S and 18S rRNA bands with a ratio of approximately 2:1.

2.3.2 Pooling RNA samples.

2.3.2.1 Microarray

For each Affymetrix GeneChip, RNA was pooled from 10 polyps (range 6-11) obtained from at least 1 mouse. As arrays were run in triplicate a minimum of 6 mice were required for each time point (0, 4, 8, 12, 24hours) and treatment (vehicle or gefitinib). Individual polyps contributed an equivalent amount of RNA to give 10 μ g total pools of RNA for each array. In total 49 mice were used to obtain sufficient polyps for each treatment time point; n=7 at time 0 hr, n=7 at time 4 hr, n=11 at time 8 hr, n=11 at time 12 hr and n=13 at time 24 hr (appendix 2.1).

RNA used for microarrays was also used in qRT-PCR to test the accuracy of the array predictions. For this a selection of the time-series fold changes induced by gefitinib were chosen with reference to gefitinib at baseline (time zero). To undertake this 1 μ g aliquots of RNA were pooled as follows: time-zero (immediately following gefitinib injection) 18 polyps (n=4 mice), 4 hr post gefitinib 28 polyps (n=3 mice), 12 hr post gefitinib 30 polyps (n=7 mice) and 24 hr post gefitinib 30 polyps (n=7 mice) (appendix 2.1). Aliquots of RNA from each the time points were used in qRT-PCR.

2.3.2.2 Biological replicates for qRT-PCR

To validate gefitinib induced transcript changes identified by the microarray analysis at 4 hr, polyp RNA for qRT-PCR was obtained from biological replicate mouse experiments. RNA from 30 polyps and 24 polyps was obtained for gefitinib (4 hr; n=3 mice) and vehicle (4 hr; n=5 mice) treated mice respectively. Similarly to explore the transcript changes induced by a monoclonal antibody against the Egfr, *Apc*^{min/+} mice were administered ME1 (1mg; n=5)

or 1XPBS (100µl; n=7) and culled 4 hr post dosing giving 30 polyps for each treatment (appendix 2.2). RNA was extracted as described (2.3.1). For each of the experimental approaches equivalent amounts of RNA from each individual polyp were pooled prior to reverse transcription reactions to produce cDNA for qRT-PCR.

2.3.2.3 Chronic gefitinib induced transcripts

To examine the relationship between transcript changes in colon polyps following acute and chronic gefitinib exposure, RNA was extracted from *Apc^{min/+}* mice exposed to chronic vehicle and chronic gefitinib (75mg/kg/day) until the development of an intestinal tumour burden requiring cull (2.1.3.3). 10 polyps were extracted from n=2 and n=3 mice respectively for vehicle and gefitinib treated mice (appendix 2.3), and 1µg aliquots of RNA were pooled for each experimental cohort prior to reverse transcription for qRT-PCR.

A small pilot study was undertaken prior to the above in 7 *Apc^{min/+}* mice exposed to long term gefitinib 75mg/kg/day (2.1.3.3) to examine tolerance and transcript expression of *Igf1r* in colon polyps upon the development resistant disease. Nine polyps were available from 2 mice treated with 0.5% Tween 80 vehicle and 9 polyps from 3 mice treated with gefitinib. Again 1µg of RNA from each polyp contributed to each experimental RNA pool.

2.3.2.4 Transcripts from autochthonous mouse models

RNA was extracted using the illustra triplePrep kit (2.5.4) from individual colon polyps from autochthonous *AhCre^{T/+}Apc^{+/-}Kras^{+/+}* and *AhCre^{T/+}Apc^{+/-}Kras^{v12/+}* mouse models exposed to gefitinib 75mg/kg for 4 hr. RNA was pooled according to *K-ras* mutation status with each polyp contributing 1µg of RNA prior to subsequent reverse transcription for qRT-PCR. As detailed (appendix 2.4) 10 polyps were available from *Apc^{+/-}Kras^{+/+}* mice (n=2) and *Apc^{+/-}Kras^{v12/+}* mice (n=3) treated with gefitinib.

2.3.2.5 Human rectal cancer specimen transcripts

Paired rectal cancer specimens (Xerxes trial 2.2.1) obtained at baseline and following 4 hr exposure to cetuximab (a monoclonal antibody against the EGF receptor) were washed in DEPC treated water prior to RNA extraction using the illustra triplePrep kit (2.5.4).

Samples were *not* pooled to allow individual comparison of transcripts from patients' tumours between the paired tissues (appendix 2.5).

2.3.3 Reverse transcription

1µg of DNased total RNA (from individual RNA samples or RNA pools) was used in the reverse transcription reaction to synthesise cDNA for qRT-PCR. The total volume was adjusted to 9µl by the addition of an appropriate volume of RNase free water (Sigma) and samples were heated to 70°C for 10 min and then allowed to equilibrate at 42°C for 1-2 min. 10µl of a stock solution containing the necessary constituents for the reverse transcription reaction (table 2.3) was freshly prepared and added to each sample including 1µl (200u/µl) of SuperScript™ II Reverse transcriptase (Invitrogen, UK). Negative control (-ve RT) samples excluded SuperScript II. Samples were then incubated for 50 min at 42°C. The reverse transcriptase enzyme was inactivated by heating to 70°C for 15 min. Finally 200µl of RNase-free water was added to each labelled cDNA sample and stored at -20°C. The reverse transcriptase reactions were performed in a PTC-100 programmable thermal controller (MJ research, Inc.)

Table 2.3 Reverse transcription reagents

Reagent	Volume(µl) per sample	Manufacturer/catalogue#
Random primers (0.5µg/µl) (hexadeoxynucleotides)	2µl (0.1µg/µl)	Promega, Madison, WI.
5x First-strand buffer (250mM Tris-HCL, pH 8.3; 375mM KCL; 15mM MgCl ₂)	4µl	Invitrogen, UK.
0.1M DTT	2µl	Invitrogen, UK.
25mM dNTPs	0.4µl	Fermentas, York, UK.
RNase free water	1.6µl	Sigma, UK.

2.3.4 Target preparation, hybridisation and scanning of Affymetrix GeneChips

RNA samples were sent on dry ice to the Patterson Institute for Cancer Research for target preparation prior to hybridisation to the array and scanning. All the protocols are available at <http://bioinformatics.picr.man.ac.uk/vice/DesignProject.vice?pid=159>.

2.4 Real-Time Qualitative Reverse Transcription Polymerase Chain Reaction (qRT-PCR)

Real-Time Qualitative Reverse Transcription Polymerase Chain Reaction is a sensitive method for the detection of mRNA expression levels. This technique allowed cDNA obtained from the reverse transcriptase reaction to act as a template for subsequent PCR amplification using primers specifically designed to detect one or more genes of interest. The SYBR Green method was used where double-stranded DNA dye in the PCR reaction binds to newly synthesized double-stranded DNA causing the release of fluorescence which is detected¹⁴⁰. It was performed using a MJ Research PTC-200 Chromo 4 continuous fluorescence detection unit.

Individual wells in each PCR plate (Bioplastics, Netherlands) received:

8.5µl cDNA

12.5µl of DyNAmo™ HS SYBR® qPCR mix (Finnzymes, Oy.)

- Hot start version of a modified *Thermos brockianus*
- Syber green I dye
- Optimised PCR buffer
- 5mM MgCl₂
- dNTP mix including dUTPs.

4µl (1mmol) forward and reverse primer mix for gene of interest (Sigma-Genosys)

25µl total volume/well

A master mix containing the required quantity of DyNAmo™ HS SYBR® qPCR mix and cDNA for the specified number of samples was made and stored on ice prior to pipetting 4µl of appropriate primer mix to each PCR well. For each gene and time point 3 duplicates were used and gave average C_T values for three identical samples.

The qRT-PCR protocol consisted of a denaturing step of 95°C for 30 sec, followed by a 30 sec annealing temperature of 60°C and extension period of 30 sec at 72°C. An anti-dimer step of 30 sec was also included at 75°C. Forty cycles were completed prior to melting curve generation between 53°C – 95°C with plate reading every 0.2°C. Melting curve analysis for each primer pair yielded sharp peaks at the melting temperature of the amplicon and, in the absence of significant fluorescent signals from negative controls, indicated that the generated products were specific and SYBER green I fluorescence a direct measure of the gene of interest. The threshold cycle (C_T) value was determined by identifying a significant increase in fluorescent signal associated with exponential growth of PCR product. The data generated was transferred to an Excel worksheet to enable further processing and calculation of fold changes. This was done using the comparative threshold $\Delta\Delta CT$ approach¹⁴¹ which enabled the relative quantification of template. This required calculating the difference (ΔCT) between the average C_T values of the target and endogenous housekeeping reference gene (B-actin or Gapdh) for triplicate paired samples. The average ΔCT value once calculated was then used to obtain the $\Delta\Delta CT$ value (average ΔCT control experiment - average ΔCT experimental treatment) which was then used to calculate the fold change difference by using the formula $2^{-\Delta\Delta CT}$.

2.4.1 Primer design for qRT-PCR

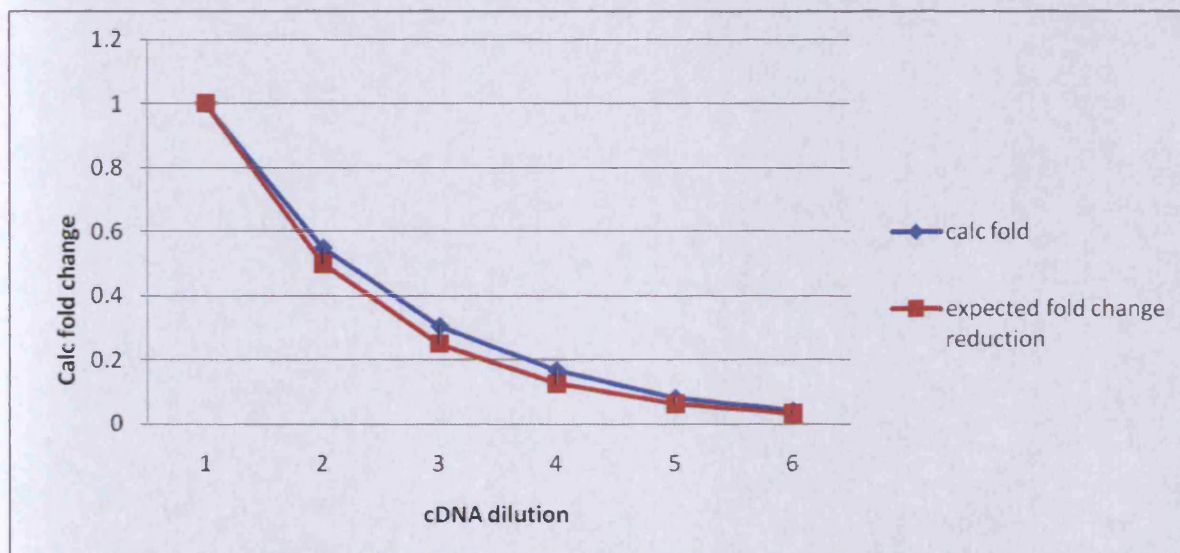
Primer design was facilitated with use of primer 3 software (<http://frodo.wi.mit.edu/primer3/>) and the mouse ensemble (<http://www.ensembl.org/index.html>) website. Primers (Sigma-Genosys, UK; table 2.4) were designed across adjacent coding exons for the gene of interest with intervening intronic sequences sufficiently large (≥ 2000 bp where possible) to impede product amplification arising from inadvertent genomic DNA contamination. Amplicons approximately 100-150 base pairs in length were produced and each primer pair was validated *in silico* using the UCSC website (<http://genome.ucsc.edu/index.html>) to ensure correct mapping to the gene

Table 2.4 Murine (5'-3') primer sequences for qRT-PCR

Gene	Forward primer sequence	Reverse primer sequence	Product size (bp)
<i>Areg</i>	CCATCATCCTCGCAGCTATT	CGAAGCCTCCTTCTTTCTTC	106
<i>Arhgef9</i>	TCAGAAGAGACAGGCTGCAA	GTTTAACGGGTCTGTGGTG	109
<i>Arid3b</i>	ACCAAAGATGCTTCCAAGG	CATCAGCATCGTCACTCCAG	115
<i>Bak1</i>	ATGGCATCTGGACAAGGAC	GCTTCGAAAGACCTCCTCTG	105
<i>Bax</i>	CCAAGAAGCTGAGCGAGTGT	CACCCGGAAGAAGACCTCTC	119
<i>Bcl-2</i>	GAGCGTCAACAGGGAGATGT	CATGCTGGGGCCATATAGTT	139
<i>Bcl-XL (BCL-2 LIKE 1 protein)</i>	AGTCGGATTGCAAGTTGGAT	GCTGCATTGTTCCCGTAGAG	110
<i>Bim (BCL-2 LIKE 11)</i>	GCGGATCGGAGACGAGTT	CAGTTGTAAGATAACCATTTGAGG	100
<i>Bmf</i>	ATCACAACCTCGGAGGCTGAG	CCTCTGACTGGAACACATCATC	102
<i>Bmp10</i>	CACAGACCGGACCTCCAT	AGGATATTTCCGGAGCCCATT	100
<i>Cbl</i>	ACGGTGGACAAGAAGATGGT	TATAAGGCGGGCTGTTCTTG	103
<i>Ccnd1</i>	AGTGCGTGCAGAAGGAGATT	AGCGGGAAGACCTCCTCTT	103
<i>Ccnd2</i>	TGATGAAGTGAACACACTCACG	AGCAGAGCTTCGATTTGCTC	111
<i>Ccne1</i>	GATGGGAAGTTCCAAGCTCA	TTCTTTGCTTGGGCTTTGTC	111
<i>Ccne2</i>	CATTCTGACCTGGAACCACA	GGGCAAGGTAAAATGTCTCC	100
<i>Cxcl10</i>	AAGTGCTGCCGTCATTTTCT	CCTATGGCCCTCATTCTCAC	129
<i>Cxcl9</i>	CGATCCACTACAAATCCCTCA	AGTCCGGATCTAGGCAGGTT	117
<i>Egfr</i>	CTGCCAGAATGTGAGCAGAG	ATTCTGGATGGCACTGGATG	110
<i>Emp1</i>	CTGGCTGGTCTCTTTGTGGT	CACCAGTGCAGTTCTTCCAA	127
<i>Epha3</i>	TTGCAATGCTGGGTATGAAG	TGGGCACTTAGCACACTTAGC	100
<i>ErbB3</i>	AATACCAACTCCAGCCATGC	TTGTATCCATGTGGCAAAGTT	112
<i>ErbB4</i>	TGGCAAGATATTGTTGGAAT	GGCCAGTGC AAGACTTATGG	100
<i>Ereg</i>	GGACGGCTACTGCTTGCAT	AGAAGTGCTCACATCGCAGA	104
<i>Fabp2</i>	ACAGTCTAGCAGACGGAACG	AGAAACCTCTCGGACAGCAA	119
<i>Gng4</i>	AGGAAAGCCGTGGAGCAG	GCACGTGGGCTTCACAGTAG	100
<i>Hbegf</i>	CAGGACTTGG AAGGGACAGA	TGAGGCATGGGTCTCTCTTC	145
<i>Hip1</i>	AGTTGGTGCTGGGATGGA	TTTCTTTTCACGGCCACTT	106
<i>Igf-1r</i>	GTGGGGGCTCGTGTTTCT	CAGCTGCTGATAGTCGTTGC	100
<i>Ikbkg</i>	CAGTTGCAGGCAGCCTATC	CTCAGCTTGCTGGAGCTGTT	108
<i>ligp1</i>	CTATGACTTCCCCGTCCTGA	TCAGAAATTGCCGCTTCTTT	125
<i>Nov</i>	TCGCCAGTGTGAGATGGTAA	ATTTCTTGGTGCGGAGACAC	113
<i>Oxtr</i>	TTCTTCGTGCAGATGTGGAG	GTTGCAGCAGCTGTTGAGG	102
<i>Phox2b</i>	GACATCTACACCAGGGAAGAGC	CCTGCTTGCGAAACTTAGCC	100
<i>Pi4kb</i>	CAAAGCTGTGCTGGCTACTG	TCGATGTGGATGATGTGACC	104
<i>Plcδ4</i>	CTGACCTCGCTCTGGAACTC	GTTTCCATCCTTCGAGCAGA	113
<i>Ptprd</i>	TATGAATGTGTGGCCTCGAA	TCAATCGTAGGGAACCCTCT	101
<i>Rassf2</i>	TGAACTTCTCCTACATCTGAAGACC	TGTTCAAGTAACCCCTCCACA	110
<i>Retnlb</i>	CGCAATGCTCCTTTGAGTCT	GTCTGCCAGAAGACGTGACA	105
<i>Ubd</i>	CACCTGTGTTGTCCGTTGAG	GAGACCTTGGTTTGGGACCT	108
<i>B-actin</i>	ACAGCT TCT TTGCAGCTCCTT	TGG TAACAATGCCATGTTCAAT	300
<i>Gapdh</i>	CACTGAGCATCTCCCTCACA	GTGGGTGCAGCGAACTTTAT	111

of interest. Each set of primers was tested using serial dilutions of cDNA to check that primer pairs and subsequent qRT-PCR accurately predicted target template quantities by plotting serial cDNA dilution against expected and calculated fold changes¹⁴¹ (e.g. fig 2.2). Negative controls for each RT-PCR reactions included water, and where possible '-ve RT' samples (RNA samples without reverse transcriptase enzyme and hence no cDNA) if sufficient RNA was available. Control samples containing genomic DNA (gDNA) were included in qRT-PCR to ensure primers were not able to amplify product originating from gDNA. The primers used for *B-actin* and *Gapdh* were designed and provided by Dr L Parry (ARC group). These two endogenous reference genes were chosen based on the absence of microarray detected fold change differences across the respective probes in response to gefitinib exposure at 4 hr. The qRT-PCR products were electrophoresed on 2.0% TAE/Agarose gels (2.11.2) and inclusion of a 100bp DNA ladder permitted confirmation of the appropriate sized primer products.

Figure 2.2. Expected and calculated fold changes ($\Delta\Delta\text{CT}$ method) for *Cbl* product using qRT-PCR primer pairs AND serial dilutions of template cDNA.



2.4.2 Human primers for qRT-PCR

Primers were designed in the same way as described for mouse primers (2.4.1) with the exception that the ensemble genome browser was referenced for human sequences (http://www.ensembl.org/Homo_sapiens/Info/Index). The primers used are outlined in

Table 2.5 Human (5'-3') primer sequences for qRT-PCR

Gene	Forward primer sequence	Reverse primer sequence	Product size (bp)
<i>BMF</i>	TCAGTGCATTGCAGACCAGT	AAGGTTGTGCAGGAAGAGGA	100
<i>CBL</i>	GACGGTGGACAAGAAGATGG	GATATAAGGTGGGCTATTCTTTAGC	106
<i>EPHA3</i>	G TTCCTGCAATGCTGGCTAT	CGGGCACTTAGCACACTTC	104
<i>ERBB3</i>	GCTGGGCTTGCTTTTCAG	GGTATTGGTTCTCAGCATCG	113
<i>HIP-1</i>	CCAGTTAACAGTGGAGATGTTTG	GCCGTCACGGACACAGAG	102
<i>IKBKG</i>	GCACCTGCCTTCAGAACAG	GCAGAATCTGGTTGCTCTGC	101
<i>GAPDH</i>	AAGGTGAAGGTCGGAGTCAAC	ATGGGTGGAATCATATTGGAAC	153

table 2.5. *GAPDH* was used as the endogenous housekeeping reference gene and qRT-PCR conditions were as described (2.4).

2.5 TriplePrep extraction (extraction of gDNA, RNA and protein)

Protein (along with genomic DNA and RNA) was extracted from individual colon polyps using the illustra™ triplePrep kit (GE Healthcare, Amersham) following the manufacturer's instructions. In essence samples were lysed (using a Precellys homogeniser) in lysis buffer 15 which contains a large amount of chaotropic salts and immediately inactivates DNase, RNase and proteases (samples were not allowed to thaw before the addition of lysis buffer). On following the protocol DNA became bound to the first column in the presence of a chaotropic solution and contaminants were removed prior to elution of DNA. The remaining flow-through contained RNA and protein. The addition of acetone bound RNA to the second column and facilitated on column DNase digestion. Following removal of contaminants RNA was eluted in appropriate buffer. Finally the remaining 'flow-through' solution contained protein which was precipitated, washed and re-suspended in 2-D DIGE buffer prior to SDS-PAGE and western blotting.

2.5.1 TriplePrep working solutions

These are described in 2.11.4

2.5.2 Sample homogenisation and lysis

Snap frozen colon polyps or polyps stored in RNA*later* solution were not permitted to thaw but immediately placed in 2ml soft tissue homogenisation tubes with 1.4mm ceramic beads (Omni Intl, US) containing 1ml of lysis buffer type 15 (+10µl 2-Mercaptoethanol) prior to homogenisation using a Precellys (Bertin technologies, Fr) machine. Samples were completely lysed after 2 separate 30sec 3D motions at 6500rpm. Following this samples were left to rest on the bench for 5 min to allow frothing to settle.

2.5.3 Genomic DNA isolation

The supernatant above was transferred by pipette into a gDNA isolation spin column housed in a 2ml collecting tubes. Each sample was centrifuged (for 1 min at 11,000 x g unless otherwise stated) and flow-through saved at room temperature for subsequent RNA

and protein isolation. The column was transferred to a new 2ml collecting tube and 500µl of wash buffer type 15 added (DNA wash 1) followed by a further spin. Flow-through was discarded. 500µl of wash buffer type 6 was added for DNA wash 2 followed by a spin and discarding of flow-through. The column was transferred to a 1.5ml eppendorf tube and 100µl of DNA elution buffer type 5 added. DNA was eluted by the final spin, samples labelled and stored at -80°C.

2.5.4 Isolation of RNA

The flow through described received 350µl of absolute acetone and was mixed by pipetting the solution up and down several times. The entire mixture was transferred to a new RNA spin-column in a new 2ml collecting tube. After a spin as above the flow-through was saved at room temperature for later protein extraction. The column was transferred to a new 2ml collecting tube and DNase treatment performed. In a separate 2ml eppendorf tube a master mix of 10µl reconstituted DNase I, 20µl of DNase reaction buffer type I and 70µl RNase free water was prepared for each sample being processed. 100µl of the diluted DNase master mix was applied directly to each sample membrane and incubated at room temperature for 10 min. Following this 500µl of wash buffer type 6 was added to the column and samples centrifuged 1 minute. The collection tube and contents were discarded and column transferred to a fresh RNase free 1.5ml eppendorf tube. 50µl of RNA elution buffer was added to the column and centrifuged to collect the purified RNA flow-through. Sample were immediately labelled and stored at -80°C.

2.5.5 Precipitation of protein

The entire flow-through described above was transferred to a new 1.5ml eppendorf tube and 600µl of protein precipitation buffer type 1 added. Samples were vortexed for 10 sec and then incubated at room temperature for 5 min to precipitate proteins. Each sample was then centrifuged for 10 min at full speed ($\geq 16,000 \times g$). Supernatants were carefully removed by decanting. 1ml of distilled water was added to the pellet and dispersed by pipetting up and down several times. The sample was then centrifuged again at full speed for 1 minute. Supernatant was removed as completely as possible (discarded) and protein re-suspended in 50µl of 2-D DIGE buffer. Samples were incubated at room temperature for 5 min prior to labelling and storage at -80°C.

2.5.6 Determination of protein concentration (2-D Quant Kit)

The 2-D Quant kit was used to accurately quantify protein samples. The procedure uses a combination of precipitant and co-precipitant to precipitate protein whilst leaving contaminants, which can otherwise interfere with protein estimation, in solution. The precipitated protein pellet is re-suspended in an alkaline solution of cupric ions which bind to the polypeptide backbone of proteins present. A colorimetric agent which binds to unbound cupric is added and therefore the resulting colour density is inversely related to the concentration of protein present in the sample. The protein concentration can be subsequently estimated by comparison to a standard curve.

2.5.6.1 Protocol

Accurate pipetting of standard curve and sample solutions is a pre-requisite for the accuracy of this assay. An appropriate volume of working colour reagent was prepared by mixing 100 parts colour reagent A with 1 part colour reagent B. Each individual assay required 1ml. Typically 24 samples would be assayed together.

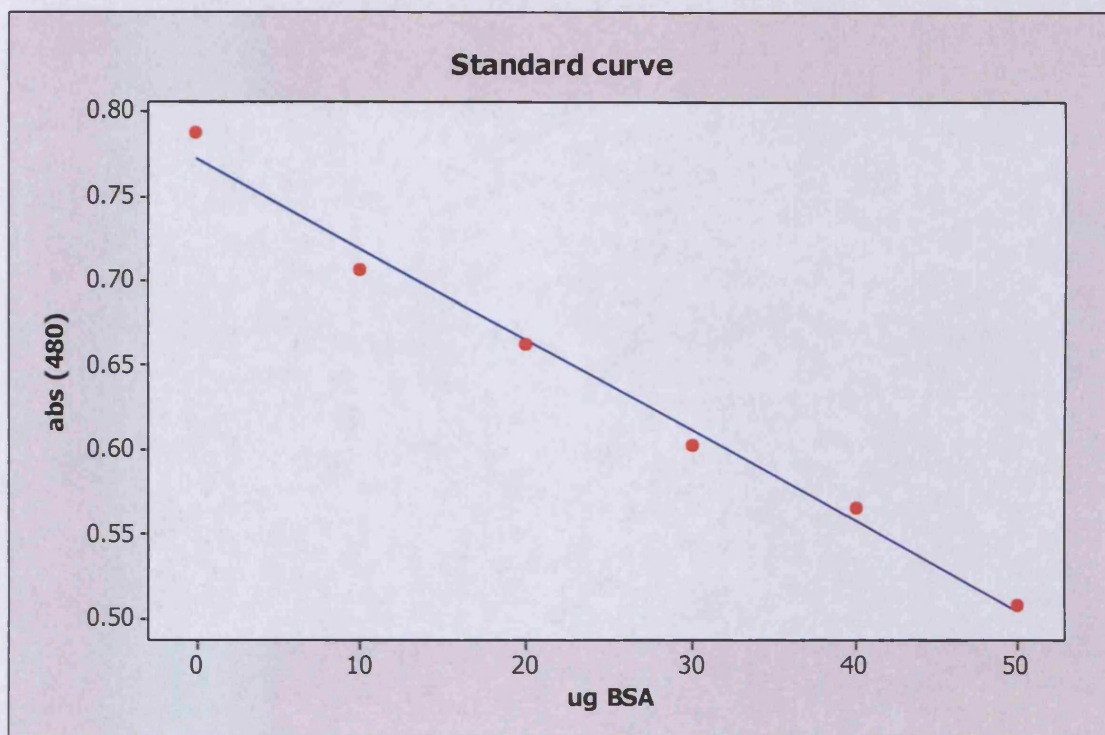
A standard curve was prepared according to the table:

Tube No.	1	2	3	4	5	6
Vol of 2mg/ml BSA standard solution	0 μ l	5 μ l	10 μ l	15 μ l	20 μ l	25 μ l
Protein quantity	0 μ g	10 μ g	20 μ g	30 μ g	40 μ g	50 μ g

Tubes containing 5 μ l of sample were prepared to be assayed. To each sample 500 μ l of precipitant was added including the standard curve tubes. Samples were vortexed briefly and incubated for 2-3 min at room temperature. 500 μ l of co-precipitant was next added to each tube and again briefly vortexed. Tubes were then centrifuged at $\geq 10,000 \times g$ for 5 min to sediment protein. Supernatant was then decanted from the protein pellet immediately following completion of centrifugation to avoid re-suspension of protein. Tubes were repositioned in the centrifuge for a short spin to help remove any remaining solution which was removed using a pipette. 100 μ l of copper solution and 400 μ l of distilled water was next added to each sample and vortexed to dissolve the precipitated protein. Finally 1ml of

working colour reagent was added to samples which were left on the bench to incubate for 20 min. The absorbance of each sample and standard was read at 480_{nm} using water as a reference. A standard curve was generated (figure 2.3) by plotting the absorbance of the standards against the quantity of protein and was used to calculate the quantity of protein in each sample.

Figure 2.3 A typical standard curve



Appendix 2.6 presents the protein quantities extracted from colon polyps from $Apc^{min/+}$ mice exposed to various drugs over short or long term experiments.

2.5.6.2 Colon polyp protein pooling

Once the protein content of each sample was determined (appendix 2.6) it was possible to pool equivalent amounts of protein from individual colon polyps (30 μ g) for different experimental treatments. Table 2.6 outlines the experimental approaches, numbers of mice and polyps obtained for pooling and subsequent western blot.

Table 2.6 Numbers of mice and colon polyps retrieved for each drug exposure time

Drug	Duration	No. mice	No. polyps
1% Tween 80	4 hr	3	19
Gefitinib (75mg/kg)	4 hr	3	26
AZ12253801 (12.5mg/kg)	4 hr	2	9
Gefitinib (75mg/kg)+ AZ12253801 (12.5mg/kg)	4 hr	3	17
1X PBS	4 hr	4	20
ME1 (1mg)	4 hr	2	20
Gefitinib (75mg/kg)	8 hr	3	22
0.5% Tween 80	8 hr	3	16
1% Tween 80	Chronic	2	7
Gefitinib (75mg/kg/day)	Chronic	3	8
AZ12253801 (12.5mg/kg/day)	Chronic	3	14

Chronic exposure refers to daily treatment until the development of tumour burden (resistant disease)

From each of the protein pools 30µg samples were used for loading SDS PAGE.

2.6 Western blotting

This technique relies upon the separation of sample proteins according to molecular weight using SDS PAGE (Sodium Dodecyl Sulphate Polyacrylamide Gel Electrophoresis) and transfer to PVDF membrane for subsequent protein interrogation, identification and estimation of quantity.

2.6.1 Sodium dodecyl sulphate polyacrylamide gel electrophoresis

The Mini-PROTEAN 3 system (Bio Rad, CA) was used to undertake gel electrophoresis. Dependent upon the size of the protein of interest resolving gels contained either 7.5% or 9.4% acrylamide content. The gel formulations are described in table 2.7

Table 2.7 Gel formulations for SDS PAGE

Reagent	Resolving gel		Stacking gel
	7.5%	9.4%	4.5%
Upper buffer	-	-	2.5ml
Lower buffer	5ml	5ml	-
Acrylamide/Bis (30%)	5ml	6.25ml	1.5ml
dH ₂ O	10ml	8.5ml	6.14ml
10% APS	200µl	200µl	100µl
TEMED	20µl	20µl	10µl

Casting gels:

Checks were made to ensure the casting stand, casting frames and glass plates were all clean and dry before starting. The Gel cassette sandwich was assembled in the casting frame and placed in the casting stand and checked for a tight seal. A comb was placed into the assembled gel cassette and a mark made 1cm below the comb teeth to note the level the resolving gel will reach when poured into the cassette. The comb was removed and the appropriate % resolving gel prepared, adding the 10% APS and TEMED to the final mixture. The monomer solution was poured to the desired mark and overlaid with a small quantity of butanol. The gel was left to set for 30 min. Once set a small piece of filter paper removed any remaining liquid on the surface of the resolving gel taking care not to disturb it. Next the stacking gel mixture was prepared again adding the 10% APS and TEMED to the final mixture and poured into the cassette sandwich until the top of the short plate was reached. Immediately the comb was carefully inserted between the spacers. The stacking gel was left to polymerise for 30 min. Once set the comb was removed and the wells rinsed with dH₂O. Next the gel cassette assembly was removed from the casting stand and the gel cassette sandwich released from the casting frame. The gel cassette sandwich was then placed behind slots on the electrode assembly and carefully loaded into the clamping frame which ensured the sandwich was clamped in place to form an inner chamber which was sealed. The inner chamber assembly was then lowered into the mini tank and 1X running buffer was poured into the inner chamber permitting overflow to reach the mid level of the gel cassette.

Sample loading:

Each sample consisted of 30µg aliquots of protein from pooled colon polyps (see 2.5.6.2) for a specific experimental approach, 0.5 volume of 10% SDS and an appropriate volume of Laemmli buffer. Samples were incubated at 70°C for 5 min and then placed on ice before gel loading. Samples were loaded in triplicate when possible. A 10-250KDa Protein marker (10µl; Bio Rad All Blue Precision Plus) was loaded into the first well of each gel.

Gel electrophoresis:

The lid was placed on the mini tank ensuring correct alignment of the colour coded banana plugs and jack. The electrical leads were connected to a power supply initially set at 50volts during migration through the stacking gel (30 min) and increased to 150volts during migration through the resolving gel (30-45 min). The reagents used and working solutions are described in 2.11.5

2.6.2 Protein transfer

Once electrophoresis was complete the power supply was turned off and electrodes disconnected. The inner chamber assembly was removed from the tank and running buffer discarded. The gel cassette sandwich was released and the two glass plates separated. The gel was removed from its glass plate by inverting both gel and plate in transfer buffer (2.11.6) and helping it float away with gentle agitation. The gel was left to equilibrate in transfer buffer for 10 min. A piece of polyvinylidene difluoride PVDF membrane (Hybond-P, Amersham) was cut to size (5cm x 8cm) and dipped in methanol before soaking in transfer buffer for 10 min. The gel was then placed on whatman paper supported by sponge (all pre-soaked in transfer buffer) and PVDF membrane was carefully positioned onto the gel forming a gel-membrane sandwich once covered by further pre-soaked whatman paper and overlying sponge. A stripette was used to roll over the sandwich to remove air bubbles. The sandwich was held together in a loading cassette and fully submerged into transfer buffer contained in a transfer tank which was kept cool by surrounding ice. The tank lid was placed onto the correct banana plugs and connected to a power supply and left to transfer at 100volts for 1.5 hr.

2.6.3 Membrane probing

2.6.3.1 Membrane incubation

Following protein transfer to PVDF membrane the latter was soaked in appropriate blocking buffer (guided by primary antibody protocol) and agitated gently on a rocking platform for 1hr at room temperature. Primary antibodies (Table 2.8) were incubated overnight at 4°C at various dilutions in the recommended blocking buffer. HRP-labelled secondary antibodies (GE Healthcare, UK) raised against the source animal primary antibody were incubated at room temperature for 1 hr at a 1:2000 dilution with blocking buffer. Membranes were washed 3 times for 5 min each using 0.1% TBST following both primary antibody and secondary antibody incubations. All buffers used in membrane incubations are described in section 2.11.7

2.6.3.2 Chemi-luminescent signal and protein identification

Once membranes were washed ECL™ standard and ECL™ Plus western blotting detection reagents (GE Healthcare, UK) were used to produce chemi-luminescent light which was detected on Fuji film and developed by Xograph imaging systems. For the ECL standard protocol 3ml of solution A and Solution B was pipetted into separate universal tubes (For ECL plus the ratio of solutions A:B was 40:1). Once in the dark room a weighing boat was used to place the PVDF membrane and solutions A and B were mixed and evenly distributed across the membrane and incubated for 1 min (5 min for ECL plus). Following this the membrane was swiftly wrapped in cling film protein side down noting the position of the protein ladder and then transferred to a developing cassette housing unexposed autoradiography film. After a series of exposure times the film was developed and viewed. The autoradiography film was viewed on a slide viewing box aligned on top of the membrane to trace its outline and help mark the location of the protein ladder. This enabled the identification of protein bands of a particular molecular weight corresponding to the protein targeted by the specific primary antibody used.

2.6.3.3 Densitometric measurements

Autoradiography films were scanned and processed using Quantiscan software v1.0 (Biosoft, kindly loaned by Dr James Matthews). Discrete blots were analysed after being defined manually and densitometric volumes reported following background subtraction.

Table 2.8 Primary antibodies used to probe protein blot membranes.

Primary Antibody	Protein molecular weight (KDa)	Source Species	Dilution	Blocking buffer	Catalogue No/Manufacturer
Akt	60	R	1/1000	B	# 9272 CST
Bmf	17	R	1/1000	B	# 4692 CST
c-Cbl	120	R	1/1000	B	# 2747 CST
Cycline E2	48	R	1/1000	B	# 4132 CST
Egfr	175	R	1/1000	B	# 2232 CST
Epha3	100	R	1/2000	M	ab52986 Abcam
ErbB3	185	R	1/500	B	# 4754 CST
Hip-1	116	Mo	1/2000	M	905-134 Assay designs
Igf-1r β	95	R	1/1000	B	# 3027 CST
Ikbkg	48	R	1/500	B	# 2685 CST
p44/42 Mapk (Erk1/2)	42/44	R	1/1000	B	# 9102 CST
Phospho-Akt (Ser473)	60	R	1/300	B	# 3787 CST
Phospho-Egfr (Tyr1068)	175	R	1/300	B	# 2234 CST
Phospho-Igf-1r (Tyr1316)	90	R	1/300	BG	AstraZeneca (MTA)
Phospho-p44/42 Mapk (Erk1/2 Thr202/Tyr204)	42/44	R	1/1000	B	# 4376 CST
Phosph-S6 (Ser240/244)	32	R	1/1000	B	#2215 CST
ribosomal protein Plcd4	90	R	1/200	M	sc-30063 SCB
S6 ribosomal protein	32	R	1/1000	B	#2217 CST
Tubulin	55	Rat	1/2000	M	ab6160 Abcam
β actin	42	Mo	1/12500	M	A2228 (AC-74 clone) Sigma

B. 5% BSA in 0.1% TBST

M. 5% Milk in 0.1% TBST

BG. 3% BSA:2% NGS in 0.1% TBST;

BSA bovine serum albumin; NGS normal goat serum.

R rabbit; Mo mouse

CST Cell Signalling Technology ,MA; SCB Santa Cruz Biotechnology Inc., CA

Sigma-Aldrich Co., UK; Assay Design Inc., MI

MTA Material transfer arrangement.

For each densitometric volume a normalised value was calculated with reference to the loading control and subsequent average densitometric values produced across duplicate or triplicate samples. Averaged densitometric values were obtained for each experimental approach and compared accordingly. Phosphorylated proteins were expressed as the total amount rather than as a proportion of the total protein in question.

2.7 Histology

2.7.1 Preparation of tissue for light microscopy

Fixed tissue samples were paraffin processed on a Leica TP 1050 fully enclosed automatic tissue processor using the following schedule:

70% Ethanol 1hr

90% Ethanol 1hr

100% Ethanol 1.5hr

100% Ethanol 2hr

100% Ethanol 2hr

This was followed by 2x 60 min washes in xylene to clear and replace the alcohol. The samples were infiltrated with paraffin wax at 60°C in 3 separate intervals overnight to replace xylene (60 min, 90 min x2; with the last 2 infiltrations under vacuum). Each sample was embedded in paraffin wax using a Leica EG1140H embedding centre. Sections were cut to a thickness of 5µ with a Leica RM2235 rotary microtome and floated on warm water and mounted on polysine microscope slides (Thermo Scientific, UK) prior to be dried overnight at 45°C. Slides were stained for Haematoxylin and Eosin (H+E) using an RA Lamb Histomate staining machine (see protocol in appendix 2.7). Sections were mounted under a cover glass using DPX mountant. All reagents and consumables were obtained from Thermo Fisher Scientific.

2.7.2 Immuno-histochemical staining

Histological sections (5 μ thickness) obtained from formalin or methacarn fixed/paraffin embedded tissues were initially washed in xylene (5 min x2) to de-wax. Sections were then rehydrated by sequential bathing in 100% ethanol (2 min), 95% ethanol (2 min x2), 70% ethanol (2 min) and finally distilled water prior antigen retrieval. At no point were slides allowed to dry. The primary antibodies used for immuno-histochemistry and the peculiarities of each protocol are summarised in table 2.9. Slides underwent epitope retrieval in 1litre of the appropriate buffer solution which was pre-heated in a microwave (900W) until boiling (10 min). Slides placed in plastic racks were immersed into a pressure cooker chamber before sealing the lid and brought up to pressure by heating for 5-10 min in a microwave (900W) until the yellow pressure indicator became elevated. At this point the microwave power was reduced to 300W and left to heat for a further 15 min. On completion the pressure cooker was removed and left to cool on the bench top for 30-60 min.

The general schema for the immuno-histochemical stain process is outlined in table 2.10 with an emphasis on the different wash buffers used (2.11.8). After antigen retrieval slides underwent endogenous peroxidase block using hydrogen peroxide and subsequent outlining of fixed tissue with a DAKO delimiting pen. As indicated in table 2.10 certain IHC protocols required a signal amplification step using the ABC method (Vectorstain ABC systems, Vector laboratories, Inc., CA). Here biotin labelled secondary antibodies were used introducing biotin into the section at the location of the primary antibody. The avidin: biotinylated enzyme complex (ABC) became bound to biotinylated secondary antibody and was localised by incubation with substrate for the enzyme. The alternative method used was the DAKO envision+ system horseradish peroxidase (HRP) IHC staining technique (DAKO North America, Inc.) where an HRP labelled polymer conjugated with secondary antibody resulted in staining when incubated with 3,3'-diaminobenzidine (DAB)+ substrate chromogen. All slides were counter stained with haematoxylin for approximately 30 sec and washed in running tap water before sequential dehydration in increasing concentrations of alcohols (70% ethanol x 5 min– 95% ethanol x5 min – 100% ethanol x2 5 min) and two washes in xylene x5 min prior to cover slip mounting. Immuno-histochemistry working solutions and reagents are described in 2.11.8.

Table 2.9 Primary antibodies and summary protocols for immuno-histochemistry

Primary antibody	Source	Antibody dilution	Antigen retrieval	Blocking buffer	Secondary antibody	Catalogue/Manufacturer
Phospho-Egfr (Tyr1068)	R	1/50	EDTA Pressure cooker 15mins	5% NGS TBST	Anti Rabbit HRP labelled polymer (Envision™+ kit, Dako)	# 2234 CST
Igf-1rβ	R	1/150	CITRATE buffer Pressure cooker 15mins	5% NGS TBST	Anti Rabbit HRP labelled polymer (Envision™+ kit, Dako)	# 3027 CST
Phospho-p44/42 Mapk (Erk1/2 Thr202/Tyr204)	R	1/75	CITRATE buffer Pressure cooker 15mins	10% NGS TBST	biotinylated goat anti-rabbit (Dako) 1:200 in 5% NGS TBST	# 4376 CST
Phospho-Akt (Ser473)	R	1/50	CITRATE buffer Pressure cooker 15mins	5% NGS TBST	biotinylated goat anti-rabbit (Dako) 1:200 in 5% NGS TBST	# 3787 CST
Anti cleaved caspase-3	R	1/200	CITRATE buffer Pressure cooker 15mins	5% NGS TBST	biotinylated anti rabbit (Vector stain ABC kit; Vector Labs) in 5% NGS TBST	#9661 CST
Anti-BrdU	Mo	1/150	CITRATE buffer Pressure cooker 15mins	1% BSA PBS	Anti Mouse HRP labelled polymer (Envision™+ kit, Dako)	N347580 BD
Anti Ki67	Mo	1/200	CITRATE buffer Pressure cooker 15mins	20% NRS TBST	biotinylated rabbit anti-mouse (Dako) 1:200 in 20% NRS TBST	VP-K452 Vector Labs, UK

R Rabbit

Mo Mouse

EDTA 1X EDTA epitope retrieval solution

NGS Normal goat serum

NRS Normal rabbit serum

BSA Bovine serum albumin

All primary antibody incubations were overnight at 4°C.

BD Becton Dickinson Immunocytometry

CST Cell signalling technology

TBST 0.1% TBS Tween 20

PBS 1X Phosphate buffered saline

Blocking buffer left for 1hr on bench

Table 2.10 Primary antibodies for IHC and overview of protocols highlighting endogenous peroxidase blocks, washes and ABC signal amplifications

Antibody	Antigen retrieval	Wash 1	Prevent endogenous staining	Wash 2	Block	Primary antibody	Wash 3	Secondary Antibody	Wash 4	Signal amplification	Wash 5	Visualisation of positivity	Wash 6
Phospho-Egfr (Tyr1068)		dH ₂ O x3	3% H ₂ O ₂ x10mins	dH ₂ O x2; 1hr	1hr	o/n 4°C	TBST x3	1hr RT	TBST x3	-	-	DAB stain 5-10min	dH ₂ O x1
Igf-1rβ		dH ₂ O x3	3% H ₂ O ₂ x10mins	dH ₂ O x2; 1hr	1hr	o/n 4°C	TBST x3	1hr RT	TBST x3	-	-	DAB stain 5-10min	dH ₂ O x1
Phospho-p44/42 Mapk (Erk1/2 Thr202/Tyr204)		dH ₂ O x1	1.5% H ₂ O ₂ x15mins	TBST x3	1hr	o/n 4°C	TBST x3	1hr RT	TBST x3	ABC x30mins	TBST x3	DAB stain 5-10min	TBST x3
Phospho-Mek1/2 (Ser221)		dH ₂ O x1	1.5% H ₂ O ₂ x15mins	TBST x3	1hr	o/n 4°C	TBST x3	1hr RT	TBST x3	ABC x30mins	TBST x3	DAB stain 5-10min	TBST x3
Phospho-Akt (Ser473)		dH ₂ O x1	3% H ₂ O ₂ x20mins	dH ₂ O x2; 1hr	1hr	o/n 4°C	TBST x3	1hr RT	TBST x3	ABC x30mins	TBST x3	DAB stain 5-10min	dH ₂ O x3
Anti cleaved caspase-3		dH ₂ O x3	3% H ₂ O ₂ x10mins	dH ₂ O x2; 1hr	1hr	o/n 4°C	TBST x3	1hr RT	TBST x3	ABC x30mins	TBST x3	DAB stain 5-10min	dH ₂ O x2
Anti-BrdU		-	Envision+ H ₂ O ₂ sol.	PBS x3	1hr	o/n 4°C	PBS x3	1hr RT	PBS x3	-	-	DAB stain 5-10min	PBS x3
Anti Ki67		dH ₂ O x1; TBST x1	0.5% H ₂ O ₂ x20mins	dH ₂ O x1	1hr	o/n 4°C	TBST x3	1hr RT	TBST x3	ABC x30mins	TBST x3	DAB stain 5-10min	TBST x3

TBST 0.1% TBS Tween 20 ; dH₂O distilled water; PBS 1X Phosphate buffer solution; ABC Avidin: Biotinylated enzyme Complex; DAB Diaminobenzidine Chromagenic substrate system. A single wash was 5mins. RT room temperature. o/n overnight incubation

2.7.3 Scoring apoptosis and cell proliferation

Haematoxylin and eosin or alternatively stained sections of tumour tissue using anti-cleaved caspase-3 or anti-BrdU antibodies were viewed using the x40 objective of an Olympus BX41 microscope attached to a U-CMAD3 digital camera utilizing Olympus colour view imaging software. Representative areas of tumour tissue were scored for the average number of epithelial cells per x40 objective field usually over 3 separate regions of a tumour. Phenotypic scoring (apoptotic bodies, cell mitoses and positive immune-reactive staining for cleaved caspase-3 or BrdU positivity) was performed by one person in a blinded fashion and the results were expressed as a percentage of the average number of epithelial cells per x40 objective field. For each experimental mouse tumour at least 1000 epithelial cells were counted in as many fields as necessary using the x40 objective and most commonly 3 tumours were scored from each animal. The average values for each phenotypic score were calculated using 3 experimental mice treated identically unless otherwise stated.

2.8 Detection of *K-ras* and *B-raf* mutations in *Apc^{min/+}* colon polyps

Genomic DNA was extracted from 30 individual colon polyps harvested from 29 *Apc^{min/+}* mice using the triplePrep kit (2.5.3). Samples were then processed by the Institute of Medical Genetics at Cardiff University. Genomic DNA from rectal cancer specimens (2.2.1) was also extracted using the same technique.

2.8.1 Pyrosequencing for *K-ras* mutations

To detect murine *K-ras* mutations in codons 12/13 and 61 pyrosequencing technology was employed. Codons 12/13 and 61 were initially amplified by PCR using the following primers sequences:-

Codon 12+13

Forward: GGCCTGCTGAAAATGACTGA

Reverse: CGCAGACTGTAGAGCAGCGTTAC

Codon 61

Forward: TGTTTCTCCCTTCTCAGGACTC

Reverse: AGAAAGCCCTCCCCAGTTC

The sequencing primers for codon 12/13 were CTTGTGGTGGTTGGAG and codon 61 GGATATTCTCGACACAGC. Pyrosequencing was semi-automated using the Pyromark ID Qiagen System and both assays were designed to detect all possible mutations in the codons examined.

codon 12/13 from human rectal cancer specimens were PCR amplified using forward primer sequence GGCCTGCTGAAAATGACTGA and reverse primer sequence AGAATGGTCCTGCACCAGTAATA, whereas *K-RAS* codon 61 was amplified using Forward primer TGTTTCTCCCTTCTCAGGATTC and reverse primer sequence AAGAAAGCCCTCCCCAGTC. The sequencing primers for codon 12/13 and 61 were CTTGTGGTAGTTGGAG and GGATATTCTCGACACAGC respectively.

2.8.2 Allelic discrimination assay for *B-raf* V600E mutation

The allelic discrimination assay permitted the detection of *B-raf* specific PCR product by measuring the increase in fluorescence of dye-labelled DNA probes. Amplification of a specific sequence of target DNA within the *B-raf* gene was achieved using forward (TTCATGAAGACCTCACAGTAAAAATAGG) and reverse (TCGATGGAGTGGGTCCCA) primer sequences. Thereafter TaqMan probes for hybridization to the target sequence within the PCR product were used to detect wild type or V600E *B-raf* mutation. The probes sequences were:-

B-raf wild type VIC-AGCTACAGTGAAATC

B-raf V600E 6FAM-CTACAGAGAAATCTC

The same probes sequences were used for human tumours as the primer annealing region and area to amplify were the identical

2.9 Statistical analysis

The Mann-Whitney statistic was used to detect significant differences between control and experimental conditions in relation to (i) tumour phenotype scoring (apoptotic bodies and mitoses) (ii) tumour immuno-phenotypic scoring (cleaved caspase 3, Anti Brdu and Ki67 positivity) (iii) densitometric assessments of western blots (iv) scores for total tumour numbers and volumes (v) Δ CT values for genes of interest and (vi) the detection of significant differences in the median expression values of *IKBKG*, *CXCL9* and *CCNE2* genes in patients with either disease control or no response to cetuximab treatment (based on data from GSE5851; 2.10.5). Kaplan Meier survival curves were generated for *Apc*^{min/+} cohorts receiving long term treatment and the Log Rank test was used for statistical comparisons between treatment arms.

All statistical tests and box plots to demonstrate small and large intestinal tumour counts and volumes were facilitated using Minitab 15 software. The error bars on charts represent ± 1 standard deviation from the mean value and are assumed to be significant when non-overlapping and *P values* of $\leq .05$ were accepted as statistically significant.

2.10 Microarray analysis

Microarray technology permits the comparison of gene expression profiles on a genomic scale across multiple RNA samples¹⁴². For this purpose biotin labelled cRNA was generated using established protocols <http://bioinformatics.picr.man.ac.uk/mbcf/protocols.jsp>. Mouse Genome 430 2.0 Affymetrix GeneChip arrays were run in triplicate at the Cancer Research U.K. facility at the Patterson Institute for Cancer Research for each time point and treatment (gefitinib or vehicle) using pooled RNA (see 2.3.2.1). As 2 treatments were used at 5 time points a total of 30 Affymetrix GeneChips were used. Different approaches were used to analyse the microarray data generated and the results for each analysis were compared to identify genes which were similarly differentially regulated enabling the creation of a target gene list for qRT-PCR.

2.10.1 AffyImGUI

AffyImGUI is a graphical user interface (GUI) permitting the analysis of Affymetrix GeneChip data¹⁴³. The package (<http://bioinf.wehi.edu.au/affyImGUI>) incorporates pre-processing methods for Affymetrix CEL files including quality assessment, background correction, normalisation and summarization of probe-set expression values. The output of the analysis provided differential expression and associated moderated *t*- statistic which is similar to an ordinary *t*- statistic and log-odds of differential expression, or *B*-statistic which is essentially equivalent to the moderated-*t* for ranking purposes. A table of top genes for the contrast gefitinib vs. vehicle at 4 hr provided the ranked order of log₂ fold change. Genes were chosen from this list if they were biologically relevant in terms of EGFR signalling, related to apoptotic and/or proliferative pathways or linked to the mechanism of action of gefitinib irrespective of *t*-statistic.

2.10.2 Time series regression analysis

BRB-ArrayTools is a software package developed by the Biometric Research Branch of the Division of Cancer Treatment & Diagnosis of the National Cancer Institute (<http://linus.nci.nih.gov/BRB-ArrayTools.html>). CEL files were uploaded and the RMA method used to compute probe set summaries. The RMA method used all the arrays simultaneously to compute the normalization and probe set summaries. Probe sets with a large percentage of detection cells that had an absent (A) value were filtered out in order to exclude probe sets considered unreliable or uninteresting because too many of the expression values were absent. A logarithmic (base 2) transformation was applied to the signal intensities before median normalisation. The time series regression analysis plug-in model was used to identify genes whose variation over time was dependent upon treatment. Once identified it was then possible to calculate gene expression fold changes taking the ratio of geometric gene signal intensities for gefitinib at 4-24 hr relative to either time zero or vehicle at 4-24 hr.

2.10.3 Fold change and ranked products analysis

Raw intensity signals generated from the microarray were initially processed using MaxD/View (<http://www.bioinf.manchester.ac.uk/microarray/maxd/download.html>) to

remove false negative and positive signals (using a cut off of at least one P value for each transcript <0.2). The data were then normalized by using the global geometric mean (GGM) normalization option within the MaxD/View-Program, as described previously¹¹⁴. Fold change and ranked product computations were performed and the two-sample t test to calculate P values for differences between vehicle and gefitinib treatment at 4 hr. Differentially expressed genes with the greatest fold change difference (top or bottom 50 genes ≤ 0.5 or ≥ 2 fold change with P value ≤ 0.05) or ranked position (top or bottom 50; P value ≤ 0.05) were favourably filtered and searched for biologically relevant candidates, in a similar fashion as for the affyImGUI analysis.

2.10.4 Significance analysis of microarrays (SAM)

The data processed using MaxD/View was also subject to SAM analysis¹⁴⁴ (<http://www-sat.stanford.edu/~tibs/SAM/>). Here contrast was made between gene expression for each of the experimental treatments at the various time points (gefitinib vs. vehicle) and for gefitinib at time 4 hr relative to time zero to identify significant genes. The cut off for significance was determined by the tuning parameter delta, which was determined by me based upon the acceptance of a defined false positive rate.

2.10.5 Analysis of the GSE5851 dataset

The GSE5851 data (<http://www.ncbi.nlm.nih.gov/geo/query/acc.cgi?acc=GSE5851>) is from a phase II exploratory pharmacogenomics study of cetuximab monotherapy in patients with advanced metastatic CRC²⁴. Here transcriptional profiling of RNA from pre-treatment metastatic colorectal cancer biopsies identified genes correlated with best clinical outcome in patients treated with cetuximab monotherapy. This data was then probed for qRT-PCR validated mouse candidate genes hypothesised to be predictive of response to Egfr blockade, using the equivalent human probe identities, to enquire if they dichotomise response category in patients (disease control group/ non responder). Transcripts with a $P \leq 0.05$ were considered discriminatory for treatment outcome and if present explored in more detail by collecting individual Affymetrix expression values for the genes of interest from each patient with *K-RAS* wild type tumours. The median expression values were calculated for each gene for disease control and non-responder groups and compared using

the Mann-Whitney test to gain insight into how the direction of expression correlates with outcome.

2.11 Working solutions, materials and reagents

2.11.1 TBE/Agarose gels for DNA electrophoresis

5X Tris-Borate-EDTA (TBE) buffer (Sigma,UK)

0.445M Tris borate

0.5mM EDTA (pH 8.3)

Made with water for injection

2.0% Agarose gel:

200mls 1X TBE buffer (40ml 5X TBE buffer: 160mls dH₂O.)

4g agarose (Eurogentech, UK)

5µl Safeview Nucleic Acid Stain (NBS biologicals, UK)

4.0% Agarose gel:

8g agarose used, otherwise as for 2% gel.

TBE electrophoresis running buffer (1000ml)

200ml 5X TBE buffer stock

800ml dH₂O

The TBE buffer/agarose mix was heated in a conical flask in a microwave until boiling and allowed to cool slightly before the addition of nucleic acid stain and poured into an electrophoresis cast to set. Gels were immersed in 1X TBE electrophoresis running buffer and electrophoresed at 120v for 30 min.

2.11.1.1 Orange G loading dye

10x Orange G loading dye

40ml 30% glycerol (Fisher Scientific, UK)

100mg Orange G (Sigma, UK)

10ml dH₂O

Sample loading per well:

5µl 1X Orange G loading dye (Track the position of 50bp DNA molecules)

10µl qRT-PCR product

2.11.2 TAE/Agarose gels for RNA electrophoresis

10X Tris-Acetate EDTA (TAE) buffer (Sigma, UK)

0.4M Tris acetate

0.01M EDTA

pH 8.3

made up with nuclease free water

1% TAE/Agarose non-denaturing RNA gel:

25ml 1X TAE

0.25g agarose (Sigma, UK)

1µl ethidium bromide solution (Sigma,UK)

1X TAE electrophoresis running buffer (1000mls)

100ml 10X TAE buffer: 900mls dH₂O

The mixture of TAE/Agarose was heated in a conical flask for 30 sec using a microwave, stirred and then re heated until boiling. Ethidium bromide was added once the solution had cooled slightly and was then poured into the electrophoresis cast to set. Gels were immersed in 1X TAE electrophoresis buffer and electrophoresed at 50volts for 20 min.

2.11.2.1 RNA loading buffer

100µl saturated bromophenol blue (Sigma,UK)

80µl 0.5M EDTA (pH 8.0) (Sigma,UK)

720µl formaldehyde (38%) (Sigma,UK)

2ml glycerol (Fisher Scientific, UK)

3.1ml formamide (Sigma,UK)

4ml 10X MOPS

1ml aliquots stored at -20°C.

10X MOPS (All reagents from Sigma, UK)

41.8g 4-Morpholinepropanesulfonic acid (free acid)

Up to 800ml with nuclease free water

pH to 7.0 with NaOH

Add 16.6ml 3M NaOH_c (sodium acetate)

Add 20ml 0.5M EDTA pH 8.0

Made up to 1L and autoclaved.

Sample loading per well:

1µl RNA sample

2µl RNA loading buffer

6µl Nuclease free water (Sigma, UK)

2.11.3 Solutions for drug suspensions

2.11.3.1 Vehicle solutions

0.5% Tween⁸⁰

50ml purite water

250µl Tween⁸⁰ (Sigma, UK)

1.0% Tween⁸⁰

50ml purite water

500µl Tween⁸⁰ (Sigma, UK)

1X Phosphate buffered saline (PBS)

5ml 10X PBS (Gibco, Invitrogen, UK)

45ml purite water

(Vehicle for ME1)

All vehicle solutions stored at 4°C.

2.11.3.2 Drug suspensions

Gefitinib stock (stored at room temperature for 24 hr)

15mg gefitinib (AstraZeneca, UK)

1ml 0.5% or 1.0% Tween⁸⁰

Vortexed thoroughly before administered.

AZ12253801 stock (stored at room temperature for 24hr)

5mg AZ12253801 (AstraZeneca,UK)

2ml 1.0% Tween⁸⁰

Vortexed thoroughly before administered.

ME1 provided as stock solution ready for injection (ImClone systems, New York)

100µl (1mg) aliquots stored at -20°C.

2.11.4 TriplePrep kit reagents and working solutions

Lysis buffer type 15 (for each sample being processed)

Aliquot 1000µl lysis buffer type 15 into DNase/RNase-free 2ml tube

Add 10µl 2-Mercaptoethanol (Sigma,UK)

Wash buffer type 6

48ml of absolute ethanol added and mixed

Absolute acetone (Sigma, UK)

DNase 1

540µl RNase free water (supplied) added to DNase vial

Aliquot and stored at -20°C

2-D DIGE buffer (40ml)

40ml dH₂O

42g Urea

15.2g Thiourea

0.36g Tris-HCl

4g CHAPS (3-3-Cholamidopropyl) dimethylammonio-1-propanesulfonate

(All reagents from Sigma, UK)

2-D DIGE Reagents mixed well and not heated beyond 37°C. Final pH adjusted to 8.5 and total volume of 40ml with distilled water. Dispensed into 5ml aliquots and stored at -20°C.

2.11.5 SDS PAGE

2.11.5.1 Upper buffer

6.6g Tris base 2-Amino-2-(hydroxymethyl)-1,3-propanediol; Roche, UK)

0.4g SDS (sodium dodecyl sulphate; Fisher Scientific, UK)

pH 6.8 with HCl (made up to 100ml dH₂O)

2.11.5.2 Lower buffer

19.8g Tris base

0.4g SDS

pH to 8.8 with HCl (made up to 100ml with dH₂O)

10% Ammonium persulfate (APS) solution

100mg APS

Made up to 1ml with dH₂O

2.11.5.3 Running buffer (10X Stock)

30.3g Tris base

144.4g Glycine

Made up to 1000ml with dH₂O

Before use 5ml of 10% (w/v) solution of SDS added to 1X solution

2.11.5.4 Laemmli buffer

1.4g Tris base

4g SDS

20g sucrose

4mg bromophenol blue

pH to 6.8 with HCl (made up to 100ml with dH₂O)

For use: 50µl β-Mercaptoethanol (Sigma, UK) added to 950µl sample buffer prior to use.

Reagents:

Acrylamide/Bis, 19:1 mixture (30%) (BioRad, CA)

APS (ammonium persulphate) (Fisher Scientific, UK)

TEMED (N,N,N',N'-Tetramethylethylenediamine) (Sigma, UK)

Glycine (Fisher Scientific, UK)

Methanol (Fisher Scientific, UK)

2.11.6 Protein transfer buffer

Transfer buffer (1000ml)

200ml 10X Running buffer (2.11.5.3)

200ml Methanol (Fisher Scientific, UK)

600ml dH₂O

Mixed well using magnetic flea stirrer

2.11.7 PVDF Membrane incubation buffers

0.1% TBS Tween²⁰ (TBST) Membrane wash buffer

1000ml 1X TBS (100ml 10X TBS made up to 1000ml with dH₂O)

1ml Tween²⁰ (Sigma, UK)

5% Milk in TBST Blocking buffer (500ml)

25g Marvel non fat dried milk powder

made up to 500ml with TBST

Heated to 37°C and mixed to help form solution (stored at 4°C)

5% BSA in TBST Blocking buffer (500ml)

25g Bovine serum albumin (Sigma, UK) replaces skimmed milk

3% BSA/2% NGS in 0.1% TBST Blocking buffer (20ml)

0.6g BSA

0.4ml NGS

Made up to 20ml with TBST

Reagents:

10X TBS (Tris buffered saline; Sigma, UK)

NGS (Normal goat serum, Dako.)

2.11.8 Immuno-histochemistry

2.11.8.1 Antigen retrieval

EDTA buffer antigen retrieval (EDTA buffer, Thermo Fisher Scientific)

10X EDTA epitope retrieval solution (10mM EDTA buffer, pH 8.0)

100ml (10X EDTA buffer stock) diluted in 900ml dH₂O

Citrate buffer antigen retrieval (Citrate buffer, Thermo Fisher Scientific)

10X Sodium Citrate buffer (100mM Sodium Citrate buffer, pH 6.0)

100ml (10X Citrate buffer stock) diluted in 900ml dH₂O

2.11.8.2 Wash buffers

TBST (0.1% TBS Tween²⁰)

1000ml TBS

1ml Tween 20

PBS (phosphate buffered saline)

10X stock PBS (pH 7.0; Invitrogen)

100ml PBS diluted in 900ml dH₂O

2.11.8.3 Blocking buffers

1% BSA in PBS

0.2g BSA bovine serum albumin (Sigma)

20ml PBS

5% NGS (Normal goat serum)

500µl NGS (Dako)

10ml TBST

20% NRS (Normal rabbit serum)

2ml NRS

10ml TBST

2.11.8.4 Endogenous peroxidase block

3% H₂O₂ solution (Hydrogen peroxide)

Stock 30% H₂O₂ (Sigma)

1ml 30% H₂O₂ diluted in 9ml dH₂O

2.11.8.5 Signal amplification and DAB staining

ABC reagents (Vectastain, Vector laboratories)

5ml TBST

Add 2 drops reagent A, mix

Add 2 drops reagent B

(Left for 30 min at room temperature before incubating on sample for 30 min at room temperature)

DAB (diaminobenzidine) +Chromogen Envision™ system (DAKO)

DAB substrate buffer solution (1ml)

Add DAB chromogen solution (1 drop)

Staining complete in 5-10 min

Chapter 3

3. Gene expression changes in *Apc^{min/+}* *K-ras* wild type colon polyps in response to EGFR blockade: Identification of novel putative biomarkers of response to anti-EGFR therapy.

3.1 Introduction

Despite advances in response prediction to EGFR targeted therapy in colorectal cancer, there remain unknown factors determining outcome in patients with *K-RAS* wild type tumours in the absence of genetic events leading to pathway activation of *B-RAF* or PI3 kinase signalling^{45, 46, 52} (1.3.4). It was hypothesised therefore that the *Apc^{min/+}* mouse would model *K-ras* wild type colorectal tumours sufficiently well to be informative in terms of gene expression changes detected in response to Egfr targeted agents and consequently increase our insight of molecular factors influencing treatment outcome. To achieve this, microarray technology has been used to identify genes differentially expressed in colon polyps harvested from *Apc^{min/+}* mice acutely exposed to gefitinib (2.3.2.1) and subsequently, transcripts similarly altered in response to a specific monoclonal antibody against the murine Egf receptor, ME1 (2.3.2.2). This work has discovered new putative molecular targets which may contribute towards predicting the outcome of EGFR targeted therapy in *K-RAS* wild type advanced colorectal cancer, in the absence of other mutations known to influence responses.

3.2 Results

3.2.1 Colon polyp *K-ras* and *B-raf* mutation status

Given the intention to use the *Apc*^{min/+} mouse as a model of *K-ras* wild type colon cancer, I initially sought to exclude the presence of the common known mutations in *K-ras* and *B-raf* occurring in colorectal cancer. Subsequent pyrosequencing (2.8.1) and allelic discrimination (2.8.2) PCRs failed to identify mutations in *K-ras* codons 12/13 and 61 or the presence of *B-raf* V600E in genomic DNA samples from 30 colon polyps harvested from 29 *Apc*^{min/+} mice. Figure 3.1 demonstrates a typical pyrogram result for *K-ras* codon 12/13. This supports the applicability of the *Apc*^{min/+} mouse model to *K-RAS* and *B-RAF* wild type colon cancer.

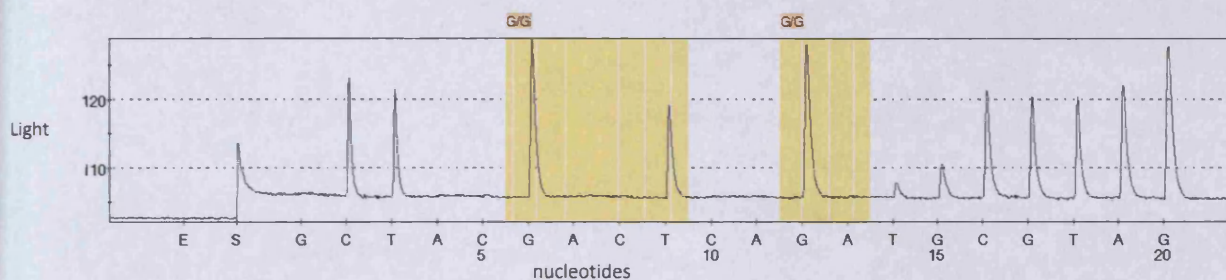


Fig 3.1 Pyrogram result from a colon polyp (sample 28D) demonstrating wild type status (GGT and GGC) of *K-ras* gene codons 12/13.

3.3 Pharmacodynamic effects of Egfr blockade in *Apc*^{min/+} intestinal tumours

As gene expression changes in response to acute Egfr exposure were to be explored in intestinal tumours from *Apc*^{min/+} mice, I next probed the immediate phenotypic effects of gefitinib and ME1 exposure. This was to ensure the doses administered induced relevant biological effects potentially associated with anti-tumour responses.

3.3.1 Small intestine and colon tumours

3.3.1.1. Gefitinib

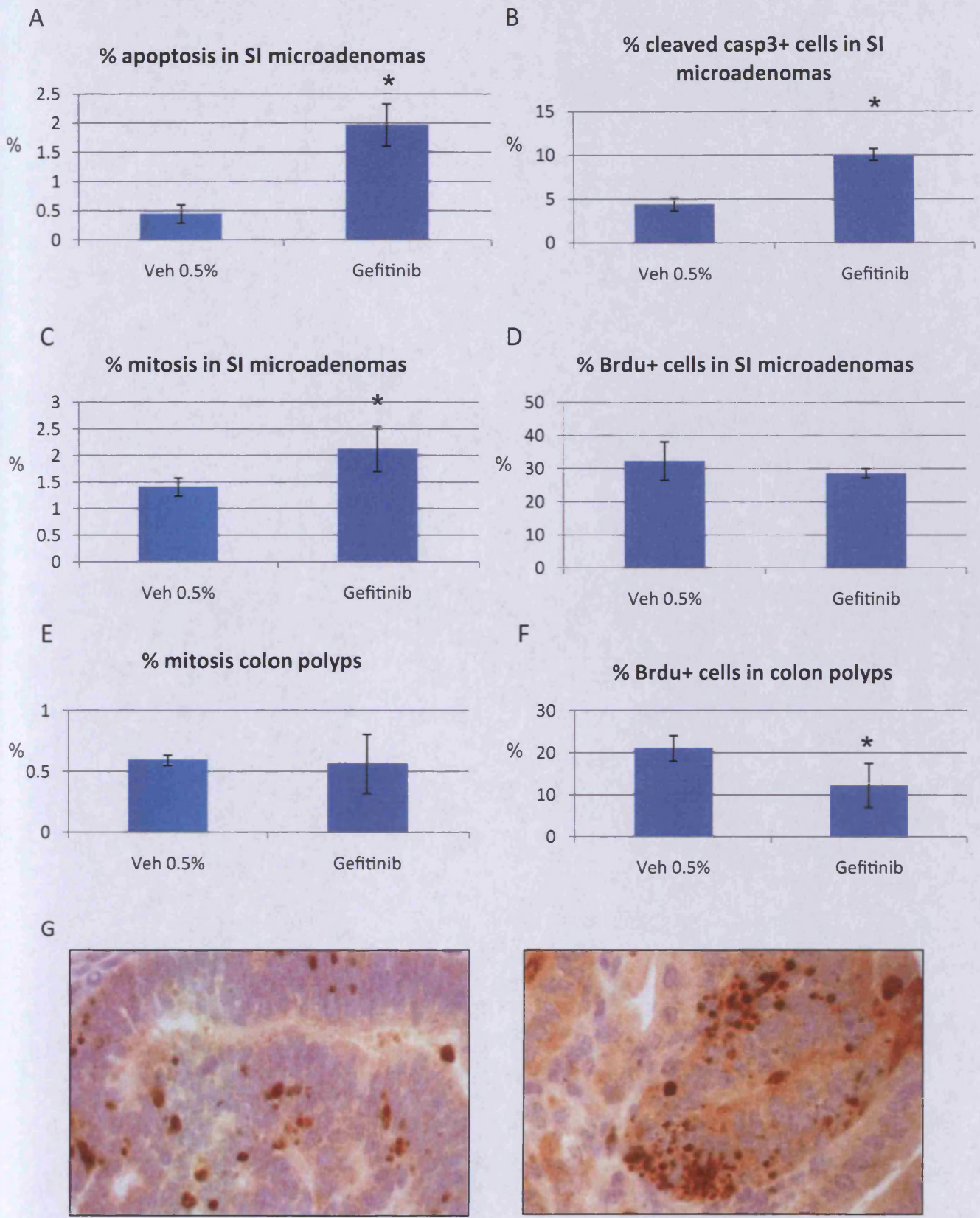
I initially exposed mice to a single dose of gefitinib 75mg/kg and obtained intestinal tumours at a 4 hour time point. The immediate pharmacodynamic consequences of gefitinib exposure in small intestinal tumours resulted in increased scoring of apoptosis assessed by

H and E ($0.45\% \pm 0.15$ [Veh] vs. $1.96\% \pm 0.36$ [Gef], $P=0.04$, Mann-Whitney, fig 3.2A) and cleaved capsase-3 staining ($4.4\% \pm 0.7$ [Veh] vs. $10.1\% \pm 0.7$ [Gef], $P=0.04$, Mann-Whitney, fig 3.2B). This was combined with increased mitotic scoring ($1.4\% \pm 0.2$ [Veh] vs. $2.1\% \pm 0.4$ [Gef], $P=0.04$, Mann-Whitney, fig 3.2C) without change in Brdu cell labelling ($32.4\% \pm 5.5$ [Veh] vs. $28.6\% \pm 1.4$ [Gef], $P=0.3$, Mann-Whitney, fig 3.2D). These findings suggest there is an accumulation of cells during M phase given the failure to demonstrate increased cell cycling and cell proliferation. Examination of colon polyps however showed evidence of reduced Brdu tumour cell labelling at 4 hours ($21.1\% \pm 3$ [Veh] vs. $12.3\% \pm 5.2$ [Gef], $P=0.04$, Mann Whitney, fig 3.2F) without a change in mitotic index ($0.60\% \pm 0.4$ [Veh] vs. $0.57\% \pm 0.24$ [Gef], $P=0.5$, Mann-Whitney, fig 3.2E). These findings suggest that cell proliferation is suppressed without alteration in M phase, perhaps due to slower cell cycling. Apoptosis was not induced in colon polyps by gefitinib (data not shown).

3.3.1.2 ME1

I next wished to determine if exposure to a monoclonal antibody raised against Egfr would alter the phenotype of intestinal tumours in a manner parallel to gefitinib exposure. To achieve this I exposed mice to 1mg of ME1, an antibody raised in rats against murine Egfr, and then harvested samples at 4 hours. In small intestinal tumours Ki67 scoring to mark cycling cells showed a decrease ($56.2\% \pm 9.6$ [Veh] vs. $42.4\% \pm 3.5$ [ME1], $P=0.04$, Mann Whitney; fig 3.3D). However, there was no change in mitotic index ($0.76\% \pm 0.3$ [Veh] vs. 0.61 ± 0.06 [ME1], $P=0.33$, Mann Whitney; fig 3.3C). These data suggest reduced proliferation, but that this does not result in changed M phase, possible reflecting slower cell cycle passage. In colonic tumours an increased mitotic count was observed ($0.40\% \pm 0.0003$ [Veh] vs. $0.55\% \pm 0.1$ [ME1], $P=0.04$, Mann Whitney; fig 3.3G) without a change in Brdu cell labelling ($23.8\% \pm 1.2$ vs. $24.7\% \pm 0.09$, $P=0.38$, Mann Whitney; fig 3.3H). These data suggest that cells may be accumulating during M phase as there is there is no apparent increase in cell transit through the cell cycle. No changes in H and E scoring for apoptosis ($0.94\% \pm 1$ [Veh] vs. $0.60\% \pm 0.3$ [ME1], $P=0.5$, Mann-Whitney, fig 3.3A; $1.24\% \pm 0.46$ [Veh] vs. 1.82 ± 0.2 [ME1], $P=0.06$, Mann-Whitney, fig 3.3E) or cleaved caspase 3 ($2.4\% \pm 1.3$ [Veh] vs. 3.6 ± 1.5 [ME1], $P=0.18$, Mann-Whitney, fig 3.3B; $8.3\% \pm 1$ [Veh] vs. $7.7\% \pm 4.9$ [ME1],

Figure 3.2 Phenotypic consequences of acute (4 hr) gefitinib exposure on *Apc^{min/+}* small and large intestinal tumours

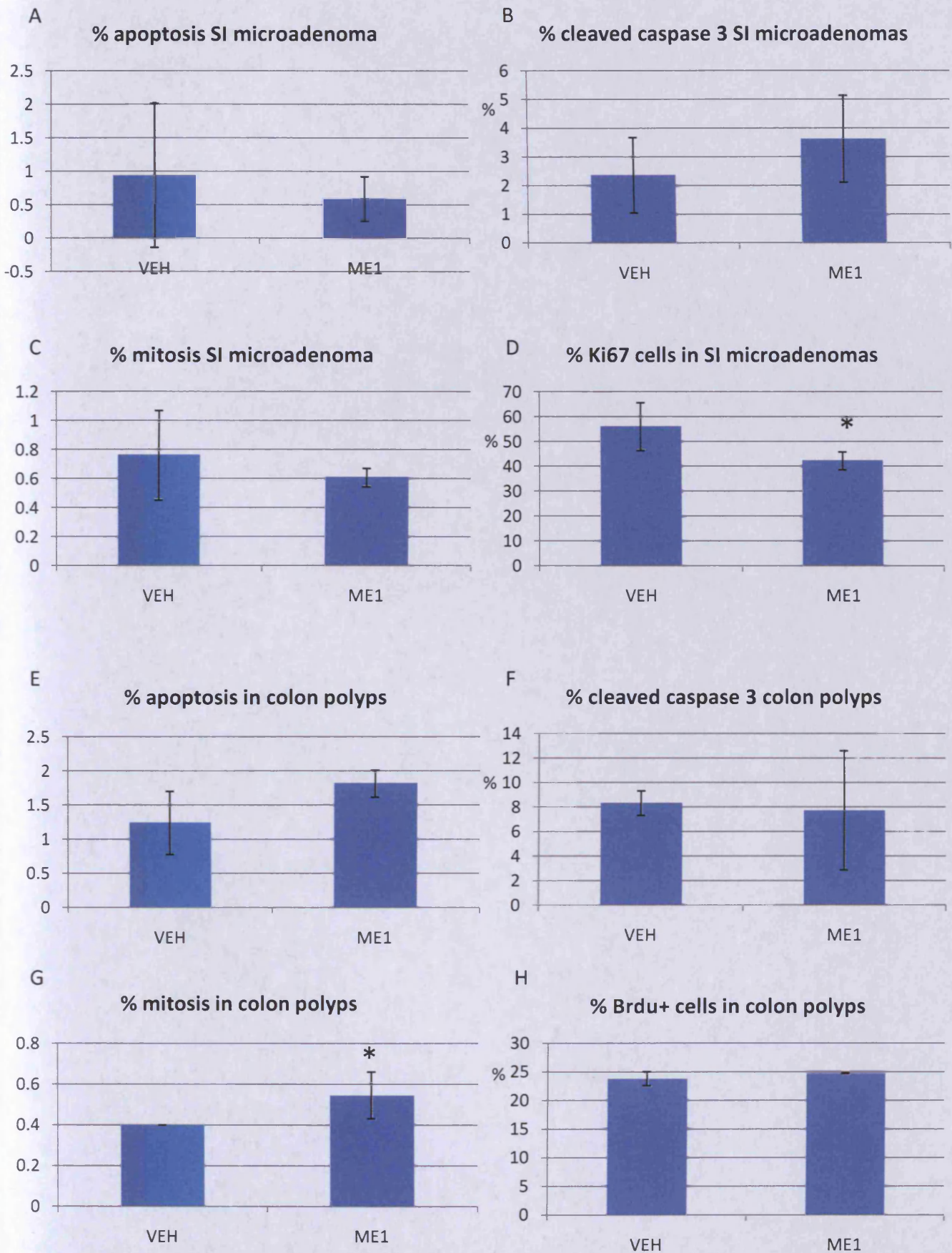


4 hr Vehicle (0.5% Tween80) exposure

4 hr Gefitinib (75mg/kg) exposure

Panel G demonstrates increased cleaved caspase-3 immuno-reactivity in small intestinal adenomas following acute gefitinib exposure. Error bars represent ± 1 standard deviation. SI small intestine; Veh 0.5% Tween 80; Gefitinib 75 mg/kg. * P=0.04 (Mann-Whitney). Panel E n=2 mice counted for gefitinib data.

Figure 3.3 Phenotypic consequences of acute (4 hr) ME1 exposure on *Apc^{min/+}* small and large intestinal tumours



SI small intestinal, VEH 1xPBS (100ul), ME1, rat monoclonal antibody against mouse EGFR (1mg)
 * P=0.04 (Mann-Whitney). Panel H, n=2 mice available for ME1 data. Error bars represent ±1 standard deviation.

P=0.3, Mann-Whitney, fig 3.3F) staining were detected in either small or large intestinal tumours respectively in response to ME1.

3.3.2 Apoptotic and cell cycle transcript changes in colon polyps

My next task was to investigate some of the molecular alterations induced by Egfr antagonism in order to explain the immediate phenotypic changes. This was done by examining colon polyp transcript changes in response to acute Egfr inhibition by gefitinib and ME1.

3.3.2.1 Gefitinib

Following 4 hour exposure to gefitinib 75mg/kg there was an approximate 2-fold induction of the pro-apoptotic genes *Bak1*, *Bax* and almost 4-fold increase in *Bcl2 modifying factor (Bmf)* expression. This was associated with an approximate 2-fold reduction in the expression of *cyclin E2*, (*Ccne2*) a component of cell cycle control (fig 3.4 A). These findings, although only examined at the mRNA level, may indicate that pro-apoptotic events are driven by changes in *Bak1*, *Bax* and *Bmf* and anti-proliferative effects influenced by reduced expression of *cyclin E2*.

3.3.2.2 ME1

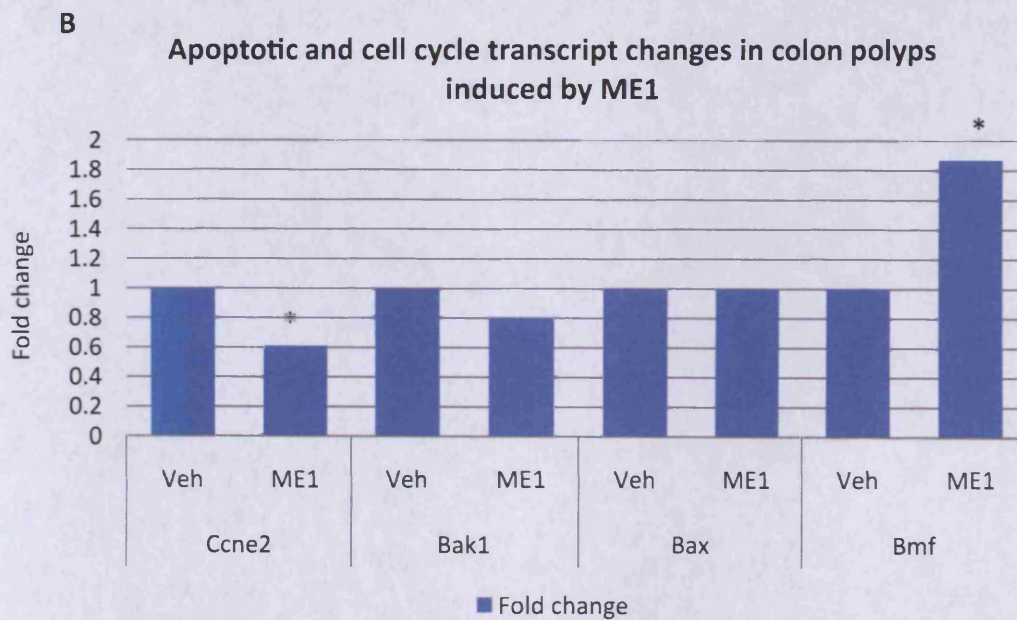
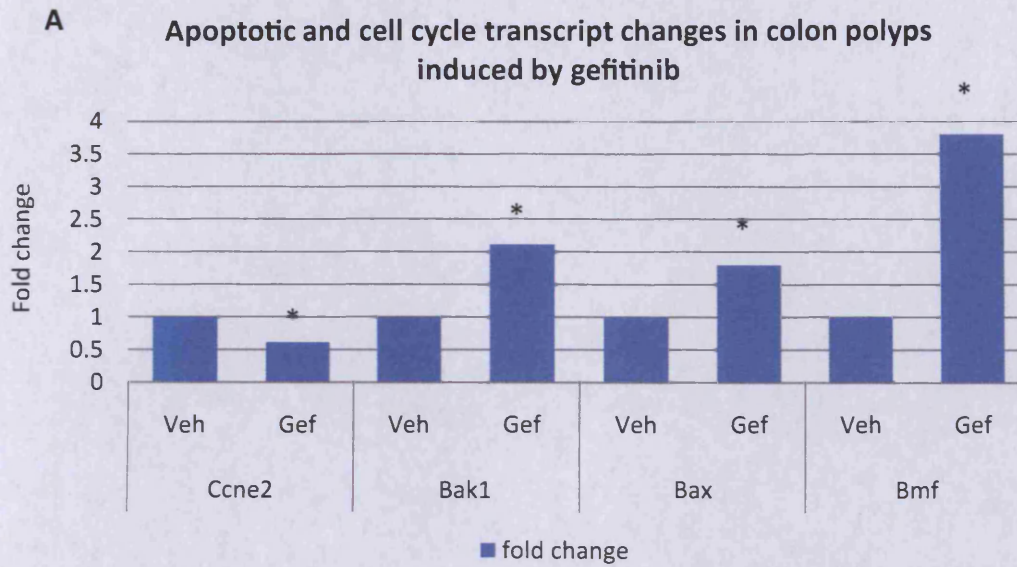
Similar transcript changes were search for in colon tumours in response the Egfr blockade driven by targeted monoclonal antibody. Here, ME1 1mg induced a 2-fold increased expression of *Bmf* and led to an approximate 2-fold decreased level of *cyclin E2* expression in colon polyps following 4 hour exposure (fig 3.4 B). Again, these changes may be important in driving the phenotypic alterations seen following acute Egfr antagonism in intestinal tumours. The pro-apoptotic transcript changes appear to be more selective in response to ME1 compared to gefitinib.

3.3.3 Downstream signalling changes in colon polyps

I next sought to identify the molecular changes in response to Egfr blockade, in terms of the acute effects upon Egfr signal transduction in *Apc^{min/+}* mouse intestinal tumours, to provide further pharmacodynamic evidence that the chosen agents were administered at an appropriate dose based upon previous work¹³². This work was



Figure 3.4. Apoptotic and cell cycle transcript changes induced in *Apc^{min/+}* colon polyps by 4 hr exposure to gefitinib or ME1



* P 0.0404 (Mann Whitney). Triplicate paired samples were available for qRT-PCR.

Figure 3.5 Signalling changes in *Apc^{min/+}* colon polyps following 4 hr Egfr antagonism with gefitinib or ME1

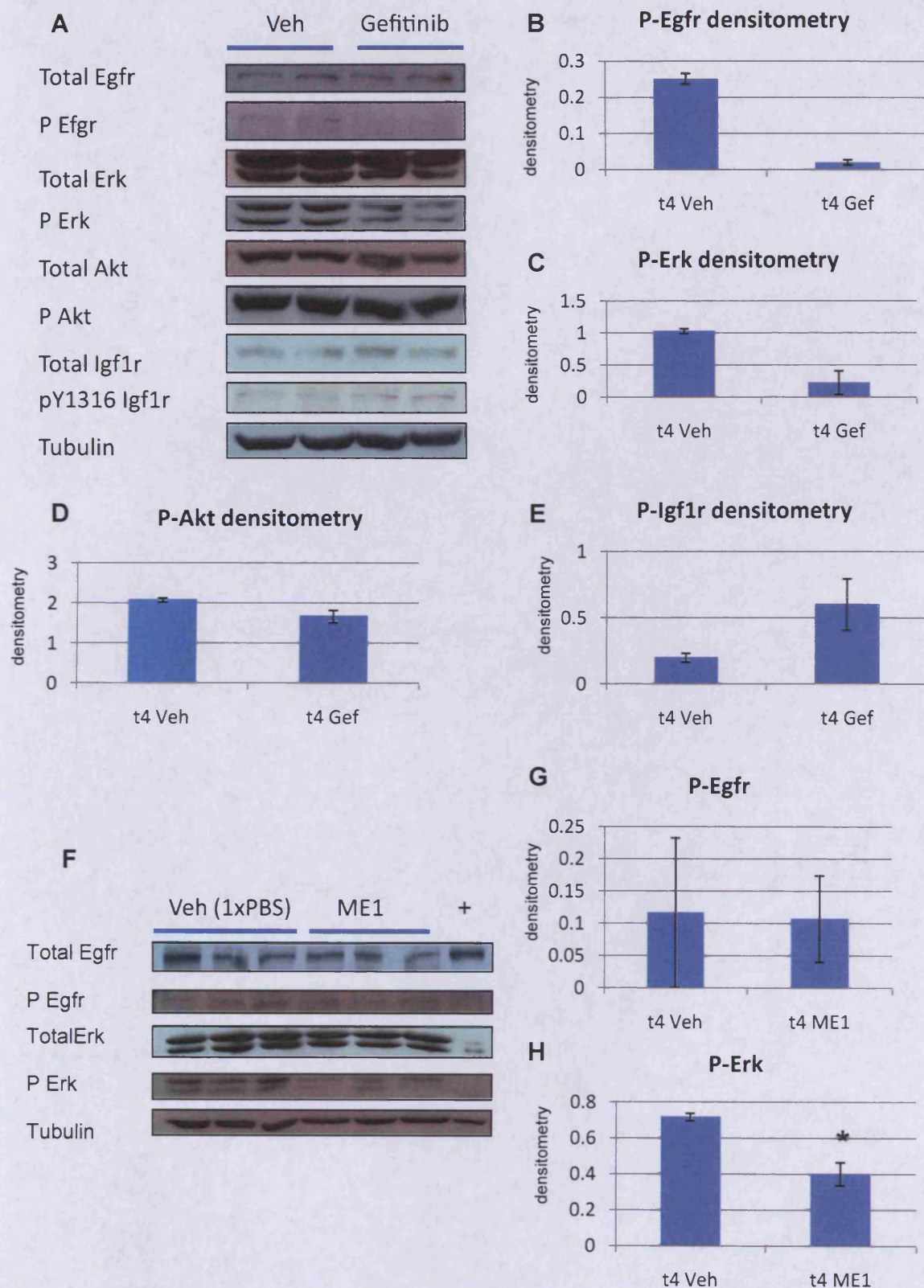


Fig3.5 Western blots of protein from pooled *Apc^{min/+}* colon polyps from mice culled 4 hr after a single intra-peritoneal injection of (A) vehicle 1% Tween 80/gefitinib (75mg/kg) or (F) vehicle 1xPBS /ME1 (1mg). Charts are densitometry results for various phospho-antibodies used. 1XPBS, phosphate buffered saline. Lane labelled + refers to positive control. * refers to P value 0.04 (Mann-Whitney). See methods 2.5.6.2 for details regarding numbers of mice and polyps pooled for each treatment. 'P', Phosphorylated protein. Error bars represent value ranges (B-E) and standard deviation G and H.

undertaken following acquisition of material for the microarray analysis, but ideally should have been performed beforehand to ensure suitable dose administration in this setting.

3.3.3.1 Gefitinib

Egfr blockade using gefitinib 75mg/kg reduced the level of phosphorylated Egfr in colon polyps and consequently suppressed downstream phosphorylation of Erk and Akt (fig 3.5 A-D). In addition there was activation of the Igf1 receptor indicated by an increased level of Igf1r phosphorylation at tyrosine 1316 position (fig 3.5 A, E).

3.3.3.2 ME1

The monoclonal antibody raised against Egfr, ME1 (1mg), resulted in suppression of *Apc^{min/+}* colon polyp Erk phosphorylation. However this was demonstrated in the absence of a detected reduction in the level of Egfr phosphorylation (fig 3.5 F-H). Signalling through Akt and Igf1r activation was not probed in response to ME1.

3.4 Microarray analysis

My next step was to identify *Apc^{min/+}* colon polyp transcript changes in response to acute Egfr exposure. This is based on the hypothesis that any induced gene alterations may represent novel candidate biomarkers indicative of clinical outcome to EGFR targeted therapy in *K-ras* wild type colorectal cancer. As described in methods (section 2.1.3.2.1 and 2.3.2.1), *Apc^{min/+}* mice with an intestinal tumour burden were exposed to acute Egfr inhibition for defined time periods prior to cull. This was followed by colon polyp RNA extraction and pooling, with subsequent RNA labelling and hybridisation to Affymetrix gene chips. Although professional bioinformatics input was not available for analysis of the microarray level data, Dr Karen Reed was of great assistance, and provided excellent support for aspects of the analysis.

3.4.1 Fold change and ranked product computations

A clear strategy for choosing potential targets for qRT-PCR validation was required given the hundreds of genes potentially differentially expressed. As described (2.10), the approach I adopted to identify targets for subsequent validation was to search transcripts repeatedly differentially expressed by different methods of microarray data enquiry. I then

Table 3.1. Top 50 up- and down-regulated genes (fold change ≤ 5 or ≥ 2 ; $P \leq 0.05$) based on microarray fold changes in *Apc^{min/+}* colon polyps in response to gefitinib at 4 hours

Probe Set ID	Gene Symbol	Gene Title	Fold change	P value
1453925_at	<i>4930429F24Rik</i>	RIKEN cDNA 4930429F24 gene	10.22	0.05
1439379_x_at	<i>Prm1</i>	protamine 1	10.06	0.00
1426132_at	---	methylase mRNA	9.92	0.04
1443126_at	---	Unclassifiable product	7.62	0.02
1447626_x_at	<i>Arid3b</i>	AT rich interactive domain 3B (BRIGHT-like)	7.48	0.04
1433145_at	<i>4933431C10Rik</i>	RIKEN cDNA 4933431C10 gene	7.34	0.01
1448514_at	<i>Cox5b</i>	cytochrome c oxidase, subunit Vb	7.27	0.01
1446352_at	---	hypothetical Alanine-rich region/Treacher Collins syndrome protein	6.96	0.03
1436258_at	<i>Arhgef9</i>	CDC42 guanine nucleotide exchange factor (GEF) 9	6.79	0.02
1425574_at	<i>Epha3</i>	Eph receptor A3	6.72	0.02
1429933_at	<i>Agtpbp1</i>	ATP/GTP binding protein 1	6.36	0.01
1431764_at	<i>2310067P03Rik</i>	RIKEN cDNA 2310067P03 gene	6.35	0.02
1432049_at	<i>4930422I22Rik</i>	RIKEN cDNA 4930422I22 gene	6.10	0.01
1445592_at	---	No transcript currently supports this probe set, though EST sequences are available from the design information.	5.90	0.01
1417943_at	<i>Gng4</i>	guanine nucleotide binding protein (G protein), gamma 4	5.86	0.00
1446211_at	---	No transcript currently supports this probe set, though EST sequences are available from the design information.	5.57	0.00
1437631_at	<i>Kcnip4</i>	Kv channel interacting protein 4	5.45	0.03
1423328_at	<i>Gdap1</i>	ganglioside-induced differentiation-associated-protein 1	5.32	0.03
1422214_at	<i>Npffr2</i>	neuropeptide FF receptor 2	5.25	0.03
1451861_at	<i>Nxn12</i>	nucleoredoxin-like 2	5.22	0.04
1456248_at	<i>Lce3f ///</i>	late cornified envelope 3F ///	5.20	0.01
1445187_at	<i>LOC630971</i>	hypothetical protein LOC630971	5.05	0.04
1438870_at	<i>9430070O13Rik</i>	RIKEN cDNA 9430070O13 gene	4.82	0.04
1456814_at	<i>Fbn1</i>	fibrillin 1	4.55	0.01
1421561_at	<i>Rrp7a</i>	ribosomal RNA processing 7 homolog A (<i>S. cerevisiae</i>)	4.50	0.03
1453526_at	<i>Bhlhe23</i>	basic helix-loop-helix family, member e23	4.49	0.00
1416196_at	<i>4930503E14Rik</i>	RIKEN cDNA 4930503E14 gene	4.46	0.02
1449380_at	<i>Rpsa</i>	ribosomal protein SA	4.41	0.02
		protein kinase C and casein kinase substrate in neurons 1		

Top 50 up-regulated genes in colon polyps in response to gefitinib exposure

Table 3.1. Top 50 up- and down-regulated genes (fold change ≤ 5 or ≥ 2 ; $P \leq 0.05$) based on microarray fold changes in *Apc^{min/+}* colon polyps in response to gefitinib at 4 hours

Probe Set ID	Gene Symbol	Gene Title	Fold change	P value
1430018_at	<i>Cdc42ep5</i>	CDC42 effector protein (Rho GTPase binding) 5	4.40	0.02
1443155_at	---	probes do not match the transcript, presumably because the 3' end of the transcript is truncated in the record	4.24	0.01
1454298_at	<i>4932430A15Rik</i>	RIKEN cDNA 4932430A15 gene	4.24	0.05
1438324_at	<i>9330182L06Rik</i>	RIKEN cDNA 9330182L06 gene	4.22	0.03
1419220_at	<i>Xirp1</i>	xin actin-binding repeat containing 1	4.16	0.02
1430306_a_at	<i>Atp6v1c2</i>	ATPase, H ⁺ transporting, lysosomal V1 subunit C2	4.16	0.02
1438884_at	<i>Shisa3</i>	shisa homolog 3 (<i>Xenopus laevis</i>)	4.10	0.02
1445817_at	<i>BB168181</i>	expressed sequence BB168181	4.10	0.04
1419294_at	<i>1700011H14Rik</i>	RIKEN cDNA 1700011H14 gene	4.07	0.03
1454054_at	<i>4930459I23Rik</i>	RIKEN cDNA 4930459I23 gene	3.95	0.00
1444605_at	<i>1700061F12Rik</i>	RIKEN cDNA 1700061F12 gene	3.93	0.05
1443599_at	---	Hypothetical protein	3.92	0.02
1444253_at	<i>Adamts18</i>	a disintegrin-like and metallopeptidase (reprolysin type) with thrombospondin type 1 motif, 18	3.87	0.02
1426150_at	<i>Gipc3</i>	GIPC PDZ domain containing family, member 3	3.76	0.02
1438194_at	<i>Slc1a2</i>	solute carrier family 1 (glial high affinity glutamate transporter), member 2	3.75	0.03
1433165_at	<i>4930570E01Rik</i>	RIKEN cDNA 4930570E01 gene	3.71	0.02
1444359_at	---	No transcripts are known to correspond to this probe set at this time, but a UniGene Cluster is known to correspond to it	3.70	0.03
1442022_at	<i>Tsepa</i>	thymocyte selection pathway associated	3.70	0.00
1435618_at	<i>Pnma2</i>	paraneoplastic antigen MA2	3.69	0.02
1431436_a_at	<i>Katnal2</i>	katanin p60 subunit A-like 2	3.66	0.02
1421422_at	<i>5033411D12Rik</i>	RIKEN cDNA 5033411D12 gene	3.65	0.02
1420418_at	<i>Syt2</i>	synaptotagmin II	3.62	0.02

Top 50 up-regulated genes in colon polyps in response to gefitinib exposure

Table 3.1. Top 50 up- and down-regulated genes (fold change ≤ 5 or ≥ 2 ; $P \leq 0.05$) based on microarray fold changes in *Apc^{min/+}* colon polyps in response to gefitinib at 4 hours

Probe Set ID	Gene Symbol	Gene Title	Fold change	P value
1455907_x_at	<i>Phox2b</i>	paired-like homeobox 2b	0.04	0.01
1459995_at	<i>1700015G11Rik</i>	RIKEN cDNA 1700015G11 gene	0.07	0.04
1447292_at	<i>Actr1b</i>	ARP1 actin-related protein 1 homolog B, centractin beta (yeast)	0.08	0.0001
1432877_at	<i>4930544N03Rik</i>	RIKEN cDNA 4930544N03 gene	0.09	0.001
1437899_at	<i>Lyg2</i>	lysozyme G-like 2	0.11	0.05
1430233_a_at	<i>Nhedc1</i>	Na ⁺ /H ⁺ exchanger domain containing 1	0.11	0.002
1440888_at	<i>Oxtr</i>	oxytocin receptor	0.13	0.02
1441695_at	---	Unclassifiable product	0.14	0.01
1444889_at	<i>Rassf2</i>	Ras association (RalGDS/AF-6) domain family member 2	0.14	0.02
1446115_at	---	Unclassifiable product	0.15	0.02
1421699_at	<i>Enam</i>	enamelin	0.15	0.02
1432481_a_at	<i>Lyzl6</i>	lysozyme-like 6	0.15	0.002
1444168_at	<i>Xpr1</i>	xenotropic and polytropic retrovirus receptor 1	0.15	0.05
1427393_at	<i>F9</i>	coagulation factor IX	0.15	0.02
1422349_at	<i>Ccr1l1</i>	chemokine (C-C motif) receptor 1-like 1	0.15	0.0006
1431976_at	<i>4930526F13Rik</i>	RIKEN cDNA 4930526F13 gene	0.16	0.05
1430112_at	<i>Wdr66</i>	WD repeat domain 66	0.16	0.0002
1437523_s_at	<i>Sgcg</i>	sarcoglycan, gamma (dystrophin-associated glycoprotein)	0.16	0.02
1440534_at	<i>ENSMUSG00000056615</i>	predicted gene, ENSMUSG00000056615	0.16	0.02
1443780_at	---	No transcripts are known to correspond to this probe set at this time, but a UniGene Cluster is known to correspond to it	0.17	0.0005
1449704_at	<i>C80171</i>	expressed sequence C80171	0.17	0.03
1443377_at	<i>Adam1a</i>	a disintegrin and metallopeptidase domain 1a	0.17	0.004
1453444_at	<i>5730437C12Rik</i>	RIKEN cDNA 5730437C12 gene	0.18	0.02
1429791_at	<i>A930004D18Rik</i>	RIKEN cDNA A930004D18 gene	0.18	0.001
1434614_at	---	hypothetical protein	0.18	0.02

Top 50 down-regulated genes in colon polyps in response to gefitinib exposure

Table 3.1. Top 50 up- and down-regulated genes (fold change ≤ 0.5 or ≥ 2 ; $P \leq 0.05$) based on microarray fold changes in *Apc^{min/+}* colon polyps in response to gefitinib at 4 hours

Probe Set ID	Gene Symbol	Gene Title	Fold change	P value
1445412_at	<i>Ccdc73</i>	coiled-coil domain containing 73	0.19	0.005
1441852_x_at	<i>Atg16l1</i>	autophagy-related 16-like 1 (yeast)	0.19	0.02
1420321_at	<i>Rsad1</i>	Radical S-adenosyl methionine domain containing 1, mRNA (cDNA clone MGC:170901 IMAGE:8862296)	0.19	0.03
1444249_at	---	No transcripts are known to correspond to this probe set at this time, but a UniGene Cluster is known to correspond to it	0.20	0.005
1457769_at	<i>H60a</i>	histocompatibility 60a	0.20	0.005
1458853_at	---	No transcript currently supports this probe set, though EST sequences are available from the design information.	0.20	0.01
1457876_at	<i>D9Ert496e</i>	DNA segment, Chr 9, ERATO Doi 496, expressed	0.21	0.04
1458102_at	---	Hypothetical protein	0.21	0.02
1430209_at	<i>4930404H21Rik</i>	RIKEN cDNA 4930404H21 gene	0.21	0.02
1443549_at	<i>4930579E17Rik</i>	RIKEN cDNA 4930579E17 gene	0.21	0.0002
1449378_at	<i>Krt27</i>	keratin 27	0.22	0.005
1425717_at	<i>Lrba</i>	LPS-responsive beige-like anchor	0.22	0.004
1430739_at	<i>4930471M09Rik</i>	RIKEN cDNA 4930471M09 gene	0.22	0.003
1442242_at	<i>C79127</i>	expressed sequence C79127	0.22	0.02
1419224_at	<i>Cecr6</i>	cat eye syndrome chromosome region, candidate 6 homolog (human)	0.22	0.02
1452437_at	<i>1110021J02Rik</i>	RIKEN cDNA 1110021J02 gene	0.22	0.01
1451600_s_at	<i>EG13909 /// Es31</i>	predicted gene, EG13909 /// esterase 31	0.22	0.003

Top 50 down-regulated genes in colon polyps in response to gefitinib exposure

Table 3.1. Top 50 up- and down-regulated genes (fold change ≤ 5 or ≥ 2 ; $P \leq 0.05$) based on microarray fold changes in *Apc^{min/+}* colon polyps in response to gefitinib at 4 hours

Probe Set ID	Gene Symbol	Gene Title	Fold change	P value
1455119_at	<i>Ppapdc1a</i>	phosphatidic acid phosphatase type 2 domain containing 1A	0.22	0.008
1437407_at	<i>Rnf222</i>	ring finger protein 222	0.22	0.008
1444873_at	---	No transcript currently supports this probe set, though EST sequences are available from the design information.	0.22	0.05
1419390_at	<i>Pde10a</i>	phosphodiesterase 10A	0.22	0.05
1442715_at	---	Unclassifiable product	0.23	0.008
1454114_a_at	<i>Nhedc1</i>	Na ⁺ /H ⁺ exchanger domain containing 1	0.23	0.003
1454308_at	<i>1700030C10Rik</i>	RIKEN cDNA 1700030C10 gene	0.23	0.003
1421763_at	<i>Bmp10</i>	bone morphogenetic protein 10	0.23	0.00004

chose candidates based on the magnitude of differential expression whilst also considering their biological relevance in the context of EGFR signalling biology and published literature. Fold change analysis (2.10.3) revealed 148 up- and 210 down-regulated transcripts (≥ 2 fold up or down-regulation with an associated P value of $P \leq .05$) in colon polyps in response to 4 hour gefitinib exposure. Table 3.1 is a selection of these genes, presenting the top 50 most up and down-regulated genes. This list of genes is complemented by table 3.2a and 3.2b which presents the top and bottom 50 genes differentially expressed according to ranked product computation (2.10.3) following 4 hour gefitinib exposure. By comparing the genes listed in these tables I searched for similarly expressed transcripts identified by both analyses. As a result *AT rich interactive domain 3B (BRIGHT-like) (Arid3b)*, *Cdc42 guanine nucleotide exchange factor (GEF) 9 (Arhgef9)*, *bone morphogenetic protein 10 (Bmp10)*, *EPH receptor A3 (Epha3)*, *guanine nucleotide binding protein (G protein), gamma 4 (Gng4)*, *oxytocin receptor (Oxtr)*, *paired-like homeobox 2b (Phox2b)* and *Ras association (RalGDS/AF-6) domain family member 2 (Rassf2)* were chosen for further assessment as potential indicators of response to EGFR blockade.

3.4.2 Time series regression analysis

The time-series regression analysis (2.10.2) provided details of temporal gene expression changes in colon polyps over 24 hours resulting from gefitinib exposure (Fig 3.6).

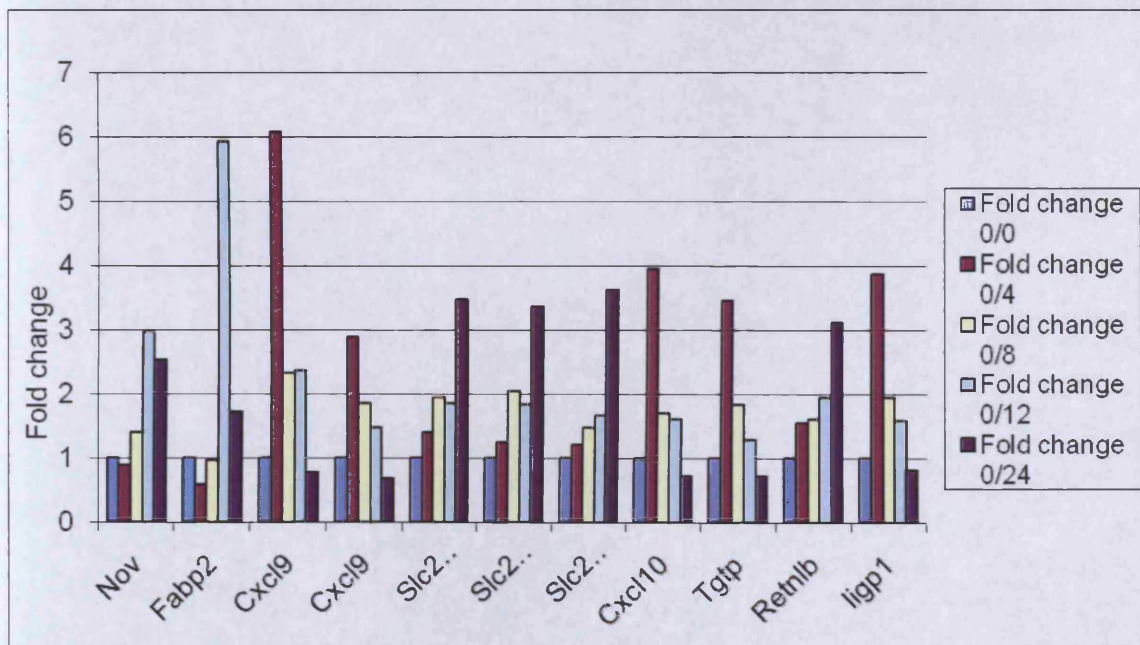


Table 3.2a. Top 50 ranked genes in *Apc^{min/+}* colon polyps in response to gefitinib

Probe Set ID	Gene Symbol	Gene Title
1430306_a_at	<i>Atp6v1c2</i>	ATPase, H ⁺ transporting, lysosomal V1 subunit C2
1439390_at	<i>1300018I17Rik</i>	RIKEN cDNA 1300018I17 gene
1425574_at	<i>Epha3</i>	Eph receptor A3
1437631_at	<i>Kcnip4</i>	Kv channel interacting protein 4
1439379_x_at	<i>Prm1</i>	protamine 1
1447626_x_at	<i>Arid3b</i>	AT rich interactive domain 3B (BRIGHT-like)
1438274_at	<i>Ikzf4</i>	IKAROS family zinc finger 4
1422214_at	<i>Npffr2</i>	neuropeptide FF receptor 2
1416776_at	<i>Crym</i>	crystallin, mu
1421561_at	<i>Bhlhe23</i>	basic helix-loop-helix family, member e23
1417943_at	<i>Gng4</i>	guanine nucleotide binding protein (G protein), gamma 4
1456248_at	<i>Lce3f</i>	late cornified envelope 3F
	<i>LOC630971</i>	hypothetical protein LOC630971
1420418_at	<i>Syt2</i>	synaptotagmin II
1431436_a_at	<i>Katnal2</i>	katanin p60 subunit A-like 2
1445187_at	<i>9430070013Rik</i>	RIKEN cDNA 9430070013 gene
1426150_at	<i>Gipc3</i>	GIPC PDZ domain containing family, member 3
1423328_at	<i>Gdap1</i>	ganglioside-induced differentiation-associated-protein 1
1438194_at	<i>Slc1a2</i>	solute carrier family 1 (glial high affinity glutamate transporter), member 2
1419220_at	<i>Xirp1</i>	xin actin-binding repeat containing 1
1416196_at	<i>Rpsa</i>	ribosomal protein SA
1449380_at	<i>Pacsin1</i>	protein kinase C and casein kinase substrate in neurons 1
1436258_at	<i>Arhgef9</i>	CDC42 guanine nucleotide exchange factor (GEF) 9
1453526_at	<i>4930503E14Rik</i>	RIKEN cDNA 4930503E14 gene

Table 3.2a. Top 50 ranked genes in *Apc^{min/+}* colon polyps in response to gefitinib

Probe Set ID	Gene Symbol	Gene Title
1444950_at	<i>Zfp509</i>	zinc finger protein 509
1444253_at	<i>Adamts18</i>	a disintegrin-like and metallopeptidase (reprolysin type) with thrombospondin type 1 motif, 18
1426132_at		methylase mRNA
1456814_at	<i>Rrp7a</i>	ribosomal RNA processing 7 homolog A (S. cerevisiae)
1438324_at	<i>9330182L06Rik</i>	RIKEN cDNA 9330182L06 gene
1432049_at	<i>4930422I22Rik</i>	RIKEN cDNA 4930422I22 gene
1454298_at	<i>4932430A15Rik</i>	RIKEN cDNA 4932430A15 gene
1444605_at	<i>1700061F12Rik</i>	RIKEN cDNA 1700061F12 gene
1451861_at	<i>Nxn12</i>	nucleoredoxin-like 2
1445930_at	<i>Fndc7</i>	fibronectin type III domain containing 7
1443599_at		Hypothetical protein
1438870_at	<i>Fbn1</i>	fibrillin 1
1438884_at	<i>Shisa3</i>	shisa homolog 3 (<i>Xenopus laevis</i>)
1433165_at	<i>4930570E01Rik</i>	RIKEN cDNA 4930570E01 gene
1431764_at	<i>2310067P03Rik</i>	RIKEN cDNA 2310067P03 gene
1453925_at	<i>4930429F24Rik</i>	RIKEN cDNA 4930429F24 gene
1446352_at		Hypothetical Alanine-rich region/Treacher Collins syndrome protein
1429933_at	<i>Agtbbp1</i>	ATP/GTP binding protein 1
1443126_at		Unclassifiable product
1447553_x_at	<i>Ric3</i>	CDNA clone IMAGE:40090175
1433145_at	<i>4933431C10Rik</i>	RIKEN cDNA 4933431C10 gene
1440945_at	<i>Glcci1</i>	Testthymin
1446211_at		CLONE=L0267B04 , EST
1448514_at	<i>Cox5b</i>	cytochrome c oxidase, subunit Vb
1442480_at		No transcripts are known to correspond to this probe set at this time, but a UniGene Cluster is known to correspond to it.
1444359_at		No transcripts are known to correspond to this probe set at this time, but a UniGene Cluster is known to correspond to it.
1445592_at		No transcript currently supports this probe set, though EST sequences are available from the design information.

Table 3.2b. Bottom 50 ranked genes in *Apc^{min/+}* colon polyps in response to gefitinib

Probe Set ID	Gene Symbol	Gene Title
1451600_s_at	<i>EG13909</i>	predicted gene, EG13909
...	<i>Es31</i>	esterase 31
1441852_x_at	<i>Atg16l1</i>	autophagy-related 16-like 1 (yeast)
1421763_at	<i>Bmp10</i>	bone morphogenetic protein 10
1449378_at	<i>Krt27</i>	keratin 27
1445412_at	<i>Ccdc73</i>	coiled-coil domain containing 73
1419390_at	<i>Pde10a</i>	phosphodiesterase 10A
1422349_at	<i>Ccr1l1</i>	chemokine (C-C motif) receptor 1-like 1
1443549_at	<i>4930579E17Rik</i>	RIKEN cDNA 4930579E17 gene
1421699_at	<i>Enam</i>	enamelin
1444889_at	<i>Rassf2</i>	Ras association (RalGDS/AF-6) domain family member 2
1432481_a_at	<i>Lyzl6</i>	lysozyme-like 6
1455119_at	<i>Ppapdc1a</i>	phosphatidic acid phosphatase type 2 domain containing 1A
1443377_at	<i>Adam1a</i>	a disintegrin and metallopeptidase domain 1a
1455907_x_at	<i>Phox2b</i>	paired-like homeobox 2b
1427393_at	<i>F9</i>	coagulation factor IX
1419224_at	<i>Cecr6</i>	cat eye syndrome chromosome region, candidate 6 homolog (human)
1437407_at	<i>Rnf222</i>	ring finger protein 222
1430209_at	<i>4930404H21Rik</i>	RIKEN cDNA 4930404H21 gene
1430112_at	<i>Wdr66</i>	WD repeat domain 66
1437523_s_at	<i>Sgcg</i>	sarcoglycan, gamma (dystrophin-associated glycoprotein)
1437899_at	<i>Lyz2</i>	lysozyme G-like 2
1425717_at	<i>Lrba</i>	LPS-responsive beige-like anchor
1454308_at	<i>1700030C10Rik</i>	RIKEN cDNA 1700030C10 gene
1440888_at	<i>Oxtr</i>	oxytocin receptor

Table 3.2b. Bottom 50 ranked genes in *Apc^{min/+}* colon polyps in response to gefitinib

Probe Set ID	Gene Symbol	Gene Title
1442242_at	<i>C79127</i>	expressed sequence C79127
1452437_at	<i>1110021J02Rik</i>	RIKEN cDNA 1110021J02 gene
1430233_a_at	<i>Nhedc1</i>	Na ⁺ /H ⁺ exchanger domain containing 1
1454114_a_at	<i>Nhedc1</i>	Na ⁺ /H ⁺ exchanger domain containing 1
1457769_at	<i>H60a</i>	histocompatibility 60a
1459995_at	<i>1700015G11Rik</i>	RIKEN cDNA 1700015G11 gene ARP1 actin-related protein 1 homolog B, centractin beta (yeast)
1447292_at	<i>Actr1b</i>	unclassifiable product
1442715_at		
1444168_at	<i>Xpr1</i>	xenotropic and polytropic retrovirus receptor 1
1441695_at		unclassifiable product
1458102_at		hypothetical protein
1429791_at	<i>A930004D18Rik</i>	RIKEN cDNA A930004D18 gene
1453444_at	<i>5730437C12Rik</i>	RIKEN cDNA 5730437C12 gene
1430739_at	<i>4930471M09Rik</i>	RIKEN cDNA 4930471M09 gene
1434614_at		hypothetical protein
1446115_at		unclassifiable product
	<i>ENSMUSG000000</i>	
1440534_at	<i>56615</i>	predicted gene, ENSMUSG00000056615
1431976_at	<i>4930526F13Rik</i>	RIKEN cDNA 4930526F13 gene
1432877_at	<i>4930544N03Rik</i>	RIKEN cDNA 4930544N03 gene
1449704_at	<i>C80171</i>	expressed sequence C80171 No transcripts are known to correspond to this probe set at this time, but a UniGene Cluster is known to correspond to it. No transcript currently supports this probe set, though EST sequences are available from the design information.
1444249_at		
1458853_at		
1420321_at	<i>Rsad1</i>	Radical S-adenosyl methionine domain containing 1, mRNA (cDNA clone MGC:170901 IMAGE:8862296) No transcript currently supports this probe set, though EST sequences are available from the design information.
1444873_at		
1443780_at		No transcripts are known to correspond to this probe set at this time, but a UniGene Cluster is known to correspond to it.
1457876_at	<i>D9Ertd496e</i>	DNA segment, Chr 9, ERATO Doi 496, expressed

Fig 3.6 Transcript changes in *Apc^{min/+}* colon polyps induced by gefitinib over 24 hours (time series regression analysis; gene false discovery rate ≤ 0.055). Plots show the gene fold changes calculated by expressing the ratio of mean geometric gene intensity values for gefitinib at 0-24 hours relative to time zero for each probe. Similar fold changes were also found by expressing the ratio of mean geometric gene intensity values for gefitinib and vehicle at each time point (data not shown). *Nov*, nephroblastoma over-expressed; *Fabp2*, fatty acid binding protein 2; *Cxcl9*, chemokine receptor ligand 9; *Slc26a3*, solute carrier family 26, member 3; *Cxcl10*, chemokine receptor ligand 10; *Tgtp*, Tcell-specific GTPase; *Retnlb*, resistin like beta; *ligp1*, Interferon inducible GTPase 1.

I next wished to test the accuracy of the microarray data by confirmatory qRT-PCR using a sample of genes identified by time series regression analysis, and the same microarray mRNA. This affirmed the capability of the microarray to detect expression changes in 5/6 genes tested by qRT-PCR (Fig 3.7).

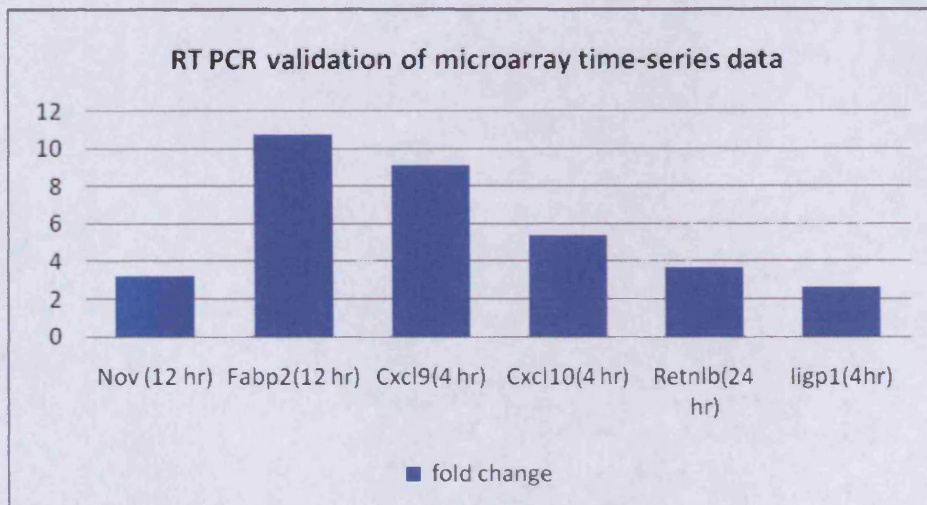


Fig 3.7 Validation of microarray transcript changes (time series regression model) by qRT-PCR using microarray mRNA. Primer design failed for *Tgtp* and *Slc26a3*. Fold changes all reach P values of 0.04 (Mann-Whitney) with the exception of *ligp1* which did not reach this level of significance.

As the time series regression analysis had identified differentially expressed genes related to gefitinib exposure, *chemokine (C-X-C motif) ligand 9 (Cxcl9)*, *chemokine (C-X-C motif) ligand 10 (Cxcl10)*, *T cell specific GTPase (Tgtp)* and *Interferon inducible GTPase 1*

Table 3.3. *Apc^{min/+}* colon polyp genes changes in response to gefitinib identified by SAM analysis

Probe set	Gene symbol	Description	Geom mean intensity T0 Gefitinib	Geom mean intensity T4 Gefitinib	Fold-change
1442786_s_at	<i>Rufy3</i>	RUN and FYVE domain containing 3	54.35	9.60	0.18
1424402_at	<i>Rufy3</i>	RUN and FYVE domain containing 3	151.97	29.07	0.19
1443746_x_at	<i>Dmp1</i>	dentin matrix protein 1	96.55	28.07	0.29
1455886_at	<i>Cbl</i>	Casitas B-lineage lymphoma	413.60	120.57	0.29
1452730_at	<i>Rps4y2</i>	ribosomal protein S4, Y-linked 2	152.68	52.45	0.34
1427515_at	<i>A530088/07Rik</i>	RIKEN cDNA A530088I07 gene	190.31	50.69	0.27
AFFX-BioC-5_at	NA	NA	743.50	274.67	0.37
1443745_s_at	<i>Dmp1</i>	dentin matrix protein 1	165.65	53.68	0.32
AFFX-BioC-3_at	NA	NA	841.14	327.05	0.39
1418652_at	<i>Cxcl9</i>	chemokine (C-X-C motif) ligand 9	381.33	2318.67	6.08
1420437_at	<i>Indo</i>	indoleamine-pyrrole 2,3 dioxygenase	125.52	872.97	6.95
1419734_at	<i>Actb</i>	actin, beta, cytoplasmic	476.91	2232.84	4.68
1417654_at	<i>Sdc4</i>	syndecan 4	415.35	1817.47	4.38
1417462_at	<i>Cap1</i>	CAP, adenylate cyclase-associated protein 1 (yeast)	112.29	479.67	4.27
1419762_at	<i>Ubd</i>	ubiquitin D	186.27	857.90	4.61
1435906_x_at	<i>Gbp2</i>	guanylate nucleotide binding protein 2	569.06	2644.60	4.65
AFFX-18SRNAMur/X0068_6_5_at	NA	NA	443.83	2498.81	5.63
1417461_at	<i>Cap1</i>	CAP, adenylate cyclase-associated protein 1 (yeast)	238.53	885.77	3.71
1418240_at	<i>Gbp2</i>	guanylate nucleotide binding protein 2	398.13	1674.11	4.20
1439197_at	<i>Pi4kb</i>	phosphatidylinositol 4-kinase, catalytic, beta polypeptide	54.56	178.35	3.27
1429509_at	<i>Lsm12</i>	LSM12 homolog (S. cerevisiae)	78.69	249.27	3.17
1449859_at	<i>Golt1b</i>	golgi transport 1 homolog B (S. cerevisiae)	58.30	182.65	3.13

Table 3.3. *Apc^{min/+}* colon polyp genes changes in response to gefitinib identified by SAM analysis

Probe set	Gene symbol	Description	Geom mean intensity T0 Gefitinib	Geom mean intensity T4 Gefitinib	Fold-change
1416497_at	<i>Pdia4</i>	protein disulfide isomerase associated 4	383.86	1167.22	3.04
1423411_at	<i>BC013481</i>	cDNA sequence BC013481	237.81	716.24	3.01
1431804_a_at	<i>Sp3</i>	trans-acting transcription factor 3	314.16	933.09	2.97
1439831_at	<i>EG240327</i>	predicted gene, EG240327	83.24	315.66	3.79
1419042_at	<i>ligp1</i>	interferon inducible GTPase 1	339.03	1315.63	3.88
1418930_at	<i>Cxcl10</i>	chemokine (C-X-C motif) ligand 10	259.98	1027.44	3.95
1418392_a_at	<i>Gbp3</i>	guanylate nucleotide binding protein 3	325.96	1120.22	3.44
1438676_at	<i>Mpa2l</i>	macrophage activation 2 like	155.88	546.18	3.50
1449009_at	<i>Tgtp</i>	T-cell specific GTPase	1570.79	5428.20	3.46
1449496_at	<i>2010109I03Rik</i>	RIKEN cDNA 2010109I03 gene	83.47	253.29	3.03
1438403_s_at	<i>Ramp2</i>	receptor (calcitonin) activity modifying protein 2	1594.34	5205.58	3.27
1427679_at	<i>Lats1</i>	large tumor suppressor	38.69	119.31	3.08

Table 3.3. *Apc^{min/+}* colon polyp genes changes in response to gefitinib identified by SAM analysis

Probe set	Gene symbol	Description	Geom mean	Geom mean	Fold-change
			intensity T0	intensity T4	
1418911_s_at	<i>Acsf4</i>	acyl-CoA synthetase long-chain family member 4	171.22	447.08	2.61
1435653_at	NA	NA	1061.63	3052.24	2.88
1422845_at	<i>Canx</i>	calnexin	919.39	2468.22	2.68
1418908_at	<i>Pam</i>	peptidylglycine alpha-amidating monooxygenase	68.48	177.39	2.59
1418536_at	<i>H2-Q8</i>	histocompatibility 2, Q region locus 8	598.81	1801.27	3.01
1426164_a_at	<i>Usf1</i>	upstream transcription factor 1	169.86	438.28	2.58
1449018_at	<i>Pfn1</i>	profilin 1	2996.31	7650.52	2.55
1437904_at	<i>Rbm45</i>	RNA binding motif protein 45	61.49	167.27	2.72
1417705_at	<i>Otub1</i>	OTU domain, ubiquitin aldehyde binding 1	249.87	615.28	2.46
1415801_at	<i>Gja1</i>	gap junction membrane channel protein alpha 1	152.52	432.10	2.83
AFFX-18SRNAMur/X00686_3_at	NA	NA	483.00	1298.97	2.69
1426226_at	<i>Dyrk1a</i>	dual-specificity tyrosine-(Y)-phosphorylation regulated kinase 1a	134.20	346.29	2.58
1417764_at	<i>Ssr1</i>	signal sequence receptor, alpha	417.63	1029.61	2.47
1421106_at	<i>Jag1</i>	jagged 1	42.08	102.73	2.44
1432646_a_at	<i>2900097C17Ri</i>	RIKEN cDNA	71.40	201.03	2.82
	<i>k</i>	2900097C17 gene			
1421341_at	<i>Axin2</i>	axin2	179.31	429.77	2.40
1447927_at	<i>Mpa2l</i>	macrophage activation 2 like	529.63	1592.47	3.01
1456907_at	<i>Cxcl9</i>	chemokine (C-X-C motif) ligand 9	116.60	336.36	2.88
1424101_at	<i>Hnrpl</i>	heterogeneous nuclear ribonucleoprotein L	387.43	910.47	2.35

The estimated false discovery rate among the 54 significant genes is 0.0087 and associated delta value used to identify the significant genes is 0.0469.

(*ligp1*) were chosen as candidates for qRT-PCR validation in biological replicate experiments. This was because these genes displayed altered expression levels at 4 hours, reflecting the same time point clinical samples would be available to interrogate the transcriptome, in response to cetuximab (Xerxes trial, 2.2.1).

3.4.3 AffymGUI and SAM analysis

AffymGUI analysis (2.10.1) identified a number of genes with less robust fold changes at 4 hours which did not all reach statistical significance but remained candidates in view of their potential biological relevance to EGFR signalling or blockade. Unfortunately SAM analysis (2.10.4) failed to identify gene changes with an acceptable FDR when comparing gefitinib induced changes at 4 hours relative to vehicle; 4 genes were each down-regulated including *ribosomal protein S4, Y-linked 2 (Rps4y2)*, *protease, serine, 22 (Prss22)*, *aquaporin 4 (Aqp4)* and *G protein-coupled receptor, family C, group 5, member A (Gprc5a)* (FDR 0.48 and delta value of 0.89). As none of these genes were obviously related to EGFR signalling and due to the poor FDR, they were disregarded as candidates for further assessment. However SAM analysis was extended to compare gefitinib induced gene changes at 4 hours relative to time zero (Table 3.3). This pragmatic approach led to the identification of *Cbl* (fold change 0.3; estimated FDR .009 and delta value .047) as a potential candidate of interest given its documented role in EGFR turnover¹⁴⁵⁻¹⁴⁷. It is worth noting that table 3.3 includes a number of genes first identified by the time series analysis (*Cxcl9*, *Cxcl10*, *ligp1* and *Tgtp*) and also *Ubd* (Ubiquitin D) which was identified as an up-regulated gene by the AffymGUI analysis and has biological relevance in terms of EGFR degradation¹⁴⁸. The SAM analysis also highlighted *Pi4kb* as a gene of potential interest given its association with phosphatidylinositol signal transduction downstream of EGFR.

As a consequence of the various analyses described above I have identified a list of candidate genes which are hypothesised to be potentially relevant in the prediction of response to EGFR targeted therapy in *K-RAS* wild type colorectal cancer (table 3.4). Target genes in this table have been expressed as 4 hour fold changes in response to gefitinib (relative to vehicle), indicating the method of microarray analyses used to identify

Table 3.4: Microarray detected gene expression fold changes in *K-ras* wild type *Apc^{min/+}* colon polyps in response to gefitinib at 4 hours: Candidates for qRT-PCR validation

Gene	Name	Probe Set	Fold change	t test	Analysis
<i>Areg</i>	amphiregulin	1421134_at	0.54	0.100	A
<i>Arhgef9</i>	CDC42 guanine nucleotide exchange factor (GEF) 9	1436258_at	6.79	0.022	F/R
<i>Arid3b</i>	AT rich interactive domain 3B (BRIGHT-like)	1447626_x_at	7.48	0.037	F/R
<i>Bcl2</i>	B-cell leukemia/lymphoma 2	1437122_at	1.32	0.152	A
<i>Bcl2L11</i>	BCL2-like 11 (apoptosis facilitator)	1435448_at	1.23	0.058	A
<i>Bmf</i>	BCL2 modifying factor	1422995_at	1.46	0.015	A
<i>Bmp10</i>	bone morphogenetic protein 10	1421763_at	0.23	0.00004	F/R
<i>Cbl</i>	casitas B-lineage lymphoma	1455886_at	.879	0.173	S
<i>Ccnd1</i>	cyclin D1	1417419_at	0.88	0.308	A
<i>Ccnd2</i>	cyclin D2	1416124_at	0.55	0.026	A
<i>Ccne1</i>	cyclin E1	1441910_x_at	0.79	0.036	A
<i>Ccne2</i>	cyclin E2	1422535_at	0.65	0.037	A
<i>Cxcl10</i>	chemokine (C-X-C motif) ligand 10	1418930_at	2.50	0.257	T
<i>Cxcl9</i>	chemokine (C-X-C motif) ligand 9	1418652_at	2.77	0.135	T
<i>Egfr</i>	epidermal growth factor receptor	1418349_at	0.74	0.013	A
<i>Emp1</i>	epithelial membrane protein 1	1459171_at	0.49	0.044	F
<i>Epha3</i>	eph receptor A3	1425574_at	6.72	0.022	A/F/R
<i>ErbB3</i>	v-erb-b2 erythroblastic leukemia viral oncogene homolog 2, neuro/glioblastoma derived oncogene homolog (avian)	1434606_at	1.20	0.069	A
<i>ErbB4</i>	v-erb-a erythroblastic leukemia viral oncogene homolog 4 (avian)	1427783_at	1.90	0.476	R
<i>Ereg</i>	epiregulin	1419431_at	0.63	0.260	A

Table 3.4: Microarray detected gene expression fold changes in *K-ras* wild type *Apc^{min/+}* colon polyps in response to gefitinib at 4 hours. Candidates for qRT-PCR validation

Gene	Name	Probe Set	Fold change	t test	Analysis
<i>Gng4</i>	guanine nucleotide binding protein (G protein), gamma 4	1417943_at	5.86	0.0004	F/R
<i>Hbegf</i>	heparin-binding EGF-like growth factor	1418350_at	0.64	0.018	A
<i>Hip1</i>	huntingtin interacting protein 1	1434557_at	1.27	0.064	A
<i>Iigp1</i>	interferon inducible GTPase 1	1419042_at	2.50	0.124	T
<i>Ikbkg</i>	inhibitor of kappaB kinase gamma	1435647_at	2.41	0.017	F
<i>Oxtr</i>	oxytocin receptor	1440888_at	0.13	0.022	F/R
<i>Phox2b</i>	paired-like homeobox 2b	1455907_x_at	0.04	0.011	F/R
<i>Pi4kb</i>	Phosphatidylinositol 4-kinase, catalytic, beta polypeptide	1439197_at	1.08	0.367	S
<i>Plcd4</i>	phospholipase C, delta 4	1437030_at	2.02	0.007	F
<i>Ptprd</i>	protein tyrosine phosphatase, receptor type, D	1444492_at	0.43	0.014	F
<i>Rassf2</i>	ras association (RalGDS/AF-6) domain family member 2	1444889_at	0.14	0.023	F/R
<i>Tgtp</i>	T-cell specific GTPase 2	1449009_at	2.41	0.111	T
<i>Ubd</i>	ubiquitin D	1419762_at	2.44	0.106	A/S

Shown are the calculated fold changes (Gefitinib: vehicle at 4 hours) for each gene along with its associated P value. Candidates were selected from genes identified by analysis of microarray data using AffyImGUI, time series regression analysis, fold change, ranked products and SAM analysis and were chosen based on their repeated differential expression by different analysis methods, magnitude of differential expression and/or biological relevance to EGFR signalling/blockade. Microarray analysis method leading to target identification, A, AffyImGui; F, fold change; R, ranked products; S, SAM; T, time-series regression analysis.

Table 3.5 qRT-PCR validation of targets identified by microarray using biological replicate experiments of 4 hour gefitinib and ME1 exposure

Gene	Microarray	qRT-PCR	
	Fold change of colon polyp transcript		
	Gef:Veh (4hr)	Gef:Veh (4hr)	ME1:Veh (4hr)
Areg	0.54	0.5	0.8
Arhgef9	6.79	3.3	1.9
Arid3b	7.48	1.2	-
Bcl2	1.32	1.4	1
Bcl2L11	1.23	0.8	-
Bmf	1.46	3.8	1.9
Bmp10	0.23	<i>fp</i>	<i>fp</i>
Cbl	0.879	2.4	1.4
Ccnd1	0.88	1	-
Ccnd2	0.55	1	-
Ccne1	0.79	1	-
Ccne2	0.65	0.6	0.6
Cxcl10	2.5	0.2	1.27
Cxcl9	2.77	0.2	0.7
Egfr	0.74	1.4	1.6
Emp1	0.49	1.37	-
Epha3	6.72	2.1	2
ErbB3	1.2	2.1	0.4
ErbB4	1.9	<i>fp</i>	<i>fp</i>
Ereg	0.63	0.4	0.7
Gng4	5.86	1.2	-
Hbegf	0.64	0.7	-
Hip1	1.27	1.7	1.2
ligp1	2.5	0.2	-
lkbkg	2.41	3.4	1.5
Oxtr	0.13	1	-
Phox2b	0.04	<i>fp</i>	<i>fp</i>
Pi4kb	1.08	1.2	-
Plcd4	2.02	2.2	2.3
Ptprd	0.43	1.7	1.3
Rassf2	0.14	1.9	1
Tgtp	2.41	<i>fp</i>	<i>fp</i>
Ubd	2.44	0.3	0.6

Bold red text indicates fold changes that reached P values of 0.04 (Mann-Whitney). Unless target expression was significantly altered by gefitinib it was not selected for detection of altered expression in response to ME1 (with the exception of EGFR). Genes with altered expression following exposure to both agents became definitive candidates of response to EGFR blockade (highlighted). *fp* failed primers. See 2.3.2.2 for further details of methods

transcripts. As transcripts have been expressed in this way, some of the gene fold changes no longer appear remarkable and/or have non-significant P values.

3.5 qRT-PCR validation of microarray candidate genes

My next task was to validate the candidate genes identified by the various microarray analyses. The genes altered in response to Egfr blockade (table 3.4) underwent evaluation by qRT-PCR, using colon polyp RNA from biological replicate animal experiments exposed to gefitinib and monoclonal antibody raised against murine Egfr, ME1 (2.3.2.2). Gene targets which displayed altered expression on qRT-PCR across such replicate experiments were deemed definitive candidates of response to EGFR blockade (table 3.5). In essence if a candidate gene in table 3.5 demonstrated significantly altered expression in response to gefitinib by qRT-PCR it was similarly assessed for transcript change in response to ME1. By taking this approach it was possible to identify 11 transcripts differentially expressed in response to EGFR blockade by either gefitinib or ME1 exposure. These genes included *Bmf*, *Cas-Br-M (murine) ecotropic retroviral transforming sequence (Cbl)*, *Ccne2*, *Cxcl9*, *Epha3*, *ErbB3*, *Epiregulin (Ereg)*, *huntingtin interacting protein 1 (Hip1)*, *inhibitor of kappa light polypeptide gene enhancer in B-cells, kinase gamma (Ikbkg)*, *phospholipase C, delta 4 (Plcd4)* and *ubiquitin D (Ubd)*. As indicated it was not possible to design primers for all possible transcripts under scrutiny (*Bmp10*, *ErbB4*, *Phox2b* and *Tgtp*) due to: (i) failure to map to the specific gene *in silico* (*Tgtp* and *Bmp10*), (ii) failure of primers to amplify a product (*ErbB4*) and (iii) failure of primers to amplify PCR product due to insufficient sample template (*Phox2b*). *Ilgp2* was not assessed in response to ME1.

3.6 Colon polyp transcript expression following chronic gefitinib exposure

I next sought to examine the relationship between immediate transcript responses to gefitinib and those induced after long term exposure as a means of exploring novel mechanism potentially mediating resistance to Egfr blockade. Table 3.6 shows the transcript changes in *Apc^{min/+}* colon polyps after chronic exposure to gefitinib 75mg/kg in relation to acute transcripts changes, for each of the 11 candidate genes, induced by gefitinib 75mg/kg and ME1 1mg. *Bmf*, *Cbl*, *ErbB3*, *Hip1* and *Ikbkg* are each up-regulated after 4 hour exposure to gefitinib and remain up-regulated after chronic dosing when tumours have become resistant to Egfr blockade, following increased *Apc^{min/+}* longevity (5.3.1). *Cxcl9* and *Ubd* are

Table 3.6 Acute and chronic transcript changes in *Apc^{min/+}* colon polyps following short term gefitinib or ME1 and long term gefitinib exposure.

Gene	Fold change (qRT-PCR)		
	Acute		Chronic
	Gef:Veh	ME1:Veh*	Gef:Veh**
<i>Bmf</i>	3.8	1.9	3.6
<i>Cbl</i>	2.4	1.4	3.2
<i>Ccne2</i>	0.6	0.6	-
<i>Cxcl9</i>	0.2	0.7	9.2
<i>Epha3</i>	2.1	2	-
<i>ErbB3</i>	2.1	0.4	5.8
<i>Ereg</i>	0.4	0.7	-
<i>Hip1</i>	1.7	1.2	3.6
<i>Ikbkg</i>	3.4	1.5	4.1
<i>Plcd4</i>	2.2	2.3	-
<i>Ubd</i>	0.3	0.6	2.8

qRT-PCR transcript fold changes are presented for the definitive hypothetical candidate biomarkers of response to anti-EGFR therapy in *Apc^{min/+}* colon polyps . The mice receiving chronic daily gefitinib (75mg/kg) are described in section 2.1.3.3 (cohort A) and 2.3.2.3. Acute refers to transcript changes at 4hrs in response to gefitinib 75mg/kg (Gef) or ME1 1mg dose. Chronic transcripts were assessed in colon polyps obtained from *Apc^{min/+}* mice culled following long term gefitinib. '-' indicates transcript not yet assessed by qRT-PCR. Veh, 0.5% Tween 80 ; Veh* 1XPBS; Veh**, 1% Tween80.

initially down-regulated in response to acute gefitinib exposure and subsequently up-regulated in colon polyps after chronic gefitinib treatment. Results are not yet available for *Ccne2*, *Epha3*, *Ereg* and *Plcd4* transcripts following chronic treatment with gefitinib.

3.7 Protein validation of candidate transcripts of response to EGFR blockade

Given the identification of prospective candidate biomarkers for response to Egfr antagonism (table 3.5), I next wanted to validate these changes at the protein level. This was achieved by western blotting (2.6). Of the specific antibodies available and that worked against the total proteins of interest (table 2.7) no differences were identified on blots comparing 4 hour ME1 exposure to vehicle (fig 3.8 A,B). In light of this, I probed protein changes at 8 hours in response to gefitinib on the basis there may be a delay between transcript alterations and protein translation. Protein probing at 8 hours induced by gefitinib compared to vehicle (fig 3.9 A) identified increased Cbl expression (1.06 ± 0.48 [Veh] vs 2.27 ± 0.35 [Gef], $P=0.04$, Mann-Whitney; fig 3.9C) and decreased protein expression of *Ccne2* (0.81 ± 0.12 [Veh] vs 0.33 ± 0.12 [Gef], $P=0.04$, Mann-Whitney; fig 3.9D), in keeping with the transcript changes demonstrated at 4 hours by Egfr blockade.

3.8 Probing human transcriptome data (GSE5851) for mouse candidate genes which dichotomise patient outcome

I next wished to find evidence that the *Apc*^{min/+} mouse candidate biomarkers of response to Egfr blockade might be retrospectively applied to human colorectal cancer transcriptome data, and predict the outcome of cetuximab monotherapy. Fortunately, the Khambata-Ford GSE 5851 dataset²⁴ provided Affymetrix expression level data from rectal cancer specimens and response outcome to cetuximab monotherapy in 68 patients with metastatic colorectal cancer (2.10.5). Thirty-nine patients were *K-RAS* wild type, 20 *K-RAS* mutant and 9 of unknown *K-RAS* status. I found that of the 11 mouse colon tumour transcripts hypothesised to predict response to Egfr targeted therapy (table 3.5) *IKBK* ($P=0.043$), *CXCL9* ($P=0.017$) and *CCNE2* ($P=0.032$) were found to be differentially expressed in the disease control versus non-responder (to cetuximab) groups in *K-RAS* wild type colorectal cancer patients (table 3.7). These transcripts may therefore represent novel biomarkers of response prediction to anti-EGFR therapy.

Fig 3.8 Protein validation of *Apc^{min/+}* colon polyp transcript changes induced by ME1 (4 hr)

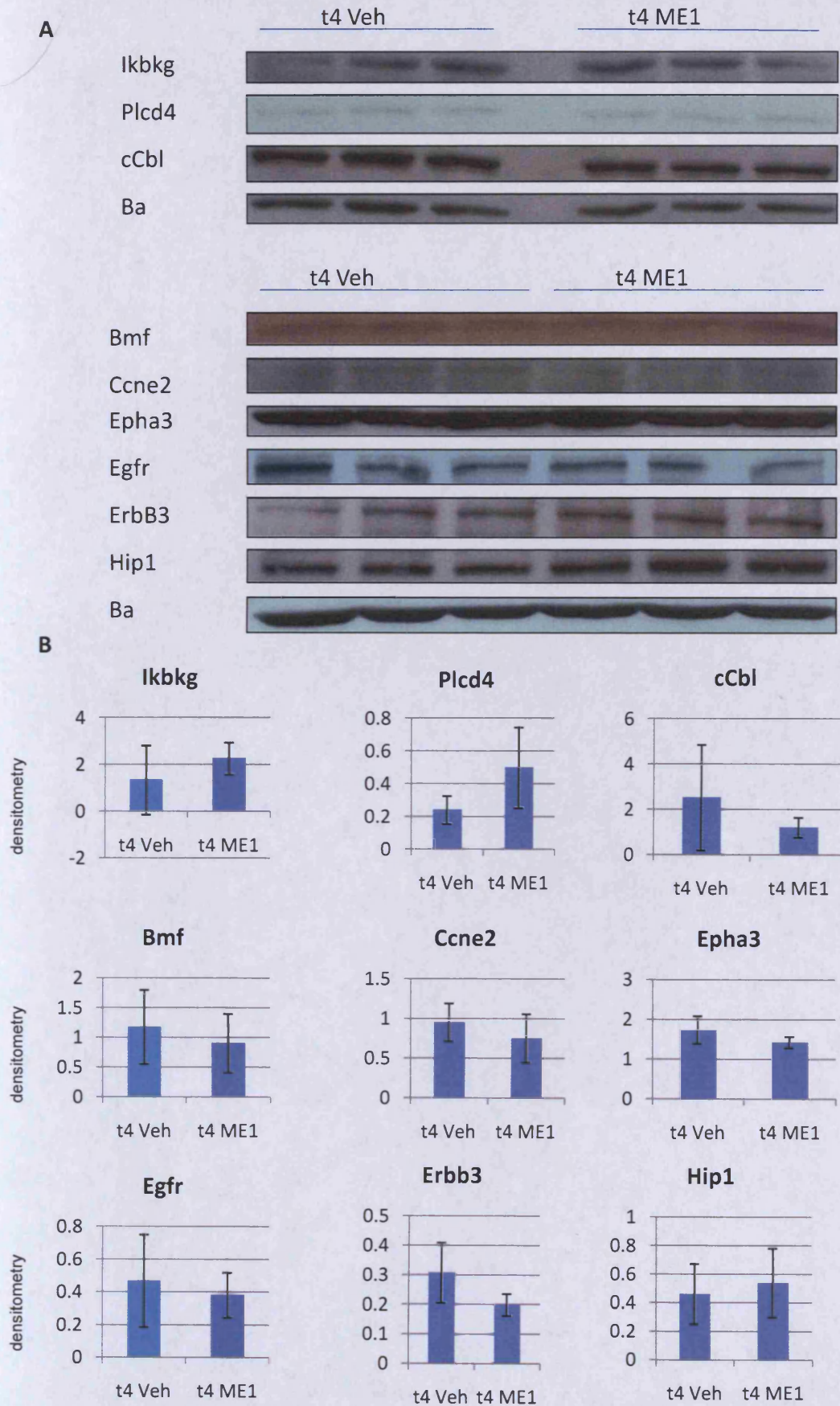


Fig 3.8 (A) Western blots of respective proteins ; t4 Veh, 4 hr exposure to 1X PBS; t4 ME1, 4 hr exposure to monoclonal antibody targeting EGFR , ME1(1mg). (B) Densitometry for each protein. See table 2.7 for protein molecular weights. Ba, beta actin. See methods 2.5.6.2 for details of colon polyp pooling. Error bars represent ±1 standard deviation.

Fig 3.9 Protein validation of *Apc^{min/+}* colon polyp transcript changes induced by gefitinib (8 hr)

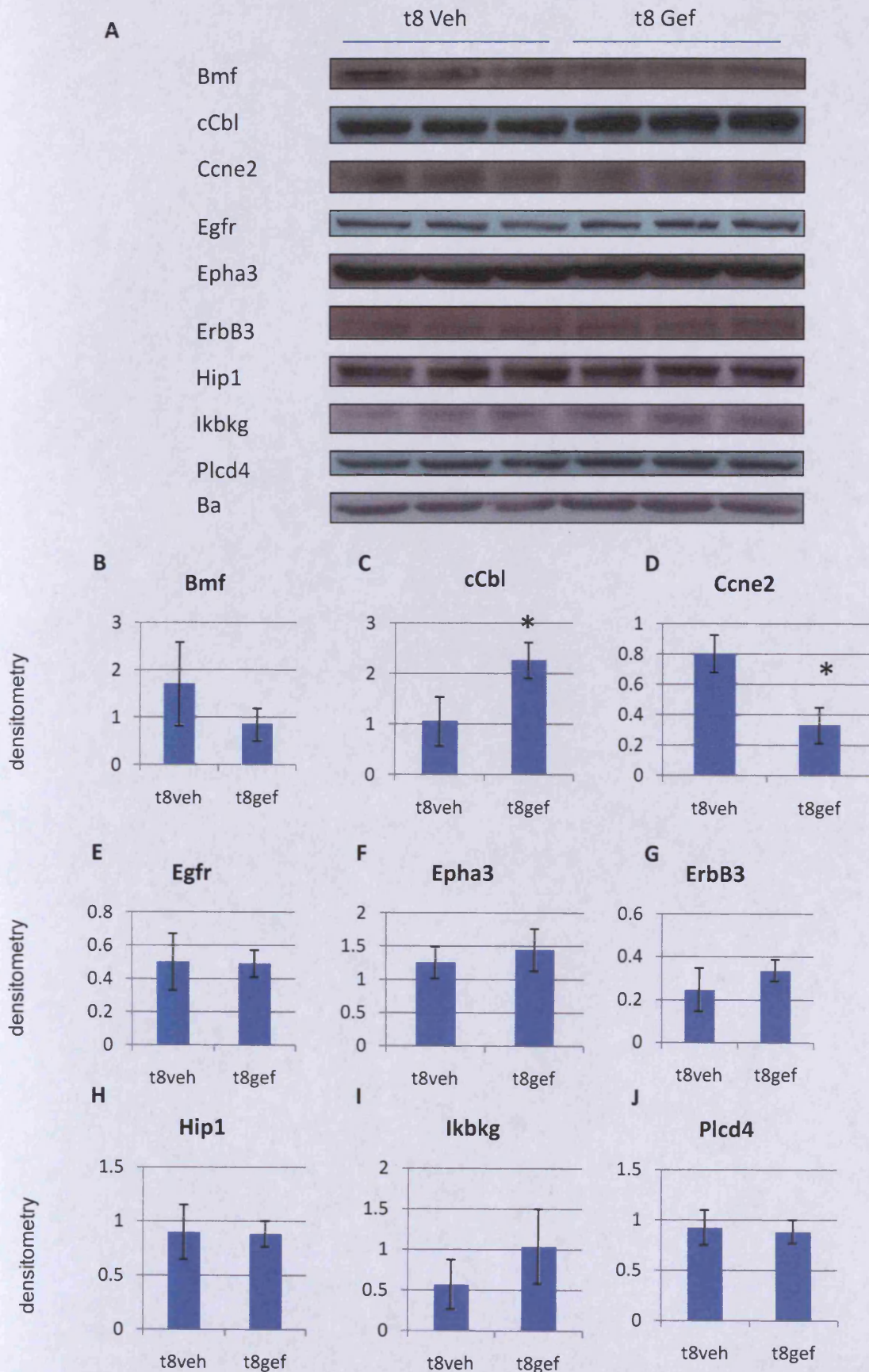


Fig 3.9 (A) Western blots of respective proteins; t8 Veh, 8 hr exposure to 0.5% Tween 80; t8 Gef, 8 hr exposure to gefitinib 75mg/kg. (B) Densitometry graph for each protein. * P=0.04 (Mann-Whitney). See table 2.7 for protein molecular weights. Ba, beta actin. See methods 2.5.6.2 for details of colon polyp pooling. Error bars represent ± 1 standard deviation

Table 3.7 Human rectal cancer transcriptome (GSE5851) probing by novel mouse candidate genes. The included mouse transcripts were present amongst the 17137 probe sets expressed in at least 10% of liver metastases samples²⁴. Bold text highlights human transcripts, identified using *Apc^{min/+}* colon polyp transcript expression changes in response to Egfr antagonism, which dichotomise response outcome to cetuximab. Disease status refers to outcomes following cetuximab monotherapy. DCG, disease control group; NR, non responder group. P value is for two-sided unequal-variance test performed on all 17137 probe sets²⁴

Gene Symbol	Affymetrix probe set	P value (t test DCG vs NR)	Gene title
CXCL9	203915_at	0.017	Chemokine (CXC type) ligand 9
CCNE2	211814_s_at	0.032	Cyclin E2
<i>EREG</i>	205767_at	1.474E-05	Epiregulin
<i>EPHA3</i>	206071_s_at	0.794	Ephrin receptor A3
<i>ERBB3</i>	202454_s_at	0.434	v-erb-b2 erythroblastic leukemia viral oncogene homolog 3 (avian)
<i>IKBKG</i>	209929_s_at	0.500	Inhibitor of kappa light polypeptide gene enhancer in B-cells, kinase gamma
IKBKG	36004_at	0.043	Inhibitor of kappa light polypeptide gene enhancer in B-cells, kinase gamma
<i>HIP1</i>	205425_at	0.502	Huntingtin interacting protein 1
<i>HIP1</i>	205426_s_at	0.720	Huntingtin interacting protein 1
<i>UBD</i>	205890_s_at	0.140	Ubiquitin D

3.9 Affymetrix expression values for genes discriminating patient outcome (GSE5851 dataset)

Figure 3.10 Affymetrix expression values for genes discriminating patient outcome in response to cetuximab monotherapy.

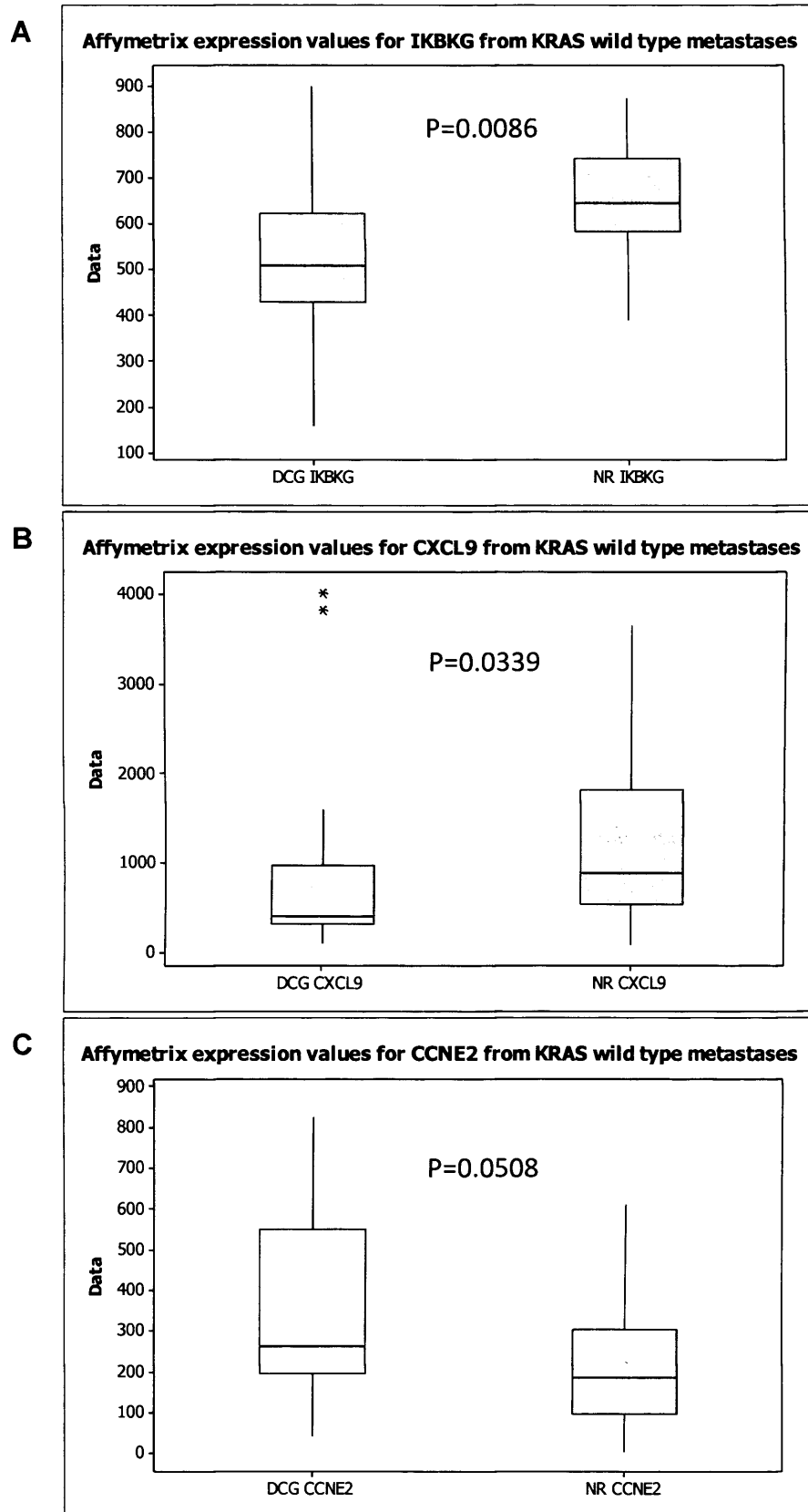


Fig 3.10 Transcripts were identified by searching *K-RAS* wild type metastatic colorectal cancer transcriptomes (GSE5851 dataset) for 11 mouse candidate genes altered in response to anti-EGFR exposure in *Apc^{min/+}* colon polyps. Median expression values were calculated using data from patients with *K-RAS* wild type colorectal metastases with either disease control (DCG) or non response to cetuximab (NR). Statistical comparisons used the Mann-Whitney test.

Having identified 3 genes which indicate response outcome to cetuximab therapy in colorectal cancer, I next wished to identify the median expression values for each of the genes in relation to outcome. The calculated median gene expression values for *CXCL9*, *CCNE2* and *IKBKG* from patients with *K-RAS* wild type metastatic colorectal cancer (2.10.05) are presented in figure 3.10. In the disease control groups *IKBKG* (P=0.0086) and *CXCL9* (P=0.0339) transcripts were both suppressed whereas *CCNE2* (P=0.0508) was increased relative to the non responding patients.

3.10 Probing Xerxes trial rectal cancer specimens for the expression of putative candidates of response to targeted anti-EGFR therapy identified using the *Apc^{min/+}* mouse.

My initial intention was to examine the expression of candidate genes, identified by the *Apc^{min/+}* mouse, in multiple rectal cancer specimens following a four hour infusion of cetuximab. However, in view of the difficulties recruiting to the Xerxes trial, a limited amount of tissue was available for such purposes. Despite this, paired human rectal cancer specimens (2.3.2.5) pre and post exposure to neo-adjuvant cetuximab were probed for 6/11 putative mouse colon tumour candidate genes postulated to be biomarkers of response to anti-EGFR exposure. Satisfactory rectal cancer biopsy samples were only available from two Xerxes trial patients harbouring *K-RAS* and *B-RAF* wild type rectal cancer (table 3.8). Unfortunately RNA quantity limited the number of transcripts that could be analysed by qRT-PCR. A 5-fold reduction in the level of tumoural *BMF* was induced at 4 hours by cetuximab infusion in patient 1 (pyT3N0 rectal cancer) whereas a 3-fold reduction in *BMF* was accompanied by a 5 and 3-fold reduction in *EPHA3* and *IKBKG* respectively in patient 2 (pyTON0 rectal cancer) in response to cetuximab. Both subjects, when last assessed, were free from disease recurrence at 3.5 years post diagnosis.

Table 3.8 *Apc^{min/+}* directed transcript expression levels in rectal cancer specimens from the Xerxes trial

Pat	Date of diagnosis	<i>K-RAS/B-RAF</i> status	% Tumour in sample		Pathol. stage	Last alive and well	<i>Apc^{min/+}</i> directed transcript expression fold change (Cetuximab 4 hours: Baseline)										
			baseline	4 hr			<i>BMF</i>	<i>CBL</i>	<i>CCNE2</i>	<i>CXCL9</i>	<i>EPHA3</i>	<i>ERBB3</i>	<i>EREG</i>	<i>HIP1</i>	<i>IKBKG</i>	<i>PLCD4</i>	<i>UBD</i>
1	14/10/2005	wt	70	40	pyT3N0	01/02/2009	0.2	0.4	-	-	0.6	0.5	-	2	3.1	-	-
2	21/11/2005	wt	40	40	pyTON0	01/03/2009	0.3	0.9	-	-	0.2	0.4	-	2.1	0.3	-	-

qRT-PCR was undertaken to obtain cetuximab induced transcript changes in rectal cancer specimens at 4 hours relative to baseline (time zero). Bold red figures signify fold changes reaching P=0.04. Limited RNA yield has prevented testing all transcripts of interest. Pat, patient; wt, wild type mutation status.

3.11 Discussion

The failure to identify common mutations in either *K-ras* or *B-raf* in colon polyps from *Apc^{min/+}* mice underscores the suitability of this mouse for the study of *K-RAS* and *B-RAF* wild type colon cancer. This has therefore offered an opportunity to translate the acute gene expression changes in response to Egfr blockade, to patients with *K-RAS* and *B-RAF* wild type colorectal cancer, in terms of hypothetical response prediction.

3.11.1 Acute pharmacodynamic effects of Egfr inhibition in *Apc^{min/+}* intestinal tumours

3.11.1.1 Apoptosis and cell proliferation

To be confident that the doses of tyrosine kinase inhibitor gefitinib (75mg/kg) and rat monoclonal antibody against Egfr, ME1 (1mg) administered to *Apc^{min/+}* mice were relevant, in terms of induced tumour gene expression changes, it was important to document phenotypic changes in intestinal tumours consequent upon drug administration. The single 4 hour dose of gefitinib 75mg/kg was sufficient to induce apoptosis as evidenced by increased H and E and elevated cleaved caspase-3 scoring in small intestinal microadenomas. In addition evidence of mitotic arrest was suggested by an increase in mitotic index without a demonstrable change in Brdu cell labelling (fig 3.2 A-D;G). Furthermore, in colon polyps, acute exposure to gefitinib inhibited cell cycling based upon reduced Brdu tumour cell labelling, in the absence of a change in mitotic activity (fig 3.2 E and F). These findings are in keeping with pro-apoptotic and anti-proliferative effects of gefitinib described *in vitro* using A431 cell lines¹³².

The only published report exploring the therapeutic effects of the monoclonal antibody targeting mouse Egfr, ME1, describes its effects on murine liver regeneration¹³⁷. Hence this is the first description of its *in vivo* anti-tumour effects. In small intestinal tumours, a single 1mg dose of ME1, at 4 hours leads to a decrease in Ki67 cell immunostaining (fig 3.3 D), indicative of reduced cell cycle progression and proliferation, without changes in cell death (fig 3.3 A,B). In colon tumours, ME1 resulted in increased mitotic scoring in the absence of change in Brdu cell labelling, suggestive of M phase arrest (fig 3.3 E-H). ME1 therefore has a predominant effect on the cell cycle in intestinal tumours without induction of apoptosis, at least at 4 hours following a single dose of 1mg.

Transcript changes were next sought to help understand the mechanism of pro-apoptotic and anti-proliferative changes seen in tumour tissue as a result of anti-Egfr exposure. This was achieved by examining gene expression in colon polyps (fig 3.4). It is attractive to speculate that the pro-apoptotic genes *Bak1*, *Bax* and *Bmf*, and reduced expression *Ccne2*, a component of cell cycle control, account at least in part for the phenotypic changes seen in small and large intestinal tumours in response to gefitinib. Furthermore, as these transcripts are from colon tumours, one might anticipate similar phenotypic change in small and large intestinal tumours, but failure to demonstrate increased apoptosis in colon tumours in response to gefitinib, may be explained by altered post transcriptional dynamics between these two tissues.

When examining the same transcripts in colon polyps exposed to ME1, only *Bmf* and *Ccne2* show altered expression. This would naturally lead to a prediction of induced apoptosis and inhibition of cell cycle/proliferation. However, given the demonstration of only altered cell cycling in both small and large intestinal tumours it may be that *Bmf* alone is not sufficient to induce apoptosis, or reflect a failure to detect apoptotic change in response to increased *Bmf*, as a consequence of a single time point being examined.

Despite these observations, it has been shown that acute exposure of *Apc^{min/+}* mice to gefitinib and ME1 leads to morphological and transcriptional changes in intestinal tumours indicative of either increased apoptosis or decreased cell cycling, confirming the biological appropriateness of the chosen drug doses. Furthermore is it attractive to suppose that early light microscopic assessments of tumour responses to treatment may act as a surrogate for long term treatment outcome, such that prolonged treatment with gefitinib or ME1 would suppress the *Apc^{min/+}* phenotype and translate into a survival advantage. Indeed this has been shown for the long term treatment with gefitinib 75mg/kg (5.3.1).

3.11.1.2 Egfr signalling

As anticipated, Egfr antagonism with gefitinib 75mg/kg resulted in reduced phosphorylation of Egfr, Erk and Akt in colon polyps from *Apc^{min/+}* mice (fig 3.5 A-D). This supports previous publications showing reduced auto-phosphorylation of EGFR by gefitinib¹³¹ and similar effects on normal mouse intestine¹⁴⁹. Interestingly, gefitinib also gave rise to increased phosphorylation of Igf1r in keeping with reports citing this as an escape

mechanism in response to EGFR antagonism⁸⁰⁻⁸² (figure 3.5 E) and forms the basis of further experiments in chapter 5.

Despite ME1 having previously been shown, at a dose of 1mg, to suppress Egfr phosphorylation in regenerating hepatocytes at tyrosine residue 992¹³⁷, no difference in Egfr phosphorylation was documented at tyrosine residue 1068, although Erk phosphorylation was inhibited downstream (fig 3.5 F-H). It is probable therefore that tyrosine residues other than 1068 display altered phosphorylation in response to ME1 leading to alterations in Erk phosphorylation, at least in colonic polyps.

3.11.2 Transcript expression changes in *Apc*^{min/+} colon polyps induced by Egfr antagonism

3.11.2.1 Microarray

In an attempt to maximise the amount of useful data provided by the microarray platform, different approaches to the analysis were adopted as described (3.4). As a consequence of this process, genes identified by the microarray were chosen as potential candidates of response prediction to Egfr targeted therapy in *K-ras* wild type colon polyps and by inference *K-RAS* wild type colorectal cancer (table 3.4).

All of the microarray gene expression analyses considered fold change differences in response to 4 hour exposure to gefitinib (75mg/kg) relative to vehicle (0.5% Tween⁸⁰) except, in an extended SAM analysis, where the comparison in transcript expression was between 4 hour gefitinib exposure relative to transcripts at time zero, immediately following an injection of gefitinib. This was undertaken as SAM analysis results were disappointing given the failure to identify genes with an acceptable false discovery rate (only 4 genes discovered with FDR of 0.48) in response to gefitinib. It could be argued that as the translational end-point is to relate transcripts from mouse to rectal cancer transcripts, this latter comparison is a closer reflection of what is happening in patients: sequential tumour transcript examination, without vehicle controls. However, this clearly makes no allowance for gene expression changes induced by vehicle, which is taken into consideration when transcript changes are expressed relative to 4 hour vehicle exposure, which was the preferred approach. Given that professional bioinformatics assistance was not used in the analysis of the microarray data, it is possible that further examination will

reveal important gene expression changes related to gefitinib exposure. Future analyses may include gene set enrichment analysis to identify pathway activation or suppression in response to Egfr blockade and a search for common transcription factors which regulate the expression of genes.

The fold change computations revealed 148 up- and 210 down-regulated genes in colon polyps following acute gefitinib 75mg/kg exposure. This relatively modest number of differentially expressed genes reflects the pooling methodology chosen which is reported to reduce the number of transcripts identified (by up to 50%) when compared to individual sample analysis¹⁵⁰. The time series regression analysis enabled identification of 4 genes differentially expressed at 4 hours including *Cxcl9*, *Cxcl10*, *Tgtp* and *ligp1* (fig 3.6) and also served as the basis for validation of the microarray by qRT-PCR using the same RNA. It is interesting to note that these genes were transiently increased at the 4 hour time point and thereafter, expression levels rapidly fell over 8-24 hours. This supports the existence of auto-regulatory pathways¹⁵¹, activated in response to Egfr blockade, which are capable of suppressing transcript expression. Auto-regulatory pathways have been observed in intestinal tumours expressing *K-Ras*^{G12D}, where despite the presence of Mek activity, downstream Erk phosphorylation is not detected due to elevated concentrations of Mkp3, an Erk phosphatase¹⁵². Despite the limitations of primer design for *Tgtp* and *Slc26a3*, the array correctly identified 5 of 6 genes with altered expression over 24 hours (fig 3.7).

All of the candidate genes of response to Egfr blockade, identified by the various microarray analyses (table 3.4), underwent evaluation by qRT-PCR using colon polyps from biological replicate animal experiments, exposed to gefitinib and subsequently ME1. This enabled the creation of a definitive list of putative biomarkers of response to Egfr exposure including *Bmf*, *Cbl*, *Ccne2*, *Cxcl9*, *Epha3*, *Erb3*, *Ereg*, *Hip1*, *Ikbkg*, *Plcd4* and *Ubd* (table 3.5).

3.11.2.1.1 Comparison of microarray and qRT-PCR results for gefitinib.

Of the definitive candidate genes of response to Egfr blockade listed in table 3.5 there is agreement between the fold change direction predicted by microarray and qRT-PCR results for gefitinib with the exception of *Cbl*, *Cxcl9* and *Ubd*. It is worth noting however that when these three genes are presented in the format of microarray fold changes (table 3.4; 4 hours gefitinib: 4 hour vehicle) none of the P values reached statistical significance showing

that the microarray failed to identify true differences in expression regardless of its direction based on qRT-PCR findings.

3.11.2.1.2 Comparison of qRT-PCR transcript changes for gefitinib and ME1.

The fold change direction of qRT-PCR data obtained for gefitinib and ME1 biological replicates are in agreement except for *ErbB3* where there is increased *ErbB3* expression following 4 hour gefitinib exposure and a decreased expression post- ME1 exposure. Given recent reports, it was anticipated that gefitinib and ME1 would both increase *ErbB3* transcripts, in keeping with *ErbB3* acting as an escape mechanism to EGFR blockade^{77, 145}. It is a challenge to interpret this observation but may reflect the different mechanisms of action between the two drugs.

3.11.2.1.3 Contextualization of identified transcripts

To put the qRT-PCR validated transcripts into context, a low induction of gene expression changes has been reported *in vitro* when HT29 and Caco-2 cell lines are exposed to EGFR blockade in combination with EGF ligand¹⁵³. Based on microarray analysis from this study, only 10 genes were up-regulated for gefitinib + EGF exposure and none for cetuximab + EGF, whereas 32 genes were down-regulated for gefitinib + EGF and only 3 were down-regulated for cetuximab + EGF. Thus the number of genes differentially regulated *in vivo* as a consequence of my research appears quite respectable.

The relatively small magnitude fold change differences identified by my efforts should not detract from their potential physiological significance. Two-fold increases in gene expression have been shown to result in strong phenotypes in the arena of imprinted genes^{154, 155} and furthermore 1.5 fold global changes in mRNA levels are of potential importance in contributing to the development or progression of cancer¹⁵⁶. This suggests small detected changes in the expression level of critical genes in response to an agent may be important in determining a biological outcome. Of related interest very small but significant microarray transcript expression changes (personal communication¹⁵⁷) have also been seen in rectal cancer specimens pre and post cetuximab treatment²⁵. It appears therefore, in keeping with published studies, that this work confirms gene fold changes

which are quite modest following acute Egfr blockade, but nonetheless, may still have biological significance.

Finally, it is worth noting that recent experiments examining transcript changes in cells lines exposed to EGFR inhibition have also revealed similar gene expression changes, to those identified by my research, although the cell type and genetic make-up of tumours differ. Down-regulation of *Ccne2* and up-regulation of *Bmf* has been described in the gefitinib *sensitive* cell line, Bam1a, which originated from a mammary tumour (in BALB-NeuT mouse)¹⁵⁸. In addition *PLCD4* has previously been reported to be differentially expressed at the transcript level in HT-29 cell lines (*K-RAS* wild type, *p53* mutant¹⁵⁹) in response to cetuximab exposure¹⁵³.

3.11.2.1.4 Protein validation of transcripts induced by Egfr blockade

Of the colon polyp transcripts it was possible to probe for at the level of protein, it was disappointing that none could be validated for their response to ME1 exposure at 4 hours (fig 3.8). This may be explained by attempts to examine both transcript and protein changes at the same time (4 hours), when it is possible insufficient time had elapsed to allow transcriptional changes to impact protein dynamics. In view of this, assessment of protein levels was repeated following an 8 hour exposure to gefitinib. At this time it was possible to validate transcript changes for *Cbl* and *Ccne2* at the protein level (fig 3.9). Minimal validation of transcripts at the protein level is not ideal. However, expectations may be too great, as it is possible that subtle alterations in gene expression translated into protein changes are beyond the sensitivity and detection of western blot technology. Developments in nano-fluidic proteomics are likely to be helpful in the future¹⁶⁰ and would have been potentially useful in this setting.

3.11.3 Probing human rectal cancer transcriptome data (GSE5851) for 'mouse' candidate genes

Searching human metastatic rectal cancer transcriptome data from the Khambata-Ford publication²⁴ (GSE5851) for qRT-PCR validated mouse candidate genes of response to EGFR exposure (table 3.5), was encouraging as it identified 3 genes, which were differentially expressed, between patients achieving disease control, and no response to

cetuximab monotherapy. These genes included *IKBK*G (also known as *NEMO* or NF-kappa B essential modifier), *CXCL9* (chemokine ligand 9) and *CCNE2* (Cyclin E2; table 3.7). Expression of *IKBK*G and *CXCL9* was reduced whereas *CCNE2* was increased in patients achieving disease control with cetuximab relative to non responding patients (fig 3.10). The fact that only 11 genes have been searched for in the GSE5851 dataset demonstrates attempts were made to counter over-fitting the transcript data.

3.11.3.1 *IKBK*G

The EGFR family of receptors have been implicated in the initiation of NF-kappaB activation¹⁶¹ and *IKBK*G is an essential regulator of NF kappaB activity¹⁶² thus providing a link between EGFR blockade and *IKBK*G. NF-kappaB is retained in the cytoplasm as an inactive complex of the inhibitory kappaB (IB), p65 and p50 mammalian rel family proteins. When activated, by phosphorylation of inhibitory kappaB by the inhibitory kappaB kinase (IKK), the p65-p50 complex is released, and translocated into the nucleus, leading to anti-apoptotic and proliferative signals¹⁶¹. Recent evidence that NF-kappaB signalling is inhibited *in vitro* by short hairpin RNA mediated knock down of *IKBK*G¹⁶³, reinforces the essential role *IKBK*G plays in NF-kappaB pathway activity. In light of this it is reasonable to interpret the finding of a reduced level of *IKBK*G, in patients achieving disease control with cetuximab (fig 3.10), as biologically relevant and possibly explained by reduced NF-kappa B activation, leading to reduced cell proliferation and increased apoptosis, thus accounting for the favoured clinical response. Indeed the clinical importance of *IKBK*G being a potential predictor of response to EGFR targeted therapy, is strengthened by the publication of data showing that decreased NF-Kappa B immuno-reactivity is correlated with improved survival, in irinotecan-refractory patients receiving cetuximab and irinotecan, for second line treatment for metastatic colorectal cancer¹⁶⁴. The *Apc*^{min/+} mouse model of colon cancer has therefore independently identified a biologically and clinically relevant gene, which appears to have a plausible role in determining the outcome of EGFR targeted therapy in colon cancer.

3.11.3.2 *CCNE2*

The finding that *CCNE2* expression levels are increased in patients with metastatic colorectal cancer achieving disease control with cetuximab, is somewhat confusing in biological terms. It is known that cetuximab mediates, at least some of its clinical effects,

through changes in cell proliferation, specifically up-regulation of p27(Kip1), which binds to and inactivates cyclin-dependent kinase-2 activity giving rise to G1 cell cycle arrest¹⁶⁵. One might therefore predict that any functional role *CCNE2* has in tumour responses would equate to a fall in its expression levels, due to its effects on the cell cycle¹⁶⁶: Up-regulation of *CCNE2* has been demonstrated in HCT116 colorectal cells resistant to 5-fluorouracil¹⁶⁷. Unless the association of increased *CCNE2* expression in patients achieving a clinical response to cetuximab is a chance finding, a biological explanation for this is lacking. Nevertheless, *Ccne2* remains a validated candidate of response to anti-EGFR exposure in *Apc^{min/+}* colon polyps based upon qRT-PCR and protein changes, and has been associated with response to treatment in breast cancer¹⁶⁸ and should remain as a candidate transcript potentially able to predict response to EGFR therapy in *K-RAS* wild type colorectal cancer despite a lack of biological insight in this setting.

3.11.3.3 CXCL9

CXCL9 (chemokine [CXC motif] ligand 9) is a member of the chemokine family which are best known for inducing directional cellular migration of leukocytes during inflammation¹⁶⁹. Chemokines have also been associated with tumour development by way of influencing angiogenesis, tumour-leukocyte interactions and tumour transformation, survival, growth, invasion and metastases. However, the role of chemokines in tumour evolution is not straight forward as some favour tumour growth whereas others enhance anti-tumour activity¹⁶⁹.

It is known that *CXCL9* interacts with its receptor *CXCR3* and has been shown to be associated with tumour growth, migration and metastasis in mouse models of colon cancer^{7, 170}. Furthermore the potential importance of *CXCR3* in colon cancer is reinforced by its constitutive expression in human colon cancer cell lines, *CXCR3* immuno-staining in 34% of colon cancer specimens, the association of *CXCR3* with lymph node metastases and significantly poorer prognosis compared to *CXCR3*-negative colon tumours¹⁷⁰. In addition a recently 'inflammatory gene card' array study examining 8 surgical colorectal tumour samples has demonstrated *CXCL9* ligand expression in colon cancer, albeit in the absence of its receptor¹⁷¹.

With this background in mind it is feasible that cetuximab may interfere with the CXCR3-CXCL9 axis by reducing CXCL9 levels. This may inhibit tumour growth, and thereby provide a therapeutic response in keeping with the reduced expression of CXCL9, and its apparent association with disease control in response to cetuximab (fig 3.10). EGFR signalling has been linked to regulation of certain chemokines¹⁷² and their receptors¹⁷³ and use of a monoclonal antibody against EGFR in an EGFR-expressing SCCHN model has been shown to alter expression of several cytokines and chemokines¹⁷⁴. Given the absence of published data specifically detailing interactions between EGFR inhibition and the CXCL9-CXCR3 axis, the evidence presented here may indicate a novel mechanism of action of cetuximab and should be explored in more detail and possibly exploited. Promotion of metastases by over-expression of *CXCR3* mRNA in colorectal cancer models and the ability to inhibit metastatic colon cancer by targeting CXCR3 with AMG487 in mouse models⁷, suggests that combined EGFR/CXCR3 antagonism may have greater therapeutic potential than cetuximab or AMG487 alone. This would be an exciting combination to explore in genetically engineered mouse models of colon cancer, using a monoclonal antibody raised against murine *Egfr*.

3.11.4 Exploring the potential biological significance of mouse candidate genes proposed to indicate putative response to EGFR targeted therapy

Having discussed *IKBKG*, *CXCL9* and *CCNE2* in the context of transcriptome information obtained from a clinical trial, the remaining mouse transcripts (*Bmf*, *Cbl*, *Epha3*, *Hip1*, *Plcd4*, *ErbB3*, *Ereg* and *Ubd*) required further exploration. This next section aims to describe how their unique biology and acute alterations in expression may contribute towards understanding their potential influence on clinical outcome to targeted anti-EGFR therapy in colon cancer. The genes were all selected by a rational approach at the initial step of sifting through the microarray data to include those that had at least some biological relevance to EGFR blockade and its downstream consequences. This was done in the belief that validated targets should be relevant rather than obscure without current biological application. Admittedly such an approach was less blue sky and more pragmatic, but it is in keeping with the set goal of attempting to translate research findings to patients.

3.11.4.1 *Bmf*

BMF or BCL2 modifying factor is a pro-apoptotic protein that binds to pro-survival BCL-2 and triggers apoptosis through its BH3 domain¹⁷⁵. Gefitinib has previously been shown to promote apoptosis in human NSCLC by inducing the expression of pro-apoptotic BCL2 associated X protein (BAX) and BCL2-like11 apoptosis facilitator (BIM) proteins⁷⁵ and *Bmf* is up-regulated in a gefitinib sensitive breast cancer cell line¹⁵⁸ in response to gefitinib as previously mentioned. Increased expression of pro-apoptotic proteins in response to EGFR inhibition is therefore expected.

Although *Bcl2* antagonist killer (*Bak1*), *Bax* and *Bmf* transcripts were all up-regulated in colon polyps after acute gefitinib exposure in *Apc^{min/+}* mice, only *Bmf* was up-regulated following acute ME1 exposure (fig 3.4) and therefore identified as a candidate gene. This naturally led to the hypothesis that alteration in the levels of *Bmf* would result in either pro-apoptotic or anti-apoptotic effects dependent upon the direction of change, assuming the balance of other determinants of apoptosis were not altered. The acute increased expression of *Bmf* following *Egfr* antagonism may therefore indicate a positive tumour response to long term *Egfr* blockade as a result of increased apoptosis.

3.11.4.2 *Cbl* (*c-Cbl*)

Casitas B-lineage lymphomas comprise 3 family members, (c-CBL, CBL-b and CBL-3), and are important for the internalisation of EGFR, by virtue of their RING finger containing E3 ubiquitin ligases, that mediate ubiquitination of the receptor¹⁷⁶. Given the demonstration of a transformed cell phenotype owing to prolonged EGFR signalling with failure of EGFR receptor down-regulation¹⁷⁷, and CBL's role in EGFR turnover¹⁴⁵⁻¹⁴⁷ it is interesting that CBL expression in colon polyps appeared to be altered in response to EGFR blockade. It is suggested that CBL is biologically capable of influencing receptor signalling and response to targeted therapy through its effect on EGF receptor degradation. Thus the observed increased level of *Cbl* in colon polyps following *Egfr* blockade may predict reduced *Egfr* signalling (due to increased ubiquitination of EGFR) and be indicative of a favourable tumour response outcome in patients with *K-RAS* wild type colorectal tumours.

3.11.4.3 *Epha3*

The Eph receptors are part of the receptor tyrosine kinase family and interact with ephrin ligands in a promiscuous fashion within each A or B class¹⁷⁸. There are several lines of evidence linking Eph/Ephrin and EGF receptor. It has recently been shown in glioma that ephrin A5-transfected glioma cells mediate ephrin A5 enhanced CBL binding to EGFR thus promoting degradation of the EGF receptor¹⁷⁹. Conversely, EPHA2 has been shown to physically interact and amplify ERBB2 signalling promoting adenocarcinoma development and progression in transgenic mice with breast cancer¹⁸⁰.

Mutations in EPHA3 have been shown to play a significant role in tumourigenesis and been found in colorectal¹⁸¹ and lung cancers¹⁸², as has high expression of Eph receptors in a variety of cancers¹⁸³. In addition, the recent demonstration that EPHA2 acts as an oncogene in the intestine, based on the suppression of intestinal tumour development in *Apc^{min/+}* mice carrying a genetic knockout of the EPHA2 gene¹⁸⁴, raises the possibility that EPHA3 may play a similar role. The documented increased level of *Epha3* in colon polyps exposed to EGFR blockade may influence response to therapy and represent a tumour escape mechanism to EGFR blockade (through cross-talk with ERBB2¹⁸⁰). Thus increased expression of *Epha3* could theoretically predict response outcome to EGFR targeted therapy. Interestingly as part of their Anti-EPHA3 program Kalobios is undertaking pre-clinical studies targeting the EPHA3 receptor with an IgG antibody based upon the hypothesis that it will disrupt tumour neovascularisation, and cause tumour cell kill through antibody dependent cell cytotoxicity and stimulation of apoptosis (http://www.kalobios.com/kb_pipeline_004.php).

3.11.4.4 *Ubd*

UBD (ubiquitin D or FAT 10) is a ubiquitin-like protein that has been shown to induce apoptosis when expressed¹⁴⁸. UBD also has a role in ubiquitin independent proteosomal degradation, mediated by fatylation¹⁴⁸. Given that *Ubd* was decreased in colon polyps following acute exposure to gefitinib or ME1, the reduction in *Ubd* may represent an attempt by tumour cells to maintain EGFR signalling, by reduced fatylation of EGFR. This may translate into continued tumour growth. It is possible therefore, in response to Egfr blockade, that *Cbl* and *Ubd* represent competing responses that together determine the effect of Egfr inhibition in a tumour. This potential interaction raises the possibility that it

may be inappropriate to base response predictions on individual transcript changes, as competing biological mechanisms are likely to be of consequence.

3.11.4.5 *Hip1*

Huntingtin interacting protein 1 is an endocytic protein predominantly expressed in the brain and known to have a role in vesicle transport¹⁸⁵. HIP1 has been shown to stabilise EGFR by influencing receptor endocytosis and enhance the phosphorylation of downstream effectors to effectively increase the half life of EGF receptor signalling^{186, 187}. These findings have been extended by Bradley et al who reported HIP1 may up-regulate or maintain EGFR over-expression in tumours by direct interaction with the EGF receptor in addition to any indirect effects of HIP1 upon receptor endocytosis¹⁸⁸. In view of this relationship the finding of *Hip1* as a transcript altered in response to EGFR blockade is of potential significance. The documented increase in *Hip1*, following acute exposure to EGFR blockade in colonic polyps, may indicate a potential mechanism of resistance (by altering the ratio of EGFR exposed to gefitinib), and would select elevated *Hip1* as a biomarker trying to overcome the effects of EGFR blockade. Of significance it has been demonstrated that colon polyps from *Apc^{min/+}* mice chronically treated with gefitinib have elevated Egfr protein expression (5.5.1) in combination with increased *Hip1* expression (table 3.6). Thus it is attractive to speculate that this increase in Egfr protein may have been mediated by *Hip1*.

3.11.4.6 *Plcd4*

Phospholipase C, delta 4 is a phosphatidyl inositol phospholipase C enzyme isoform that shows increased expression in fast proliferating hepatoma cells¹⁸⁹. Investigation of human PLCD4 protein, by forced ectopic expression in MCF-7 breast cancer cells, has demonstrated up-regulation of EGFR and HER2, leading to ERK1/2 signalling activity and proliferation¹⁹⁰. There is therefore evidence of interaction between PLCD4 and receptor tyrosine kinase proteins. In light of this and the finding of up-regulated levels of *Plcd4* in colon polyps following acute EGFR inhibition, it is suggested *Pclcd4* may represent a mechanism to circumvent the effects of EGFR blockade and be an emergent resistance pathway predictive of non-response to EGFR inhibition.

3.11.4.7 *ErbB3*

ERBB3 is the 3rd member of the EGF receptor tyrosine kinase family and interest has grown recently due to its central role in driving oncogenic signals in tumours¹⁹¹. For example the intestinal specific deletion of *ErbB3* in *Apc^{min/+}* mice has shown a dramatic reduction in intestinal tumours mediated by reduced PI3K/AKT signalling and caspase 3 mediated apoptosis¹⁹². It has also been demonstrated both *in vitro* and in tumours *in vivo* that resistance to tyrosine kinase inhibitors (TKIs) is driven through up-regulation of ERBB3 and consequent PI3K/Akt signalling⁷⁷. Furthermore cell culture experiments have found prolonged cetuximab exposure promotes up-regulation of EGFR through altered internalisation and degradation with resultant activation of ERBB3¹⁴⁵ leading to resistance.

In view of these findings, the increase in *ErbB3* expression in colon polyps following acute and chronic gefitinib exposure (table 3.6) is significant as *ErbB3* is likely to be driving resistance to EGFR blockade in the *Apc^{min/+}* mouse. Experiments using this model reinforce the potential importance of *ErbB3* in tumourigenesis and raise the possibility that the direction of early *ERBB3* expression changes, in response to EGFR blockade, may have a role in determining the outcome of such treatment in *K-RAS* wild type colorectal cancer. If it does, then therapies targeting *ERBB3* may be useful in circumventing such mechanisms and could be tested in the *Apc^{min/+}* mouse in a similar way IGF1R antagonists have been explored (Chapter 5).

3.11.4.8 *Ereg*

Epiregulin is one of many ligands which bind to the EGFR family having a low affinity for EGFR and ErbB4, but increased affinity when ErbB2 is present with ErbB4 and ErbB3¹⁹³. Epiregulin drives tumour growth through EGFR signalling and interference with TKIs has been shown to produce anti-tumour effects^{194, 195}. Furthermore, disruption of ligand binding to the EGF receptor by cetuximab, has been proposed to explain the association between increased tumoural *EREG* and response to cetuximab in *K-RAS* wild type colorectal cancer^{24, 49}. Similarly the *Apc^{min/+}* model system also shows dramatic up-regulation of epiregulin in colon polyps¹⁹⁶. Taken together it is suggested that the documented fall in expression of *Ereg* in *Apc^{min/+}* colon polyps, in response to acute Egfr blockade, contributes to the observed positive response gefitinib therapy has in *Apc^{min/+}* mice (5.3.1). Thus an acute

reduction in epiregulin in response to EGFR blockade is postulated to represent a positive biomarker of clinical outcome.

3.11.5 Transcript expression after chronic gefitinib exposure

The initial gene signature in response to EGFR blockade was chosen at 4 hours on the basis this would capture a 'pure' molecular signal of tumour cell response to agents. It is reasoned that this avoided additional 'molecular noise' a later time point would introduce, when a greater number of molecular events drive dividing cells. Despite this it remained of interest to examine the relationship between early transcript changes and the molecular changes responsible for or at least associated with resistant tumour growth following long term administration of gefitinib (Chapter 5).

3.11.5.1 Chronic transcripts affirming gefitinib induced 4 hour transcript changes

It has only been possible to examine the fold changes of a limited number of transcripts from colon polyps following long term administration of gefitinib (2.1.3.3). However, despite this *Bmf*, *Cbl*, *ErbB3*, *Hip1* and *Ikbkg* are all up-regulated in *Apc^{min/+}* colon polyps exposed to chronic gefitinib to a greater extent than their 4 hour counter parts (table 3.6).

It has been hypothesised that a positive tumour response may follow increased *Bmf* or *Cbl* gene expression at 4 hours given the pro-apoptotic and anti-EGFR signalling effects of these proteins. That both transcripts remain elevated in *Apc^{min/+}* colon polyps assumed to be resistant to gefitinib, does not necessarily negate their hypothesised predictive potential. However this suggests the presence of resistance mechanisms countering any positive contribution *Bmf* or *Cbl* had toward inhibition of tumour growth. It is attractive to speculate the transcripts responsible for resistance to Egfr blockade in *Apc^{min/+}* mice might include *ErbB3*, *Hip1* and *Ikbkg*.

The increased longevity of *Apc^{min/+}* mice following gefitinib treatment (5.3.1) and associated up-regulated expression of *ErbB3*, *Hip1* and *Ikbkg* is potentially relevant to our understanding of resistance mechanisms to EGFR blockade in *K-RAS* wild type colon cancer, especially in light of the discussed biologically plausible evidence supporting such transcripts in this process (3.11.3.1, 3.11.4.5, 3.11.4.7). If these transcripts are important it appears

they initiate resistance mechanisms soon after the first dose of gefitinib; it would therefore be of great interest to inhibit each of these putative resistance mechanisms in the *Apc^{min/+}* mouse to identify optimal drug sequencing and timing. Such experiments could improve our understanding of resistance mechanisms and potentially improve patient outcomes if translated in clinical trials.

3.11.5.2 Chronic transcripts opposing gefitinib induced 4 hour transcript changes

Cxcl9 and *Ubd* were both down-regulated at 4 hours but show up-regulated colon polyp expression in response to chronic gefitinib (table 3.6). It is possible that induced molecular pathways produce this pattern of transcript change, over time, causing the reversal of any hypothetical biological effects each transcript initially had. One may therefore speculate that increased expression of *Ubd* reflects attempts to increase fatylation of up-regulated *Egfr*, following chronic gefitinib exposure (5.5.1), as a consequence of increased Hip1 activity.

3.11.6 Transcripts identified in patients' rectal cancer specimens

The availability of good quality rectal cancer tissue biopsies has hampered this aspect of my research, which consequently remains anecdotal. The two patients included harboured *K-RAS* and *B-RAF* wild type rectal cancers and in common demonstrated reduced expression of *BMF*, remaining free from disease recurrence (table 3.8). It was not possible to examine the expression level of all transcripts given the low yield of RNA, but of those tested patient 2 also demonstrated reduce levels of *EPHA3* and *IKBK*G.

No conclusions can be drawn, but it is encouraging that some of the transcripts identified by the mouse model are also differentially expressed in human rectal cancer specimens, in response acute cetuximab exposure. Low level expression of *IKBK*G and *EPHA3* may represent biological mechanisms contributing towards the favourable outcome in patient 2 reflected by reduced NF-kappaB¹⁶² and oncogenic activity of *EPHA3*. This takes no account of the reduced expression of *BMF* however, which would be predicted to promote tumour cell survival. If there is any credibility in this approach, it would be necessary to interpret the spectrum of induced transcript changes together, whilst

accepting certain transcripts may have a dominant effect. Clearly this work is at an early stage.

The Xerxes trial highlights some of the challenges faced when undertaking translational research. Rectal cancers are accessible to sequential biopsy to assess the molecular effects of cetuximab monotherapy but, multimodal therapy for rectal cancer has complicated the assessment cetuximab therapy alone can have on treatment outcome. In addition, recruitment has been difficult in view of the reduced complete pathological response rate (5-9%) when pre-operative radiotherapy plus cetuximab is combined with capecitabine ± oxaliplatin^{56, 57}. This compares with pathological complete response rates of 16%⁵⁸ when cetuximab is excluded. At best it was hoped sufficient rectal cancer biopsy material would be available to demonstrate that targets identified using the mouse model, could be shown in human samples exposed to cetuximab. This data may have led to further hypotheses regarding their potential predictive significance.

In light of this, further investigation of the role identified mouse transcripts play, either together or as isolated targets, in response to cetuximab monotherapy, is required. This may be achieved by examining archival FFPE samples from patients in a prospective randomised controlled trial⁴⁶, including *K-RAS* wild type metastatic colorectal cancers, for correlations between transcript expression and known response outcomes to therapy.

3.11.7 Summary

Colon polyps from the *Apc*^{min/+} mouse have been shown to be wild type for *K-ras* and *B-raf* underscoring the relevance of this model for the study of *K-RAS* and *B-RAF* wild type colorectal cancer. Furthermore, acute exposure of *Apc*^{min/+} mice to Egfr blockade has been shown to suppress Egfr, Erk and Akt phosphorylation, in keeping with its known action as an inhibitor of EGFR tyrosine kinase activity, resulting in morphological change consistent with acute anti-tumour effects in the intestine. In addition the transcript changes identified using *Apc*^{min/+} colon polyps and acute Egfr blockade, has led to the clinically purposeful identification of novel biomarkers of response to cetuximab in *K-RAS* wild type metastatic colorectal cancer (*IKBKKG*, *CCNE2* and *CXCL9*). Biological consideration of the remaining mouse transcripts has also helped build a picture of how acute gene expression changes can be interpreted and hypothesised to represent favourable or unfavourable tumour

responses. As a result, novel resistance mechanisms to EGFR blockade have been proposed (*HIP1* and *IKBK3*) or reinforced (*ERBB3*). Applying this knowledge to patients' tumours could be a means of identifying new drug combinations to overcome EGFR resistance pathways, which may appear immediately after a single drug exposure. The *Apc^{min/+}* mouse may therefore be used to investigate and inhibit resistance pathways, and by testing novel drug combinations, help make progress towards better treatment combinations for future colorectal cancer patients.

Chapter 4

4. Verification of *K-ras* wild type specific transcript changes in colon polyps using a conditional transgenic mouse model of colon tumourigenesis

4.1 Introduction

Having identifying putative targets of response to Egfr blockade in *Apc^{min/+}* *K-ras* wild type colon tumours, by excluding the presence of common *K-ras* mutations in harvested colon polyps, I wanted to verify these transcript changes using an alternative model of intestinal tumourigenesis harbouring a mutant *K-ras* allele. This was made possible by using a conditional transgenic model of colon cancer which under the control of the *AhCre* promoter is able to induce intestinal specific loss of *Apc* with or without expression of an endogenous mutant *K-ras* (V12) allele¹¹⁴. As a consequence I have been able to examine transcript changes in response to gefitinib in mouse models with or without *K-ras* mutant colon polyps. On the assumption Egfr inhibition would have negligible effects upon the transcriptional profile of colon polyps harbouring mutant *K-ras* it was anticipated that comparison between *K-ras* wild type and mutant transcriptional profiles would reveal *K-ras* wild type specific expression changes. Use of this approach has also allowed verification of transcript changes in a mixed genetic background more akin to that seen in humans.

This work has help identify *Apc^{min/+}* colon polyp transcripts which have been validated as *K-ras* specific gene changes in response to Egfr blockade, and therefore provides a means of prioritising transcripts which should be tested in human specimens for their ability to predict outcome in response to EGFR targeted therapy in *K-RAS* wild type colorectal cancer.

4.2 Results

4.2.1 Gefitinib induced transcript changes in the context of *K-ras* mutation status.

The putative biomarkers of response to Egfr blockade identified using the *Apc^{min/+}* mouse (table 4.1) were probed for in colon polyps harvested from *AhCre^{T/+} Apc^{fl/+} Kras^{v12/+}* mice exposed to gefitinib 75mg/kg for 4 hours (2.3.2.4) and expressed relative to transcript expression in similarly exposed *AhCre^{T/+} Apc^{fl/+} Kras^{+/+}* colon polyps (table 4.1). On examination of the transcript changes, gefitinib exposure in mice with endogenous *K-ras* allele activation results in reduced colon polyp expression of *Ikbkg*, *Cxcl9*, *Ccne2*, *Cbl* and *Ereg* and increased expression of *Plcd4* and *ErbB3*.

If comparison is made between the fold changes for the different experimental conditions, then one would anticipate that an increased transcript expression in *Apc^{min/+} K-ras* wild type polyps, in response to gefitinib, would be associated with the induction of opposite expression changes in *K-ras* mutant polyps relative to *K-ras* wild type polyps. Failure to comply with this would suggest that a transcript change is not specific to *K-ras* wild type status. With this in mind *Ikbkg* and *Cbl* are therefore identified as *K-ras* wild type specific changes in response to gefitinib. However, the remaining transcripts, identified from *K-ras* mutant tumours, do not appear to be specific to *K-ras* wild type tumours as they demonstrate either no gene expression differences (*Epha3*, *Bmf* and *Hip1*) or increased expression (*Plcd4*, *ErbB3*, *Cxcl9*, *Ccne2* and *Ereg*).

Transcript	Fold change (Gef <i>K-ras</i> mutant: Gef <i>K-ras</i> wt)	Fold change Gef:Veh (<i>Apc^{min/+} K-ras</i> wt)
<i>Ikbkg</i>	0.8	3.4
<i>Plcd4</i>	2.1	2.2
<i>Epha3</i>	1.1	2.1
<i>ErbB3</i>	2.3	2.1
<i>Cxcl9</i>	0.38	0.2
<i>Ccne2</i>	0.46	0.6
<i>Bmf</i>	0.8	3.8
<i>Cbl</i>	0.75	2.4

Transcript	Fold change (Gef <i>K-ras</i> mutant: Gef <i>K-ras</i> wt)	Fold change Gef:Veh (<i>Apc</i> ^{min/+} <i>K-ras</i> wt)
<i>Ereg</i>	0.5	0.4
<i>Hip1</i>	0.9	1.7
<i>Ubd</i>	-	0.3

Table 4.1 Altered gene expression patterns (qRT-PCR) in *K-ras* mutant colon polyps relative to *K-ras* wild type colon polyps in response to gefitinib at 4 hours. Transcripts identified as definitive candidates of response to Egfr blockade using *K-ras* wild type colon polyps from the *Apc*^{min/+} model showing the fold changes in response to gefitinib (75mg/kg) at 4 hours relative to vehicle (0.5% Tween⁸⁰) are also presented. Bold red numbers indicate a P value of 0.04 was reached (Mann-Whitney). '-' transcript not examined.

4.3 Discussion

With the approach taken, I have assumed that a target previously up-regulated in response to gefitinib in *Apc*^{min/+} colon polyps, would also be up-regulated in *K-ras* wild type colon polyps harvested from the *AhCre*^{T/+} *Apc*^{fl/+} *Kras*^{+/+} conditional transgenic model. As gefitinib induced transcript changes in *K-ras* mutant colon polyps have been expressed relative to *K-ras* wild type transcripts it follows an up-regulated target in *K-ras* wild type tissue would be reflected by down-regulation of the same target in *K-ras* mutant tissue. With this in mind *Ikbkg* and *Cbl* transcripts were the only transcripts verified by this approach and confirmed as gefitinib induced *K-ras* wild type specific changes. The importance of *Ikbkg* and *Cbl* and their potential relevance to *K-ras* wild type tumour responsiveness to Egfr targeted therapy has been discussed in detail (3.11.3.1 and 3.11.4.2).

It is worth noting that the gefitinib induced *Apc*^{min/+} targets were defined using a greater pool of colon polyps than for the conditional transgenic model which incorporates the *K-ras* mutation. This could affect the accuracy of the data obtained for the latter as smaller sample sizes increase the likelihood of including false positive extreme values. The failure to detect corresponding transcript changes in the remaining candidates excluding *Ikbkg* and *Cbl* may reflect differences in the genetic background of the animals used¹⁹⁷. The transcript changes seen in response to Egfr blockade may therefore no longer be seen or 'off target' transcript changes may be detected which bear no association with Egfr signalling.

The question arises whether failure to confirm some of the transcript changes (*Epha3*, *Bmf*, *Hip1*, *Plcd4*, *ErbB3*, *Cxcl9*, *Ccne2* and *Ereg*) using the conditional transgenic model means disregarding them altogether? Certainly if a series of patients with mixed genetic backgrounds is sufficient to obscure the identified target genes, then this is of concern, however *Cxcl9* and *Ccne2* have been shown to dichotomise clinical response to cetuximab monotherapy using transcriptome data from patients with *K-ras* wild type colorectal metastatic tumour (3.11.3). This suggests there is potential value in evaluating the targets in other ways. One approach to this would be to examine the relationship between the candidate genes and their ability to associate with clinical response status to cetuximab monotherapy in the context clinical trials. This could be achieved by examining

archival FFPE *K-RAS* wild type metastatic colorectal cancer specimens from a prospectively randomised controlled trial of cetuximab monotherapy vs. best supportive care to test the ability of the transcripts to dichotomise clinical response. The same approach could be repeated in *K-RAS* mutant tumour samples from the same trial with the expectation that none of the transcripts would be associated with outcome if they are specific to *K-RAS* wild type tumours.

The finding that gefitinib up-regulated *ErbB3* (2.3 fold) in *K-ras* mutant relative to *K-ras* wild type colon polyps is particularly interesting especially in light of a recent report showing *K-ras* mutant HCT116 colon cancer cells lines are attenuated by increased apoptosis in the presence of siRNA against *ErbB3*¹⁹². *ErbB3* activity may therefore not only be a mechanism of resistance to gefitinib in *K-ras* wild type tumours (3.11.4.7) but also play a role in mediating molecular responses in the setting of *K-ras* mutations. Indeed evidence is accumulating that EGFR targeted therapy in patients with *K-RAS* mutant colorectal cancer is detrimental⁴⁷. A possible explanation for this may be increased mitogenic signalling, as a consequence of EGFR blockade up-regulating ERBB3 in patients with *K-RAS* mutant colorectal cancer, leading to increased PI3K/AKT pathway activation in addition to constitutive pathway activation downstream of *K-RAS*.

These findings may also have relevance in relation to resistance mechanisms which may arise in *K-RAS* mutant colon cancers treated using MEK inhibitors (Chapter 7). It is possible that similar up-regulation of ERBB3 could occur leading to activation of parallel PI3K/AKT signalling activity and circumvention of disruption of MEK/ERK signalling. It will therefore be important to examine this possibility in tumour tissue from mouse experiments incorporating prolonged MEK inhibition.

In summary, the use of a conditional transgenic mouse model carrying *K-ras* mutations has helped to reinforce *Ikbkg* and *Cbl* as potential *K-ras* wild type specific gene expression changes in response to Egfr blockade. Having not validated all transcripts by this method is disappointing, but on reflection perhaps highlights those transcripts which should be prioritised for further study using human tissue samples, to assess their ability to predict outcome in response to EGFR targeted therapy in *K-RAS* wild type colorectal cancer.

Chapter 5

5. Investigating Igf1r pathway activation in *Apc^{min/+}* *K-ras* wild type colon polyps in response to Egfr blockade

5.1 Introduction

Previously (Chapter 3) I have shown that exposure to the Egfr inhibitor, gefitinib, led to elevated phosphorylation of the insulin-like growth factor 1 receptor (Igf1r) in *Apc^{min/+}* colonic polyps. This observation implicates the Igf-1 pathway in response to Egfr blockade. This finding was particularly relevant given the accumulating evidence that IGF1R pathway activity may be important in conferring resistance to EGF receptor blockade⁸⁰⁻⁸², based upon *in vitro* cell culture and xenograft studies. I therefore next wanted to test the importance of the Igf pathway, in promoting resistance to Egfr blockade, in a relevant *in vivo* model using the *Apc^{min/+}* mouse, which I have shown develops intestinal colon tumours which are wild type for *K-ras* and *B-raf*. This is a clinically important area to explore in the setting of *K-RAS* and *B-RAF* wild type colorectal cancer given monoclonal antibodies targeting the EGF receptor are now licensed for use and tumour resistance will be an inevitable consequence.

I have tested the hypothesis that blockade of Egfr signalling is being tempered by compensatory activation of the Igf pathway by examining the effect of chronic suppression of Igf1r using AZ12253801, a small molecular tyrosine kinase inhibitor of Igf1r (2.1.3.1.2), alone and in combination with gefitinib. *Apc^{min/+}* mice were treated for a period of 8 weeks with gefitinib and then subsequently exposed to single agent gefitinib or combination therapy against Egfr and Igf1r (2.1.3.3; fig 2.1). In addition to having already shown concurrent suppression of Egfr and induction of Igf signalling in murine intestinal tumours, combined dosing with gefitinib and AZ12253801 suppressed both small and large intestinal tumourigenesis relative to vehicle and single agent controls. As well as establishing a rationale for combinatorial therapy, this data also implicates Erk phosphorylation in response to chronic Igf1r inhibition, suggesting that Mek inhibition may abrogate against resistance to Igf1r inhibition. Finally, I have provided direct *in vivo* proof of the concept that early molecular pathway changes may be useful as biomarkers for response/resistance prediction.

5.2 Results

My initial work was aimed at choosing an appropriate dose of investigational drugs for long term studies in *Apc^{min/+}* mice. Pilot studies were therefore undertaken which also tested, at transcript level, whether increased *Igf1r* levels occurred in intestinal tumours in response to chronic Egfr inhibition.

5.2.1 AZ12253801 test doses

The company brochure recommended a dosing schedule of AZ12253801 12.5mg/kg 12 hourly, but this was not feasible at a practical level. AZ12253801 was therefore administered 12.5mg/kg twice daily (8 hours apart). This unfortunately resulted in weight loss over a 5 day period of treatment and was clearly dose limiting. I therefore reduced the dose level to 12.5mg/kg once daily which was much better tolerated without weight loss. This became the favoured dosing regimen. Company data available for AZ12253801 describes significant anti-tumour effects of doses ranging from 6.25mg/kg to 25mg/kg/day (AZ12253801 Investigators brochure). A single dose of AZ12253801 25mg/kg in *Apc^{min/+}* mice resulted in marked hyperglycaemia and would not be tolerated in a long term study. No public information was available regarding alternative AZ12253801 dosing regimens.

5.2.2 Gefitinib test doses

The dose of gefitinib was initially chosen based on xenograft studies that demonstrated a radio-sensitising effect of gefitinib 75mg/kg administered as a suspension in 0.5% Tween^{80 132}. Chronic once daily dosing of gefitinib 75mg/kg was tolerated well by intra-peritoneal injection in a pilot study involving 7 *Apc^{min/+}* mice (2.3.2.3). This pilot study also provided evidence to support the importance and rationale of the experimental approach by the demonstrating a 2-fold increase in *Igf1r* transcript in pooled colon polyps exposed to chronic gefitinib relative to vehicle treatment (fig 5.1).

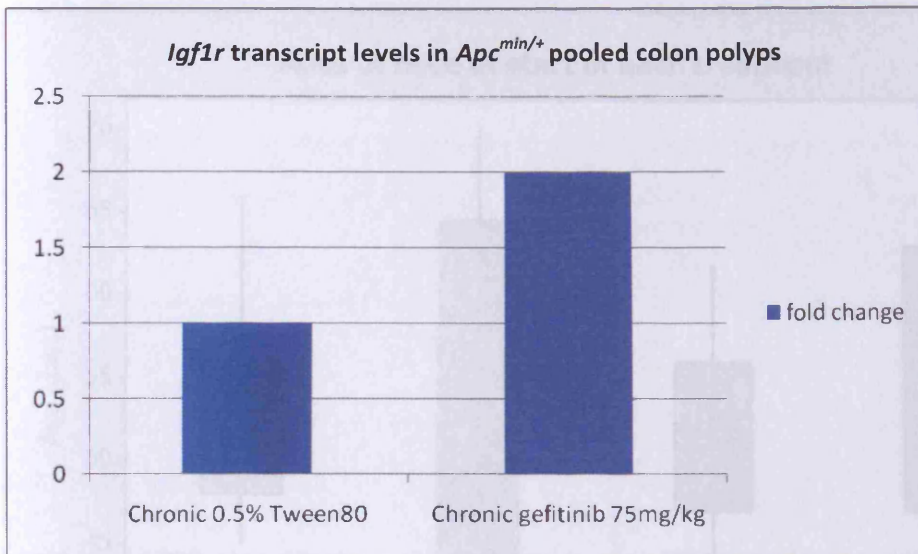


Figure 5.1 qRT-PCR determined transcript expression of *Igf1r* in colon polyps from *Apc^{min/+}* mice treated with long term vehicle (1% Tween80) or gefitinib (75mg/kg) until the development of an intestinal tumour burden. Primer sequences are listed in table 2.4.

I next determined the influence of each chronic treatment upon *Apc^{min/+}* mice in terms of longevity and intestinal tumour metrics.

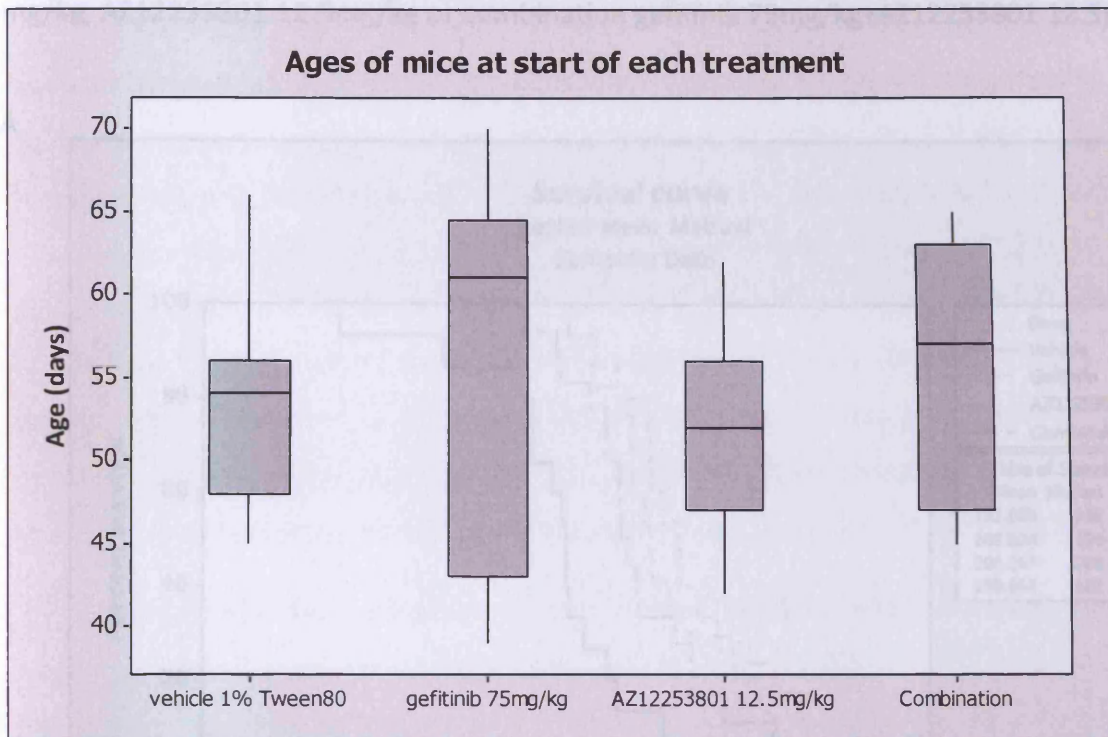
5.3 Consequences of chronic treatments in *Apc^{min/+}* mice upon survival, tumour volume and tumour counts

It was important from the outset to ensure that the age of mice starting treatments, in each cohort, was the same to exclude this as a factor which could influence various endpoint measurements. There were however no detectable differences in the median ages of mice starting experimental treatments (fig 5.2; median age vehicle 54 days vs. gefitinib 61 days, $P=0.14$; vehicle 54 days vs. AZ12253801 52 days, $P=0.56$; vehicle 54 days vs. combination 57 days, $P=0.28$; combination 57 days vs. gefitinib 61 days, $P=0.63$; combination 57 days vs. AZ12253801 52 days, $P=0.07$; gefitinib 61 days vs. AZ12253801 52 days, $P=0.1$; Mann-Whitney).

Figure 5.2 Box plots showing the age range of mice at the start of each treatment

5.3.2 AZ12253801 (*Igf1r* inhibition)

Figure 5.3. Survival and intestinal tumour metrics of *Apc^{min/+}* mice treated with once daily gefitinib



I next determined the influence of each chronic treatment upon *Apc^{min/+}* mice in terms of longevity and intestinal tumour metrics:-

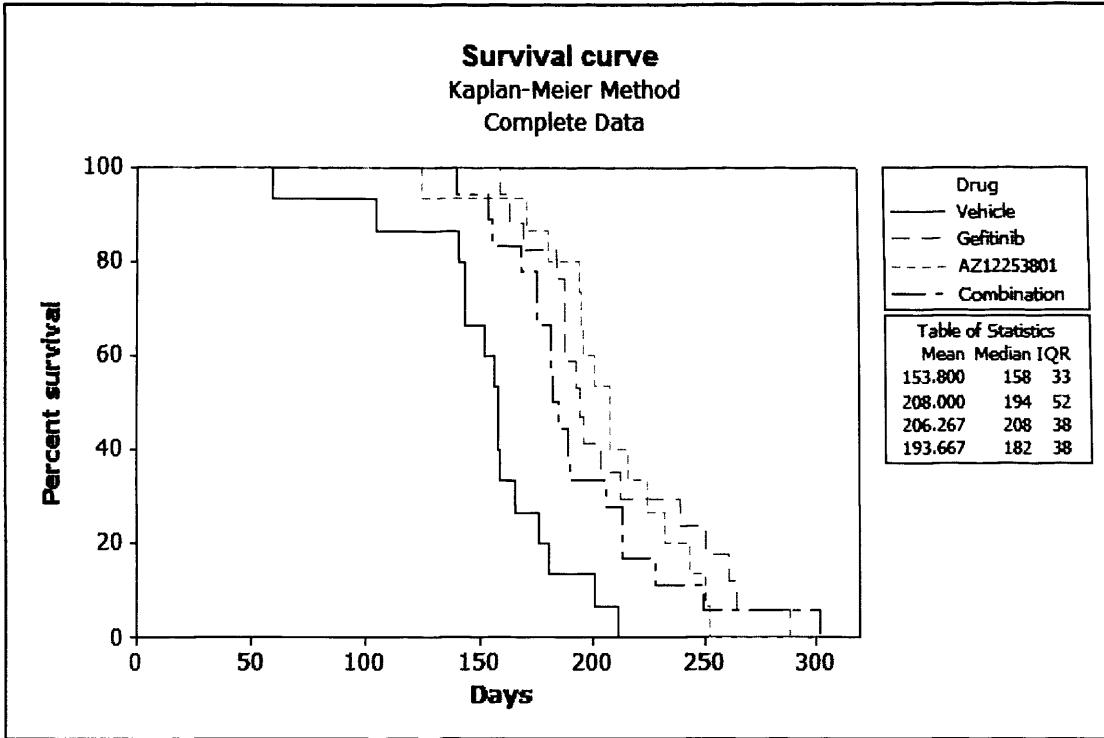
5.3.1 Gefitinib (Egfr inhibition)

Apc^{min/+} mice receiving chronic daily gefitinib 75mg/kg had an improved median survival relative to vehicle treatment (158 days vs. 194 days, $P < 0.0001$; log rank test; fig 5.3 A). Median colon polyp numbers at death were significantly reduced in gefitinib treated animals compared to vehicle treatment (2 vs. 8 colon polyps, $P = 0.002$; fig 5.3E). However, no difference was observed in colon tumour volume between gefitinib and vehicle treatments (8mm^3 vs. 158.5mm^3 , $P = 0.136$; Mann-Whitney test; fig 5.3D), indicating that the reduced number of colon tumours in gefitinib treated mice grew to a larger size, presumably as a direct consequence of enhanced longevity. No differences were observed at death in the median number of small intestinal tumours (37.5 vs. 29, $P = 0.2664$; Mann-Whitney test; fig 5.3C) or small intestinal tumour volumes (128mm^3 vs. 123mm^3 , $P = 0.4998$; Mann-Whitney test; fig 5.3B), despite increased longevity. These data therefore argue that gefitinib exposure delays both small and large intestinal tumourigenesis.

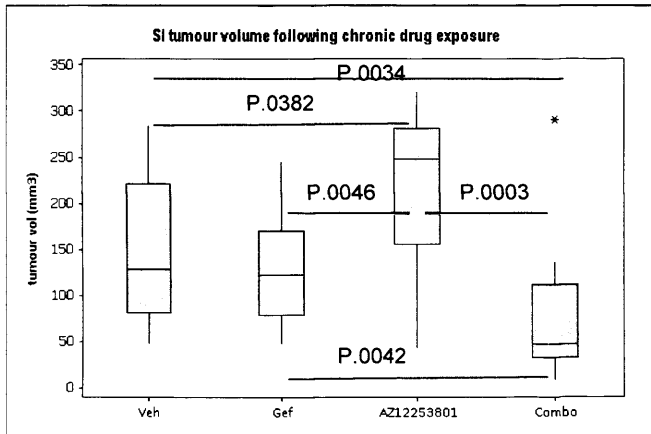
5.3.2 AZ12253801 (Igf1r inhibition)

Figure 5.3. Survival and intestinal tumour metrics of *Apc^{min/+}* mice treated with once daily gefitinib 75mg/kg, AZ12253801 12.5mg/kg or combination gefitinib 75mg/kg+AZ12253801 12.5mg/kg.

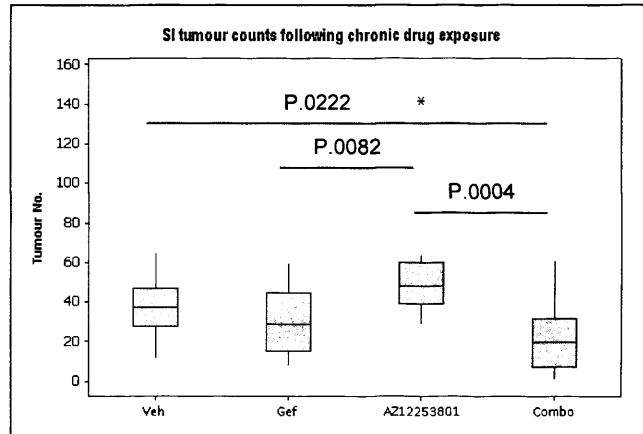
A



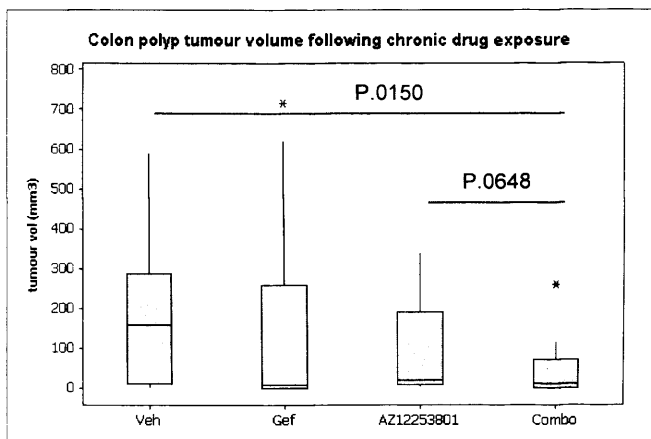
B



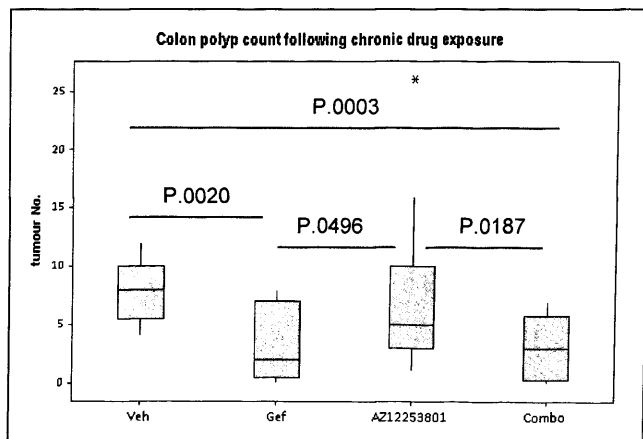
C



D



E



The median survival of *Apc*^{min/+} mice receiving once daily AZ12253801 12.5mg/kg was also increased relative to vehicle controls (158 days vs. 208 days, P<0.001; log rank test; fig 5.3A). At the time of death there was an increase in median small intestinal tumour volume relative to vehicle (248.5mm³ vs. 128.5 mm³, P=0.0382; Mann-Whitney test; fig 5.3B) which in the absence of a detected difference in the small intestinal tumour count (37.5mm³ vs. 48 mm³, P0.0668, fig 5.3C) indicates tumours grew to a larger size in the AZ12253801 treated cohort. However, there were no differences in median colon polyp tumour volume (158 mm³ vs. 19.5 mm³, P0.2280; fig 5.3D) or colon polyp number despite increased longevity of the mice (8 vs. 5, P0.2217, fig 5.3E). These data indicate that exposure to AZ12253801 increases survival specifically through a reduction in colon polyp burden.

Interestingly, small intestinal tumour volume and both small and large intestinal tumour counts were greater in single agent Igf1r inhibitor treated *Apc*^{min/+} mice relative to Egfr inhibitor and dual Egfr/Igf1r inhibitor cohorts (median small intestinal tumour volume 248 mm³ [AZ12253801] vs. 123 mm³ [Gef], P=0.0046 and 47 mm³ [Combo], P=0.0003; median small intestinal tumour counts 48 [AZ12253801] vs. 29 [Gef], P=0.0082 and 20 [Combo], P=0.0004 and median colon polyp tumour counts 5 [AZ12253801] vs. 2 [Gef], P=0.0496 and 3 [Combo], P=0.0187; Mann-Whitney test fig 5.3B-E). This suggests loss of a protective effect of continuous gefitinib when it is withdrawn after 8 weeks treatment in the AZ12253801 monotherapy cohort.

5.3.3 Combined Gefitinib with AZ12253801 (Dual Egfr and Igf1r inhibition)

Combined once daily gefitinib 75mg/kg and AZ12253801 12.5mg/kg treatment similarly resulted in a prolongation of *Apc*^{min/+} median survival (158 days vs. 182 days, P=0.002; log rank test; fig 5.3A) and at the time of death significantly reduced small and large intestinal tumourigenesis relative vehicle as measured by both tumour number and volume (median number small intestinal tumours 20 vs. 37.5, P=0.0222; median number colon polyps 3 vs. 8, P=0.0003; Mann Whitney; median small intestine tumour volume 47 mm³ vs. 128.5mm³, P=0.0034; median colon tumour volume 10.5 mm³ vs. 158.5mm³, P=0.0150; fig 5.3B-E). The combination of Egfr/Igf1r blockade therefore appears to improve survival by delaying both small and large intestinal tumourigenesis.

When comparison is made between the three chronic treatment regimes, combination treatment reduced the median small intestinal tumour number compared to lgf1r inhibition (20 [combo] vs. 48 [AZ12253801], $P=0.0004$) but not against gefitinib (20 [combo] vs. 29 [gefitinib], $P=0.22$; fig 5.3C). Similarly, in the large intestine, combined therapy reduced colon polyp number compared to AZ12253801 treatment, but not against gefitinib (3 [combo] vs. 5 [AZ12253801], $P=0.0187$ and 3 [combo] vs. 2 [gefitinib], $P=0.718$; fig 5.3E). No differences were observed in median colon polyp tumour volume between the treatments (10.5mm^3 [combo] vs. 19.5mm^3 [AZ12253801], $P=0.0648$ and 10.5mm^3 [combo] vs. 8mm^3 [gefitinib], $P=0.482$; fig 5.3D). It is clear however that combination treatment leads to reduced median small intestinal tumour volume (47mm^3 [comb] vs. 248mm^3 [AZ12253801], $P=0.0003$ and 47mm^3 [comb] vs. 123mm^3 [gefitinib], $P=0.0042$; fig 5.3B).

Although combined treatment reduced tumour burden at death compared to single agent exposure, the survival data for the different regimens showed that all three regimens resulted in similar increased longevity compared to vehicle controls (median survival 158 days [Veh] vs. 194 days [Gef], $P<0.0001$; vs. 208 days [AZ12253801], $P<0.0001$; vs. 182 days [Combo], $P=0.002$; 182 days [Combo] vs. 208 days [AZ12253801], $P=0.301$; 182 days [Combo] vs. 194 days [Gef], $P=0.370$; 194 days [Gef] vs. 208 days [AZ12253801], $P=0.0723$, log rank method).

5.3.4 Adverse effects of chronic treatment

In keeping with pilot experiments, chronic treatment of *Apc^{min/+}* mice with the various drugs was well tolerated. Weekly assessments showed that mice maintained their weight throughout treatment until the development of an intestinal tumour load which indicated the end point of the study. Mice receiving chronic gefitinib developed wavy fur (fig 5.4A), without obvious distress. Five mice receiving combination AZ12253801 12.5mg/kg and gefitinib 75mg/kg developed intra-abdominal collections (presumed to be abscesses) of varying severity (Fig 5.4B) resulting in early cull. A separate survival analysis however, excluding mice developing intra-abdominal pathology, had no effect on the end result, suggesting this complication did not obscure a survival advantage for combination therapy. Blood glucose samples were unfortunately not taken from any mice when culled, and would

Figure 5.5 Phenotypic changes in *Apc^{min/+}* small intestinal tumours post 4 hr drug exposure

have been potentially helpful in determining whether hyperglycaemia contributed to the pathogenesis of the intra-abdominal lesions.

Fig 5.4

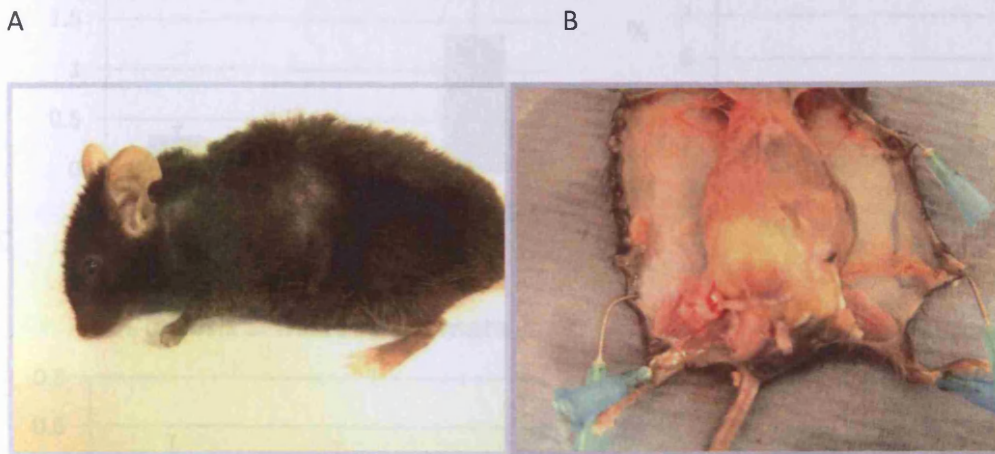


Fig 5.4 Adverse effects of chronic administration of drugs in mice.

Chronic administration of once daily gefitinib 75mg/kg leads to wavy hair in the *Apc^{min/+}* mouse (A). An intra-abdominal abscess at the site of intra-peritoneal injection in a mouse receiving chronic AZ12253801 12.5mg/kg in combination with gefitinib 75mg/kg (B).

5.4 Acute effects of drug exposure in tumours from *Apc^{min/+}* mice

I next sought to dissect the mechanisms of response to these targeted agents in terms of the acute effects upon *Apc^{min/+}* intestinal tumours with respect to cell death and proliferation and the underlying molecular effects.

5.4.1 Tumour phenotypic change

Following 4 hour exposure of *Apc^{min/+}* mice to combined EGFR/IGF1R antagonism there is increased small intestinal tumour apoptosis ($1.37\% \pm 0.5$ [combo] vs. $0.33\% \pm 0.1$ [vehicle] and $1.37\% \pm 0.5$ [combo] vs. $0.34\% \pm 0.1$ [AZ12253801]) and a trend towards elevated cleaved caspase 3 positivity ($5.18\% \pm 3.8$ [combo] vs. $1.3\% \pm 0.9$ [vehicle] and $5.18\% \pm 3.8$ [combo] vs. $2.1\% \pm 0.9$ [AZ12253801]; fig 5.5 A, B). No differences in small intestinal tumour mitotic rate or Brdu cell labelling were however identified when comparing vehicle, AZ12253801 or combination treatments at 4 hours (Fig 5.5 C, D). In colon

Figure 5.5 Phenotypic changes in *Apc^{min/+}* small intestinal tumours post 4 hr drug exposure

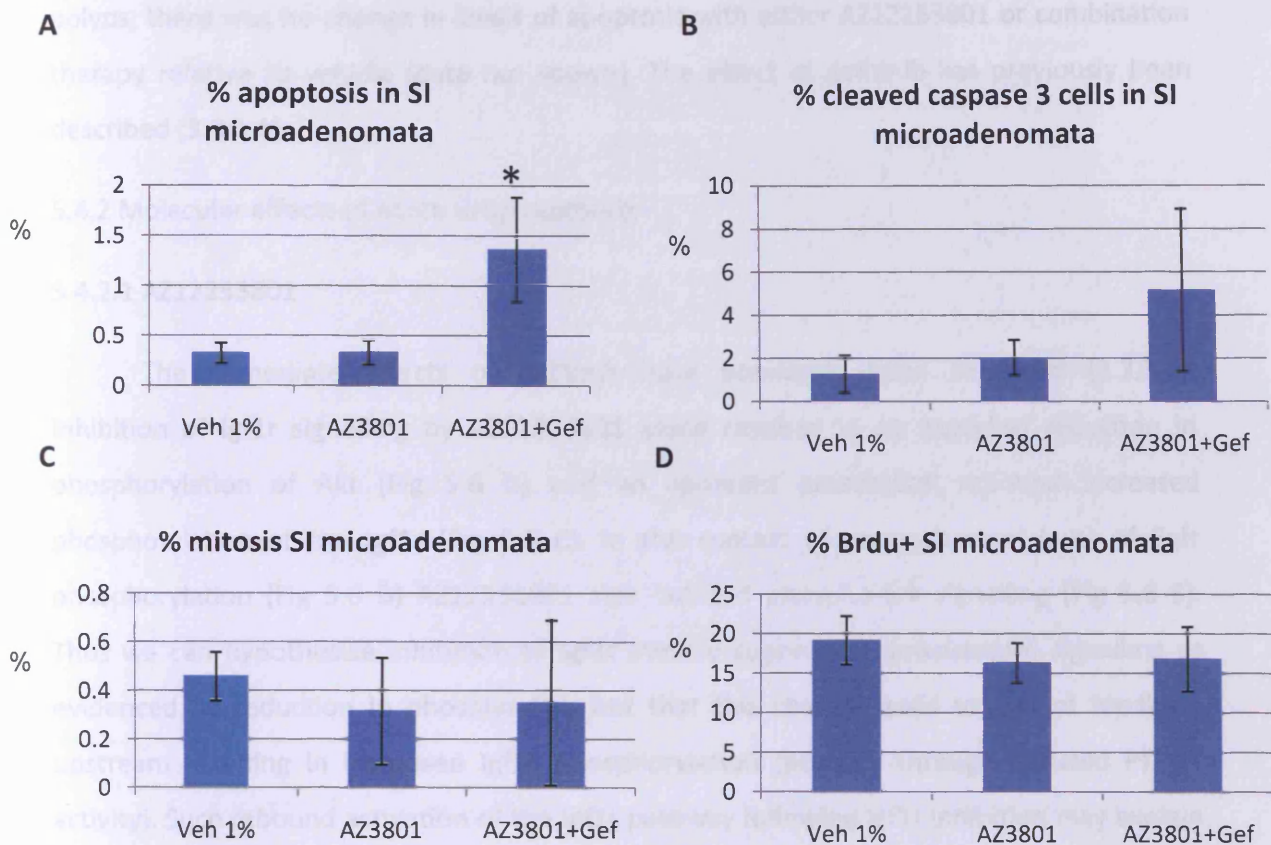


Fig 5.5 (A). Plot of % apoptosis counts from haematoxylin and eosin stained sections (B). % Cleaved caspase-3 immuno-reactivity . (C) % Mitosis counts from haematoxylin and eosin stained sections and (D)% Brdu positive immuno-reactivity. (A-D) represent counts in small intestinal (SI) tumours exposed to respective drug for 4 hr. 3 mice were used for each drug exposure. Error bars represent ± 1 standard deviation. * P value = 0.04 (Mann-Whitney). Veh 1% = 1% Tween80, AZ3801= AZ12253801 12.5mg/kg, AZ3801+Gef= AZ12253801 12.5mg/kg+Gefitinib75mg/kg.

polyps, there was no change in levels of apoptosis with either AZ12253801 or combination therapy relative to vehicle (data not shown). The effect of gefitinib has previously been described (3.3.1.1).

5.4.2 Molecular effects of acute drug exposure

5.4.2.1 AZ12253801

The immediate effects of gefitinib have previously been described (3.3.3.1). Inhibition of Igf1r signalling by AZ12253801 alone resulted in an expected reduction in phosphorylation of Akt (Fig 5.6 D) and an apparent paradoxical rebound increased phosphorylation of the Igf1r (Fig 5.6 C). In the context of an unchanged level of Egfr phosphorylation (Fig 5.6 B) AZ12253801 also induced phospho-Erk signalling (Fig 5.6 E). Thus we can hypothesise inhibition of Igf1r initially suppresses downstream signalling as evidenced by reduction in phospho-Akt, but that this change leads to loss of feedback upstream resulting in increased Igf1r phosphorylation (possibly through reduced PTPB1 activity). Such rebound activation of the Igf1r pathway following Igf1r inhibition may explain the increased level of Erk phosphorylation or alternatively reflect altered Egfr trafficking.

5.4.2.2 Combined Gefitinib with AZ12253801

In view of the signalling changes described for Egfr and Igf1r inhibition alone, I anticipated combined Egfr/Igf1r inhibition would produce either competing or additive molecular effects four hours after exposure. The former is demonstrated for both Egfr and Erk phosphorylation (Fig 5.6 B, E) where the level of activity is between that for each agent alone. For phospho-AKT suppression, an additive effect is demonstrated compared to either treatment in isolation (Fig 5.6 D). For phospho-Igf1r, combination therapy resulted in either similar (Igf1r inhibition) or reduced (Egfr inhibition) levels compared to individual treatments (Fig 5.6 C).

5.5 Molecular signalling changes in tumours chronically exposed to drugs

I next examined signal transduction pathway changes associated with chronic drug to determine potential tumour resistance mechanisms and ask if the acute signalling

Figure 5.6 Acute downstream signalling changes in *Apc^{min/+}* colon polyps post 4 hr drug exposure

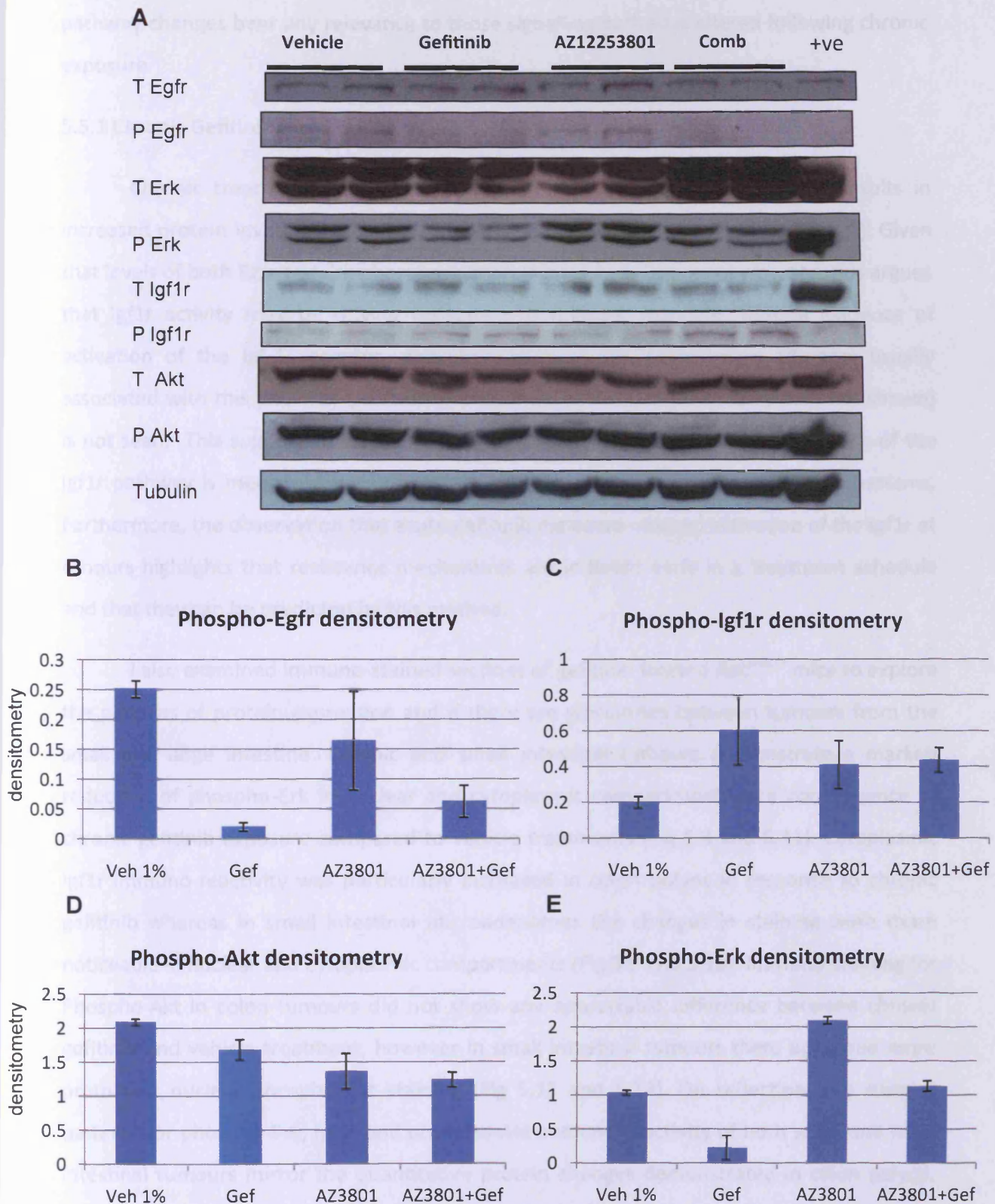


Fig 5.6 (A) Western blots to show immediate (4 hr) effect of 1% Tween80 (Veh), Gefitinib 75mg/kg (Gef), AZ12253801 (AZ3801) 12.5mg/kg and AZ12253801 12.5mg/kg+Gefitinib 75mg/kg on the respective proteins. Loading controls were either B actin or tubulin. Polyps were pooled from 3 mice for each treatment (further detail in appendix 2.6) (B-E) Densitometry readings for phospho-proteins.+ve signifies positive control. Error bars represent range of values.

pathway changes bear any relevance to those signalling pathways altered following chronic exposure.

5.5.1 Chronic Gefitinib

Chronic treatment of *Apc^{min/+}* mice with gefitinib (relative to vehicle) results in increased protein levels of total Egfr, total Igf1r and phospho-Igf1r (Fig 5.7A, B, E, F). Given that levels of both Egfr and Erk phosphorylation (Fig 5.7 A, C, D) are not elevated, this argues that Igf1r activity may be driving resistance to therapy. However, despite evidence of activation of the Igf-1 receptor, phosphorylation of the downstream effectors usually associated with this pathway (Akt and s6 ribosomal protein- densitometry data not shown) is not seen. This suggests that, in the setting of chronic blockade of Egfr, activation of the Igf1r pathway is mediating tumour growth through alternative, unidentified mechanisms. Furthermore, the observation that acute gefitinib exposure induced activation of the Igf1r at 4 hours highlights that resistance mechanisms are initiated early in a treatment schedule and that they can be predicted by this method.

I also examined immuno-stained sections of gefitinib treated *Apc^{min/+}* mice to explore the patterns of protein expression and if there are similarities between tumours from the small and large intestine. Colonic and small intestinal tumours demonstrate a marked reduction of phospho-Erk in nuclear and cytoplasmic compartments as a consequence of chronic gefitinib exposure compared to vehicle treatments (Fig 5.8 and 5.11). Cytoplasmic Igf1r immuno-reactivity was particularly increased in colon polyps in response to chronic gefitinib whereas in small intestinal microadenomas the changes in staining were more noticeable in nuclear and cytoplasmic compartments (Fig 5.9 and 5.10). Immuno-staining for Phospho-Akt in colon tumours did not show any appreciable difference between chronic gefitinib and vehicle treatment, however in small intestinal tumours there appeared more prominent nuclear phospho-Akt staining (Fig 5.12 and 5.13). On reflection, the staining patterns for phospho-Erk, Igf1r and phospho-Akt immuno-reactivity of both small and large intestinal tumours mirror the quantitative protein changes demonstrated in colon polyps, suggesting the same molecular changes occur irrespective of tumour site.

5.5.2 Chronic AZ12253801

Figure 5.7 Signalling pathways in *Apc^{min/+}* tumours following chronic treatment

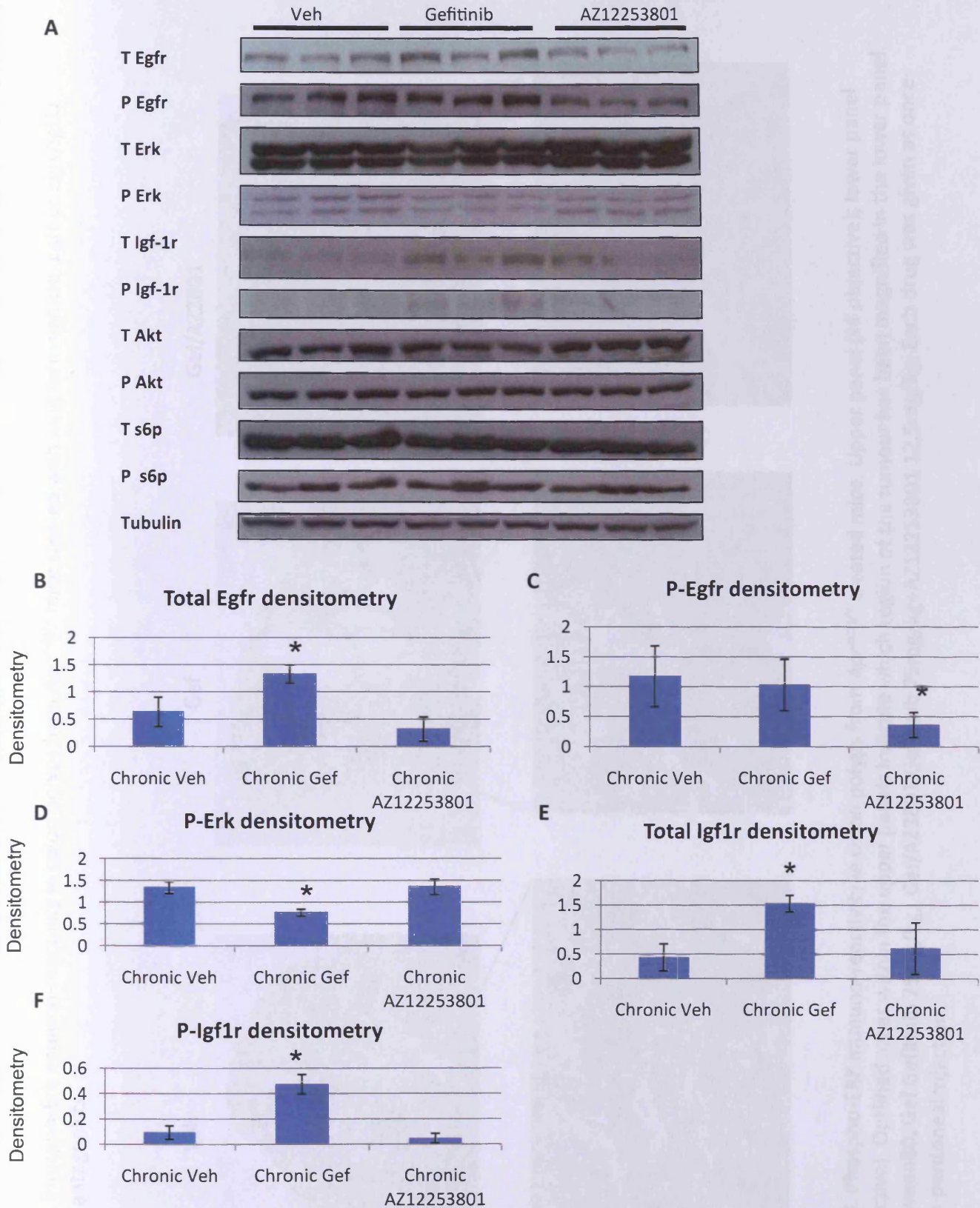


Fig 5.7 (A) Western blots to demonstrate the chronic effect of 1% Tween80 (Veh), Gefitinib (Gef) 75mg/kg, AZ12253801 (AZ3801) 12.5mg/kg and combination AZ12253801 12.5mg/kg+Gefitinib 75mg/kg upon the respective protein. Equivalent quantities of protein were pooled from 3 mice for each treatment except vehicle (n=2). In total 7 polyps pooled for vehicle, 8 polyps for gefitinib and 13 polyps for AZ12253801 treatments. (B-D) Densitometry plots for phospho-proteins which were altered in response to drugs. Loading control was tubulin. * P=0.04 (Mann-Whitney). Error bars represent ± 1 standard deviation.

Figure 5.8. Phospho-Erk immuno-reactivity in colon polyps from *Apc^{min/+}* mice treated with long term vehicle, Egfr or Egfr/Igf1r combined antagonists.

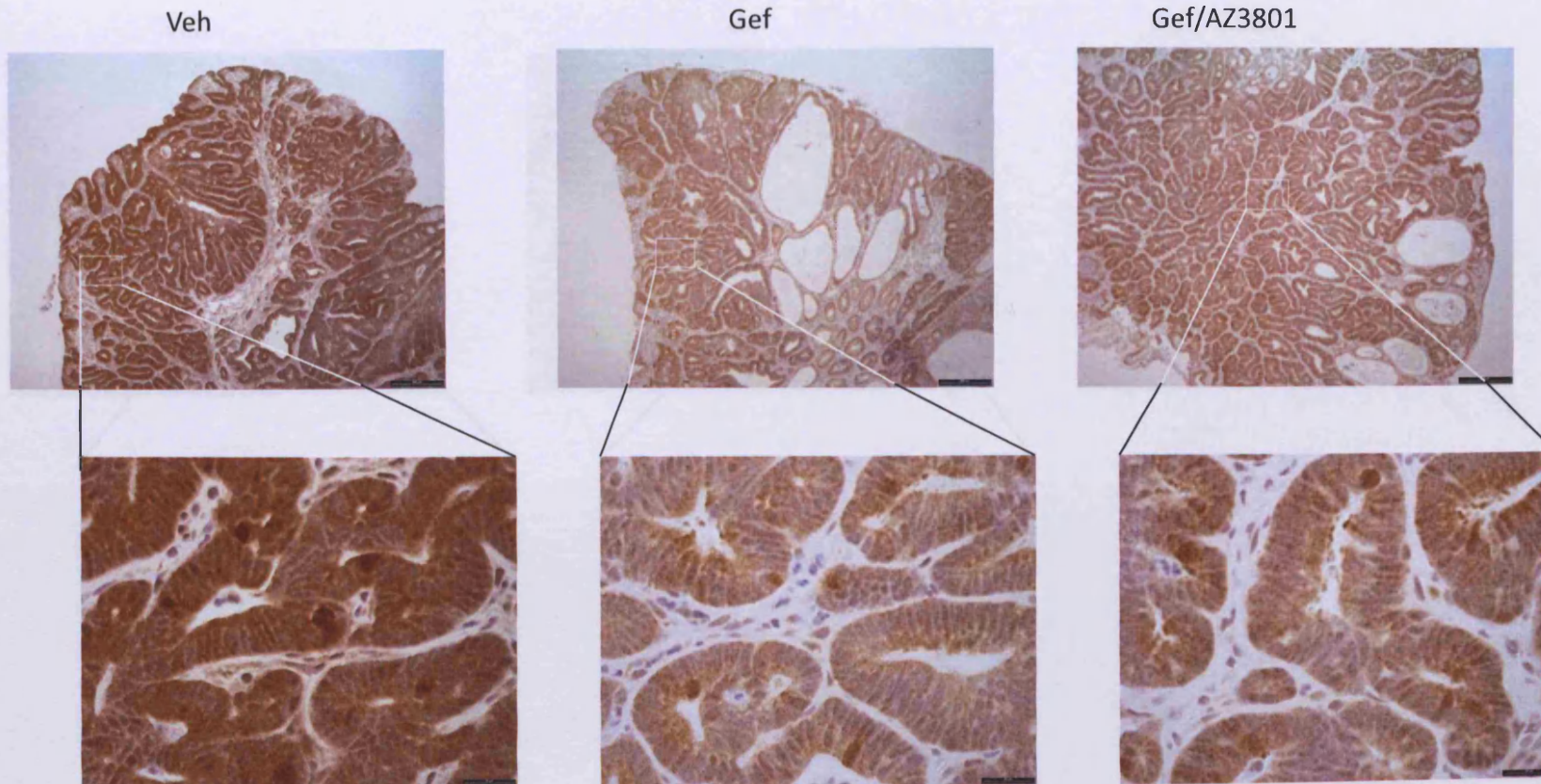


Figure 5.8. Phospho-ERK immuno-reactivity in colon polyps from *Apc^{min/+}* treated mice. Upper panel (x4 objective); lower panel (x40 objective). Outlined areas within the upper panels indicate which region of the tumour has been magnified in the lower panel. Veh 1% Tween80, Gef Gefitinib 75mg/kg, Gef/AZ3801 Gefitinib 75mg/kg+AZ12253801 12.5mg/kg. Each drug was given as once daily intra-peritoneal injection.

Figure 5.9 Igf1r immuno-reactivity in colon polyps from *Apc^{min/+}* mice treated with long term vehicle, Egfr or Egfr/Igf1r combined antagonists.

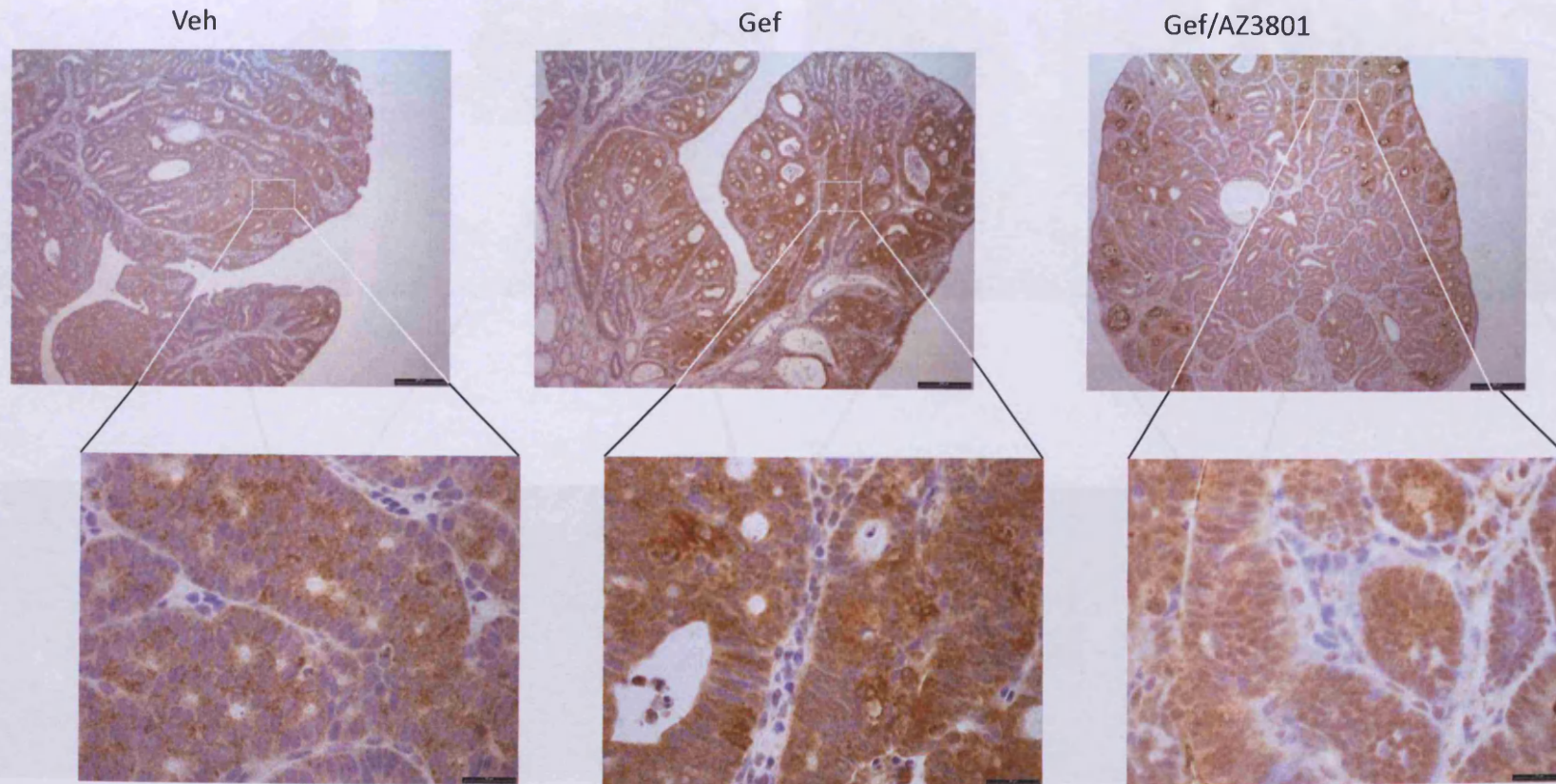


Figure 5.9. Igf1r immuno-reactivity in colon polyps from *Apc^{min/+}* treated mice. Upper panel (x4 objective); lower panel (x40 objective). Outlined areas within the upper panels indicate which region of the tumour has been magnified in the lower panel. Veh 1% Tween80, Gef Gefitinib 75mg/kg, Gef/AZ3801 Gefitinib 75mg/kg+AZ12253801 12.5mg/kg. Each drug was given as once daily intra-peritoneal injection.

Figure 5.10. Igf1r immuno-reactivity in small intestinal adenomas from *Apc^{min/+}* mice treated with long term vehicle, Egfr, Igf1r or Egfr/Igf1r combined antagonists.

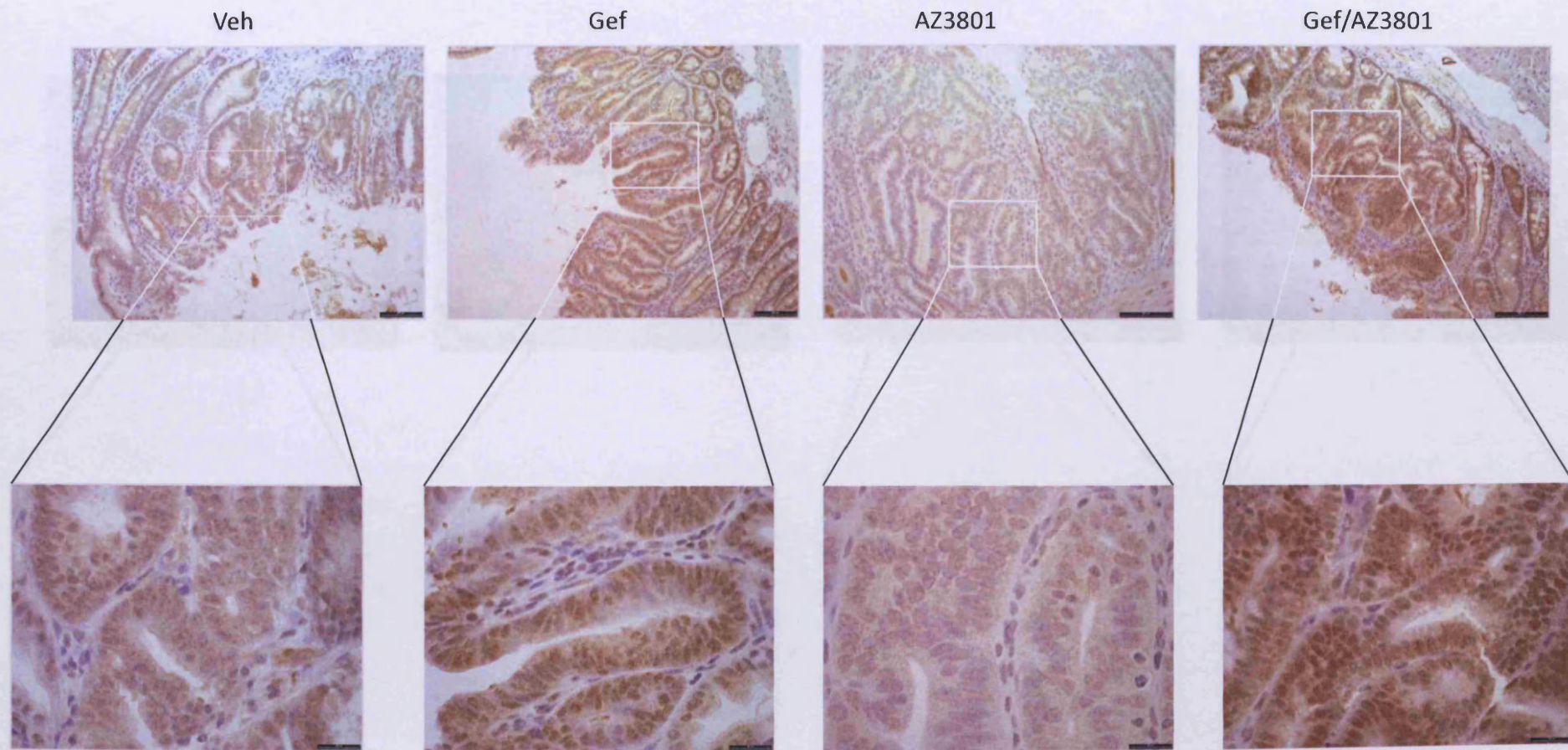


Figure 5.10. Igf1r immuno-reactivity in small intestinal adenomas from *Apc^{min/+}* treated mice. Upper panel (x10 objective); lower panel (x40 objective). Outlined areas within the upper panels indicate which region of the tumour has been magnified in the lower panel. Veh 1% Tween80, Gef Gefitinib 75mg/kg, AZ3801 AZ12253801 12.5mg/kg, Gef/AZ3801 Gefitinib 75mg/kg+AZ12253801 12.5mg/kg. Each drug was given as once daily intra-peritoneal injection.

Figure 5.11. Phospho-Erk immuno-reactivity in small intestinal adenomas from *Apc^{min/+}* mice treated with long term vehicle, Egfr, Igf1r or Egfr/Igf1r combined antagonists.

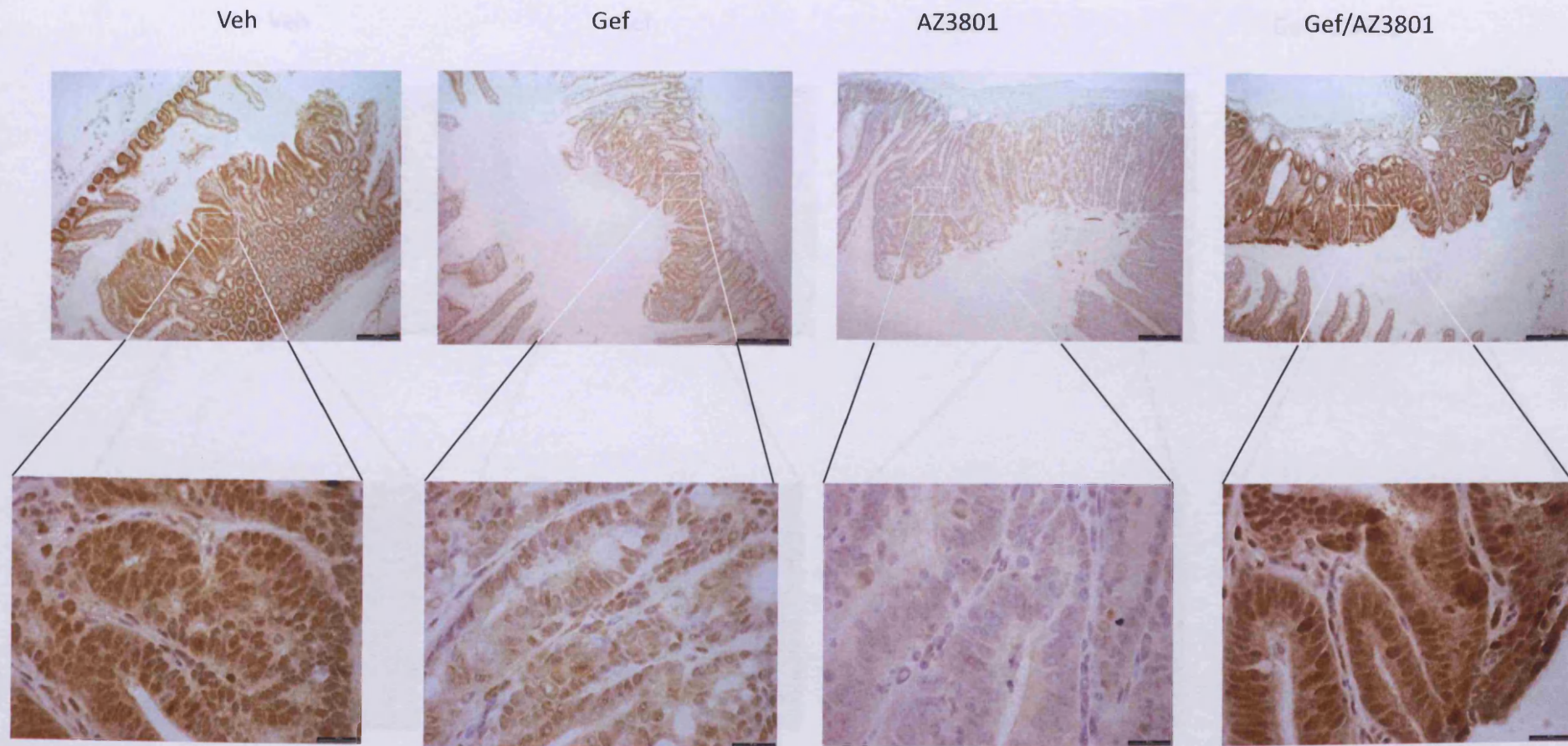


Figure 5.11. Phospho-Erk immuno-reactivity in small intestinal adenomas from *Apc^{min/+}* treated mice. Upper panel (x4 objective); lower panel (x40 objective). Outlined areas within the upper panels indicate which region of the tumour has been magnified in the lower panel. Veh 1% Tween80, Gef Gefitinib 75mg/kg, AZ3801 AZ12253801 12.5mg/kg, Gef/AZ3801 Gefitinib 75mg/kg+AZ12253801 12.5mg/kg. Each drug was given as once daily intra-peritoneal injection.

Figure 5.12. Phospho-Akt immuno-reactivity in small intestinal adenomas from *Apc^{min/+}* mice treated with long term vehicle, Igf1r or Egfr/Igf1r combined antagonists.

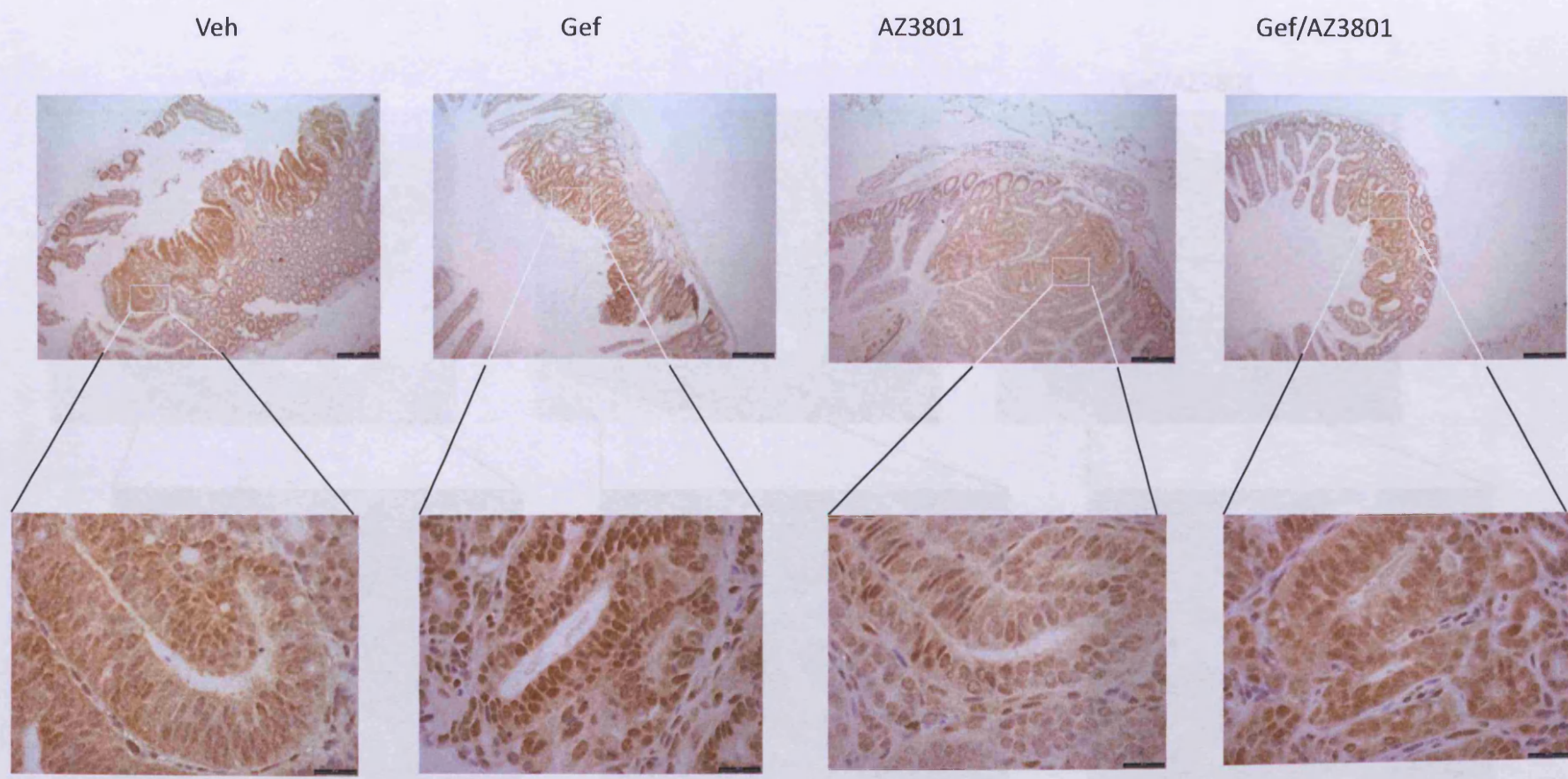


Figure 5.12. Phospho-Akt immuno-reactivity in small intestinal adenomas from *Apc^{min/+}* treated mice. Upper panel (x4 objective); lower panel (x40 objective). Outlined areas within the upper panels indicate which region of the tumour has been magnified in the lower panel. Veh 1% Tween80, Gef Gefitinib 75mg/kg, AZ3801 AZ12253801 12.5mg/kg, Gef/AZ3801 Gefitinib 75mg/kg+AZ12253801 12.5mg/kg. Each drug was given as once daily intra-peritoneal injection.

Figure 5.13. Phospho-Akt immuno-reactivity in colon polyps from *Apc^{min/+}* mice treated with long term vehicle, Egfr or Egfr/Igf1r combined antagonists.

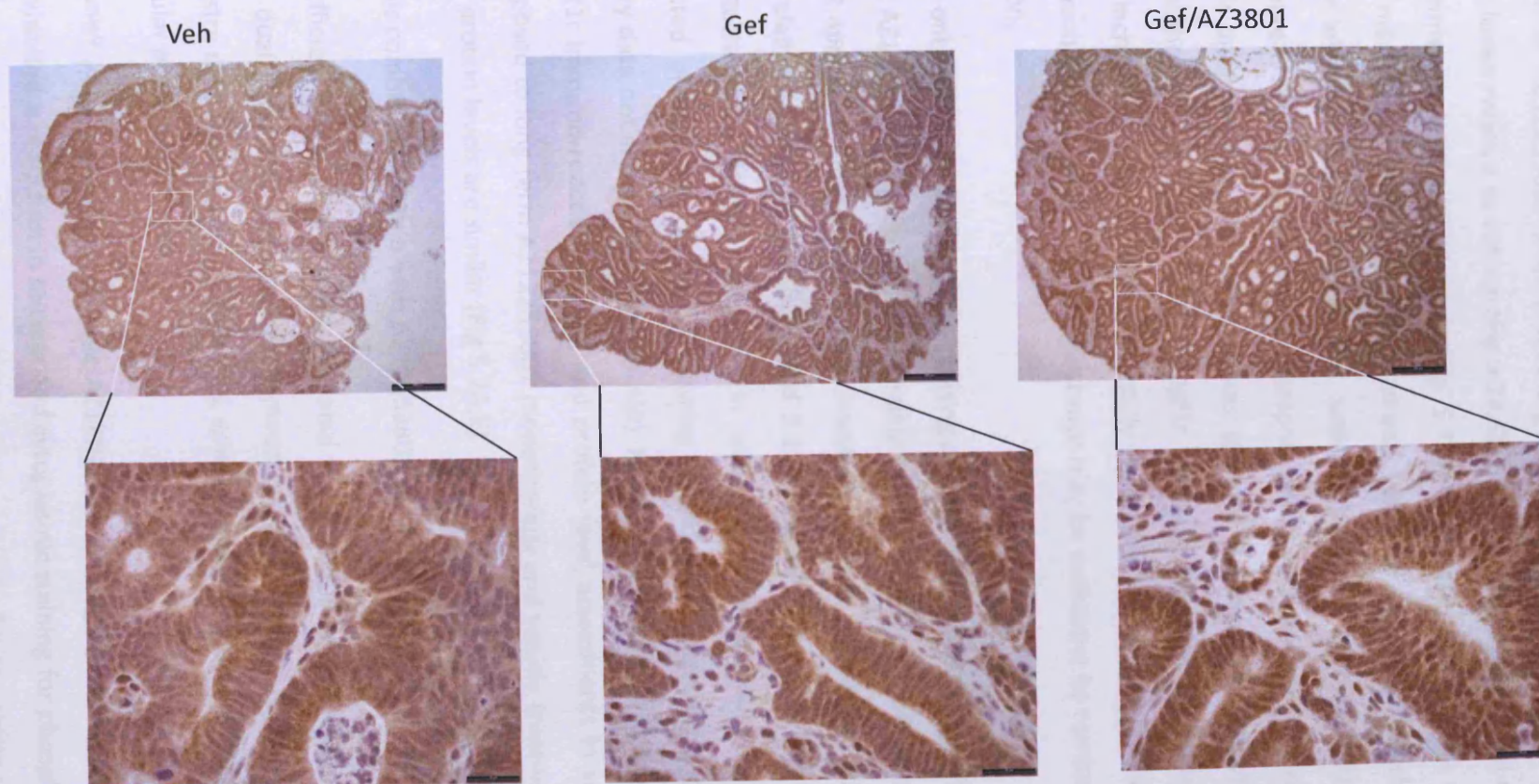


Figure 5.13. Phospho-Akt immuno-reactivity in colon polyps from *Apc^{min/+}* treated mice. Upper panel (x4 objective); lower panel (x40 objective). Outlined areas within the upper panels indicate which region of the tumour has been magnified in the lower panel. Veh 1% Tween80, Gef Gefitinib 75mg/kg, Gef/AZ3801 Gefitinib 75mg/kg+AZ12253801 12.5mg/kg. Each drug was given as once daily intra-peritoneal injection.

The only change observed following chronic inhibition of Igf1r through administration of AZ12253801 after 8 weeks gefitinib monotherapy was a reduction in phospho-Egfr levels relative to vehicle (Fig 5.7A-F). Given the suppressed level of phospho-Egfr, the maintenance of phospho-Erk (Fig 5.7 A, D) is presumed to be via an Egfr independent mechanism, such as repression of an inhibitor of phospho-Erk such as sprouty. Chronic Igf1r inhibition results in different pathway dynamics to acute Igf1r inhibition, where I observed reciprocal activation of phospho-Egfr (to a level similar to vehicle where Egfr activity is unopposed in promoting tumour growth) and increased phospho-Erk. If the level of phospho-Erk is crucial in driving Igf1r resistant tumours, then the acute data showing an increase in phospho-Erk potentially reflects a mechanism of resistance. This raises the possibility that Igf1r inhibitor resistance may be overcome by combined Igf1r and Mek inhibition.

I was only able to probe immuno-staining of small intestinal tumours after treatment with chronic AZ12253801, which was not possible for colon tumours. Both phospho-Erk and phospho-Akt appeared suppressed in small intestinal tumours in response to AZ12253801 treatment relative to vehicle (Fig 5.11 and 5.12). This demonstrates the limitations of immuno-histochemistry as no difference in small intestinal tumours levels of either phosphorylated protein was evident following quantitative assessment (Fig 5.7 A, D; densitometry data not shown for phospho-Akt). However, there was a better concordance between Igf1r immuno-reactive staining and protein level assessments in small intestinal tumours exposed to long term AZ12253801 monotherapy and vehicle treatments (Fig 5.10) where Igf1r protein levels are similar (Fig 5.7A,E).

5.5.3 Chronic combined Gefitinib with AZ12253801

Insufficient colon polyps were available for quantitative pathway analysis of the effects of dual Egfr/Igf1r therapy on tumours. This led to a reliance on immuno-histochemistry data from intestinal tumours, which although not quantitative, gave insight into molecular pathway changes.

Apc^{min/+} mice exposed to chronic AZ12253801 12.5mg/kg combined with gefitinib 75mg/kg exhibited a reduction in nuclear and cytoplasmic staining for phospho-Erk in colon tumours whereas staining in small intestinal tumours was similar to vehicle treatments (Fig

5.8 and 5.11). The level of phospho-Akt staining appears similar in small intestinal tumours treated with combination therapy and vehicle (Fig 5.12), whereas for colon tumours there is a propensity for increased nuclear staining associated with dual therapy relative to vehicle (Fig 5.13). Immuno-staining against Igf1r appeared increased in small and large intestinal tumours from *Apc^{min/+}* mice treated with either gefitinib containing regimen, although the pattern of staining was restricted to the cytoplasm in colonic tumours (Fig 5.9, 5.10).

5.6 Discussion

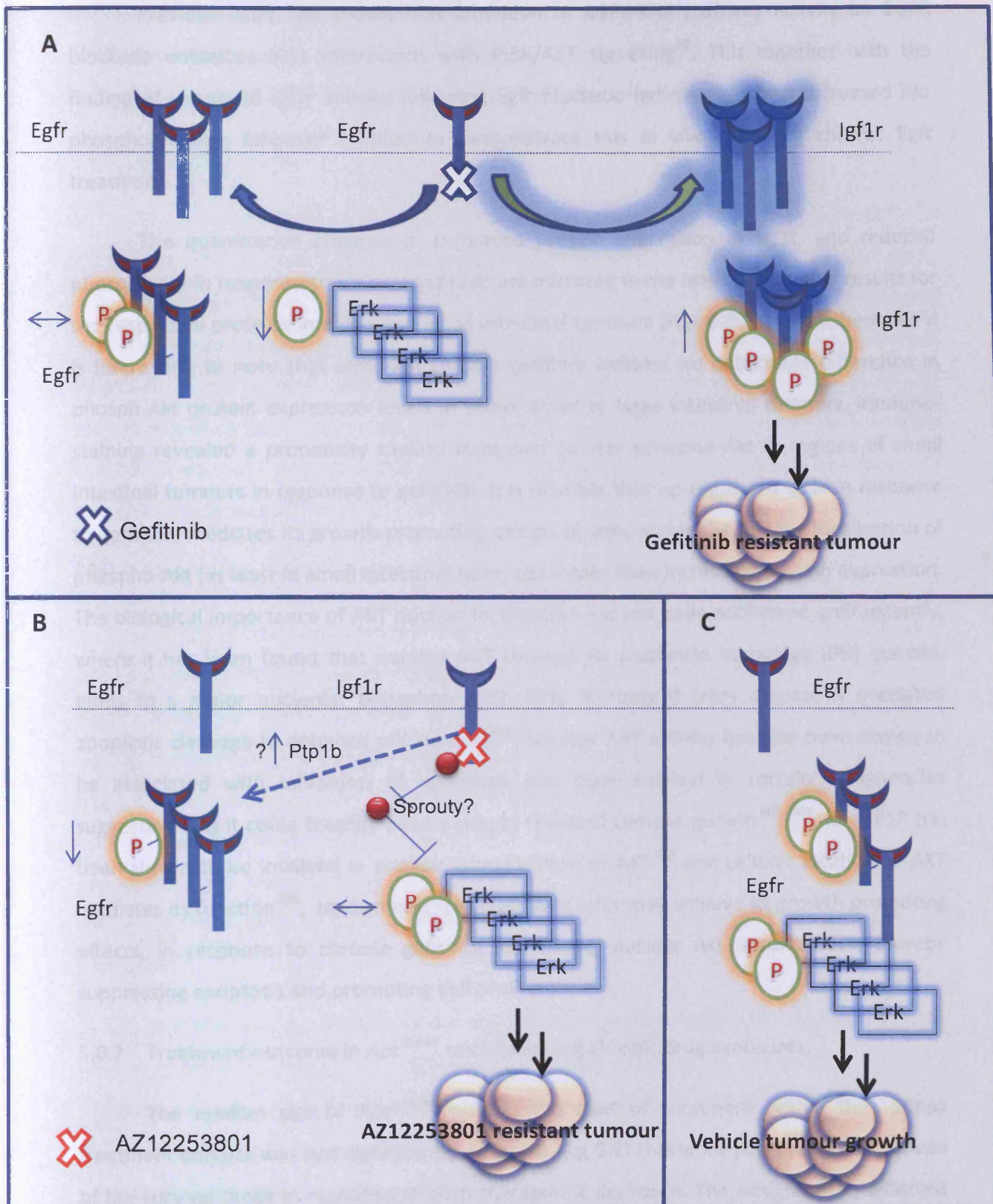
I have described the acute and chronic effects of inhibiting Egfr and Igf1r alone and in combination in the *Apc^{min/+}* mouse. Given that *K-RAS* and *B-RAF* wild type status is predictive of EGFR targeted response in patients^{46, 50}, and having demonstrated that *Apc^{min/+}* mice intestinal polyps remain wild type for *K-ras* and *B-raf* (3.2), underscores the relevance of this model for studying EGFR blockade. In terms of responsiveness to agents that target EGFR and IGF1R, there is increasing evidence for cross communication between these two pathways from both cell line and xenograft studies^{77, 80, 81, 95, 96, 198, 199}. Here I have now extended this analysis to an autochthonous *in vivo* animal model.

5.6.1 Igf1r up-regulation and activation in response to chronic gefitinib treatment

I have confirmed the significance of early gefitinib induced Igf1r signalling in colon polyps in relation to resistance as Igf1r and Igf1r phosphorylation are increased at the protein level in chronic gefitinib exposed resistant tumours (fig 5.14). Furthermore this data suggests resistance mechanisms are initiated very early in a treatment schedule and that it may be possible to sample tumours early in a course of treatment to assess molecular responses and identify biomarkers predictive of resistance.

Interestingly phospho-Akt and phospho-s6p were not activated despite Igf1r pathway activity, suggesting an alternate pathway is responsible for signal transduction promoting tumour growth. It appears that tumour cells in an attempt to overcome Egfr blockade also increase Egfr protein but fail to increase activation of Egfr signalling as shown by an absence of change in Egfr phosphorylation and reduced Erk phosphorylation (fig 5.14). It is possible that certain transcripts differentially expressed in colon tumour tissue, in response to long term gefitinib (Cbl, Ubd and Hip1), are involved in up-regulated expression of Egfr through their previously discussed effects on Egfr turnover (3.11.4.2, 3.11.4.4, 3.11.4.5). Egfr is able to engage with alternate effector pathways, such as Src/Fak, Stat or Plcy/Pkc⁶⁷ which I have not probed, but may be responsible for mitogenic signal transmission. EGFR-IGF1R hetero-dimerisation has been reported in response to gefitinib treatment of human NSCLC cell lines²⁰⁰ and may explain a role for increased Egfr expression, to circumvent Egfr blockade, in concert with up-regulated Igf1r.

Fig 5.14. Resistance mechanisms postulated as a consequence of chronic Egfr or Igf1r inhibition in *Apc^{min/+}* mice



Resistance mechanisms in *Apc^{min/+}* tumours in response to Egfr and Igf1r inhibition. (A) Chronic gefitinib, leads to increased expression of Igf1r and p-Igf1r and resistant tumour growth. Egfr protein is increased without activity downstream. (B) Chronic AZ12253801 results in reduced phospho-Egfr which may be mediated via increased PTP1B activity. Erk activity is speculated to be maintained by repression of an inhibitor of phospho-Erk (sprouty). (C) Unopposed Egfr signalling with vehicle control.

Previous work has shown that inhibition of EGFR-ERK pathway activity by EGFR blockade enhances IRS1 interaction with PI3K/AKT signalling⁸⁰. This together with the finding of increased Igf1r activity following Egfr blockade led me to expect increased Akt phosphorylation, however I failed to demonstrate this *in vivo* following chronic Egfr treatment.

The quantitative changes of increased protein expression of Igf1r, and reduced phospho-Erk in response to chronic gefitinib are mirrored in the immuno-staining results for the respective proteins in colon and small intestinal tumours (Figs 5.8-5.11). Furthermore it is interesting to note that although chronic gefitinib induced no detectable difference in phosph-Akt protein expression levels in either small or large intestinal tumours, immuno-staining revealed a propensity toward increased nuclear phospho-Akt in regions of small intestinal tumours in response to gefitinib. It is possible that up-regulated Igf1r in response to gefitinib, mediates its growth promoting effects by influencing the cellular localisation of phospho-Akt (at least in small intestinal tumours) rather than increasing protein expression. The biological importance of AKT nuclear localisation has not been addressed until recently, where it has been found that nuclear AKT through its pleckstrin homology (PH) domain, binds to a major nucleolar phosphoprotein B23, rescuing it from caspase 3 mediated apoptotic cleavage to enhance cell survival²⁰¹. Nuclear AKT activity has also been shown to be associated with inhibition of apoptosis and poor survival in certain malignancies suggesting that it could feasibly have a role in resistant tumour growth^{202, 203}. As IGF1R has been shown to be involved in nuclear translocation of AKT²⁰⁴ and cellular location of AKT regulates its function²⁰⁵, leads me to speculate that Igf1r may achieve its growth promoting effects, in response to chronic gefitinib, by driving nuclear Akt accumulation thereby suppressing apoptosis and promoting cell proliferation.

5.6.2 Treatment outcome in *Apc^{min/+}* mice following chronic drug exposures.

The median age of *Apc^{min/+}* mice at the start of treatment within the various treatment cohorts was not significantly different (Fig 5.2) therefore permitting comparison of the survival times in response to each therapeutic approach. The design of the different treatment schedules (Fig2.1) with the exception of vehicle control, incorporated an initial 8 week period of gefitinib exposure on the assumption this would drive gefitinib resistant

tumour clones. In retrospect it would have been useful to incorporate a small pilot study to confirm the presence of intestinal tumours, subject to treatment, and also show the up-regulated expression Igf1r driving gefitinib resistant tumour growth.

5.6.2.1 Chronic Gefitinib

There was a clear survival advantage in *Apc^{min/+}* mice treated with once daily gefitinib 75mg/kg as median survival was extended by 36 days or 23% (158 days vs. 194 days, $P < 0.0001$; log rank test; Fig 5.3A). This was a consequence of cell cycle inhibition and increased apoptosis (3.3.1.1) leading to reduced intestinal tumourigenesis (delayed small intestinal tumourigenesis and inhibition of colon polyp initiation). The observation of perturbed cell cycling supports an earlier report of gefitinib reducing proliferation and the number of aberrant crypt foci and colonic microadenomas in an azoxymethane model of colonic carcinogenesis¹⁴⁹.

5.6.2.2 Chronic AZ12253801

The IGF1R has been implicated in the development of tumours in various settings⁸⁶ and I anticipated inhibition of the Igf1r would be of potential therapeutic significance in this model, which has been confirmed; Igf1r inhibition (following gefitinib monotherapy for 8 weeks) improved median survival compared to vehicle by 50 days or 32% (158 days vs. 208 days, $P < 0.001$; log rank test; Fig 5.3A). In demonstrating Egfr blockade enhanced Igf1r activity and that monotherapy against Igf1r enhances survival in *Apc^{min/+}* mice I have provided further additional support for the *in vivo* proof of concept that Igf1r targeted therapy is of benefit in tumours expressing high receptor levels and is a potential predictive biomarker²⁰⁶.

At the time of death there was an increase in median small intestinal tumour volume relative to vehicle, which in the absence of a detected difference in the small intestinal tumour count, indicated tumours grew to a larger size in the AZ12253801 treated cohort. This increase in small intestinal tumour burden is also observed for AZ12253801 exposure relative to single agent gefitinib and combined gefitinib/AZ12253801 treatment in addition to an increase in small and large intestinal tumour counts. This appears to reflect the loss of a therapeutic effect of gefitinib in the AZ1253801 cohort of mice which only received

gefitinib for 8 weeks prior to AZ12253801 monotherapy, suggesting that the scheduling sequence of short term gefitinib is sub-optimal despite the survival advantage documented. It is possible that the withdrawal of gefitinib at 8 weeks results in loss or reduced expression of Igf1r, the target of AZ12253801, and could explain why continued EGFR blockade with gefitinib is necessary to maximally suppress small intestinal tumour growth. Ideally to investigate the timing of Igf1r expression in relation to EGFR blockade, *Apc^{min/+}* should have been treated for 8 weeks to confirm up-regulation of tumoural Igf1r expression and subsequent loss or reduced expression demonstrated upon withdrawal thereafter to support this hypothesis.

The failure to detect changes in cell death and proliferation arising from acute AZ12253801 exposure is likely to reflect the selection of an inappropriate time point as the prolongation in survival afforded by AZ12253801 monotherapy must be reflected by anti-tumour phenotypic changes. Unfortunately it was not feasible to re-examine cell death and proliferation at further time points which would be a logical step forward.

5.6.2.3 Chronic combined Gefitinib with AZ12253801

The acute increase in Igf1r activity in colon polyps following exposure to Egfr blockade raises the possibility of testing tumour specimens or circulating tumour cells²⁰⁷ for their initial response to drug. Such responsiveness could then be considered in determining therapeutic combinations. To address this approach, I determined if the acute activity in Igf1r predicted improved outcome (in terms of tumour burden/survival) when Igf1r inhibition was combined with Egfr blockade. I have demonstrated a dramatic suppression of intestinal tumourigenesis with combination treatment relative to vehicle as evidenced by an almost 3 fold reduction of small intestinal tumour volume and 16 fold reduction of median colon tumour volume. The documented increase in apoptosis in small intestinal tumours following acute (4 hour) exposure to combined Egfr/Igf1r blockade (fig 5.5A), without a difference in Brdu labelling, suggests increased cell death is the important determinant of this response. Similar reports of enhanced apoptosis with the combination have been published with⁸¹ or without increased anti-proliferative effects^{80,95}.

The reduction in small intestinal volume remains equally impressive when compared to gefitinib treatment alone reinforcing the therapeutic advantage of adding Igf1r blockade

to gefitinib. Surprisingly however, although a survival advantage is seen compared to vehicle treatment (158 days vs. 182 days), there was no improvement in survival for this combination beyond that seen for either gefitinib or Igf1r inhibitor monotherapy.

The finding that none of the treatment arms exhibited a superior median survival in favour of a particular treatment regimen may at first appear confusing. However the mouse cohorts may not have been large enough to detect a true but small significant difference in survival that exists between the treatment arms. And in addition, if tumour response is a primary albeit non-exclusive determinant of survival and response rates are less than 50%, which is likely here, it follows that the median survival measured at the point 50% of animals have died is controlled by the non-responding groups²⁰⁸. Therefore in this setting the median survivals are unlikely to be different across the treatment arms given response rates for the treatment arms are probably less than 50%.

5.6.2.4 Adverse effects

Previous experiments have described a wavy hair phenotype in *wa-2* homozygous mice arising from a point mutation in the EGFR tyrosine kinase domain (glycine to valine substitution at residue 743) resulting in impaired kinase activity²⁰⁹. This clearly explains the phenotype of wavy fur in *Apc^{min/+}* mice in response to chronic gefitinib (fig 5.4A) and provides biological evidence that EGFR tyrosine kinase has been targeted in the experiments.

The development of abdominal collections at sites of intra-peritoneal injection in mice receiving combination treatment with AZ12253801 12.5mg/kg and gefitinib 75mg/kg, was clearly a problem in a small number of animals, which were culled as a consequence (fig 5.4B). Given that EGFR signalling has been shown to have important roles in cutaneous wound healing²¹⁰ and innate immunity²¹¹, and that Igf1r blockade can impair blood sugar homeostasis, it is likely these factors contributed to the observed abdominal wall complications seen with *Egfr/Igf1r* inhibition. It is highly probable therefore, that the combination of impaired wound healing and drug induced diabetes gave rise to intra-abdominal infection and early death, thus concealing any potential survival advantage for dual inhibitor blockade. Furthermore, as mice on combined treatment were culled before reaching the experimental primary endpoint, i.e. anaemia secondary to an intestinal tumour

burden, a reduced tumour burden was observed at death in the absence of a survival advantage. Further enquiry could include exposure of wild type mice to the combined treatments, with blood sugar monitoring and microscopy and culture of any subsequent intra-abdominal wall lesions, to examine if fatalities are linked with deregulated glucose metabolism and infection. These complications may have been avoided had the drugs been administered via oral gavage and it is of some reassurance that the agents have been designed for oral ingestion, reducing the concern of serious skin complications in patients enrolled in early phase trials testing Egfr/Igf1r combinations.

5.6.3 Acute downstream molecular effects of drug treatments

Analysis of the acute signalling pathway changes following drug administration was undertaken to increase understanding of mechanisms accounting for drug treatment effects and possible early indications of stimulated resistance mechanisms.

Acute exposure of *Apc^{min/+}* mice to gefitinib suppressed Egfr, Erk and Akt phosphorylation in keeping with its known action as an inhibitor of EGFR tyrosine kinase activity¹³¹. This combined with published evidence of the importance of Egfr signalling in *Apc^{min/+}* mouse intestinal tumours¹⁰⁹ including genetic manipulation studies with hypomorphic Egfr alleles (*Egfr^{wa2}* allele) and pharmacologic manipulation¹¹⁰, supports a role for Egfr in intestinal tumour development. Short term exposure to gefitinib led to increased apoptosis and mitotic blockade in small intestinal tumours and reduced cell cycling in colon polyps. I also observed increased Igf1r phosphorylation. These observations predicted long term exposure to gefitinib may improve survival by delaying the development of intestinal tumours and furthermore, that gefitinib resistance may develop, possibly through deregulation of pathways such as Igf1r. This early observation indicated to me that this model would be useful to test the effect of Igf1r antagonism alone and in combination with gefitinib, which has been confirmed.

Signalling pathway changes in response to acute Igf1r inhibition (fig 5.6 A-E) resulted in an expected reduction in Akt phosphorylation but also a paradoxical increase in Igf1r phosphorylation along with an increased level of Erk phosphorylation in the absence of any change in Egfr activity. I propose that AZ12253801 initially suppresses Igf1r phosphorylation leading to the observed reduction in Akt activity, with this itself triggering feedback leading

to increased Igf1r phosphorylation, possibly through reduced protein tyrosine phosphatase 1B (PTP1B) activity (Fig 5.15). Support for this comes from evidence showing interaction between PTP1B and IGF1R and the regulation of IGF1R kinase activity and function by PTP1B^{212, 213}. Alternatively the increase in Igf1r phosphorylation may be due to induction of cytosolic reactive oxygen species by tyrosine kinase inhibitors⁷⁷ which are known to inhibit PTPs²¹⁴. This rebound activity in Igf1r signalling may account for the marked increase in Erk phosphorylation. Alternatively, the increased Erk activity may be consequent upon subtle changes in Egfr trafficking in the absence of a detectable change in Egfr phosphorylation or secondary to suppression of cytoplasmic phosphatases DUSP 6,7 or 9²¹⁵.

Taken together, I speculate that the predominant initial response to AZ12253801 is suppression of Akt signalling, followed by a switch to predominant Erk signalling resulting in loss of response and increased adenoma growth. If this hypothesis is correct it may be possible to suppress or prevent tumour resistance to Igf1r blockade by inhibiting Erk activity; indeed partial inhibition of Erk phosphorylation is seen by adding gefitinib to Igf1r inhibition (fig 5.6E). Such incomplete Erk inhibition may explain why combination with Egfr blockade therapy ultimately fails, and also suggests that more potent suppression of Erk activity for example with a Mek inhibitor in the context of Igf1r inhibition may be a preferred combination⁸⁰.

In terms of understanding the mechanism of adenoma suppression with combined Egfr/Igf1r treatment, I undertook protein analysis four hours following Egfr and Igf1r blockade alone and in combination. I anticipated demonstrating maximal suppression of Akt phosphorylation for the combination against both drug comparisons^{80, 81} however, I found only suppression of tumoural Akt signalling for combination against vehicle and gefitinib treatment (fig 5.6 D), but not Igf1r inhibition. Expectation of maximal suppression of Akt signalling for the combination does assume a simple additive relationship in terms of the effects seen by either drug in isolation, and it is possible that in combination the relationship between pathways is more complicated such that at the level of Akt, pathway inhibition and loss of negative feedback does not equate with an additive outcome *in vivo* as expected. Therefore in terms of understanding the signalling responsible for combinatorial

Figure 5.15. Rebound activation of Igf1r signalling following Igf1r inhibition through reduced Ptp1b activity.

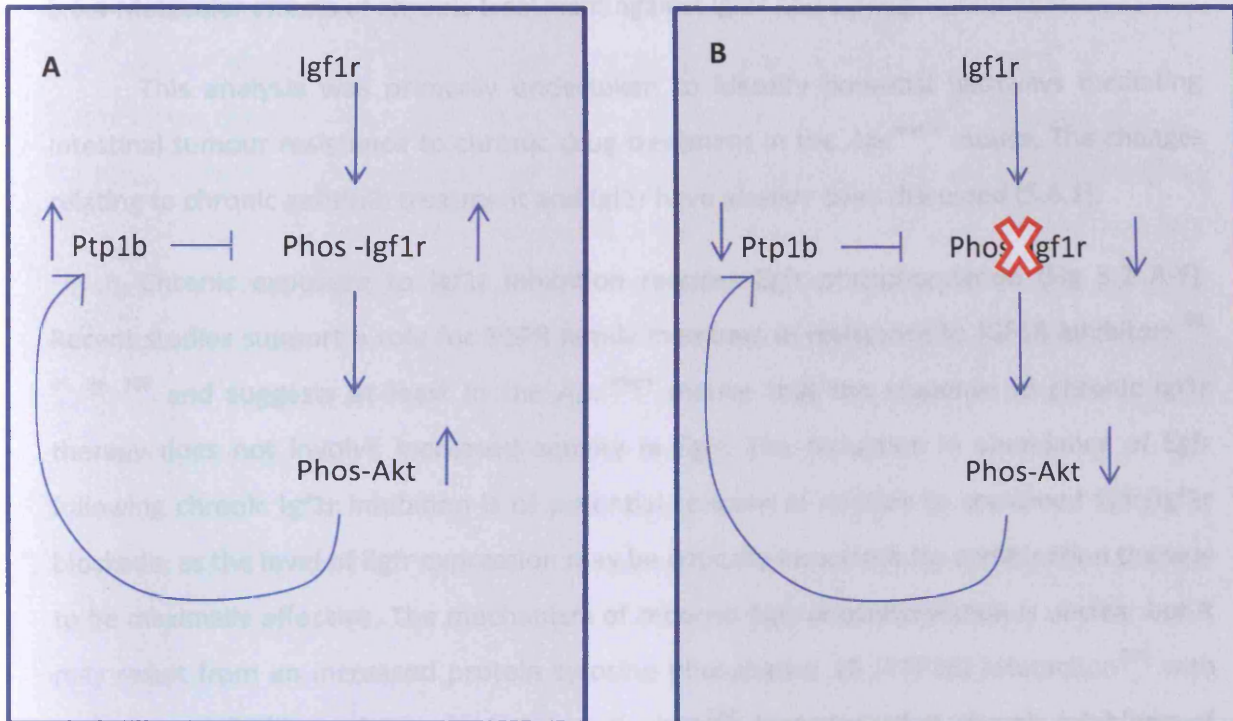


Fig 5.15. (A) Represents a tumour cell which is dependent upon Igf1r activation to promote growth. Activation leads to increased phospho-Akt activity which creates a feedback loop controlling the rate at which Igf1 receptors are de-phosphorylated via the phosphatase activity of protein tyrosine phosphatase 1B (Ptp1b). (B) In the presence of AZ12253801, it is suggested that immediate inhibition of Igf1r phosphorylation leads to reduced phospho-Akt which subsequently leads to suppressed activity of Ptp1b creating a situation where de-phosphorylation of Igf1r is reduced, thereby increasing the phosphorylation status of Igf1r.

tumour suppression I can conclude that relative to vehicle, a reduction in Egfr and Akt phosphorylation appears to be important.

5.6.4 Molecular effects of chronic treatment against Igf1r and Egfr/Igf1r inhibition

This analysis was primarily undertaken to identify potential pathways mediating intestinal tumour resistance to chronic drug treatment in the *Apc^{min/+}* mouse. The changes relating to chronic gefitinib treatment and Igf1r have already been discussed (5.6.1).

Chronic exposure to Igf1r inhibition reduces Egfr phosphorylation (Fig 5.7 A-F). Recent studies support a role for EGFR family members in resistance to IGF1R inhibitors^{80, 95, 96, 198} and suggests at least in the *Apc^{min/+}* mouse that the response to chronic Igf1r therapy does not involve increased activity in Egfr. The reduction in abundance of Egfr following chronic Igf1r inhibition is of potential concern in relation to combined Egfr/Igf1r blockade, as the level of Egfr expression may be critically important for combination therapy to be maximally effective. The mechanism of reduced Egfr phosphorylation is unclear but it may result from an increased protein tyrosine phosphatase 1B (PTP1B) interaction²¹⁶ with endocytosed EGFR on the endoplasmic reticulum²¹⁷. I propose that chronic inhibition of Igf1r in the absence of Egfr activation may reflect repression of an inhibitor of phospho-Erk (e.g. sprouty²¹⁵) resulting in Erk activity equivalent to vehicle treatment culminating in intestinal tumour growth. It would be of interest to examine the role of Erk signalling in this setting by testing the therapeutic effect of additional Erk1/2 signalling inhibition. This could be achieved by combining Igf1r antagonism with Mek inhibition. Enhanced IGF1R directed AKT signalling⁸⁰ has been documented with Mek inhibitor monotherapy making this a logical approach for this additional reason.

Weak immuno-staining for phospho-Erk and phospho-Akt in small intestinal tumours (fig 5.11 and 5.12) is inconclusive given that quantitative protein level data for Erk and Akt phosphorylation (fig 5.7A and E) does not suggest a difference in expression between chronic vehicle and Igf1r inhibition. Igf1r immuno-staining of small intestinal adenomas is in agreement with protein level data showing similar levels of Igf1r expression between chronic vehicle and Igf1r inhibitor treatment (Fig 5.10). Based on the available protein level data, Igf1r protein expression appears to be driven by continuous gefitinib exposure (fig 5.7 E). As gefitinib was only administered for 8 weeks to mice receiving Igf1r inhibitor

monotherapy, I propose that withdrawal of Egfr blockade removes the stimulus to up-regulate Igf1r expression compromising the therapeutic effect of Igf1r inhibition in terms of intestinal tumour suppression.

In the absence of protein level data for pathway changes in response to chronic combination therapy, immuno-staining was undertaken to help identify potential changes occurring in tumours following chronic drug exposure. The apparent increase in phospho-Erk staining in small intestinal tumours (fig 5.11) may suggest that Erk activity mediates resistance in response to chronic combined therapy, although this pattern is not repeated in colon polyps (fig 5.8). The mechanism for this observed increase in small intestinal tumour phospho-Erk immuno-staining following chronic Egf/Igf-1 receptor blockade may be secondary to suppression of auto-regulatory feedback loops acting at nodal levels in the MAPK pathway^{151, 218}. An alternative response to dual Egfr/Igf1r inhibition may be determined by the pattern of phospho-Akt staining which is predominantly nuclear in colon polyps in particular, following chronic treatment (fig 5.12 and 5.13). This nuclear localisation of phospho-Akt may reflect a mechanism of inhibiting apoptosis²⁰¹ or promoting cell proliferation²⁰⁴ to confer resistance and therefore signify an important biological response which needs further investigation. Quantification of the immuno-histological changes would have introduced a more objective assessment.

5.7 Summary

In summary I have shown that, in *Apc^{min/+}* intestinal tumours, acute Egfr blockade by gefitinib reduces Egfr signalling, but activates Igf1r, a potential resistance pathway. Chronic monotherapy against either Egfr or Igf1r enhances survival but ultimately adenomas still develop. Combination Egfr/Igf1r blockade produced the most effective tumour suppression, and this data therefore supports the concept of Egfr resistance mediated through induced Igf1r signalling, and provides a rationale for combinatorial therapy.

Finally, the ability to detect the emergence of activated Igf1r following *de novo* exposure to gefitinib raises hope in our ability to identify drug resistance pathways very early within treatment schedules. Applying this principle could increase our ability to stratify patients according to drug induced tumour molecular responses to determine which additional pathways should be targeted to maximise anti-tumour responses (Fig 5.16).

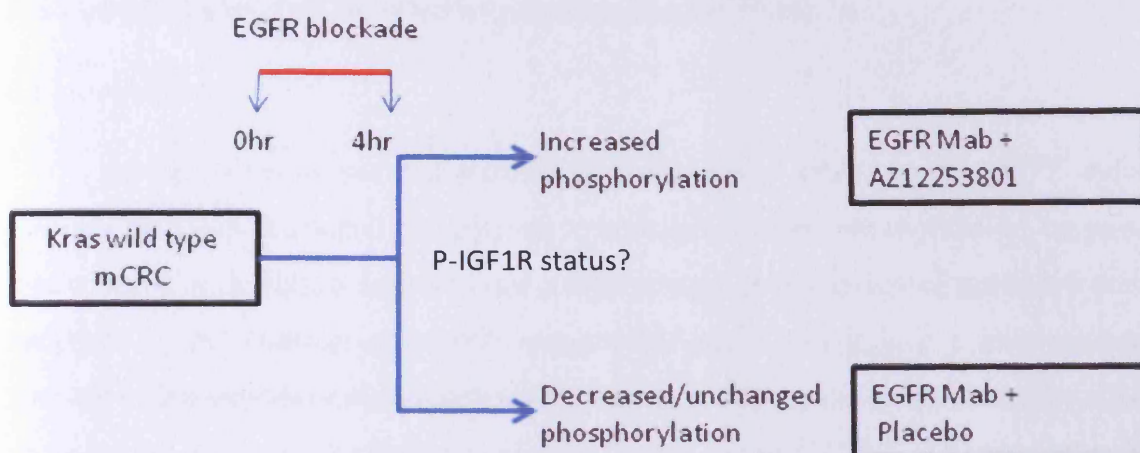


Figure 5.16. Hypothetical clinical trial stratifying patients according to drug induced tumour molecular profile. In the absence of a validated surrogate (tissue/blood), sequential tumour biopsies are taken at baseline and 4 hours following EGFR blockade with targeted monoclonal antibody. Comparison is made of IGF1R phosphorylation (P-IGF1R) status between time zero and 4 hours and used to allocate treatment with or without IGF1R inhibition with AZ12253801. The primary endpoint of the study would be % progression free and alive a 3 months from start of treatment. This design assumes a proportion of tumours will not become resistant to EGFR blockade through IGF1R activation and gain no benefit from IGF1R inhibition. mCRC metastatic colorectal cancer.

Chapter 6

6. Enhancing the therapeutic effect of gefitinib in the *Apc^{min/+}* mouse

6.1 Introduction

Having demonstrated that gefitinib has anti-tumour effects in the *Apc^{min/+}* mouse (Chapter 5) I was interested in exploring how this treatment effect could be improved. Recent work using NSCLC cell lines has demonstrated enhancement of gefitinib-induced apoptosis by the addition of a BH-3 mimetic ABT-737⁷⁵. This drug is a small molecule inhibitor of the anti-apoptotic proteins Bcl-2, Bcl-X_L and Bcl-w and does not directly initiate apoptosis but mediates its effects by enhancing death signals¹²⁹ (1.8.1). It is now known that tumour sensitivity to ABT-737 correlates with increased levels of BCL-2, BCL-X_L, NOXA and BIM and low expression of MCL-1^{128, 130}. With this in mind it was of great interest to find that the expression of *Bim* (also known as *Bcl2l11*) was 2.2 fold increased in *Apc^{min/+}* small intestinal tumours²¹⁹.

This led to the hypothesis that increased levels of *Bim* in *Apc^{min/+}* intestinal tumours may indicate sensitivity to ABT-737 and that combined ABT-737/ gefitinib treatment would therefore maximise cell death¹²⁸ and build upon the improved *Apc^{min/+}* survival already demonstrated for chronic gefitinib treatment (5.3.1). BH-3 mimetics have been shown to potentiate the effects of oncogenic kinase inhibitors by converting predominant cytostatic responses into cytotoxicity¹²⁸.

This chapter describes ongoing work to explore the therapeutic potential of ABT-737 in the *Apc^{min/+}* mouse. I will describe short term effects of ABT-737 with and without gefitinib in intestinal tumours and plans to exploit therapy in longer term studies.

6.2 Results

I initially sought evidence that would confirm increased *Bim* expression in *Apc^{min/+}* intestinal tumours as a predictor of sensitivity to the BH-3 mimetic, ABT-737.

6.2.1 Probing *Apc^{min/+}* microarray data for *Bim* transcript levels

Previous work in the ARC laboratory (Dr Karen Reed, unpublished) has explored microarray gene expression changes in *Apc^{min/+}* colon tumours relative to adjacent normal colonic tissue. By mining the microarray database for probe ID's attached to *Bim* (*Bcl2like11*) it was possible to calculate fold change differences in colon polyps relative to normal colon for this gene (Table 6.1). As shown, four of the five probe IDs indicate statistically significantly increased expression of *Bim* transcripts in *Apc^{min/+}* colon tumours relative to normal colon. The increased expression of *Bim* transcript in intestinal tumours points to the increase likelihood ABT-737 would have an anti-tumour effect in this setting.

Probe ID	Fold change Tumour/Normal	t-test
1426334_a_at	4.8	0.00586661
1435449_at	3.5	3.16E-05
1456005_a_at	1.6	0.12099079
1456006_at	1.9	0.00495264
1435448_at	2.7	0.00553042

Table 6.1. Mouse GeneChip 430 2.0 array probe ID's linked to *Bim* (*Bcl2l11*) and associated transcript fold changes in *Apc^{min/+}* colon polyps relative to normal adjacent colon tissue. P values were obtained using the two sample t test. Colon polyps from 3 *Apc^{min/+}* mice were obtained and equal quantities of RNA from individual polyps pooled for each mouse prior to hybridisation on 3 gene chips. RNA from adjacent normal colon tissue from each mouse was also obtained for reference (For further detail regarding fold change calculations and statistics see 2.10.3).

As I have previously shown, the immediate phenotypic effects of targeted agents can be assessed *in vivo* using the *Apc^{min/+}* mouse to determine mechanisms of anti-tumour drug effects. In addition, the acute effects of a compound may be used as a surrogate for therapeutic anti-tumour activity supporting the design of expensive long term pre-clinical

studies. I therefore proceeded to examine the immediate effects of ABT-737 drug combinations on intestinal tumours from *Apc^{min/+}* mice.

6.2.2 Acute effects of drug exposure in tumours from *Apc^{min/+}* mice

Mice received a single intra-peritoneal dose of 75mg/kg ABT-737 in acute pharmacodynamic experiments as this dose has previously been well tolerated for up to 21 days in xenograft studies demonstrating significant anti-tumour effects¹²⁹. ABT-737 dosed at 100mg/kg (i.p) has previously demonstrated apoptosis as early as 2 hours after treatment with a 12-fold increase evident within 16 hours¹²⁹; a 4 hour time-point for assessment of induced effects was chosen based on this data.

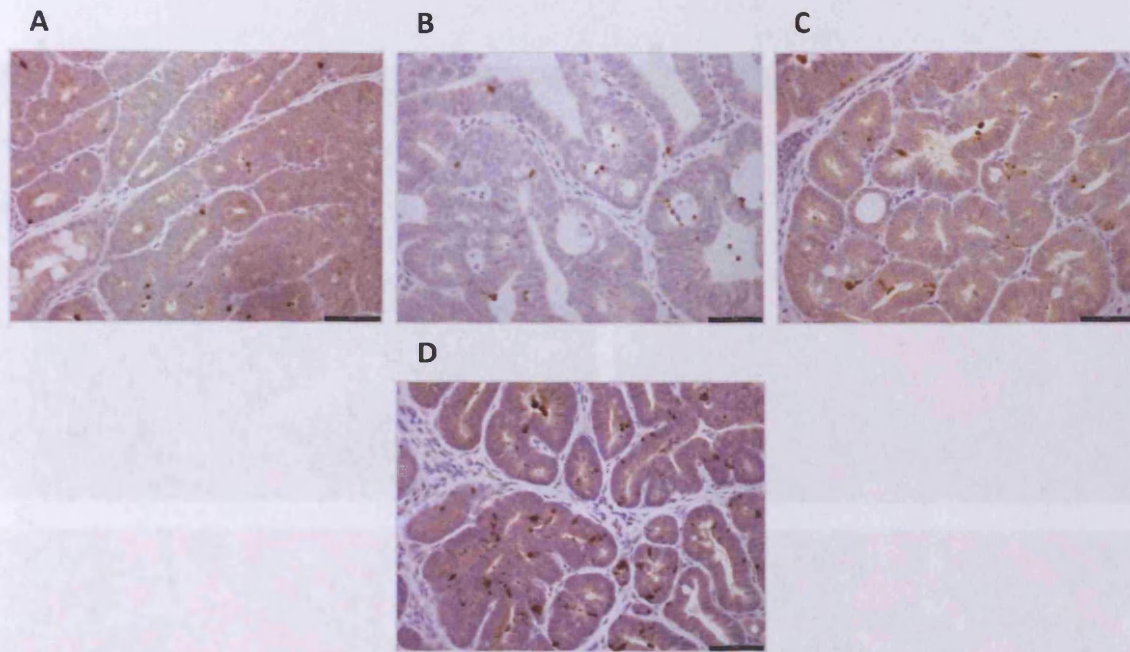
6.2.2.2 Colon tumours

There is a statistically significant approximate 3-fold increase in cleaved caspase 3 immuno-staining of colon tumours exposed to combined gefitinib 75mg/kg with ABT-737 75mg/kg relative to gefitinib 75mg/kg or ABT-737 75mg/kg alone. Caspase-3 immuno-reactivity in colon tumours across the different treatments is shown in fig 6.1 A-D. These data suggest that the immediate effect of combination treatment is to enhance cell death in colon tumours relative to single agents alone (14.8%±5.2 [Combo] vs. 5.7%±1.9 [Gef], P0.05; vs. 5.8%±0.7 [ABT-737], P0.03, Mann-Whitney; Fig 6.1 E). Gefitinib 75mg/kg monotherapy, in keeping with previous results (3.3.1.1) did not induce increased caspase-3 staining (5.7%±1.9 [Gef] vs. 7.2%±2.1 [Veh 0.5%], P0.19, Mann-Whitney) and surprisingly, ABT-737 75mg/kg alone also failed to increase caspase-3 immuno-staining in colon tumours compared to vehicle at 4 hours (5.8%±0.7 [ABT-737] vs. 5.9%±2.5 [ABT-737 Veh], P0.47, Mann-Whitney).

6.2.2.3 Small intestinal microadenomas

Haematoxylin and Eosin stained sections of small intestinal adenomas from *Apc^{min/+}* mice at a 4 hour time point following intra-peritoneal injection of ABT737 75mg/kg in combination with gefitinib 75mg/kg also demonstrated increased levels of apoptosis, although a formal count is outstanding (Fig 6.2 A-D).

Fig 6.1 Caspase 3 immuno-staining in *Apc^{min/+}* colon tumours at a 4 hr time point following ABT-737 administration with and without gefitinib and gefitinib alone



E

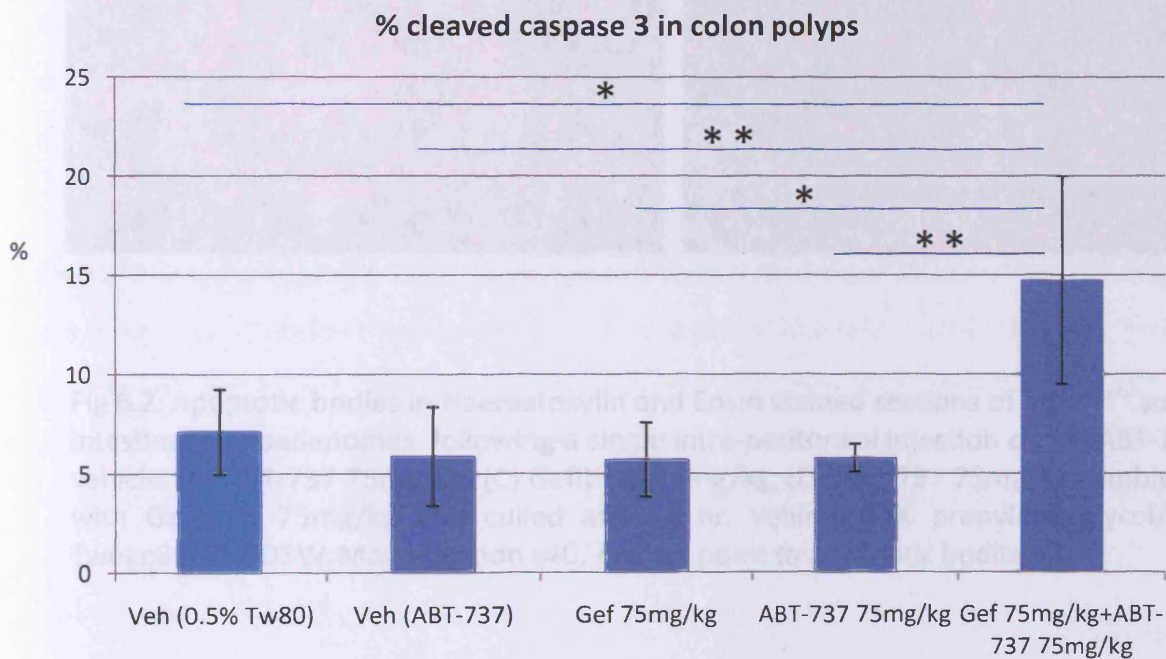


Fig 6.1. Caspase-3 immuno-reactivity at 4 hr in colon tumour from *Apc^{min/+}* mice administered a single intra-peritoneal injection of: (A) ABT-737 vehicle, (B) ABT-737 75mg/kg, (C) Gefitinib 75mg/kg, (D) ABT-737 75mg/kg combined with Gefitinib 75mg/kg. (E) % cleaved caspase 3 scoring in colon tumours at a 4 hour time point following exposure to single doses of various drugs. Veh (0.5% Tw80), 0.5% Tween80, Veh (ABT-737) 30% propylene glycol/5% Tween80/65% D5W, Gef Gefitinib. 4 mice used for each drug exposure except Veh (0.5% Tw80) and Gefitinib where 3 mice were used, 3 tumours were scored from each mouse in 15/18 mice. Error bars represent mean value \pm 1x standard deviation. * P values calculated using Mann-Whitney test, *P= 0.05, ** P=0.03.

Fig 6.2 Apoptosis in *Apc^{min/+}* small intestinal microadenomas at a 4 hr time point following ABT-737 administration with and without gefitinib and gefitinib alone

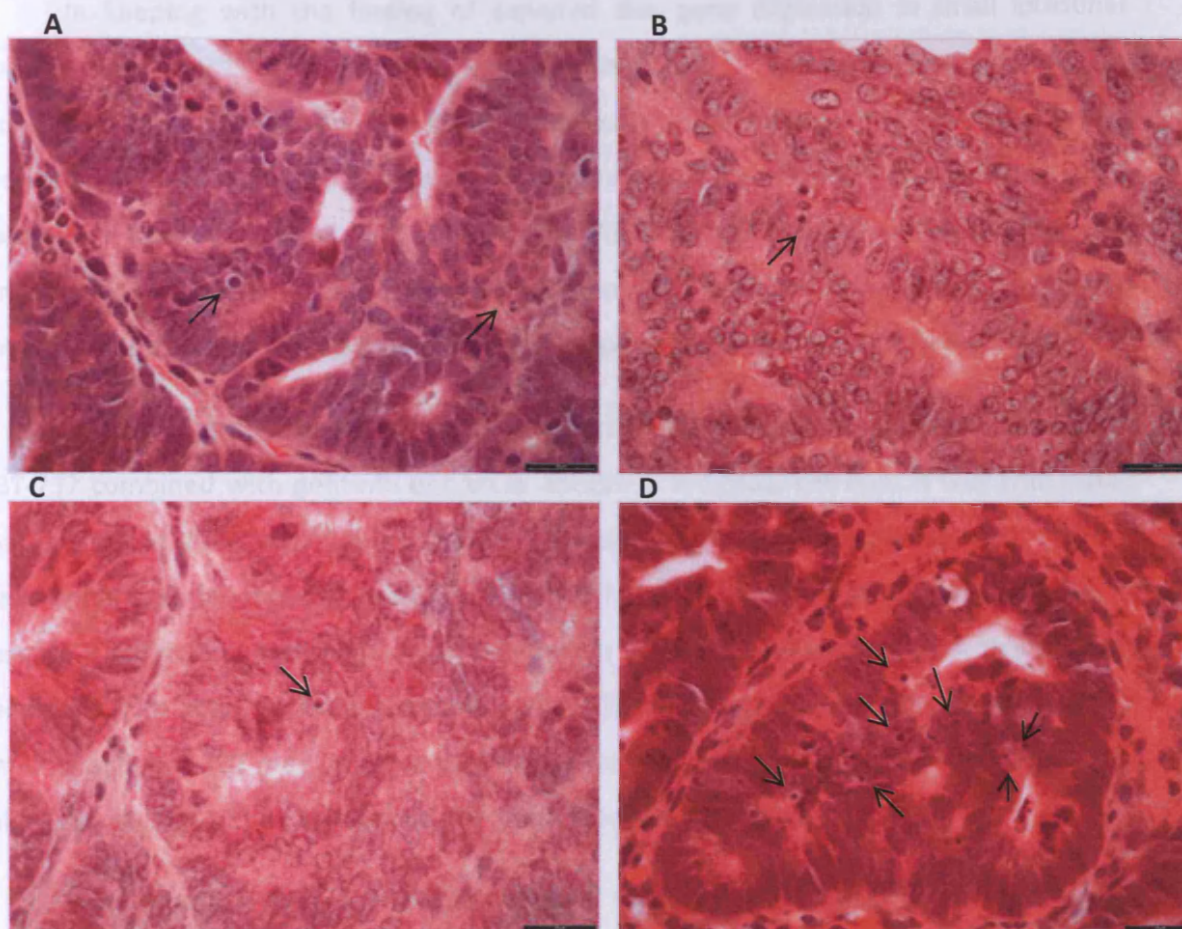


Fig 6.2. Apoptotic bodies in Haematoxylin and Eosin stained sections of *Apc^{min/+}* small intestinal microadenomas following a single intra-peritoneal injection of: (A) ABT-737 vehicle, (B) ABT-737 75mg/kg, (C) Gefitinib 75mg/kg, (D) ABT-737 75mg/kg combined with Gefitinib 75mg/kg and culled after 4 hr. Vehicle 30% propylene glycol/5% Tween80/65%D5W. Magnification x40. Arrows point to apoptotic bodies.

6.3 Discussion

In keeping with the finding of elevated *Bim* gene expression in small intestinal tumours from *Apc^{min/+}* mice²¹⁹ it is apparent that *Apc^{min/+}* colon tumours also express increased levels of *Bim* based upon *Apc^{min/+}* microarray data (table 6.1). As *Bim* can bind and sequester all anti-apoptotic Bcl2 family members with high affinity¹²⁸ its up-regulation is naturally important in mediating sensitivity to ABT-737 cell death²²⁰; ABT-737 effectively binds and saturates Bcl-2, Bcl-X_L and Bcl-w pro-survival proteins allowing *Bim* freedom to bind MCL1 and A1 such that all pro-survival pro-apoptotic family members are blocked¹²⁸.

In view of the increased level of *Bim* in *Apc^{min/+}* intestinal tumours and evidence that ABT-737 combined with gefitinib enhances apoptosis in NSCLC cell lines it was anticipated that this would also hold true for intestinal tumours exposed to the combination. This has been confirmed by showing combined ABT-737/Gefitinib results in a 3-fold increase in caspase-3 activity beyond single agent treatments in colon tumours (fig 6.1). A similar effect seems likely in small intestinal tumours (fig 6.2). This suggests that the combination of gefitinib and ABT-737 may improve the median survival of gefitinib monotherapy in *Apc^{min/+}* mice (194 days; 5.3.1) by enhancing cell death in intestinal tumours.

Not expected was the demonstration that ABT-737 75mg/kg did not induce apoptosis beyond that seen for vehicle, given the increased expression of *Bim* transcript in colon tumours. However this takes no account of protein translation which may not result in greater *Bim* levels. Furthermore, the dose of ABT-737 may have been too small or the apoptotic effects assessed too early following the single intra-peritoneal dose. The dynamics of tumour response, pharmacokinetics and pharmacodynamics are likely to be context dependent and different for *in vivo* *Apc^{min/+}* colon tumours rather than xenograft studies used to assess ABT-737.

A further explanation may relate to the level of *Mcl-1* in *Apc^{min/+}* intestinal tumours which is a known predictor of resistance to apoptosis by ABT-737¹²⁸. Cox inhibition has been shown to reduce colorectal polyps in familial adenomatous polyposis²²¹ possibly mediated through reduced *Mcl-1* expression²²². *Mcl-1* may therefore be a factor driving anti-apoptotic signals in colon polyps as a consequence of Cox-2 derived PGE2²²³. In view of this I have probed the differential expression of *Mcl-1* transcripts in *Apc^{min/+}* colon tumours using the

Apc^{min/+} microarray data described earlier (6.2.1). By examining probes identities linked to *Mcl-1* (table 6.2), an approximate 2-fold reduction in colon polyp *Mcl-2* transcript expression was evident suggesting *Mcl-1* is not responsible for the lack of an apoptotic in response to ABT-737 75mg/kg, indeed this would indicate sensitivity¹²⁸. Further investigation is required and will begin by examining qRT-PCR mRNA and protein expression levels of *Bim* and *Mcl-1* in colon polyps exposed to ABT-737 relative to vehicle.

Table 6.2. *Mcl-1* microarray probe transcript changes in *Apc*^{min/+} colon tumours relative to adjacent normal colon.

Probe ID	Fold change Tumour/Normal	t-test
1416881_at	0.63	0.272804
1448503_at	0.62	0.018483
1456243_x_at	0.67	0.004526
1437527_x_at	0.64	0.000309
1456381_x_at	0.64	0.010769
1416880_at	0.64	0.072075

Given the enhancement of apoptosis seen with combined ABT-737 and gefitinib, long term experiments are being designed to test the hypothesis that combined therapy in the *Apc*^{min/+} mouse will translate into a therapeutic effect improving survival beyond that seen for single agent gefitinib 75mg/kg or ABT-737 75m/kg.

To test this cohorts of *Apc*^{min/+} mice (n=20) will begin treatment with once daily intra-peritoneal injections of either (A) ABT-737 75mg/kg, (B) Gefitinib 75mg/kg (C) ABT-737 75mg/kg plus Gefitinib 75mg/kg or (D) vehicle control 30% propylene glycol/5% Tween80/65% D5W (Dextrose 5% water) upon the earliest develop of an intestinal tumour burden (pale feet or rectal bleeding). Animals will need to be closely monitored for potential complications related to thrombocytopenia and lymphopenia which was reported in 21 day dosing schedules on ABT-737 75mg/kg¹²⁹. Treatment will continue until intestinal tumour burdens are clearly increasing at which point the survival endpoint will be reached. The Kaplan Meier method will be used to determine differences in survival and tumour metrics assessed as previously described (Chapter 5).

Interestingly, circulating biomarkers of cell death after treatment with ABT-737 have been used in a xenograft study of lung cancer demonstrating early increases in cleaved cytokeratin 18 map to drug specific tumour regression, and that intact cytokeratin 18 levels correlate with tumour burden²²⁴. By applying these finding, I plan to incorporate blood sampling into the above long term experiments to test how monitoring intact cytokeratin 18 and cleaved cytokeratin 18 levels correlate with presumed initial response and eventual resistance to the proposed treatments. One difficulty will be to address the impact non-tumour derived epithelial cleaved and intact cytokeratin 18 may have as a potential confounding factor as expression has been reported in normal colonic mucosa in addition to adenomas and carcinomas²²⁵. Pilot studies looking at the expression of both cleaved and intact cytokeratin 18 levels in mice without tumours in response to ABT-737 and vehicle will help assess how great a contribution this may be. As cytokeratins are not expressed in haematopoietic cells, thrombocytopenia and lymphopenia toxicities should not confound the measurement of cytokeratins²²⁶.

Finally, examining the immediate effect of signal transduction inhibitors and inducers of apoptosis upon pathway activation and anti-tumour phenotypic changes provides an opportunity to optimise drug sequencing and dosing strategies in mouse models of cancer. Combining this approach, with the potential of introducing other treatment modalities such as radiotherapy, has the potential therefore to define novel, rationale interventional strategies which can be taken forward into early clinical trial design.

In summary, combined exposure to ABT-737 and gefitinib enhances cell death in *Apc^{min/+}* intestinal tumours. This combination may translate into improved *Apc^{min/+}* longevity when administered long term and build upon the survival advantage demonstrated for chronic gefitinib monotherapy. The relationship between tumour responses and expression of BCL-2 family members needs to be explored in further detail and longer term studies may also test the ability of circulating biomarkers to predict treatment responses.

Chapter 7

7. Investigating the immediate effect of Mek inhibition in a genetically defined and clinically relevant autochthonous model of human colorectal cancer.

7.1 Introduction

Bowel cancer is the 2nd most common cause of cancer death in the UK, with 16,000 deaths pa. Approximately 9% of patients present with Dukes D disease at diagnosis with a 5 year survival figure of only 7%¹. However, patients with colorectal liver metastases treated with hepatic resection have improved 5 year survival rates of between 28-41%²²⁷. Unfortunately, 50% of patients who have undergone potentially curative surgery for early stage disease will relapse with metastatic disease making it a significant burden of disease².

Despite treatment advances a large proportion of patients with metastatic colorectal cancer remain refractory due to the common presence of *K-RAS* mutations, which predict poor response and outcome to cytotoxic drugs and targeted monoclonal antibodies against the epidermal growth factor receptor (EGFR)^{45-47, 228}. There is therefore a pressing need for new therapeutic strategies to improve outcomes for patients with *K-RAS* mutant tumours which currently represent an unmet clinical need. Here I have used mouse models of colon cancer harbouring the same mutations seen in human colorectal cancer to test the hypothesis that inhibition of MEK is a rational treatment approach.

Currently, the extent of experimental data derived from an *in vivo* setting to support MEK inhibition remains relatively limited largely by virtue of the experimental systems used. To counter this, my research employs Mek inhibition in conditional transgenic mouse models of colon cancer (*Apc* deleted and endogenous *K-ras* activated¹¹⁴: 1.6.2), where I plan to examine the immediate and long term effect of targeting the Raf/Mek/Erk pathway. This is an attractive approach as MEK inhibition targets a pathway known to be deregulated in colorectal cancer¹²¹ and the model described avoids cell based assays and tumour bearing xenografts which are unreliable predictors of clinical drug activity⁹⁹. The results from these experiments have the potential to influence the design of future clinical studies in metastatic colon cancer and set new standards for preclinical drug assessment using this *in vivo* platform.

This next section describes my preliminary work examining the acute effects of Mek inhibition using AZD6244 in the *Apc^{min/+}* model of colon tumorigenesis (wild type for *K-ras* and *B-raf*; 3.2) and *AhCre^{T/+}Apc^{fl/+}Kras^{+/+}* and *AhCre^{T/+}Apc^{fl/+}Kras^{v12/+}* conditional transgenic models.

7.2 Results

7.2.1 Phosphorylated Erk levels in *AhCre^{T/+}Apc^{fl/+}Kras^{+/+}* and *AhCre^{T/+}Apc^{fl/+}Kras^{v12/+}* intestinal tumours

It is important to validate the mouse models in terms of their ability to mirror activated Erk signalling in preparation for targeted inhibition. My initial efforts therefore sought to define the degree of Raf/Mek/Erk intestinal tumour pathway activation in the models used, as measured by Erk phosphorylation due to presence or absence of a constitutive *K-ras* mutation.

Phosphorylated-Erk immuno-staining of both small and large intestinal tumours obtained from *AhCre^{T/+}Apc^{fl/+}Kras^{+/+}* and *AhCre^{T/+}Apc^{fl/+}Kras^{v12/+}* mice demonstrates more intense staining of both cytoplasm and nuclei in *AhCre^{T/+}Apc^{fl/+}Kras^{v12/+}* tumours (Fig 7.1 and 7.2), in keeping with the presence of an activated Ras/Raf/Erk pathway as anticipated.

7.2.2 Acute pharmacodynamic effects of Mek inhibition using AZD6244 delivered by intra-peritoneal injection

7.2.2.1 *AhCre^{T/+}Apc^{fl/+}Kras^{v12/+}* derived intestinal tumours

The acute effects of exposure to 30mg/kg AZD6244 in *AhCre^{T/+}Apc^{fl/+}Kras^{v12/+}* intestinal tumours are provisional given that vehicle treatments only include n=2 mice. Despite this, at 4 hours there is a trend towards an increased level of H and E scored apoptosis and cleaved caspase-3 scoring in colon tumours from *AhCre^{T/+}Apc^{fl/+}Kras^{v12/+}* mice exposed to AZD6244 (apoptosis, 0.7% ± 0.003 [Veh] vs. 4.2 % ±4.0 [AZD6244]; cleaved caspase-3, 1.8% ± 0.7 [Veh] vs. 5.0% ± 3.9 [AZD6244]; Fig 7.3 A, B). This is in keeping with a trend towards increased cell death. There is no alteration in the level of mitotic activity (0.3% ± 0.1 [Veh] vs. 0.4% ± 0.3 [AZD6244]; fig 3.7C) but an increase in the percentage of cells labelled by Brdu (6.1% ± 2.6 [Veh] vs. 16.7 ± 2.6 [AZ6244]; fig 7.3D). These findings may indicate that more cells are going through S phase, but increased cell death is occurring, so the M phase component remains unchanged. Alternatively cells may be trapped in S phase (S phase block) due to reduced cell exiting.

Fig 7.1 *AhCre^{T/+}Apc^{fl/+}Kras^{+/+}* and *AhCre^{T/+}Apc^{fl/+}Kras^{v12/+}* derived colon polyps immuno-stained for Erk phosphorylation.

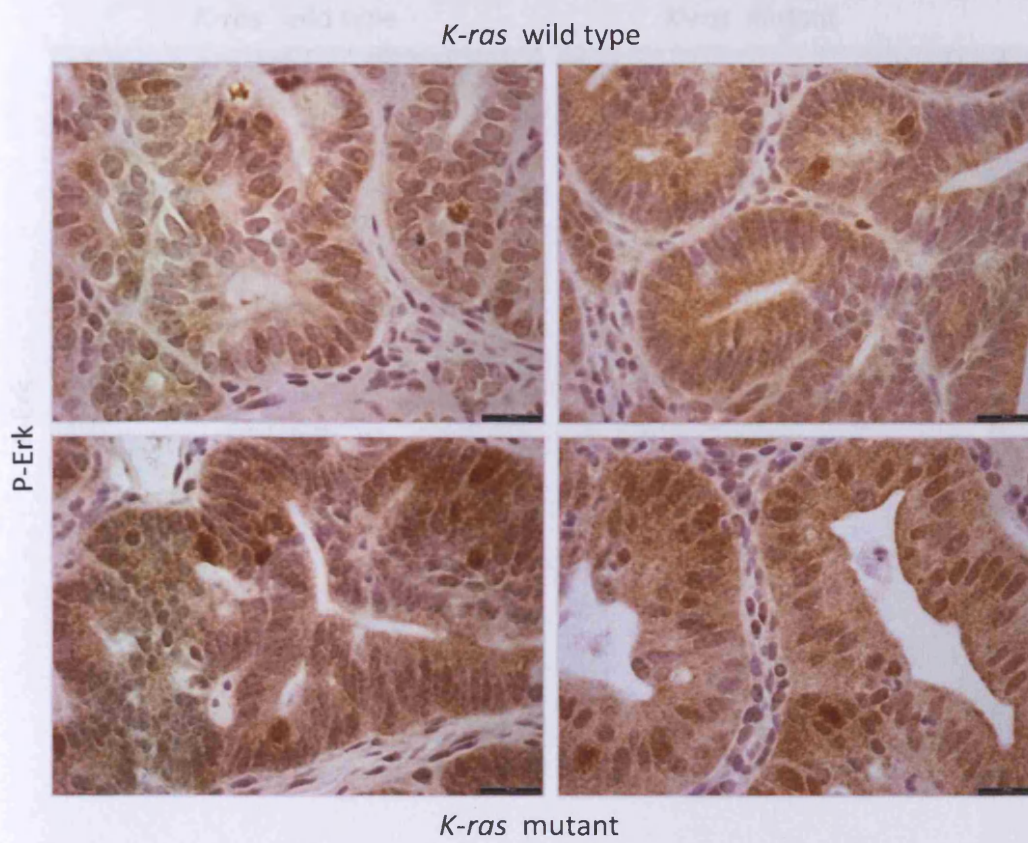


Fig 7.2 P-Erk immuno-staining in *K-ras* mutant small intestinal adenomas (right panel) demonstrate more intense staining of cytoplasmic and nuclear components.

Fig 7.1 P-Erk immuno-staining in *K-ras* mutant colon polyps (lower panel) demonstrates more intense staining of cytoplasmic and nuclear components consistent with activation of the Erk signalling pathway as a consequence of an activated *K-ras* mutant allele. Each tumour image (x40) is from an individual mouse (total n=4)

Fig 7.2 *AhCre^{T/+}Apc^{fl/+}Kras^{+/+}* and *AhCre^{T/+}Apc^{fl/+}Kras^{v12/+}* derived small intestinal microadenomas immuno-stained for Erk phosphorylation.

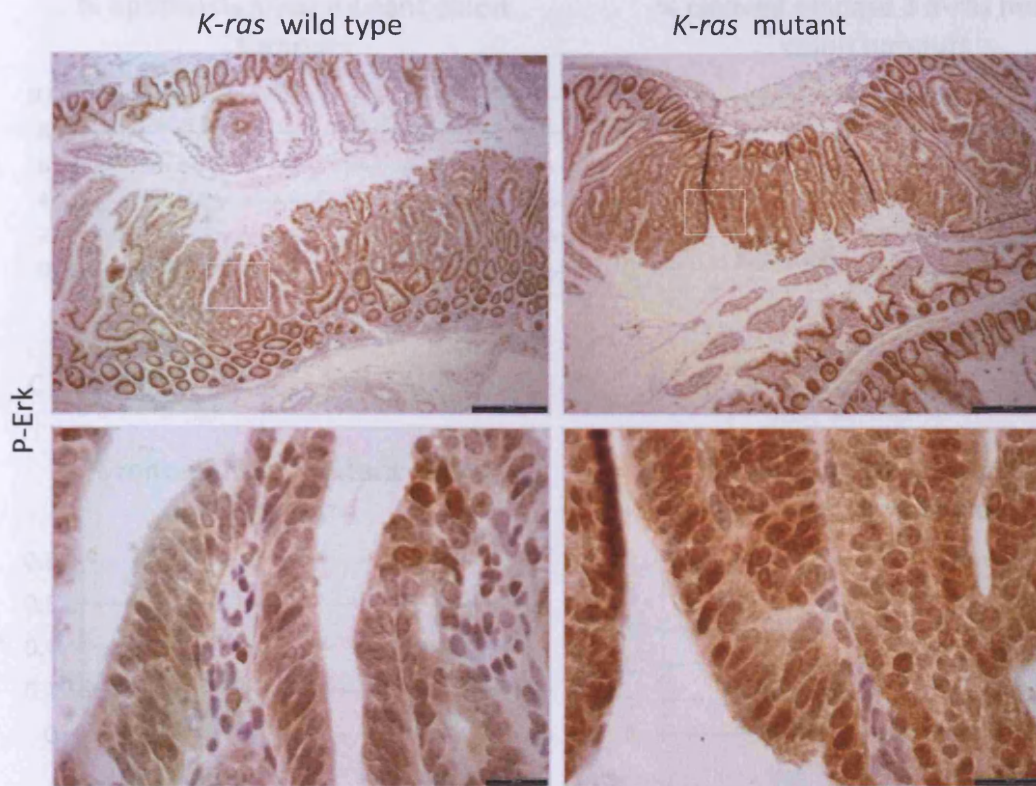


Fig 7.2 P-Erk immuno-staining in *K-ras* mutant small intestinal microadenomas (right panel) demonstrate more intense staining of cytoplasmic and nuclear components consistent with activation of the Erk signalling pathway as a consequence of an activated *K-ras* mutant allele. Upper panel x4 magnification and lower panel x40. Inset white box indicates region of tumour enlarged.

Fig 7.3 The acute effects of a single intra-peritoneal dose of 250 mg/kg or vehicle are shown with respect to (A) apoptosis, (B) immuno-staining against tumour protein markers (C) apoptosis and (D) Ki-67 labelling in colon tumours. (E) Apoptosis index in colon adenoma (F) Ki-67 labelling in colon adenoma. (G) Apoptosis and (H) Ki-67 labelling in small intestinal adenomas. *AhCre^{T/+}Apc^{fl/+}* mice were sacrificed at 4 hr following 250 mg/kg (n=4) and vehicle (0.3% hydroxypropyl methylcellulose (HPMC) T40, 200 µl) the acute dose is presented in view of mouse numbers and is reflected in the absence of statistical tests. *S* Small intestinal tumours. Error bars represent mean \pm 2x standard deviation.

Fig 7.3 Acute effect of AZ6244 in *AhCre^{T/+}Apc^{fl/+}Kras^{v12/+}* colon and small intestinal tumours.

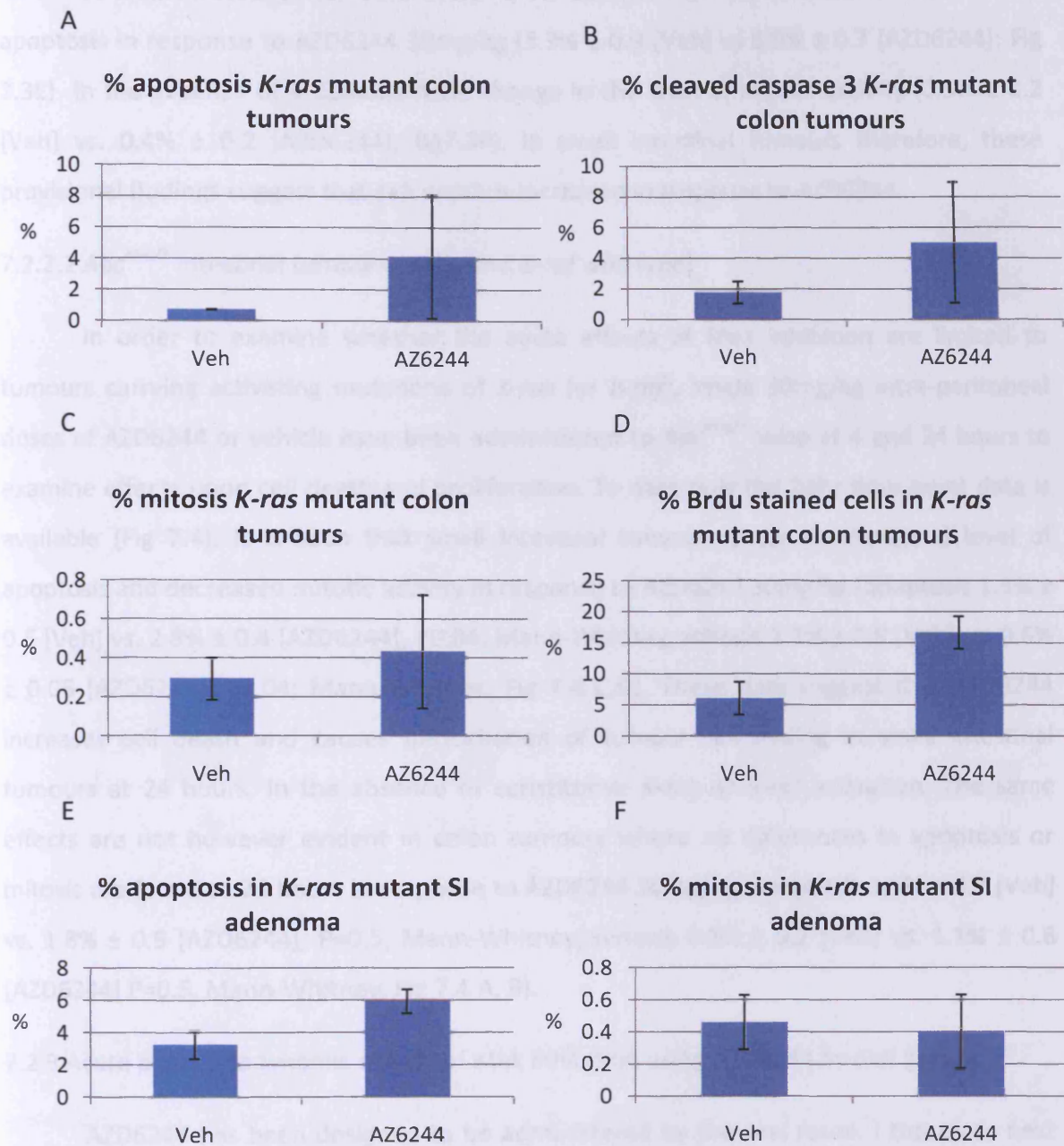


Fig 7.3 The acute effects of a single intra-peritoneal dose of AZ6244 30mg/kg or vehicle are shown with respect to (A) apoptosis, (B) immuno-staining against cleaved caspase-3, (C) mitosis and (D) Brdu cell labelling in colon tumours, (E) apoptosis and (F) mitosis in small intestinal adenomas from *AhCre^{T/+}Apc^{fl/+}Kras^{v12/+}* mice. Mice were culled at 4 hr following AZ6244 30mg/kg (n=4) and vehicle, 0.5% hydroxypropyl methylcellulose 0.1% Tween80 (n=2). The acute data is provisional in view of mouse numbers and is reflected in the absence of statistical tests. SI small intestinal tumours. Error bars represent mean ± 1x standard deviation.

In small intestinal tumours there is an apparent 2-fold increase in the level of apoptosis in response to AZD6244 30mg/kg (3.3% ± 0.9 [Veh] vs 5.9% ± 0.7 [AZD6244]; Fig 7.3E) in the absence of a demonstrable change in the level of mitotic activity (0.5% ± 0.2 [Veh] vs. 0.4% ± 0.2 [AZD6244]; fig7.3F). In small intestinal tumours therefore, these provisional findings suggest that cell death is increased in response to AZD6244.

7.2.2.2 *Apc*^{min/+} intestinal tumours (*K-ras* and *B-raf* wild type)

In order to examine whether the acute effects of Mek inhibition are limited to tumours carrying activating mutations of *K-ras* (or *B-raf*), single 30mg/kg intra-peritoneal doses of AZD6244 or vehicle have been administered to *Apc*^{min/+} mice at 4 and 24 hours to examine effects upon cell death and proliferation. To date only the 24hr time point data is available (Fig 7.4). It is seen that small intestinal tumours show an increased level of apoptosis and decreased mitotic activity in response to AZD6244 30mg/kg (apoptosis 1.3% ± 0.6 [Veh] vs. 2.8% ± 0.4 [AZD6244], P0.04, Mann-Whitney; mitosis 1.3% ± 0.8 [Veh] vs. 0.6% ± 0.05 [AZD6244], P0.04; Mann-Whitney, Fig 7.4 C,D). These data suggest that AZD6244 increases cell death and causes perturbation of tumour cell cycling in small intestinal tumours at 24 hours, in the absence of constitutive *K-ras* or *B-raf* activation. The same effects are not however evident in colon tumours where no differences in apoptosis or mitosis are found at 24 hours in response to AZD6244 30mg/kg (apoptosis 1.6% ± 0.7 [Veh] vs. 1.8% ± 0.9 [AZD6244], P=0.5, Mann-Whitney; mitosis 0.8% ± 0.2 [Veh] vs. 1.1% ± 0.8 [AZD6244] P=0.5, Mann-Whitney; Fig 7.4 A, B).

7.2.3 Acute pharmacodynamic effects of Mek inhibition using AZD6244 by oral gavage

AZD6244 has been designed to be administered by the oral route. I therefore next tested the effect of AZD6244 by this route.

A single dose of AZD6244 30mg/kg via oral gavage in *Apc*^{min/+} mice showed a 2 fold-increase in apoptosis in colon tumours (2.2% ± 0.4 [Veh] vs. 4.4% ± 0.4 [AZD6244], P=0.04, Mann Whitney; fig7.5) without a detected change in mitosis at 4 hours (0.9% ± 0.1 [Veh] vs. 0.8% ± 0.3 [AZD6244], P0.33, Fig 7.5). This suggests oral AZD6244 administration is able to increase immediate cell death, supporting the notion that the effects of Mek inhibition are not confined to the presence of activating *K-ras* and *B-raf* mutations.

Fig 7.4 Acute effect of AZD6244 in *Apc^{min/+}* colon and small intestinal tumours at 24 hr.

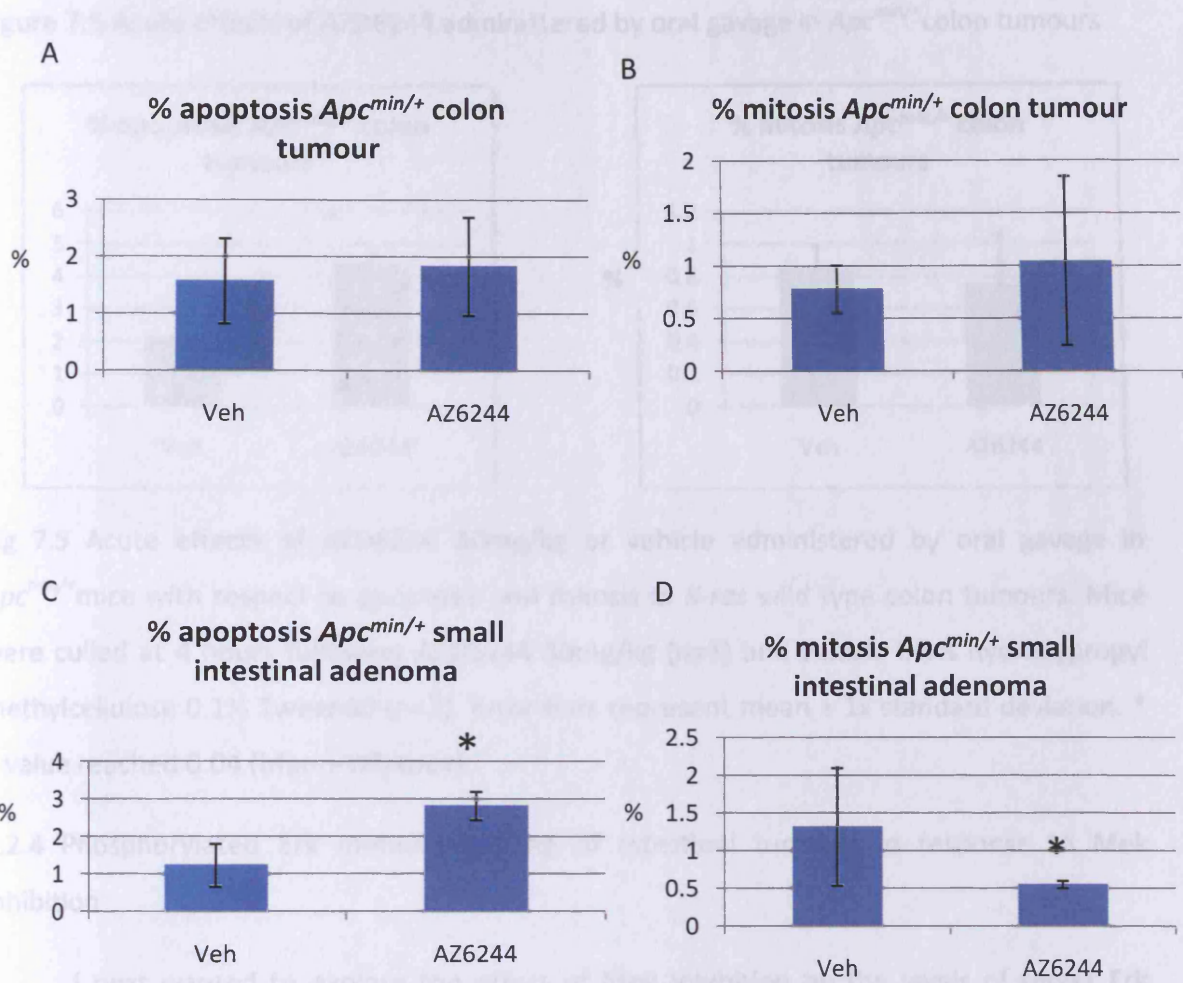


Fig 7.4 The acute effects of a single intra-peritoneal dose of AZ6244 30mg/kg or vehicle are shown with respect to (A) apoptosis, (B) mitosis in *Apc^{min/+}* colon polyps and (C) apoptosis and (D) mitosis in *Apc^{min/+}* small intestinal tumours. Mice were culled at 24 hr following AZ6244 30mg/kg (n=3) and vehicle, 0.5% hydroxypropyl methylcellulose 0.1% Tween80 (n=3). Error bars represent mean \pm 1x standard deviation. * P values reached 0.04 (Mann-Whitney test).

Figure 7.5 Acute effects of AZD6244 administered by oral gavage in $Apc^{min/+}$ colon tumours

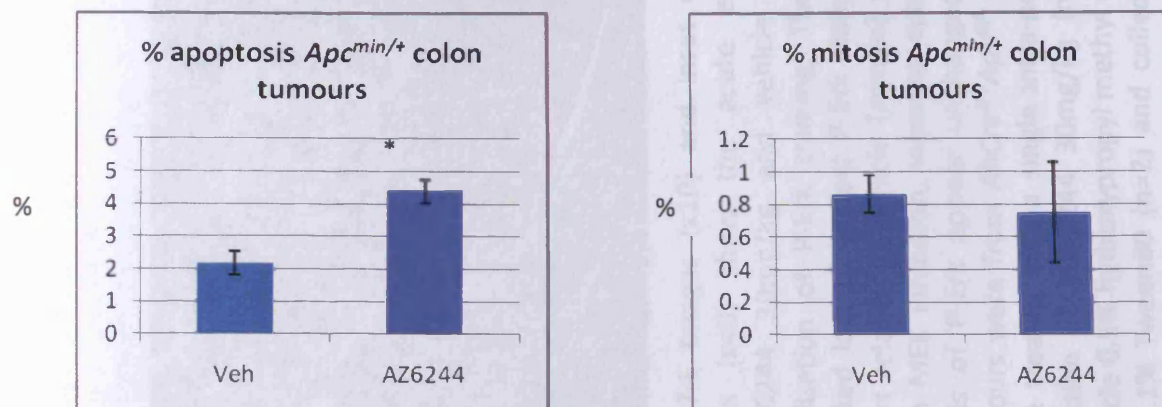


Fig 7.5 Acute effects of AZD6244 30mg/kg or vehicle administered by oral gavage in $Apc^{min/+}$ mice with respect to apoptosis and mitosis in $K-ras$ wild type colon tumours. Mice were culled at 4 hours following AZD6244 30mg/kg (n=3) and vehicle 0.5% hydroxypropyl methylcellulose 0.1% Tween80 (n=3). Error bars represent mean \pm 1x standard deviation. * P value reached 0.04 (Mann-Whitney).

7.2.4 Phosphorylated Erk immuno-staining of intestinal tumours in response to Mek inhibition

I next wanted to explore the effect of Mek inhibition on the levels of target Erk activity in intestinal tumours with and without $K-ras$ mutations.

A single intra-peritoneal dose of AZD6244 30mg/kg results in a reduction of nuclear phospho-Erk immuno-staining compared to vehicle control in colon tumours from $AhCre^{T/+}Apc^{fl/+}Kras^{v12/+}$ mice at a 4 hour time point (Fig 7.6). A similar pattern of staining as a consequence of AZD6244 30mg/kg is also seen in small intestinal adenomas from mice of the same genotype (Fig 7.7). Conversely, cytoplasmic phospho-Erk staining in both small and large intestinal tumours appears relatively unchanged. Therefore the acute immuno-histochemical response to Mek inhibition in both small and large intestinal $K-ras$ mutant tumours is reduced nuclear accumulation of phospho-Erk.

A similar 4 hour comparison of phospho-Erk immuno-reactivity examining the immediate effect of AZD6244 30mg/kg in $Apc^{min/+}$ colon and small intestinal tumours is not yet available, however Erk phosphorylation in $Apc^{min/+}$ colon tumours 24 hours following

Fig 7.6 Phospho-Erk immuno-reactive staining of colon tumours from *AhCre^{T/+}Apc^{fl/+} Kras^{v12/+}* mice exposed to MEK inhibitor (AZD6244) and Vehicle for 4 hours

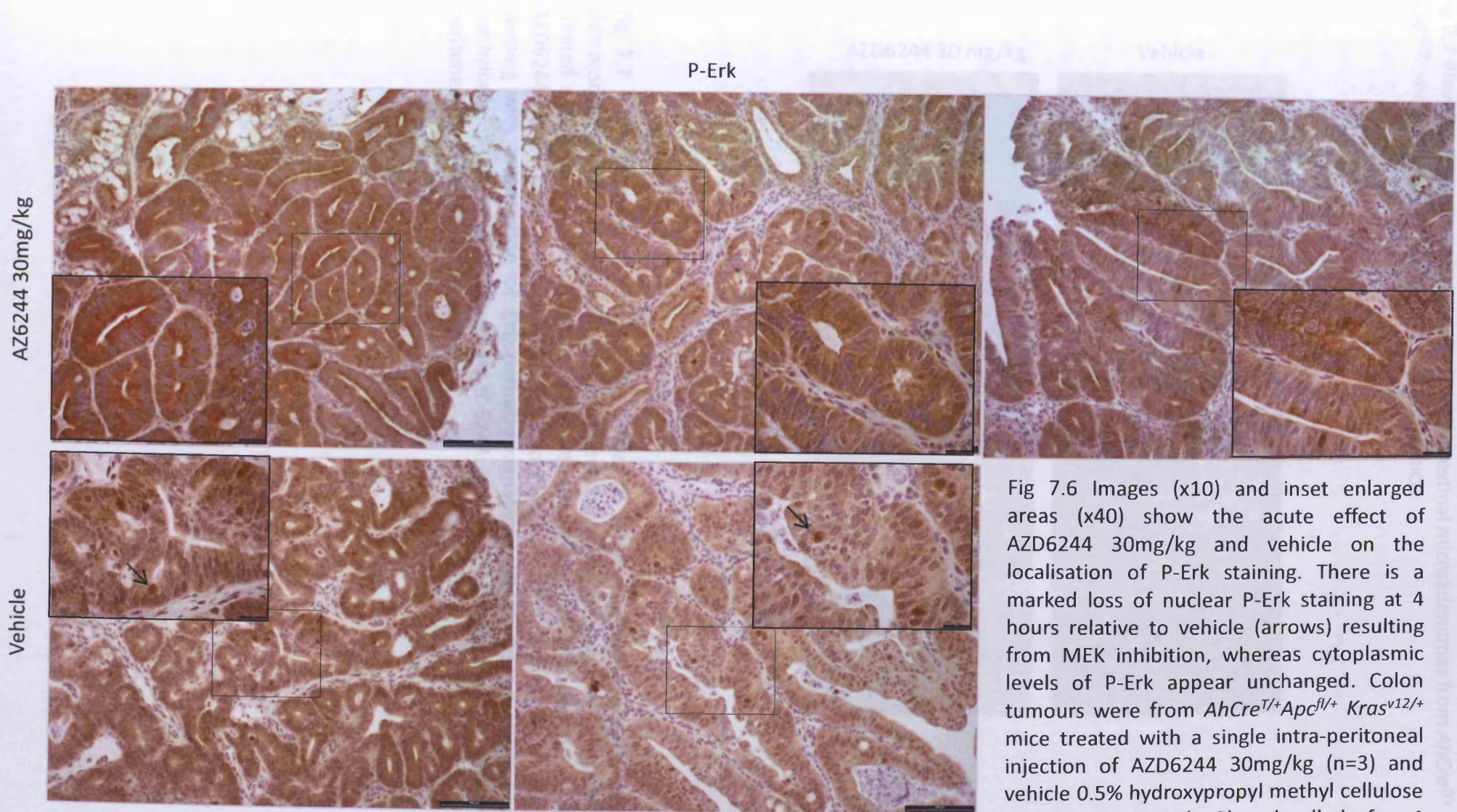


Fig 7.6 Images (x10) and inset enlarged areas (x40) show the acute effect of AZD6244 30mg/kg and vehicle on the localisation of P-Erk staining. There is a marked loss of nuclear P-Erk staining at 4 hours relative to vehicle (arrows) resulting from MEK inhibition, whereas cytoplasmic levels of P-Erk appear unchanged. Colon tumours were from *AhCre^{T/+}Apc^{fl/+} Kras^{v12/+}* mice treated with a single intra-peritoneal injection of AZD6244 30mg/kg (n=3) and vehicle 0.5% hydroxypropyl methyl cellulose in 0.1% Tween80 (n=2) and culled after 4 hours.

Fig 7.7 Phospho-Erk immuno-staining of small intestinal microadenomas from *AhCre^{T/+} Apc^{fl/+} Kras^{v12/+}* mice exposed to acute AZD6244 and Vehicle

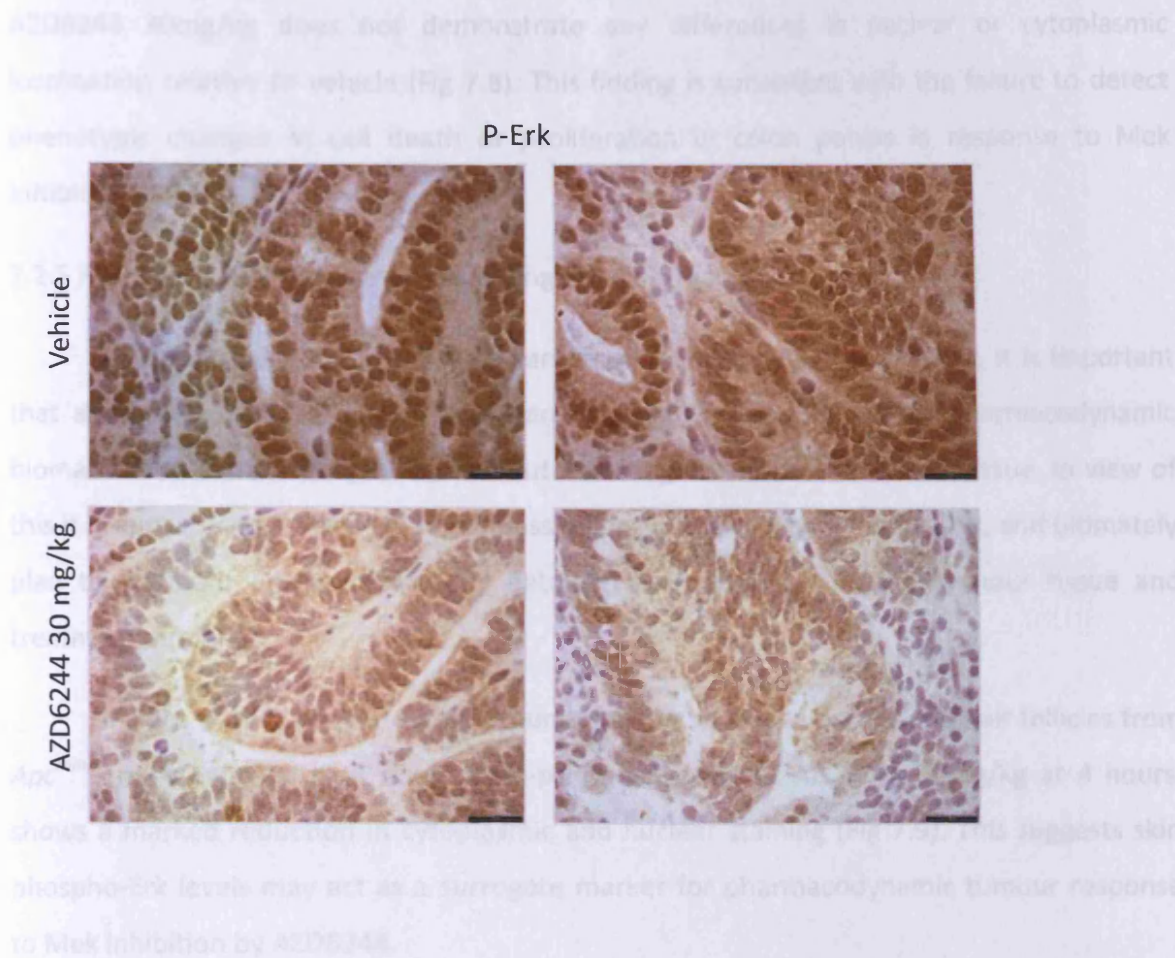


Fig 7.7 P-Erk immuno-staining in *K-ras* mutant small intestinal microadenomas demonstrate more intense staining of nuclear components at 4 hours in vehicle treated mice (top panel) consistent with activation of the Erk signalling pathway . AZD6244 30mg/kg treated mice at 4 hours show less intense nuclear P-Erk staining in keeping with interruption of Erk pathway signalling. Vehicle 0.5% hydroxypropyl methylcellulose 0.1% Tween80, and AZD6244 30mg/kg both administered via intraperitoneal injection. Magnification x40.

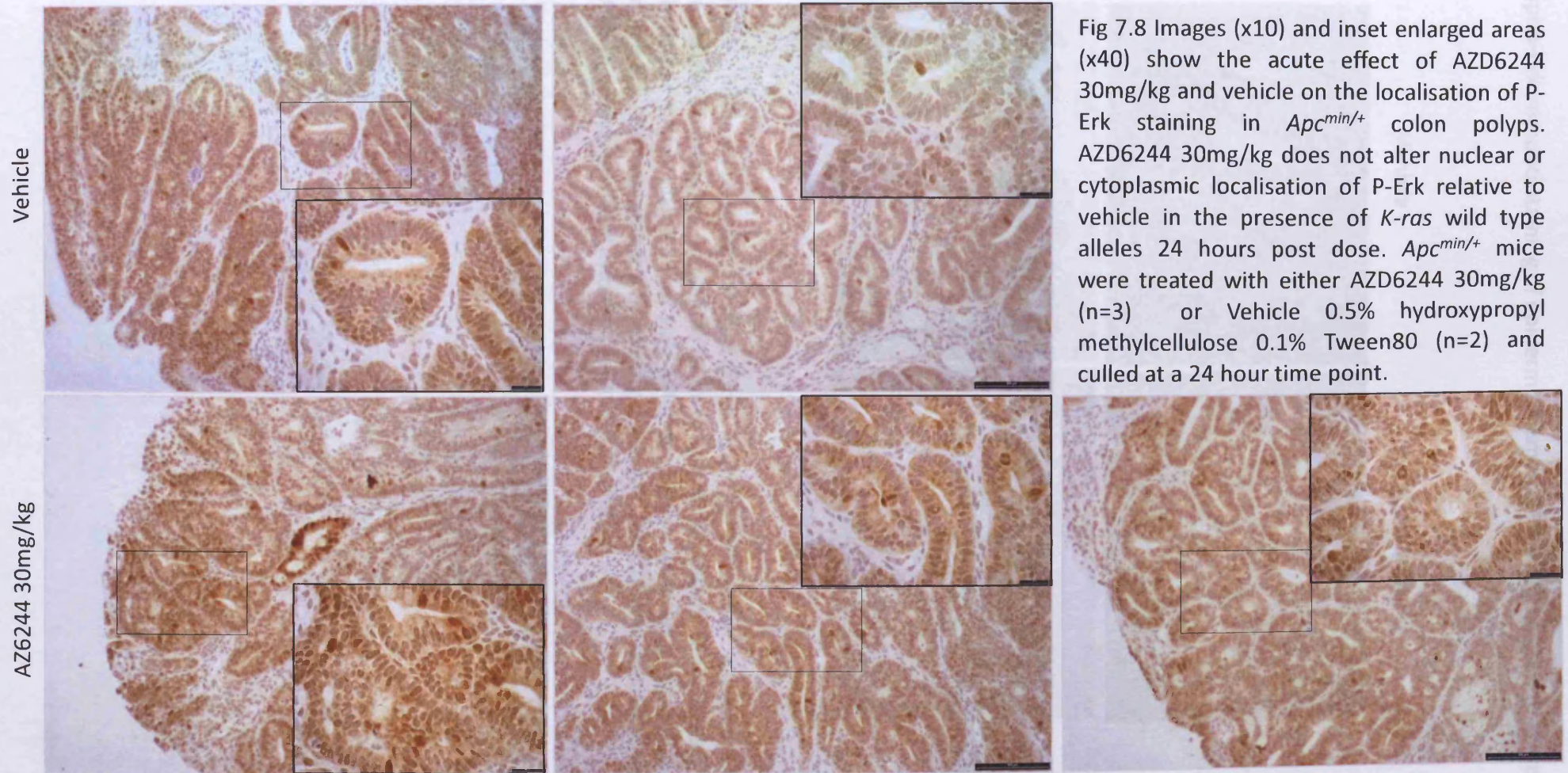
AZD6244 30mg/kg does not demonstrate any differences in nuclear or cytoplasmic localisation relative to vehicle (Fig 7.8). This finding is consistent with the failure to detect phenotypic changes in cell death or proliferation in colon polyps in response to Mek inhibition at 24 hours (7.2.2.2)

7.2.5 Phosphorylated Erk immuno-staining of epidermal tissue

As sequential tumour biopsies can be difficult to obtain in patients, it is important that alternative non tumoural tissue can be used to show activity of pharmacodynamic biomarkers to confirm target hit, without resorting to the use of tumour tissue. In view of this it is appropriate to explore these possibilities in the mouse models used, and ultimately plan to compare pharmacodynamic data between tumour and non-tumour tissue and treatment outcome.

In light of this, phospho-Erk immuno-staining of the epidermis and hair follicles from *Apc^{min/+}* mice exposed to a single intra-peritoneal dose of AZD6244 30mg/kg at 4 hours, shows a marked reduction in cytoplasmic and nuclear staining (Fig 7.9). This suggests skin phospho-Erk levels may act as a surrogate marker for pharmacodynamic tumour response to Mek inhibition by AZD6244.

Fig 7.8 Phospho-Erk immuno-staining of *K-ras* wild type *Apc^{min/+}* colon polyps from mice treated with acute AZD6244 or Vehicle treatments



7.3 Discussion

The frequency of *K-RAS* mutations in metastatic colorectal cancer, prognosis and paucity of treatment options for this subset of patients, has stimulated me to explore how genetically modified mouse models of colon cancer can be used to fill an unmet clinical need. The data I have presented is part of ongoing work in response to this need, exploring the activity of Mek inhibition in colon cancer mouse models carrying *K-ras* mutations.

Although not a quantitative assessment of Erk signalling activity, phospho-Erk immuno-staining shows increased nuclear and cytoplasmic staining in small and large intestinal tumours harbouring an activated *K-ras* mutant allele compared to tumours wild type for *K-ras* (Fig 7.1 and 7.2). Interestingly, the original paper describing this model¹¹⁴, did not report gross activation of the pathway in all small intestinal adenomas, describing only occasional positive nuclei for phospho-Erk in a proportion of intestinal adenomas (10%) arising in *AhCre^{T/+}Apc^{fl/+}Kras^{v12/+}* mice. In addition phospho-Erk staining of colon tumours was not reported but now evidence showing increased Erk activity in colonic tumours from *AhCre^{T/+}Apc^{fl/+} Kras^{v12/+}* mice is shown. Ras/Raf/Erk pathway signalling is therefore activated in intestinal tumours from this mouse model carrying an endogenously activated *K-ras* allele and underscores its use to test the activity of a targeted Mek inhibitor. Protein level quantitative assessments of phospho-Erk to confirm this finding are underway.

The data available to examine the acute phenotypic effects of AZD6244 30mg/kg upon *K-ras* mutant intestinal tumours is limited to date (n=2 mice, vehicle) and consequently the results presented require further repetition. However these preliminary results show that AZD6244 30mg/kg induces cell death (Fig 7.3 E), as shown by an increase in apoptosis and cleaved caspase-3 scoring in small intestinal tumours and a trend towards increased cell death in colonic tumours following acute administration (Fig 7.3 A and B). The phenotypic changes induced by Mek inhibition in the setting of *K-ras* mutant intestinal tumorigenesis therefore concurs with previous work showing AZD6244 25mg/kg significantly increases cleaved caspase 3 scoring in tumour bearing xenografts of Calu-6 (NSCLC *K-ras* mutant) or Colo-205 (CRC *B-raf* mutant) cell lines after 8 hours exposure (by gavage)¹²². A 4 hour time point was chosen to examine apoptosis rather than 8 hours (for

the published gavage study¹²²) reasoning that pharmacokinetics would favour assessment at an earlier time point with intra-peritoneal administration.

Documenting an increased level of Brdu cell labelling in colonic tumours (Fig 7.3 D) may result from more cells passing through S phase as a consequence of AZD6244 exposure. This has not consequently elevated the number of cells in M phase possibly through attrition of cells due to increased apoptotic cell death. Alternatively this may reflect an S phase block induced by AZD6244, leading to cell accumulation in S phase due to reduced cell exit. Previous work has shown that cell proliferation is reduced in xenografts after 24 hour exposure to AZD6244 25mg/kg¹²², but this time point has yet to be assessed in the *AhCre^{T/+} Apc^{fl/+} Kras^{v12/+}* model.

To explore the relationship between Mek inhibition and its acute anti-tumour phenotypic effects in relation to the activation status of Ras/Raf/Mek/Erk pathway signalling, AZD6244 30mg/kg was administered to *Apc^{min/+}* mice permitting an assessment of its effects on intestinal tumours in the absence of constitutive activation of either *K-ras* or *B-raf* alleles (section 3.2). With this approach it has been shown that 24 hours following a 30mg/kg dose of AZD6244, there is an approximate 2-fold increase in apoptosis and a comparable decrease in mitosis in *Apc^{min/+}* small intestinal tumours (Fig 7.4 C and D) without detected changes in colon tumour cell death or proliferation (Fig 7.4 A and B). Therefore in *K-ras* and *B-raf* wild type small intestinal tumours, AZD6244 increases cell death and reduces M phase activity. This contrasts with evidence of S phase block and unchanged M phase activity possibly due to elevated levels of cell death, induced by AZD6244 at 4 hours in the setting of *K-ras* mutant colon tumours.

Based on these *Apc^{min/+}* small intestinal tumour findings, it is possible that AZD6244 may have useful therapeutic activity in *K-ras* wild type intestinal tumours due to interruption of signalling pathways downstream of the EGF receptor which is known to be activated in *Apc^{min/+}* intestinal tumours¹⁰⁹. That AZD6244 30mg/kg (by oral gavage) also induces a 2 fold increase in apoptosis in *K-ras* wild type colon tumours from *Apc^{min/+}* mice at 4 hours (Fig 7.5) adds further support to the notion that the effects of Mek inhibition may not be restricted to *K-ras* mutant intestinal tumours. Such findings suggest that *K-ras* mutation status may not be a reliable predictor of response to Mek inhibition, at least in the

in vivo models described, contrary to published data¹²⁵. Thus any long term treatment effect of AZD6244 30mg/kg may be very similar to that seen with chronic administration of gefitinib 75mg/kg (5.3.1). What remains to be seen is whether chronic dosing with AZD6244 will be any more effective (in terms of tumour burden/longevity) in the setting of *K-ras* mutant intestinal tumours. The effect of Mek inhibition on the 24 hour tumour phenotype in *AhCre^{T/+}Apc^{fl/+}Kras^{v12/+}* mice will be of particular interest in this respect. If there is no difference in the treatment effects of long term Mek inhibitor dosing according to tumoural *K-ras* mutation status, and assuming AZD6244 30mg/kg is the optimal anti-tumour dose, this may reflect failure to counter critical 'addicted' pathway(s) driving mutant *K-ras* tumour growth.

The loss of phospho-Erk nuclear staining consequent upon AZD6244 30mg/kg in small and large intestinal tumours from *AhCre^{T/+}Apc^{fl/+}Kras^{v12/+}* mice (Fig 7.6 and 7.7) is consistent with published findings¹²², which have reported a greater reduction of phospho-Erk nuclear staining compared to cytoplasmic signals in xenografts following acute AZD6244 (25mg/kg by oral gavage)¹²². This loss of tumoural nuclear phospho-Erk may be mechanistically linked with the acute effects of AZD6244 30mg/kg based on the association with increased apoptosis in small intestinal tumours and trend towards increased apoptosis in colon tumours from *AhCre^{T/+}Apc^{fl/+}Kras^{v12/+}* mice (Fig 7.3). Indeed this fits with evidence showing that translocation of ERK to the nucleus is important in the regulation of mitogenic signals²²⁹ and that nucleo-cytoplasmic distribution of ERK is relevant to the control of ERK signalling²³⁰. Furthermore, nuclear phospho-ERK localisation has been associated with resistance to cisplatin-induced apoptosis in OVCAR-3/CDDP cells²³¹ suggesting that loss in nuclear phospho-Erk may indicate increased apoptosis. The failure to observe alterations in nuclear localisation of phospho-Erk immuno-reactivity in colon tumours from *Apc^{min/+}* mice, 24 hours post AZD6244 30mg/kg dosing (Fig 7.8) is in keeping with the absence of any detected change in apoptotic or mitotic activity at this time in colon tumours (Fig 7.4). It will thus be of great interest to confirm reduced nuclear localisation of phospho-Erk in *Apc^{min/+}* colon polyps in view of increased apoptosis in response to AZD6244 30mg/kg at 4 hours. Similarly, given increased apoptosis and reduced mitotic counts in *Apc^{min/+}* small intestinal tumours 24 hours following AZD6244 30mg/kg, the pattern of nuclear phospho-Erk localisation in these tumours will be of interest.

As sequential tumour biopsies are not always possible or comfortable for patients, attempts are being made to sample substitute tissues to examine the status of pharmacodynamic biomarkers in clinical studies. With this in mind it has been possible to show a marked loss of nuclear and cytoplasmic phospho-Erk immuno-staining of *Apc^{min/+}* epidermis and hair follicles (Fig 7.9) following acute AZD6244 dosing. Given the correlation with increased apoptosis in *Apc^{min/+}* mice colon tumours at 4 hours, it is attractive to postulate that hair follicles for phospho-Erk staining could have potential value as a future surrogate biomarker of *in vivo* pharmacodynamic activity. Unfortunately, in a phase I study however, skin biopsies following 15 days AZD6244 treatment (± 7 days) has been found to be uninformative due to variability and minimal baseline levels of phospho-Erk immunoreactivity¹³⁹. Nevertheless, being able to explore the potential utility of pharmacodynamic or predictive biomarkers in surrogate tissues from genetically modified animal models exposed to experimental drugs, may help to refine the approach taken in early phase clinical trials.

7.3.1 Future direction

Preliminary data using *AhCre^{T/+}Apc^{fl/+}Kras^{+/+}* and *AhCre^{T/+}Apc^{fl/+}Kras^{v12/+}* mouse models has pointed to increased intestinal tumour Raf/Mek/Erk signalling activity compatible with the model being potentially useful for investigating the effects of Mek inhibition with AZD6244. In addition to any acute anti-tumour effects of AZD6244 in *Apc^{min/+}* tumours, it has been demonstrated that this Mek inhibitor induces immediate anti-tumour phenotypic changes in small intestinal if not colonic tumours arising in *AhCre^{T/+}Apc^{fl/+}Kras^{v12/+}* mice, associated with a loss of nuclear phospho-Erk accumulation (pharmacodynamic biomarker). In light of these results, long term experimental treatment cohorts of *AhCre^{T/+}Apc^{fl/+}Kras^{+/+}* and *AhCre^{T/+}Apc^{fl/+}Kras^{v12/+}* will be dosed with AZD6244 30mg/kg and vehicle to specifically test whether *K-ras* mutation status sensitises tumours to chronic Mek inhibition. Treatment will start once symptoms of an intestinal tumour burden have developed (earliest evidence of pale feet, rectal prolapse, swollen abdomen or rectal bleeding). Mice of each genotype (n=20) will receive once daily AZD6244 30mg/kg or vehicle, 0.5% hydroxypropyl methylcellulose 0.1% Tween80 via oral gavage until any treatment effect is lost and the survival endpoint is reached. Kaplan Meier survival curves

will be plotted for each genotype/treatment and the log rank test used to calculate statistically significant differences in survival (Fig 7.10)

Fig 7.10 Theoretical survival curves for long term treatment with AZD6244 in *AhCre^{T/+}Apc^{fl/+}Kras^{+/+}* and *AhCre^{T/+}Apc^{fl/+}Kras^{v12/+}* mouse models

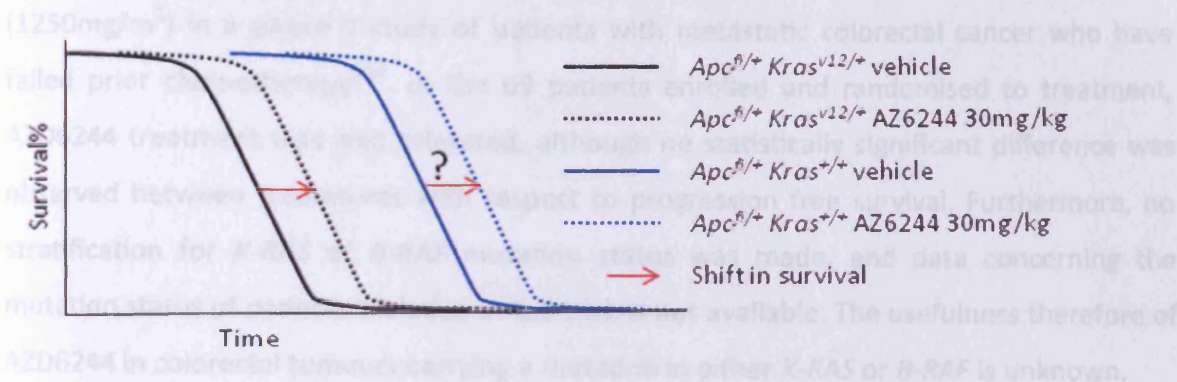


Fig 7.10 Theoretical survival curves of *Apc^{fl/+}Kras^{+/+}* and *Apc^{fl/+}Kras^{v12/+}* mouse cohorts in response to AZD6244 30mg/kg. The survival of mice carrying the *Kras^{v12/+}* allele is known to be reduced compared to mice with wild type alleles, *Kras^{+/+122}*. It is anticipated that once daily treatment with AZD6244 30mg/kg will shift the *Apc^{fl/+}Kras^{v12/+}* survival curve to the right; whether any treatment effect will be restricted to this genotype is unknown and will be tested by long term treatment of *Apc^{fl/+}Kras^{+/+}* cohorts.

As previously described for experiments incorporating long term treatment of *Apc^{min/+}* cohorts with gefitinib and AZ12253801 (5.5), at the survival endpoint, tumours will be harvested for signalling pathway analysis to probe the potential mechanism(s) responsible for resistance, assuming a survival advantage is documented. It will be of particular interest to examine activity in PI3K/AKT signalling where evidence of increased AKT activity may explain resistance to MEK inhibition^{84, 232}. As increased levels of phospho-Igf-1r were previously found as early as 4 hours post gefitinib dosing in *Apc^{min/+}* colon tumours (3.3.3.1), levels of phospho-Akt will also be examined in tumours from *AhCre^{T/+}Apc^{fl/+}Kras^{v12/+}* intestinal tumours to see if pathway activation is acutely initiated. If Pi3k/Akt pathway activation in response to Mek inhibition is confirmed, the natural step forward will be to combine inhibition of both Mek and Pi3k/Akt signalling pathways in future experiments using the *AhCre^{T/+}Apc^{fl/+}Kras^{v12/+}* model. This combination has already been shown to be therapeutically advantageous in the setting of *Kras^{G12D}* induced mouse

lung tumours²³³. Indeed Phase I studies testing the combination of dual blockade of MEK and AKT inhibition are underway using MK2206 and AZD6244 (<http://clinicaltrials.gov/ct2/show/NCT01021748>).

From a clinical standpoint, AZD6244 (100mg bid) has been compared to capecitabine (1250mg/m²) in a phase II study of patients with metastatic colorectal cancer who have failed prior chemotherapy²³⁴. In the 69 patients enrolled and randomised to treatment, AZD6244 treatment was well tolerated, although no statistically significant difference was observed between treatments with respect to progression free survival. Furthermore, no stratification for *K-RAS* or *B-RAF* mutation status was made, and data concerning the mutation status of patients included in the trial, is not available. The usefulness therefore of AZD6244 in colorectal tumours carrying a mutation in either *K-RAS* or *B-RAF* is unknown.

In summary I have designed a trial protocol to test the role of MEK inhibition using AZD6244 in patients completing first line therapy for metastatic colorectal cancer (Fig 7.11). Trials of this design are a potentially useful way to test new agents early in the trajectory of metastatic cancer treatments, with incorporation of therapy during the interval normally free from treatment, when patients have a low burden of disease. If long term treatment with AZD6244 proves to be successful in *AhCre^{T/+}Apc^{fl/+}Kras^{v12/+}* mouse cohorts, then the impetus to undertake this or a similar early clinical study will be reinforced.

Fig 7.11 Interval therapy in colorectal cancer using AZD6244

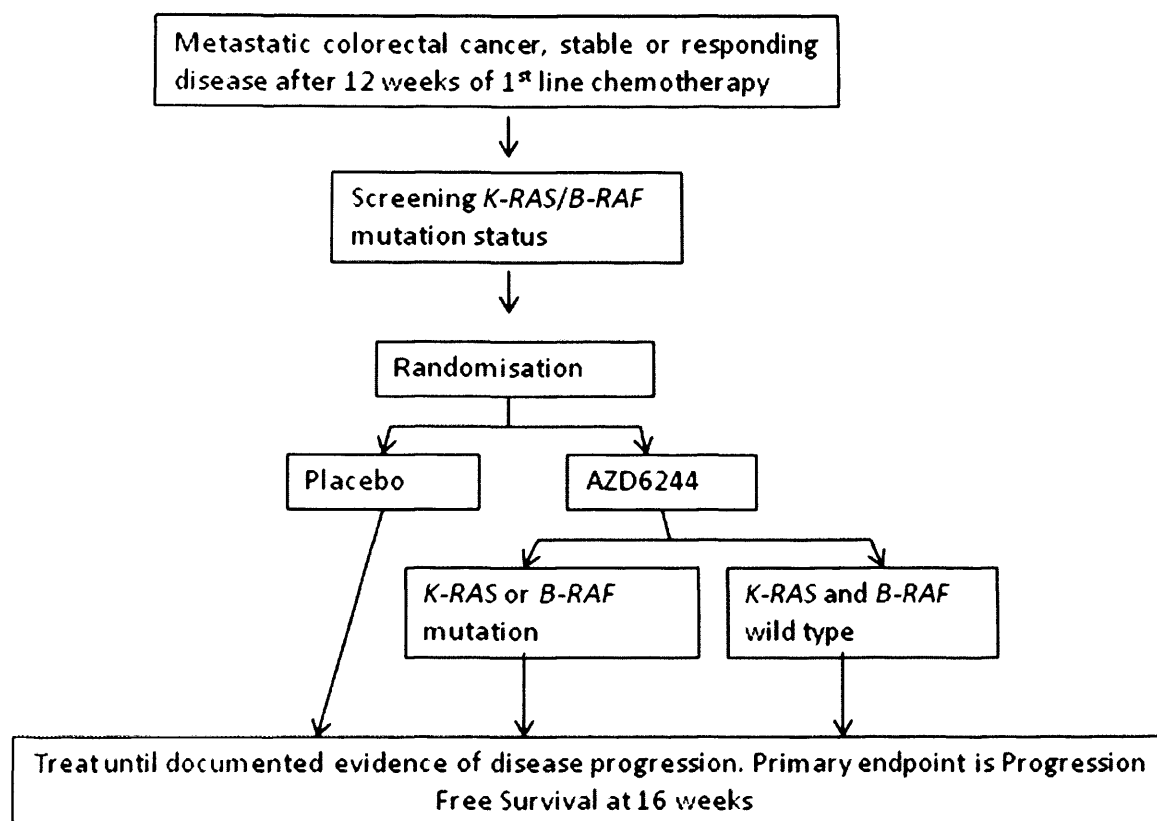


Fig 7.11 A three arm double blind placebo-controlled randomised phase 2 trial is proposed with progression free survival at 16 weeks as the primary endpoint. Patients with metastatic colorectal cancer who have received 12 weeks of standard palliative first line chemotherapy and have stable or responding disease will be eligible. At screening, consent will be obtained to type tumour samples for *K-RAS* and *B-RAF* mutation status. Patients with measurable disease will be allocated randomly to receive either AZD6244 (100mb bid) or placebo. Those in the AZD6244 group will be split into two arms; those with tumours carrying *K-RAS* and/or *B-RAF* mutation and those wild type for both *K-RAS* and *B-RAF* mutations. Patients will be monitored until progressive disease is documented at which time conventional chemotherapy will be re-started. The trial protocol was developed with Prof Tim Maughan and Gareth Griffiths and trial design discussed at the 10th ECCO-AACR-ASCO Workshop Methods in Clinical Cancer Research, Flims, Switzerland, 21-27th June 2008.

Chapter 8

Conclusion

This work has demonstrated how genetically engineered mouse models of colon tumourigenesis can be used to explore biomarker discovery, target validation, therapeutic trials and modelling resistance to targeted agents. Such discoveries have potential translational relevance which now needs to be defined in order to test the true utility of these autochthonous *in vivo* platforms compared to tumour-bearing xenografts.

Given *K-RAS* wild type status is predictive of response to EGFR targeted therapy in colorectal cancer patients⁴⁶, determining that *Apc*^{min/+} mouse colon polyps were *K-ras* and *B-raf* wild type underscores the relevance of this model for studying Egfr blockade. This is important as prediction of response to EGFR targeted therapy in approximately 30% of colorectal cancer patients is unknown⁵¹. I have shown that acute exposure to gefitinib suppresses downstream Egfr signalling, in keeping with its known action as an inhibitor of EGFR tyrosine kinase activity, resulting in morphological change consistent with anti-tumour effects in the intestine. In addition, probing the associated transcript change in *Apc*^{min/+} *K-ras* wild type colon polyps has identified 11 putative predictive biomarkers of response to Egfr targeted therapy. When transcriptome level data from *K-RAS* wild type metastatic colorectal cancer patients is examined for murine gene expression changes, *IKBKG*, *CCNE2* and *CXCL9* have been identified. These genes are therefore postulated to have clinical value in terms of segregating clinical response outcome to cetuximab monotherapy. Interpretation of the remaining mouse transcripts, in terms of their known biological function, has made it possible to build a picture of how expression patterns may hypothetically influence tumour response to anti-EGFR targeted therapy. As a consequence, novel resistance mechanisms to EGFR targeted therapy have been proposed through altered levels of gene expression (e.g. *HIP1* and *EPHA3*) or reinforced as in the case of increased expression of *ERBB3*. Such data may help devise clinical strategies to overcome resistance to EGFR targeted agents.

SAM analysis revealed an interesting 2.4 fold increased expression of *Axin2*, a known target of Wnt signalling which constitutes a negative feedback loop controlling its activity²³⁵. This data therefore reinforces the published evidence of cross talk between Egfr and

Wnt pathways. EGFR has been shown to be a target of Wnt pathway activation and suggested to drive mitogenic signals in a beta catenin driven model of mouse liver cancer²³⁶. Furthermore in mammary cancer, Wnt signalling has been shown to increase levels of cyclin D1 through activated MAPK via induction of EGFR²³⁷. It is possible therefore that *Axin2* may represent a mechanism of action mediating a therapeutic response to gefitinib through negative regulation of Wnt pathway activity in *Apc^{min/+}* tumours. As such this early response could be an important predictor of outcome to EGFR targeted therapy and should be examined in more detail. Drugs which are able to induce negative regulators of Wnt signalling may therefore be attractive targets for therapeutic development.

Given the accumulating evidence that IGF1R pathway activation may be important in conferring resistance to EGF receptor blockade⁸⁰⁻⁸², the finding that exposure to the Egfr inhibitor, gefitinib, led to elevated phosphorylation of the insulin-like growth factor 1 receptor (Igf1r), in *Apc^{min/+}* colonic polyps, further implicates the Igf-1 pathway in response to Egfr blockade. I have subsequently shown that chronic monotherapy against either Egfr or Igf1r enhances survival but that ultimately adenomas still develop. However, combined Egfr/Igf1r blockade produced the most effective tumour suppression and supports the concept that Egfr resistance is mediated through Igf-1 receptor signalling, and also provides a rationale for combinatorial therapy in *K-RAS* wild type colorectal cancer.

Of further potential clinical significance is the finding that molecular changes following acute drug exposures occur within 4 hours. This raises the attractive opportunity of being able to identify drug resistance pathways very early within a treatment schedule following a single drug exposure and tumour biopsy. This approach could increase the future ability to stratify patients in clinical trials according to drug induced molecular changes and is also a means of highlighting which pathways should be antagonised to minimise activated drug resistance pathways. This will have particular relevance if circulating tumour cells or tumour tissue substitutes can be effectively used for such purposes.

Examining the molecular effects of chronic drug administration in *Apc^{min/+}* mice has been shown to facilitate analysis of pathways mediating intestinal tumour resistance. In the case of long term gefitinib exposure, acute Igf1r pathway activity is reinforced by elevated

Igf1r protein expression. This is accompanied by increased Egfr protein levels. Having noted gefitinib induced transcript changes (*Cbl*, *Ubd* and *Hip1*) include functions linked with EGFR turnover, it is clear that this model has been useful in terms of increasing understanding of the mechanisms underlying tumour resistance mechanisms. Taking a similar approach in mice treated with chronic Igf1r inhibition has challenged recent evidence supporting EGFR family members in resistance to Igf1r blockade^{80, 95, 96, 198}, suggesting at least in the *Apc*^{min/+} mouse that response to chronic Igf1r therapy does not involve increased Egfr activity. Interestingly, Erk activity appears to be maintained in such tumours, suggesting this may be a means of driving tumour growth. This finding may indicate that combined Igf1r and Mek inhibition would provide additional therapeutic activity.

I have also investigated Mek inhibition with AZD6244 in different genetically engineered mouse models, namely *AhCre*^{T/+}*Apc*^{fl/+}*Kras*^{v12/+} and *AhCre*^{T/+}*Apc*^{fl/+}*Kras*^{+/+} in addition to *Apc*^{min/+} mice. This has enabled preliminary investigation of its anti-tumour effects with respect to *K-ras* mutation status. This is of translational importance in light of the need for targeted therapy in *K-RAS* mutant colorectal cancer and initial data suggesting tumour cells with *K-RAS* mutations are likely to be sensitive to MEK inhibition^{122, 125}.

Elevated Erk phosphorylation, indicating Ras/Raf/Erk pathway signalling, has been demonstrated in intestinal tumours from *AhCre*^{T/+}*Apc*^{fl/+}*Kras*^{v12/+} mice carrying an endogenously activated *K-ras* allele and again underscores its use as an *in vivo* platform to test the activity of AZD6244. The anti-tumour effects of AZD6244 are more apparent in small intestinal tumours, including induction of cell death and perturbation of the cell cycle. However these effects are not limited to *K-ras* mutant intestinal tumours which have also shown a reduction in nuclear Erk activity in response to Mek inhibition. Based on these early findings, any long term treatment effect of AZD6244 may be independent of *K-ras* mutation status producing similar survival for mice with and without *K-ras* mutations. The added benefit from such work will potentially increase understanding of resistance mechanisms in response to Mek inhibition. The results from a chronic dosing study may also help guide whether MEK inhibitor therapy is worth pursuing in future clinical studies restricted to *K-RAS* mutant colorectal cancers.

Finally, acute exploration of the effects of a BH-3 mimetic in combination with gefitinib has been explored, in the hope that improvements in *Apc^{min/+}* survival in response to gefitinib monotherapy, can be achieved. A 3 fold elevation in cell death has been shown for the combination in *Apc^{min/+}* colon tumours after acute exposure, raising expectation that this may translate into an additional survival advantage with chronic administration. If a positive outcome is shown, clinical studies may incorporate the addition of a BH-3 mimetic to monoclonal antibody targeting EGFR. The interruption of signalling pathways combined with induction of apoptosis provides an opportunity to optimise drug sequencing and dosing strategies based upon immediate anti-tumour phenotypic effects. The *Apc^{min/+}* mouse model may also serve to increase knowledge of how BCL-2 protein levels influence intestinal tumour response to BH-3 mimetics.

Taken together, the mouse models have served as a useful resource with potential clinical relevance. To determine their true value and the significance of the presented data, further clinical evaluation is required. My hope is this work will be of value and perhaps contribute towards improving cancer patients' lives.

References

1. **CRUK. UK cancer mortality statistics for common cancers, 2007**
2. **Obrand DI, Gordon PH. Incidence and patterns of recurrence following curative resection for colorectal carcinoma. *Dis Colon Rectum* 1997;40:15-24.**
3. **Chau I, Cunningham D. Treatment in advanced colorectal cancer: what, when and how? *Br J Cancer* 2009;100(11):1704-19.**
4. **Van Cutsem E, Kohne CH, Hitre E, Zaluski J, Chang Chien CR, Makhson A, D'Haens G, Pinter T, Lim R, Bodoky G, Roh JK, Folprecht G, Ruff P, Stroh C, Tejpar S, Schlichting M, Nippgen J, Rougier P. Cetuximab and chemotherapy as initial treatment for metastatic colorectal cancer. *N Engl J Med* 2009;360:1408-17.**
5. **Sobrero AF, Maurel J, Fehrenbacher L, Scheithauer W, Abubakr YA, Lutz MP, Vega-Villegas ME, Eng C, Steinhauer EU, Prausova J, Lenz HJ, Borg C, Middleton G, Kroning H, Luppi G, Kisker O, Zubel A, Langer C, Kopit J, Burris HA, 3rd. EPIC: phase III trial of cetuximab plus irinotecan after fluoropyrimidine and oxaliplatin failure in patients with metastatic colorectal cancer. *J Clin Oncol* 2008;26:2311-9.**
6. **Jonker DJ, O'Callaghan CJ, Karapetis CS, Zalcborg JR, Tu D, Au HJ, Berry SR, Krahn M, Price T, Simes RJ, Tebbutt NC, van Hazel G, Wierzbicki R, Langer C, Moore MJ. Cetuximab for the treatment of colorectal cancer. *N Engl J Med* 2007;357:2040-8.**
7. **Cambien B, Karimjee BF, Richard-Fiardo P, Bziouech H, Barthel R, Millet MA, Martini V, Birnbaum D, Scoazec JY, Abello J, Saati TA, Johnson MG, Sullivan TJ, Medina JC, Collins TL, Schmid-Alliana A, Schmid-Antomarchi H. Organ-specific inhibition of metastatic colon carcinoma by CXCR3 antagonism. *Br J Cancer* 2009.**
8. **Bell DW, Lynch TJ, Haserlat SM, Harris PL, Okimoto RA, Brannigan BW, Sgroi DC, Muir B, Riemenschneider MJ, Iacona RB, Krebs AD, Johnson DH, Giaccone G, Herbst RS, Manegold C, Fukuoka M, Kris MG, Baselga J, Ochs JS, Haber DA. Epidermal growth factor receptor mutations and gene amplification in non-small-cell lung cancer: molecular analysis of the IDEAL/INTACT gefitinib trials. *J Clin Oncol* 2005;23:8081-92.**

9. Imai K, Takaoka A. Comparing antibody and small-molecule therapies for cancer. *Nat Rev Cancer* 2006;6:714-27.
10. Weinstein IB. Cancer. Addiction to oncogenes--the Achilles heel of cancer. *Science* 2002;297:63-4.
11. Weinstein IB, Joe AK. Mechanisms of disease: Oncogene addiction--a rationale for molecular targeting in cancer therapy. *Nat Clin Pract Oncol* 2006;3:448-57.
12. Simon R. ASCO Education book: American Society of clinical oncology, 2006.
13. Simon R, Wang SJ. Use of genomic signatures in therapeutics development in oncology and other diseases. *Pharmacogenomics J* 2006;6:166-73.
14. Eckhardt G. Incorporation of biological correlative studies into early clinical trials, In *Methods in Clinical Cancer Research*, Vail, 2009.
15. Sargent DJ, Conley BA, Allegra C, Collette L. Clinical trial designs for predictive marker validation in cancer treatment trials. *J Clin Oncol* 2005;23:2020-7.
16. Lipshutz RJ, Morris D, Chee M, Hubbell E, Kozal MJ, Shah N, Shen N, Yang R, Fodor SP. Using oligonucleotide probe arrays to access genetic diversity. *Biotechniques* 1995;19:442-7.
17. Simon R. Roadmap for developing and validating therapeutically relevant genomic classifiers. *J Clin Oncol* 2005;23:7332-41.
18. Quackenbush J. Microarray analysis and tumor classification. *N Engl J Med* 2006;354:2463-72.
19. Nannini M, Pantaleo MA, Maleddu A, Astolfi A, Formica S, Biasco G. Gene expression profiling in colorectal cancer using microarray technologies: results and perspectives. *Cancer Treat Rev* 2009;35:201-9.
20. Mariadason JM, Arango D, Shi Q, Wilson AJ, Corner GA, Nicholas C, Aranes MJ, Lesser M, Schwartz EL, Augenlicht LH. Gene expression profiling-based prediction of response of colon carcinoma cells to 5-fluorouracil and camptothecin. *Cancer Res* 2003;63:8791-812.

21. Arango D, Wilson AJ, Shi Q, Corner GA, Aranes MJ, Nicholas C, Lesser M, Mariadason JM, Augenlicht LH. Molecular mechanisms of action and prediction of response to oxaliplatin in colorectal cancer cells. *Br J Cancer* 2004;91:1931-46.
22. Del Rio M, Molina F, Bascoul-Mollevis C, Copois V, Bibeau F, Chalbos P, Bareil C, Kramar A, Salvetat N, Fraslon C, Conseiller E, Granci V, Leblanc B, Pau B, Martineau P, Ychou M. Gene expression signature in advanced colorectal cancer patients select drugs and response for the use of leucovorin, fluorouracil, and irinotecan. *J Clin Oncol* 2007;25:773-80.
23. Ghadimi BM, Grade M, Difilippantonio MJ, Varma S, Simon R, Montagna C, Fuzesi L, Langer C, Becker H, Liersch T, Ried T. Effectiveness of gene expression profiling for response prediction of rectal adenocarcinomas to preoperative chemoradiotherapy. *J Clin Oncol* 2005;23:1826-38.
24. Khambata-Ford S, Garrett CR, Meropol NJ, Basik M, Harbison CT, Wu S, Wong TW, Huang X, Takimoto CH, Godwin AK, Tan BR, Krishnamurthi SS, Burris HA, 3rd, Poplin EA, Hidalgo M, Baselga J, Clark EA, Mauro DJ. Expression of epiregulin and amphiregulin and K-ras mutation status predict disease control in metastatic colorectal cancer patients treated with cetuximab. *J Clin Oncol* 2007;25:3230-7.
25. Debucquoy A, Haustermans K, Daemen A, Aydin S, Libbrecht L, Gevaert O, De Moor B, Tejpar S, McBride WH, Penninckx F, Scalliet P, Stroh C, Vlassak S, Sempoux C, Machiels JP. Molecular response to cetuximab and efficacy of preoperative cetuximab-based chemoradiation in rectal cancer. *J Clin Oncol* 2009;27:2751-7.
26. Li X, Quigg RJ, Zhou J, Gu W, Nagesh Rao P, Reed EF. Clinical utility of microarrays: current status, existing challenges and future outlook. *Curr Genomics* 2008;9:466-74.
27. Braun MS, Richman SD, Quirke P, Daly C, Adlard JW, Elliott F, Barrett JH, Selby P, Meade AM, Stephens RJ, Parmar MK, Seymour MT. Predictive biomarkers of chemotherapy efficacy in colorectal cancer: results from the UK MRC FOCUS trial. *J Clin Oncol* 2008;26:2690-8.
28. Saltz LB, Meropol NJ, Loehrer PJ, Sr., Needle MN, Kopit J, Mayer RJ. Phase II trial of cetuximab in patients with refractory colorectal cancer that expresses the epidermal growth factor receptor. *J Clin Oncol* 2004;22:1201-8.

29. **Cunningham D, Humblet Y, Siena S, Khayat D, Bleiberg H, Santoro A, Bets D, Mueser M, Harstrick A, Verslype C, Chau I, Van Cutsem E. Cetuximab monotherapy and cetuximab plus irinotecan in irinotecan-refractory metastatic colorectal cancer. N Engl J Med 2004;351:337-45.**
30. **Burstein HJ. The distinctive nature of HER2-positive breast cancers. N Engl J Med 2005;353:1652-4.**
31. **Chung KY, Shia J, Kemeny NE, Shah M, Schwartz GK, Tse A, Hamilton A, Pan D, Schrag D, Schwartz L, Klimstra DS, Fridman D, Kelsen DP, Saltz LB. Cetuximab shows activity in colorectal cancer patients with tumors that do not express the epidermal growth factor receptor by immunohistochemistry. J Clin Oncol 2005;23:1803-10.**
32. **Etienne-Grimaldi MC, Cayre A, Penault-Llorca F, Francoual M, Formento JL, Benchimol D, Bourgeon A, Milano G. EGFR expression in colon cancer: a break in the clouds. Ann Oncol 2006;17:1850-1.**
33. **Francoual M, Etienne-Grimaldi MC, Formento JL, Benchimol D, Bourgeon A, Chazal M, Letoublon C, Andre T, Gilly N, Delpero JR, Lasser P, Spano JP, Milano G. EGFR in colorectal cancer: more than a simple receptor. Ann Oncol 2006;17:962-7.**
34. **Barber TD, Vogelstein B, Kinzler KW, Velculescu VE. Somatic mutations of EGFR in colorectal cancers and glioblastomas. N Engl J Med 2004;351:2883.**
35. **Moroni M, Veronese S, Benvenuti S, Marrapese G, Sartore-Bianchi A, Di Nicolantonio F, Gambacorta M, Siena S, Bardelli A. Gene copy number for epidermal growth factor receptor (EGFR) and clinical response to antiEGFR treatment in colorectal cancer: a cohort study. Lancet Oncol 2005;6:279-86.**
36. **Lenz HJ, Van Cutsem E, Khambata-Ford S, Mayer RJ, Gold P, Stella P, Mirtsching B, Cohn AL, Pippas AW, Azarnia N, Tsuchihashi Z, Mauro DJ, Rowinsky EK. Multicenter phase II and translational study of cetuximab in metastatic colorectal carcinoma refractory to irinotecan, oxaliplatin, and fluoropyrimidines. J Clin Oncol 2006;24:4914-21.**
37. **Mulloy R, Ferrand A, Kim Y, Sordella R, Bell DW, Haber DA, Anderson KS, Settleman J. Epidermal growth factor receptor mutants from human lung cancers exhibit enhanced catalytic activity and increased sensitivity to gefitinib. Cancer Res 2007;67:2325-30.**

38. Kallioniemi OP, Kallioniemi A, Kurisu W, Thor A, Chen LC, Smith HS, Waldman FM, Pinkel D, Gray JW. ERBB2 amplification in breast cancer analyzed by fluorescence in situ hybridization. *Proc Natl Acad Sci U S A* 1992;89:5321-5.
39. Perez-Soler R, Saltz L. Cutaneous adverse effects with HER1/EGFR-targeted agents: is there a silver lining? *J Clin Oncol* 2005;23:5235-46.
40. Siena S, Sartore-Bianchi A, Di Nicolantonio F, Balfour J, Bardelli A. Biomarkers predicting clinical outcome of epidermal growth factor receptor-targeted therapy in metastatic colorectal cancer. *J Natl Cancer Inst* 2009;101:1308-24.
41. Shia J, Klimstra DS, Li AR, Qin J, Saltz L, Teruya-Feldstein J, Akram M, Chung KY, Yao D, Paty PB, Gerald W, Chen B. Epidermal growth factor receptor expression and gene amplification in colorectal carcinoma: an immunohistochemical and chromogenic in situ hybridization study. *Mod Pathol* 2005;18:1350-6.
42. Spindler KL, Lindebjerg J, Nielsen JN, Olsen DA, Bisgard C, Brandslund I, Jakobsen A. Epidermal growth factor receptor analyses in colorectal cancer: a comparison of methods. *Int J Oncol* 2006;29:1159-65.
43. Ross JS, Fletcher JA, Bloom KJ, Linette GP, Stec J, Symmans WF, Pusztai L, Hortobagyi GN. Targeted therapy in breast cancer: the HER-2/neu gene and protein. *Mol Cell Proteomics* 2004;3:379-98.
44. Lievre A, Bachet JB, Le Corre D, Boige V, Landi B, Emile JF, Cote JF, Tomasic G, Penna C, Ducreux M, Rougier P, Penault-Llorca F, Laurent-Puig P. KRAS mutation status is predictive of response to cetuximab therapy in colorectal cancer. *Cancer Res* 2006;66:3992-5.
45. Amado RG, Wolf M, Peeters M, Van Cutsem E, Siena S, Freeman DJ, Juan T, Sikorski R, Suggs S, Radinsky R, Patterson SD, Chang DD. Wild-type KRAS is required for panitumumab efficacy in patients with metastatic colorectal cancer. *J Clin Oncol* 2008;26:1626-34.
46. Karapetis CS, Khambata-Ford S, Jonker DJ, O'Callaghan CJ, Tu D, Tebbutt NC, Simes RJ, Chalchal H, Shapiro JD, Robitaille S, Price TJ, Shepherd L, Au HJ, Langer C, Moore MJ, Zalberg JR. K-ras mutations and benefit from cetuximab in advanced colorectal cancer. *N Engl J Med* 2008;359:1757-65.

47. **Bokemeyer C, Bondarenko I, Makhson A, Hartmann JT, Aparicio J, de Braud F, Donea S, Ludwig H, Schuch G, Stroh C, Loos AH, Zubel A, Koralewski P. Fluorouracil, leucovorin, and oxaliplatin with and without cetuximab in the first-line treatment of metastatic colorectal cancer. J Clin Oncol 2009;27:663-71.**
48. **De Roock W, Piessevaux H, De Schutter J, Janssens M, De Hertogh G, Personeni N, Biesmans B, Van Laethem JL, Peeters M, Humblet Y, Van Cutsem E, Tejpar S. KRAS wild-type state predicts survival and is associated to early radiological response in metastatic colorectal cancer treated with cetuximab. Ann Oncol 2008;19:508-15.**
49. **Jonker D. High epiregulin gene expression plus Kras wild type status as predictors of cetuximab benefit in the treatment of advanced colorectal cancer. Results from NCIC CTG CO.17 - A phase III trial of cetuximab versus best supportive care, In 45th Annual meeting of the American Society of Clinical Oncology, Chicago, 2009.**
50. **Di Nicolantonio F, Martini M, Molinari F, Sartore-Bianchi A, Arena S, Saletti P, De Dosso S, Mazzucchelli L, Frattini M, Siena S, Bardelli A. Wild-type BRAF is required for response to panitumumab or cetuximab in metastatic colorectal cancer. J Clin Oncol 2008;26:5705-12.**
51. **Sartore-Bianchi A, Martini M, Molinari F, Veronese S, Nichelatti M, Artale S, Di Nicolantonio F, Saletti P, De Dosso S, Mazzucchelli L, Frattini M, Siena S, Bardelli A. PIK3CA Mutations in Colorectal Cancer Are Associated with Clinical Resistance to EGFR-Targeted Monoclonal Antibodies. Cancer Res 2009.**
52. **Di Nicolantonio F, Sartore-Bianchi A, Molinari F, Martini M. BRAF, PIK3CA and KRAS mutations and loss of PTEN expression impair response to EGFR targeted therapies in metastatic colorectal cancer, In American Association for Cancer Research, Denver, CO, 2009.**
53. **Jhawer M, Goel S, Wilson AJ, Montagna C, Ling YH, Byun DS, Nasser S, Arango D, Shin J, Klampfer L, Augenlicht LH, Perez-Soler R, Mariadason JM. PIK3CA mutation/PTEN expression status predicts response of colon cancer cells to the epidermal growth factor receptor inhibitor cetuximab. Cancer Res 2008;68:1953-61.**
54. **Perrone F, Lampis A, Orsenigo M, Di Bartolomeo M, Gevorgyan A, Losa M, Frattini M, Riva C, Andreola S, Bajetta E, Bertario L, Leo E, Pierotti MA, Pilotti S. PI3KCA/PTEN deregulation contributes to impaired responses to cetuximab in metastatic colorectal cancer patients. Ann Oncol 2009;20:84-90.**

55. **Bonner JA, Harari PM, Giralt J, Azarnia N, Shin DM, Cohen RB, Jones CU, Sur R, Raben D, Jassem J, Ove R, Kies MS, Baselga J, Youssoufian H, Amellal N, Rowinsky EK, Ang KK. Radiotherapy plus cetuximab for squamous-cell carcinoma of the head and neck. N Engl J Med 2006;354:567-78.**
56. **Machiels JP, Sempoux C, Scalliet P, Coche JC, Humblet Y, Van Cutsem E, Kerger J, Canon JL, Peeters M, Aydin S, Laurent S, Kartheuser A, Coster B, Roels S, Daisne JF, Honhon B, Duck L, Kirkove C, Bonny MA, Haustermans K. Phase I/II study of preoperative cetuximab, capecitabine, and external beam radiotherapy in patients with rectal cancer. Ann Oncol 2007;18:738-44.**
57. **Rodel C, Arnold D, Hipp M, Liersch T, Dellas K, Ilesniels I, Hermann RM, Lordick F, Hinke A, Hohenberger W, Sauer R. Phase I-II trial of cetuximab, capecitabine, oxaliplatin, and radiotherapy as preoperative treatment in rectal cancer. Int J Radiat Oncol Biol Phys 2008;70:1081-6.**
58. **Rodel C, Liersch T, Hermann RM, Arnold D, Reese T, Hipp M, Furst A, Schwella N, Bieker M, Hellmich G, Ewald H, Haier J, Lordick F, Flentje M, Sulberg H, Hohenberger W, Sauer R. Multicenter phase II trial of chemoradiation with oxaliplatin for rectal cancer. J Clin Oncol 2007;25:110-7.**
59. **Cohen S. Isolation of a mouse submaxillary gland protein accelerating incisor eruption and eyelid opening in the new-born animal. J Biol Chem 1962;237:1555-62.**
60. **Carpenter G, Cohen S. Epidermal growth factor. Annu Rev Biochem 1979;48:193-216.**
61. **Cohen S. The stimulation of epidermal proliferation by a specific protein (EGF). Dev Biol 1965;12:394-407.**
62. **O'Keefe E, Hollenberg MD, Cuatrecasas P. Epidermal growth factor. Characteristics of specific binding in membranes from liver, placenta, and other target tissues. Arch Biochem Biophys 1974;164:518-26.**
63. **Ullrich A, Coussens L, Hayflick JS, Dull TJ, Gray A, Tam AW, Lee J, Yarden Y, Libermann TA, Schlessinger J, et al. Human epidermal growth factor receptor cDNA sequence and aberrant expression of the amplified gene in A431 epidermoid carcinoma cells. Nature 1984;309:418-25.**

64. **Carpenter G, King L, Jr., Cohen S. Epidermal growth factor stimulates phosphorylation in membrane preparations in vitro. *Nature* 1978;276:409-10.**
65. **Holbro T, Hynes NE. ErbB receptors: directing key signaling networks throughout life. *Annu Rev Pharmacol Toxicol* 2004;44:195-217.**
66. **Hynes NE, Lane HA. ERBB receptors and cancer: the complexity of targeted inhibitors. *Nat Rev Cancer* 2005;5:341-54.**
67. **Laurent-Puig P, Lievre A, Blons H. Mutations and response to epidermal growth factor receptor inhibitors. *Clin Cancer Res* 2009;15:1133-9.**
68. **Holbro T, Civenni G, Hynes NE. The ErbB receptors and their role in cancer progression. *Exp Cell Res* 2003;284:99-110.**
69. **Alvarado D, Klein DE, Lemmon MA. ErbB2 resembles an autoinhibited invertebrate epidermal growth factor receptor. *Nature* 2009;461:287-91.**
70. **Gschwind A, Fischer OM, Ullrich A. The discovery of receptor tyrosine kinases: targets for cancer therapy. *Nat Rev Cancer* 2004;4:361-70.**
71. **Yarden Y, Sliwkowski MX. Untangling the ErbB signalling network. *Nat Rev Mol Cell Biol* 2001;2:127-37.**
72. **Janmaat ML, Giaccone G. The epidermal growth factor receptor pathway and its inhibition as anticancer therapy. *Drugs Today (Barc)* 2003;39 Suppl C:61-80.**
73. **Fang JY, Richardson BC. The MAPK signalling pathways and colorectal cancer. *Lancet Oncol* 2005;6:322-7.**
74. **Ciardiello F, Caputo R, Bianco R, Damiano V, Pomatico G, De Placido S, Bianco AR, Tortora G. Antitumor effect and potentiation of cytotoxic drugs activity in human cancer cells by ZD-1839 (Iressa), an epidermal growth factor receptor-selective tyrosine kinase inhibitor. *Clin Cancer Res* 2000;6:2053-63.**
75. **Cragg MS, Kuroda J, Puthalakath H, Huang DC, Strasser A. Gefitinib-induced killing of NSCLC cell lines expressing mutant EGFR requires BIM and can be enhanced by BH3 mimetics. *PLoS Med* 2007;4:1681-89; discussion 1690.**

76. Rubin BP, Duensing A. Mechanisms of resistance to small molecule kinase inhibition in the treatment of solid tumors. *Lab Invest* 2006;86:981-6.
77. Sergina NV, Rausch M, Wang D, Blair J, Hann B, Shokat KM, Moasser MM. Escape from HER-family tyrosine kinase inhibitor therapy by the kinase-inactive HER3. *Nature* 2007;445:437-41.
78. Soltoff SP, Carraway KL, 3rd, Prigent SA, Gullick WG, Cantley LC. ErbB3 is involved in activation of phosphatidylinositol 3-kinase by epidermal growth factor. *Mol Cell Biol* 1994;14:3550-8.
79. Luo J, Emanuele MJ, Li D, Creighton CJ, Schlabach MR, Westbrook TF, Wong KK, Elledge SJ. A genome-wide RNAi screen identifies multiple synthetic lethal interactions with the Ras oncogene. *Cell* 2009;137:835-48.
80. Buck E, Eyzaguirre A, Rosenfeld-Franklin M, Thomson S, Mulvihill M, Barr S, Brown E, O'Connor M, Yao Y, Pachter J, Miglarese M, Epstein D, Iwata KK, Haley JD, Gibson NW, Ji QS. Feedback mechanisms promote cooperativity for small molecule inhibitors of epidermal and insulin-like growth factor receptors. *Cancer Res* 2008;68:8322-32.
81. Guix M, Faber AC, Wang SE, Olivares MG, Song Y, Qu S, Rinehart C, Seidel B, Yee D, Arteaga CL, Engelman JA. Acquired resistance to EGFR tyrosine kinase inhibitors in cancer cells is mediated by loss of IGF-binding proteins. *J Clin Invest* 2008;118:2609-19.
82. Lu Y, Zi X, Zhao Y, Mascarenhas D, Pollak M. Insulin-like growth factor-I receptor signaling and resistance to trastuzumab (Herceptin). *J Natl Cancer Inst* 2001;93:1852-7.
83. Dallas NA, Xia L, Fan F, Gray MJ, Gaur P, van Buren G, 2nd, Samuel S, Kim MP, Lim SJ, Ellis LM. Chemoresistant colorectal cancer cells, the cancer stem cell phenotype, and increased sensitivity to insulin-like growth factor-I receptor inhibition. *Cancer Res* 2009;69:1951-7.
84. Meng J, Peng H, Dai B, Guo W, Wang L, Ji L, Minna JD, Chresta CM, Smith PD, Fang B, Roth JA. High level of AKT activity is associated with resistance to MEK inhibitor AZD6244 (ARRY-142886). *Cancer Biol Ther* 2009;8:2073-80.

85. **Rodriguez-Viciano P, Warne PH, Dhand R, Vanhaesebroeck B, Gout I, Fry MJ, Waterfield MD, Downward J. Phosphatidylinositol-3-OH kinase as a direct target of Ras. Nature 1994;370:527-32.**
86. **Pollak M. Insulin and insulin-like growth factor signalling in neoplasia. Nat Rev Cancer 2008;8:915-28.**
87. **Chitnis MM, Yuen JS, Protheroe AS, Pollak M, Macaulay VM. The type 1 insulin-like growth factor receptor pathway. Clin Cancer Res 2008;14:6364-70.**
88. **Weber MM, Fottner C, Liu SB, Jung MC, Engelhardt D, Baretton GB. Overexpression of the insulin-like growth factor I receptor in human colon carcinomas. Cancer 2002;95:2086-95.**
89. **Zhang L, Zhou W, Velculescu VE, Kern SE, Hruban RH, Hamilton SR, Vogelstein B, Kinzler KW. Gene expression profiles in normal and cancer cells. Science 1997;276:1268-72.**
90. **Hassan AB, Howell JA. Insulin-like growth factor II supply modifies growth of intestinal adenoma in Apc(Min/+) mice. Cancer Res 2000;60:1070-6.**
91. **Harper J, Burns JL, Foulstone EJ, Pignatelli M, Zaina S, Hassan AB. Soluble IGF2 receptor rescues Apc(Min/+) intestinal adenoma progression induced by Igf2 loss of imprinting. Cancer Res 2006;66:1940-8.**
92. **Klinakis A, Szabolcs M, Chen G, Xuan S, Hibshoosh H, Efstratiadis A. IGF1R as a therapeutic target in a mouse model of basal-like breast cancer. Proc Natl Acad Sci U S A 2009;106:2359-64.**
93. **Gualberto A, Pollak M. Emerging role of insulin-like growth factor receptor inhibitors in oncology: early clinical trial results and future directions. Oncogene 2009;28:3009-21.**
94. **Carden CP, Molife LR, de Bono JS. Predictive biomarkers for targeting insulin-like growth factor-I (IGF-I) receptor. Mol Cancer Ther 2009;8:2077-8.**
95. **Haluska P, Carboni JM, TenEyck C, Attar RM, Hou X, Yu C, Sagar M, Wong TW, Gottardis MM, Erlichman C. HER receptor signaling confers resistance to the insulin-like growth factor-I receptor inhibitor, BMS-536924. Mol Cancer Ther 2008;7:2589-98.**

96. Huang F, Greer A, Hurlburt W, Han X, Hafezi R, Wittenberg GM, Reeves K, Chen J, Robinson D, Li A, Lee FY, Gottardis MM, Clark E, Helman L, Attar RM, Dongre A, Carboni JM. The mechanisms of differential sensitivity to an insulin-like growth factor-1 receptor inhibitor (BMS-536924) and rationale for combining with EGFR/HER2 inhibitors. *Cancer Res* 2009;69:161-70.
97. Cunningham MP, Thomas H, Marks C, Green M, Fan Z, Modjtahedi H. Co-targeting the EGFR and IGF-IR with anti-EGFR monoclonal antibody ICR62 and the IGF-IR tyrosine kinase inhibitor NVP-AEW541 in colorectal cancer cells. *Int J Oncol* 2008;33:1107-13.
98. Shaw P, Clarke AR. Murine models of intestinal cancer: recent advances. *DNA Repair (Amst)* 2007;6:1403-12.
99. Sharpless NE, Depinho RA. The mighty mouse: genetically engineered mouse models in cancer drug development. *Nat Rev Drug Discov* 2006;5:741-54.
100. Moser AR, Pitot HC, Dove WF. A dominant mutation that predisposes to multiple intestinal neoplasia in the mouse. *Science* 1990;247:322-4.
101. Su LK, Kinzler KW, Vogelstein B, Preisinger AC, Moser AR, Luongo C, Gould KA, Dove WF. Multiple intestinal neoplasia caused by a mutation in the murine homolog of the APC gene. *Science* 1992;256:668-70.
102. Groden J, Thliveris A, Samowitz W, Carlson M, Gelbert L, Albertsen H, Joslyn G, Stevens J, Spirio L, Robertson M, et al. Identification and characterization of the familial adenomatous polyposis coli gene. *Cell* 1991;66:589-600.
103. Luongo C, Moser AR, Gledhill S, Dove WF. Loss of Apc⁺ in intestinal adenomas from Min mice. *Cancer Res* 1994;54:5947-52.
104. Bienz M, Clevers H. Linking colorectal cancer to Wnt signaling. *Cell* 2000;103:311-20.
105. van de Wetering M, Sancho E, Verweij C, de Lau W, Oving I, Hurlstone A, van der Horn K, Batlle E, Coudreuse D, Haramis AP, Tjon-Pon-Fong M, Moerer P, van den Born M, Soete G, Pals S, Eilers M, Medema R, Clevers H. The beta-catenin/TCF-4 complex imposes a crypt progenitor phenotype on colorectal cancer cells. *Cell* 2002;111:241-50.

106. Miyoshi Y, Nagase H, Ando H, Horii A, Ichii S, Nakatsuru S, Aoki T, Miki Y, Mori T, Nakamura Y. Somatic mutations of the APC gene in colorectal tumors: mutation cluster region in the APC gene. *Hum Mol Genet* 1992;1:229-33.
107. Dietrich WF, Lander ES, Smith JS, Moser AR, Gould KA, Luongo C, Borenstein N, Dove W. Genetic identification of Mom-1, a major modifier locus affecting Min-induced intestinal neoplasia in the mouse. *Cell* 1993;75:631-9.
108. Cormier RT, Hong KH, Halberg RB, Hawkins TL, Richardson P, Mulherkar R, Dove WF, Lander ES. Secretory phospholipase Pla2g2a confers resistance to intestinal tumorigenesis. *Nat Genet* 1997;17:88-91.
109. Moran AE, Hunt DH, Javid SH, Redston M, Carothers AM, Bertagnolli MM. Apc deficiency is associated with increased Egfr activity in the intestinal enterocytes and adenomas of C57BL/6J-Min/+ mice. *J Biol Chem* 2004;279:43261-72.
110. Roberts RB, Min L, Washington MK, Olsen SJ, Settle SH, Coffey RJ, Threadgill DW. Importance of epidermal growth factor receptor signaling in establishment of adenomas and maintenance of carcinomas during intestinal tumorigenesis. *Proc Natl Acad Sci U S A* 2002;99:1521-6.
111. Torrance CJ, Jackson PE, Montgomery E, Kinzler KW, Vogelstein B, Wissner A, Nunes M, Frost P, Discafani CM. Combinatorial chemoprevention of intestinal neoplasia. *Nat Med* 2000;6:1024-8.
112. Ritland SR, Gendler SJ, Burgart LJ, Fry DW, Nelson JM, Bridges AJ, Andress L, Karnes WE, Jr. Inhibition of epidermal growth factor receptor tyrosine kinase fails to suppress adenoma formation in ApcMin mice but induces duodenal injury. *Cancer Res* 2000;60:4678-81.
113. Marsh V, Winton DJ, Williams GT, Dubois N, Trumpp A, Sansom OJ, Clarke AR. Epithelial Pten is dispensable for intestinal homeostasis but suppresses adenoma development and progression after Apc mutation. *Nat Genet* 2008;40:1436-44.
114. Sansom OJ, Meniel V, Wilkins JA, Cole AM, Oien KA, Marsh V, Jamieson TJ, Guerra C, Ashton GH, Barbacid M, Clarke AR. Loss of Apc allows phenotypic manifestation of the transforming properties of an endogenous K-ras oncogene in vivo. *Proc Natl Acad Sci U S A* 2006;103:14122-7.
115. Rajewsky K, Gu H, Kuhn R, Betz UA, Muller W, Roes J, Schwenk F. Conditional gene targeting. *J Clin Invest* 1996;98:600-3.

116. Shibata H, Toyama K, Shioya H, Ito M, Hirota M, Hasegawa S, Matsumoto H, Takano H, Akiyama T, Toyoshima K, Kanamaru R, Kanegae Y, Saito I, Nakamura Y, Shiba K, Noda T. Rapid colorectal adenoma formation initiated by conditional targeting of the Apc gene. *Science* 1997;278:120-3.
117. Ireland H, Kemp R, Houghton C, Howard L, Clarke AR, Sansom OJ, Winton DJ. Inducible Cre-mediated control of gene expression in the murine gastrointestinal tract: effect of loss of beta-catenin. *Gastroenterology* 2004;126:1236-46.
118. Guerra C, Mijimolle N, Dhawahir A, Dubus P, Barradas M, Serrano M, Campuzano V, Barbacid M. Tumor induction by an endogenous K-ras oncogene is highly dependent on cellular context. *Cancer Cell* 2003;4:111-20.
119. Bos JL. ras oncogenes in human cancer: a review. *Cancer Res* 1989;49:4682-9.
120. Downward J. Targeting RAS signalling pathways in cancer therapy. *Nat Rev Cancer* 2003;3:11-22.
121. Lee SH, Lee JW, Soung YH, Kim SY, Nam SW, Park WS, Kim SH, Yoo NJ, Lee JY. Colorectal tumors frequently express phosphorylated mitogen-activated protein kinase. *Apmis* 2004;112:233-8.
122. Davies BR, Logie A, McKay JS, Martin P, Steele S, Jenkins R, Cockerill M, Cartlidge S, Smith PD. AZD6244 (ARRY-142886), a potent inhibitor of mitogen-activated protein kinase/extracellular signal-regulated kinase 1/2 kinases: mechanism of action in vivo, pharmacokinetic/pharmacodynamic relationship, and potential for combination in preclinical models. *Mol Cancer Ther* 2007;6:2209-19.
123. Cragg MS, Jansen ES, Cook M, Harris C, Strasser A, Scott CL. Treatment of B-RAF mutant human tumor cells with a MEK inhibitor requires Bim and is enhanced by a BH3 mimetic. *J Clin Invest* 2008;118:3651-9.
124. Solit DB, Garraway LA, Pratilas CA, Sawai A, Getz G, Basso A, Ye Q, Lobo JM, She Y, Osman I, Golub TR, Sebolt-Leopold J, Sellers WR, Rosen N. BRAF mutation predicts sensitivity to MEK inhibition. *Nature* 2006;439:358-62.
125. Yeh JJ, Routh ED, Rubinas T, Peacock J, Martin TD, Shen XJ, Sandler RS, Kim HJ, Keku TO, Der CJ. KRAS/BRAF mutation status and ERK1/2 activation as biomarkers for MEK1/2 inhibitor therapy in colorectal cancer. *Mol Cancer Ther* 2009;8:834-43.

126. Emery CM, Vijayendran KG, Zipser MC, Sawyer AM, Niu L, Kim JJ, Hatton C, Chopra R, Oberholzer PA, Karpova MB, MacConaill LE, Zhang J, Gray NS, Sellers WR, Dummer R, Garraway LA. MEK1 mutations confer resistance to MEK and B-RAF inhibition. *Proc Natl Acad Sci U S A* 2009;106:20411-6.
127. Hotchkiss RS, Strasser A, McDunn JE, Swanson PE. Cell death. *N Engl J Med* 2009;361:1570-83.
128. Cragg MS, Harris C, Strasser A, Scott CL. Unleashing the power of inhibitors of oncogenic kinases through BH3 mimetics. *Nat Rev Cancer* 2009;9:321-6.
129. Oltersdorf T, Elmore SW, Shoemaker AR, Armstrong RC, Augeri DJ, Belli BA, Bruncko M, Deckwerth TL, Dinges J, Hajduk PJ, Joseph MK, Kitada S, Korsmeyer SJ, Kunzer AR, Letai A, Li C, Mitten MJ, Nettesheim DG, Ng S, Nimmer PM, O'Connor JM, Oleksijew A, Petros AM, Reed JC, Shen W, Tahir SK, Thompson CB, Tomaselli KJ, Wang B, Wendt MD, Zhang H, Fesik SW, Rosenberg SH. An inhibitor of Bcl-2 family proteins induces regression of solid tumours. *Nature* 2005;435:677-81.
130. Fesik S. Bcl-2 family inhibitors for the treatment of cancer, In *The Institute of Cancer Centenary Conference, London, 2009*.
131. Wakeling AE, Guy SP, Woodburn JR, Ashton SE, Curry BJ, Barker AJ, Gibson KH. ZD1839 (Iressa): an orally active inhibitor of epidermal growth factor signaling with potential for cancer therapy. *Cancer Res* 2002;62:5749-54.
132. Solomon B, Hagekyriakou J, Trivett MK, Stacker SA, McArthur GA, Cullinane C. EGFR blockade with ZD1839 ("Iressa") potentiates the antitumor effects of single and multiple fractions of ionizing radiation in human A431 squamous cell carcinoma. Epidermal growth factor receptor. *Int J Radiat Oncol Biol Phys* 2003;55:713-23.
133. Kendrew J, Ballard P, Hutchison M, Ducrozet F, Barnett S, Wedge S, Wakeling AE. Pharmacokinetic/Pharmacodynamic examination of gefitinib activity in a human xenograft model, In *AACR, Toronto, 2003*.
134. McKillop D, Partridge EA, Kemp JV, Spence MP, Kendrew J, Barnett S, Wood PG, Giles PB, Patterson AB, Bichat F, Guilbaud N, Stephens TC. Tumor penetration of gefitinib (Iressa), an epidermal growth factor receptor tyrosine kinase inhibitor. *Mol Cancer Ther* 2005;4:641-9.

135. Wang S, Guo P, Wang X, Zhou Q, Gallo JM. Preclinical pharmacokinetic/pharmacodynamic models of gefitinib and the design of equivalent dosing regimens in EGFR wild-type and mutant tumor models. *Mol Cancer Ther* 2008;7:407-17.
136. Favelyukis S, Till JH, Hubbard SR, Miller WT. Structure and autoregulation of the insulin-like growth factor 1 receptor kinase. *Nat Struct Biol* 2001;8:1058-63.
137. Van Buren G, 2nd, Yang AD, Dallas NA, Gray MJ, Lim SJ, Xia L, Fan F, Somcio R, Wu Y, Hicklin DJ, Ellis LM. Effect of molecular therapeutics on liver regeneration in a murine model. *J Clin Oncol* 2008;26:1836-42.
138. Haass NK, Sproesser K, Nguyen TK, Contractor R, Medina CA, Nathanson KL, Herlyn M, Smalley KS. The mitogen-activated protein/extracellular signal-regulated kinase kinase inhibitor AZD6244 (ARRY-142886) induces growth arrest in melanoma cells and tumor regression when combined with docetaxel. *Clin Cancer Res* 2008;14:230-9.
139. Adjei AA, Cohen RB, Franklin W, Morris C, Wilson D, Molina JR, Hanson LJ, Gore L, Chow L, Leong S, Maloney L, Gordon G, Simmons H, Marlow A, Litwiler K, Brown S, Poch G, Kane K, Haney J, Eckhardt SG. Phase I pharmacokinetic and pharmacodynamic study of the oral, small-molecule mitogen-activated protein kinase kinase 1/2 inhibitor AZD6244 (ARRY-142886) in patients with advanced cancers. *J Clin Oncol* 2008;26:2139-46.
140. Dorak M. Real Time PCR. Taylor and Francis Group, 2006.
141. Livak KJ, Schmittgen TD. Analysis of relative gene expression data using real-time quantitative PCR and the $2^{-\Delta\Delta C(T)}$ Method. *Methods* 2001;25:402-8.
142. Smyth GK. Linear models and empirical bayes methods for assessing differential expression in microarray experiments. *Stat Appl Genet Mol Biol* 2004;3:Article3.
143. Smyth GK. Limma: Linear models for microarray data. In: Bioinformatics and computational biology solutions using R and Bioconductor. Springer, 2005.
144. Tusher VG, Tibshirani R, Chu G. Significance analysis of microarrays applied to the ionizing radiation response. *Proc Natl Acad Sci U S A* 2001;98:5116-21.

145. Wheeler DL, Huang S, Kruser TJ, Nechrebecki MM, Armstrong EA, Benavente S, Gondi V, Hsu KT, Harari PM. Mechanisms of acquired resistance to cetuximab: role of HER (ErbB) family members. *Oncogene* 2008;27:3944-56.
146. Wiley HS, Shvartsman SY, Lauffenburger DA. Computational modeling of the EGF-receptor system: a paradigm for systems biology. *Trends Cell Biol* 2003;13:43-50.
147. Shankaran H, Wiley HS, Resat H. Receptor downregulation and desensitization enhance the information processing ability of signalling receptors. *BMC Syst Biol* 2007;1:48.
148. Hoeller D, Hecker CM, Dikic I. Ubiquitin and ubiquitin-like proteins in cancer pathogenesis. *Nat Rev Cancer* 2006;6:776-88.
149. Fichera A, Little N, Jagadeeswaran S, Dougherty U, Sehdev A, Mustafi R, Cerda S, Yuan W, Khare S, Tretiakova M, Gong C, Tallero M, Cohen G, Joseph L, Hart J, Turner JR, Bissonnette M. Epidermal growth factor receptor signaling is required for microadenoma formation in the mouse azoxymethane model of colonic carcinogenesis. *Cancer Res* 2007;67:827-35.
150. Jolly RA, Goldstein KM, Wei T, Gao H, Chen P, Huang S, Colet JM, Ryan TP, Thomas CE, Estrem ST. Pooling samples within microarray studies: a comparative analysis of rat liver transcription response to prototypical toxicants. *Physiol Genomics* 2005;22:346-55.
151. Amit I, Citri A, Shay T, Lu Y, Katz M, Zhang F, Tarcic G, Siwak D, Lahad J, Jacob-Hirsch J, Amariglio N, Vaisman N, Segal E, Rechavi G, Alon U, Mills GB, Domany E, Yarden Y. A module of negative feedback regulators defines growth factor signaling. *Nat Genet* 2007;39:503-12.
152. Haigis KM, Kendall KR, Wang Y, Cheung A, Haigis MC, Glickman JN, Niwa-Kawakita M, Sweet-Cordero A, Sebolt-Leopold J, Shannon KM, Settleman J, Giovannini M, Jacks T. Differential effects of oncogenic K-Ras and N-Ras on proliferation, differentiation and tumor progression in the colon. *Nat Genet* 2008;40:600-8.
153. Solmi R, Lauriola M, Francesconi M, Martini D, Voltattorni M, Ceccarelli C, Ugolini G, Rosati G, Zanotti S, Montroni I, Mattei G, Taffurelli M, Santini D, Pezzetti F, Ruggeri A, Castellani G, Guidotti L, Coppola D, Strippoli P. Displayed correlation between gene expression profiles and submicroscopic alterations in response to cetuximab, gefitinib and EGF in human colon cancer cell lines. *BMC Cancer* 2008;8:227.

154. **Andrews SC, Wood MD, Tunster SJ, Barton SC, Surani MA, John RM. Cdkn1c (p57Kip2) is the major regulator of embryonic growth within its imprinted domain on mouse distal chromosome 7. BMC Dev Biol 2007;7:53.**
155. **Wutz A, Theussl HC, Dausman J, Jaenisch R, Barlow DP, Wagner EF. Non-imprinted Igf2r expression decreases growth and rescues the Tme mutation in mice. Development 2001;128:1881-7.**
156. **Pollack JR, Sorlie T, Perou CM, Rees CA, Jeffrey SS, Lonning PE, Tibshirani R, Botstein D, Borresen-Dale AL, Brown PO. Microarray analysis reveals a major direct role of DNA copy number alteration in the transcriptional program of human breast tumors. Proc Natl Acad Sci U S A 2002;99:12963-8.**
157. **Debuquoy A. Molecular response to cetuximab in rectal cancer. In: Shaw P, ed, 2009.**
158. **Piechocki MP, Yoo GH, Dibley SK, Lonardo F. Breast cancer expressing the activated HER2/neu is sensitive to gefitinib in vitro and in vivo and acquires resistance through a novel point mutation in the HER2/neu. Cancer Res 2007;67:6825-43.**
159. **Lebedeva IV, Su ZZ, Emdad L, Kolomeyer A, Sarkar D, Kitada S, Waxman S, Reed JC, Fisher PB. Targeting inhibition of K-ras enhances Ad.mda-7-induced growth suppression and apoptosis in mutant K-ras colorectal cancer cells. Oncogene 2007;26:733-44.**
160. **Fan AC, Deb-Basu D, Orban MW, Gotlib JR, Natkunam Y, O'Neill R, Padua RA, Xu L, Taketa D, Shirer AE, Beer S, Yee AX, Voehringer DW, Felsher DW. Nanofluidic proteomic assay for serial analysis of oncoprotein activation in clinical specimens. Nat Med 2009;15:566-71.**
161. **Biswas DK, Iglehart JD. Linkage between EGFR family receptors and nuclear factor kappaB (NF-kappaB) signaling in breast cancer. J Cell Physiol 2006;209:645-52.**
162. **Rothwarf DM, Zandi E, Natoli G, Karin M. IKK-gamma is an essential regulatory subunit of the IkappaB kinase complex. Nature 1998;395:297-300.**
163. **Meylan E, Dooley AL, Feldser DM, Shen L, Turk E, Ouyang C, Jacks T. Requirement for NF-kappaB signalling in a mouse model of lung adenocarcinoma. Nature 2009;462:104-7.**

164. Scartozzi M, Bearzi I, Pierantoni C, Mandolesi A, Loupakis F, Zaniboni A, Catalano V, Quadri A, Zorzi F, Berardi R, Biscotti T, Labianca R, Falcone A, Cascinu S. Nuclear factor-kB tumor expression predicts response and survival in irinotecan-refractory metastatic colorectal cancer treated with cetuximab-irinotecan therapy. *J Clin Oncol* 2007;25:3930-5.
165. Fan Z, Shang BY, Lu Y, Chou JL, Mendelsohn J. Reciprocal changes in p27(Kip1) and p21(Cip1) in growth inhibition mediated by blockade or overstimulation of epidermal growth factor receptors. *Clin Cancer Res* 1997;3:1943-8.
166. Zariwala M, Liu J, Xiong Y. Cyclin E2, a novel human G1 cyclin and activating partner of CDK2 and CDK3, is induced by viral oncoproteins. *Oncogene* 1998;17:2787-98.
167. de Angelis PM, Fjell B, Kravik KL, Haug T, Tunheim SH, Reichelt W, Beigi M, Clausen OP, Galteland E, Stokke T. Molecular characterizations of derivatives of HCT116 colorectal cancer cells that are resistant to the chemotherapeutic agent 5-fluorouracil. *Int J Oncol* 2004;24:1279-88.
168. Sotiriou C, Paesmans M, Harris A. Cyclin E1 (CCNE1) and E2 (CCNE2) as prognostic and predictive markers for endocrine therapy (ET) in early breast cancer *Journal of Clinical Oncology* 2004;22.
169. Vandercappellen J, Van Damme J, Struyf S. The role of CXC chemokines and their receptors in cancer. *Cancer Lett* 2008;267:226-44.
170. Kawada K, Hosogi H, Sonoshita M, Sakashita H, Manabe T, Shimahara Y, Sakai Y, Takabayashi A, Oshima M, Taketo MM. Chemokine receptor CXCR3 promotes colon cancer metastasis to lymph nodes. *Oncogene* 2007;26:4679-88.
171. Erreni M, Bianchi P, Laghi L, Mirolo M, Fabbri M, Locati M, Mantovani A, Allavena P. Expression of chemokines and chemokine receptors in human colon cancer. *Methods Enzymol* 2009;460:105-21.
172. Mascia F, Mariani V, Girolomoni G, Pastore S. Blockade of the EGF receptor induces a deranged chemokine expression in keratinocytes leading to enhanced skin inflammation. *Am J Pathol* 2003;163:303-12.

173. Phillips RJ, Mestas J, Gharaee-Kermani M, Burdick MD, Sica A, Belperio JA, Keane MP, Strieter RM. Epidermal growth factor and hypoxia-induced expression of CXC chemokine receptor 4 on non-small cell lung cancer cells is regulated by the phosphatidylinositol 3-kinase/PTEN/AKT/mammalian target of rapamycin signaling pathway and activation of hypoxia inducible factor-1alpha. *J Biol Chem* 2005;280:22473-81.
174. Hoffmann TK, Schirlau K, Sonkoly E, Brandau S, Lang S, Pivarcsi A, Balz V, Muller A, Homey B, Boelke E, Reichert T, Friebe-Hoffmann U, Greve J, Schuler P, Scheckenbach K, Schipper J, Bas M, Whiteside TL, Bier H. A novel mechanism for anti-EGFR antibody action involves chemokine-mediated leukocyte infiltration. *Int J Cancer* 2009;124:2589-96.
175. Puthalakath H, Villunger A, O'Reilly LA, Beaumont JG, Coultas L, Cheney RE, Huang DC, Strasser A. Bmf: a proapoptotic BH3-only protein regulated by interaction with the myosin V actin motor complex, activated by anoikis. *Science* 2001;293:1829-32.
176. Sorkin A, Goh LK. Endocytosis and intracellular trafficking of ErbBs. *Exp Cell Res* 2009;315:683-96.
177. Wells A, Welsh JB, Lazar CS, Wiley HS, Gill GN, Rosenfeld MG. Ligand-induced transformation by a noninternalizing epidermal growth factor receptor. *Science* 1990;247:962-4.
178. Pasquale EB. Eph receptor signalling casts a wide net on cell behaviour. *Nat Rev Mol Cell Biol* 2005;6:462-75.
179. Li JJ, Liu DP, Liu GT, Xie D. EphrinA5 acts as a tumor suppressor in glioma by negative regulation of epidermal growth factor receptor. *Oncogene* 2009;28:1759-68.
180. Brantley-Sieders DM, Zhuang G, Hicks D, Fang WB, Hwang Y, Cates JM, Coffman K, Jackson D, Bruckheimer E, Muraoka-Cook RS, Chen J. The receptor tyrosine kinase EphA2 promotes mammary adenocarcinoma tumorigenesis and metastatic progression in mice by amplifying ErbB2 signaling. *J Clin Invest* 2008;118:64-78.
181. Bardelli A, Parsons DW, Silliman N, Ptak J, Szabo S, Saha S, Markowitz S, Willson JK, Parmigiani G, Kinzler KW, Vogelstein B, Velculescu VE. Mutational analysis of the tyrosine kinome in colorectal cancers. *Science* 2003;300:949.

182. Wood LD, Calhoun ES, Silliman N, Ptak J, Szabo S, Powell SM, Riggins GJ, Wang TL, Yan H, Gazdar A, Kern SE, Pennacchio L, Kinzler KW, Vogelstein B, Velculescu VE. Somatic mutations of GUCY2F, EPHA3, and NTRK3 in human cancers. *Hum Mutat* 2006;27:1060-1.
183. Vearing C, Lee FT, Wimmer-Kleikamp S, Spirkoska V, To C, Stylianou C, Spanevello M, Brechbiel M, Boyd AW, Scott AM, Lackmann M. Concurrent binding of anti-EphA3 antibody and ephrin-A5 amplifies EphA3 signaling and downstream responses: potential as EphA3-specific tumor-targeting reagents. *Cancer Res* 2005;65:6745-54.
184. Bogan C, Chen J, O'Sullivan MG, Cormier RT. Loss of EphA2 receptor tyrosine kinase reduces ApcMin/+ tumorigenesis. *Int J Cancer* 2009;124:1366-71.
185. Waelter S, Scherzinger E, Hasenbank R, Nordhoff E, Lurz R, Goehler H, Gauss C, Sathasivam K, Bates GP, Lehrach H, Wanker EE. The huntingtin interacting protein HIP1 is a clathrin and alpha-adaptin-binding protein involved in receptor-mediated endocytosis. *Hum Mol Genet* 2001;10:1807-17.
186. Hyun TS, Rao DS, Saint-Dic D, Michael LE, Kumar PD, Bradley SV, Mizukami IF, Oravec-Wilson KI, Ross TS. HIP1 and HIP1r stabilize receptor tyrosine kinases and bind 3-phosphoinositides via epsin N-terminal homology domains. *J Biol Chem* 2004;279:14294-306.
187. Hyun TS, Ross TS. HIP1: trafficking roles and regulation of tumorigenesis. *Trends Mol Med* 2004;10:194-9.
188. Bradley SV, Holland EC, Liu GY, Thomas D, Hyun TS, Ross TS. Huntingtin interacting protein 1 is a novel brain tumor marker that associates with epidermal growth factor receptor. *Cancer Res* 2007;67:3609-15.
189. Santi P, Solimando L, Zini N, Santi S, Riccio M, Guidotti L. Inositol-specific phospholipase C in low and fast proliferating hepatoma cell lines. *Int J Oncol* 2003;22:1147-53.
190. Leung DW, Tompkins C, Brewer J, Ball A, Coon M, Morris V, Waggoner D, Singer JW. Phospholipase C delta-4 overexpression upregulates ErbB1/2 expression, Erk signaling pathway, and proliferation in MCF-7 cells. *Mol Cancer* 2004;3:15.
191. Baselga J, Swain SM. Novel anticancer targets: revisiting ERBB2 and discovering ERBB3. *Nat Rev Cancer* 2009;9:463-75.

192. Lee D, Yu M, Lee E, Kim H, Yang Y, Kim K, Pannicia C, Kurie JM, Threadgill DW. Tumor-specific apoptosis caused by deletion of the ERBB3 pseudo-kinase in mouse intestinal epithelium. *J Clin Invest* 2009;119:2702-13.
193. Jones JT, Akita RW, Sliwkowski MX. Binding specificities and affinities of egf domains for ErbB receptors. *FEBS Lett* 1999;447:227-31.
194. Fujimoto N, Wislez M, Zhang J, Iwanaga K, Dackor J, Hanna AE, Kalyankrishna S, Cody DD, Price RE, Sato M, Shay JW, Minna JD, Peyton M, Tang X, Massarelli E, Herbst R, Threadgill DW, Wistuba, II, Kurie JM. High expression of ErbB family members and their ligands in lung adenocarcinomas that are sensitive to inhibition of epidermal growth factor receptor. *Cancer Res* 2005;65:11478-85.
195. Zhang J, Iwanaga K, Choi KC, Wislez M, Raso MG, Wei W, Wistuba, II, Kurie JM. Intratumoral epiregulin is a marker of advanced disease in non-small cell lung cancer patients and confers invasive properties on EGFR-mutant cells. *Cancer Prev Res (Phila Pa)* 2008;1:201-7.
196. Lee D, Pearsall RS, Das S, Dey SK, Godfrey VL, Threadgill DW. Epiregulin is not essential for development of intestinal tumors but is required for protection from intestinal damage. *Mol Cell Biol* 2004;24:8907-16.
197. Galvan A, Noci S, Mancuso M, Pazzaglia S, Saran A, Dragani TA. Genetic background modulates gene expression profile induced by skin irradiation in ptch1 mice. *Int J Radiat Oncol Biol Phys* 2008;72:1582-6.
198. Desbois-Mouthon C, Baron A, Blivet-Van Eggelpoel MJ, Fartoux L, Venot C, Bladt F, Housset C, Rosmorduc O. Insulin-like growth factor-1 receptor inhibition induces a resistance mechanism via the epidermal growth factor receptor/HER3/AKT signaling pathway: rational basis for cotargeting insulin-like growth factor-1 receptor and epidermal growth factor receptor in hepatocellular carcinoma. *Clin Cancer Res* 2009;15:5445-56.
199. Kaulfuss S, Burfeind P, Gaedcke J, Scharf JG. Dual silencing of insulin-like growth factor-I receptor and epidermal growth factor receptor in colorectal cancer cells is associated with decreased proliferation and enhanced apoptosis. *Mol Cancer Ther* 2009;8:821-33.
200. Morgillo F, Kim WY, Kim ES, Ciardiello F, Hong WK, Lee HY. Implication of the insulin-like growth factor-IR pathway in the resistance of non-small cell lung cancer cells to treatment with gefitinib. *Clin Cancer Res* 2007;13:2795-803.

201. Lee SB, Xuan Nguyen TL, Choi JW, Lee KH, Cho SW, Liu Z, Ye K, Bae SS, Ahn JY. Nuclear Akt interacts with B23/NPM and protects it from proteolytic cleavage, enhancing cell survival. *Proc Natl Acad Sci U S A* 2008;105:16584-9.
202. Cinti C, Vindigni C, Zamparelli A, La Sala D, Epistolato MC, Marrelli D, Cevenini G, Tosi P. Activated Akt as an indicator of prognosis in gastric cancer. *Virchows Arch* 2008;453:449-55.
203. Gately K, Stewart D, Waller D, Davies A, O'Byrne K. Phosphorylation and nuclear localisation of AKT is induced by hypoxia and associated with a poor prognosis in malignant pleural mesothelioma. *American Society of Clinical Oncology*. Chicago, 2008.
204. Borgatti P, Martelli AM, Bellacosa A, Casto R, Massari L, Capitani S, Neri LM. Translocation of Akt/PKB to the nucleus of osteoblast-like MC3T3-E1 cells exposed to proliferative growth factors. *FEBS Lett* 2000;477:27-32.
205. Wang R, Brattain MG. AKT can be activated in the nucleus. *Cell Signal* 2006;18:1722-31.
206. Zha J, O'Brien C, Savage H, Huw LY, Zhong F, Berry L, Lewis Phillips GD, Luis E, Cavet G, Hu X, Amler LC, Lackner MR. Molecular predictors of response to a humanized anti-insulin-like growth factor-I receptor monoclonal antibody in breast and colorectal cancer. *Mol Cancer Ther* 2009;8:2110-21.
207. de Bono JS, Attard G, Adjei A, Pollak MN, Fong PC, Haluska P, Roberts L, Melvin C, Repollet M, Chianese D, Connely M, Terstappen LW, Gualberto A. Potential applications for circulating tumor cells expressing the insulin-like growth factor-I receptor. *Clin Cancer Res* 2007;13:3611-6.
208. Lokich J. Tumor response and survival end points in clinical trials: a clinician's perspective. *Am J Clin Oncol* 2004;27:494-6.
209. Luetteke NC, Phillips HK, Qiu TH, Copeland NG, Earp HS, Jenkins NA, Lee DC. The mouse waved-2 phenotype results from a point mutation in the EGF receptor tyrosine kinase. *Genes Dev* 1994;8:399-413.
210. Repertinger SK, Campagnaro E, Fuhrman J, El-Abaseri T, Yuspa SH, Hansen LA. EGFR enhances early healing after cutaneous incisional wounding. *J Invest Dermatol* 2004;123:982-9.

211. Pastore S, Mascia F. Novel acquisitions on the immunoprotective roles of the EGF receptor in the skin. *Expert Rev Dermatol* 2008;3:525-527.
212. Blanquart C, Boute N, Lacasa D, Issad T. Monitoring the activation state of the insulin-like growth factor-1 receptor and its interaction with protein tyrosine phosphatase 1B using bioluminescence resonance energy transfer. *Mol Pharmacol* 2005;68:885-94.
213. Buckley DA, Cheng A, Kiely PA, Tremblay ML, O'Connor R. Regulation of insulin-like growth factor type I (IGF-I) receptor kinase activity by protein tyrosine phosphatase 1B (PTP-1B) and enhanced IGF-I-mediated suppression of apoptosis and motility in PTP-1B-deficient fibroblasts. *Mol Cell Biol* 2002;22:1998-2010.
214. Tonks NK. Redox redux: revisiting PTPs and the control of cell signaling. *Cell* 2005;121:667-70.
215. Owens DM, Keyse SM. Differential regulation of MAP kinase signalling by dual-specificity protein phosphatases. *Oncogene* 2007;26:3203-13.
216. Haj FG, Markova B, Klamann LD, Bohmer FD, Neel BG. Regulation of receptor tyrosine kinase signaling by protein tyrosine phosphatase-1B. *J Biol Chem* 2003;278:739-44.
217. Eden ER, White IJ, Futter CE. Down-regulation of epidermal growth factor receptor signalling within multivesicular bodies. *Biochem Soc Trans* 2009;37:173-7.
218. Pratilas CA, Taylor BS, Ye Q, Viale A, Sander C, Solit DB, Rosen N. (V600E)BRAF is associated with disabled feedback inhibition of RAF-MEK signaling and elevated transcriptional output of the pathway. *Proc Natl Acad Sci U S A* 2009;106:4519-24.
219. Paoni NF, Feldman MW, Gutierrez LS, Ploplis VA, Castellino FJ. Transcriptional profiling of the transition from normal intestinal epithelia to adenomas and carcinomas in the APCMin/+ mouse. *Physiol Genomics* 2003;15:228-35.
220. Deng J, Carlson N, Takeyama K, Dal Cin P, Shipp M, Letai A. BH3 profiling identifies three distinct classes of apoptotic blocks to predict response to ABT-737 and conventional chemotherapeutic agents. *Cancer Cell* 2007;12:171-85.

221. Steinbach G, Lynch PM, Phillips RK, Wallace MH, Hawk E, Gordon GB, Wakabayashi N, Saunders B, Shen Y, Fujimura T, Su LK, Levin B. The effect of celecoxib, a cyclooxygenase-2 inhibitor, in familial adenomatous polyposis. *N Engl J Med* 2000;342:1946-52.
222. Rudner J, Elsaesser SJ, Muller AC, Belka C, Jendrossek V. Differential effects of anti-apoptotic Bcl-2 family members Mcl-1, Bcl-2, and Bcl-xL on celecoxib-induced apoptosis. *Biochem Pharmacol*;79:10-20.
223. Wang D, DuBois RN. Cyclooxygenase 2-derived prostaglandin E2 regulates the angiogenic switch. *Proc Natl Acad Sci U S A* 2004;101:415-6.
224. Micha D, Cummings J, Shoemaker A, Elmore S, Foster K, Greaves M, Ward T, Rosenberg S, Dive C, Simpson K. Circulating biomarkers of cell death after treatment with the BH-3 mimetic ABT-737 in a preclinical model of small-cell lung cancer. *Clin Cancer Res* 2008;14:7304-10.
225. Fujisaki J, Shimoda T. Expression of cytokeratin subtypes in colorectal mucosa, adenoma, and carcinoma. *Gastroenterol Jpn* 1993;28:647-56.
226. Chu PG, Weiss LM. Keratin expression in human tissues and neoplasms. *Histopathology* 2002;40:403-39.
227. Adam R, de Haas RJ, Wicherts DA, Aloia TA, Delvart V, Azoulay D, Bismuth H, Castaing D. Is hepatic resection justified after chemotherapy in patients with colorectal liver metastases and lymph node involvement? *J Clin Oncol* 2008;26:3672-80.
228. Rougier P, Storojakovski D, Kohne CH, Chang Chien CR, Lim R, Pinter T, Bodoky G, Stroh C, Nippgen J, Van Cutsem E. Addition of cetuximab to FOLFIRI in first line metastatic colorectal cancer (mCRC): Updated survival data and influence of KRAS on outcome in the CRSTAL study, In *Gastrointestinal cancers symposium (ASCO)*, Chicago, 2009.
229. Brunet A, Roux D, Lenormand P, Dowd S, Keyse S, Pouyssegur J. Nuclear translocation of p42/p44 mitogen-activated protein kinase is required for growth factor-induced gene expression and cell cycle entry. *Embo J* 1999;18:664-74.
230. Kolch W. Coordinating ERK/MAPK signalling through scaffolds and inhibitors. *Nat Rev Mol Cell Biol* 2005;6:827-37.

231. Lee S, Yoon S, Kim DH. A high nuclear basal level of ERK2 phosphorylation contributes to the resistance of cisplatin-resistant human ovarian cancer cells. *Gynecol Oncol* 2007;104:338-44.
232. Wee S, Jagani Z, Xiang KX, Loo A, Dorsch M, Yao YM, Sellers WR, Lengauer C, Stegmeier F. PI3K pathway activation mediates resistance to MEK inhibitors in KRAS mutant cancers. *Cancer Res* 2009;69:4286-93.
233. Engelman JA, Chen L, Tan X, Crosby K, Guimaraes AR, Upadhyay R, Maira M, McNamara K, Perera SA, Song Y, Chirieac LR, Kaur R, Lightbown A, Simendinger J, Li T, Padera RF, Garcia-Echeverria C, Weissleder R, Mahmood U, Cantley LC, Wong KK. Effective use of PI3K and MEK inhibitors to treat mutant Kras G12D and PIK3CA H1047R murine lung cancers. *Nat Med* 2008;14:1351-6.
234. Lang I, Adenis A, Boer K, Escudero P, Kim T, Valladares M, Sanders N, Pover G, Douillard J. AZD6244 versus capecitabine in patients with metastatic colorectal cancer who have failed prior chemotherapy, In American Society for Clinical Oncology, Chicago, 2008.
235. Lustig B, Jerchow B, Sachs M, Weiler S, Pietsch T, Karsten U, van de Wetering M, Clevers H, Schlag PM, Birchmeier W, Behrens J. Negative feedback loop of Wnt signaling through upregulation of conductin/axin2 in colorectal and liver tumors. *Mol Cell Biol* 2002;22:1184-93.
236. Tan X, Apte U, Micsenyi A, Kotsagrelis E, Luo JH, Ranganathan S, Monga DK, Bell A, Michalopoulos GK, Monga SP. Epidermal growth factor receptor: a novel target of the Wnt/beta-catenin pathway in liver. *Gastroenterology* 2005;129:285-302.
237. Mohinta S, Wu H, Chaurasia P, Watabe K. Wnt pathway and breast cancer. *Front Biosci* 2007;12:4020-33.

Publications

Shaw P and Clarke AR. Murine models of intestinal cancer: recent advances. *DNA Repair (Amst)* 2007;6:1403-12

Shaw P, Maughan, TS and Clarke, AR. Dual inhibition of Egf and Igf1 receptors reduces intestinal tumours in the $Apc^{min/+}$ mouse. Submitted to *Gastroenterology* (Feb 2010)

Appendix 2.1 Colon polyp RNA pooling for specific *Apc*^{min/+} treatment times.

Sample	Mouse	Injection	Timepoint	Tissue	Size (mm)	Abs 260/280	RNA (ng/ul)	RNA (ug/ul)
1	min169	0.5%tween80	0hr	polyp	5	2.08	239.35	0.24
2	min169	0.5%tween80	0hr	polyp	5	2.10	183.00	0.18
3	min169	0.5%tween80	0hr	polyp	5	2.07	241.80	0.24
4	min169	0.5%tween80	0hr	polyp	4	2.11	151.10	0.15
5	min169	0.5%tween80	0hr	polyp	3	2.09	184.40	0.18
6	min169	0.5%tween80	0hr	polyp	3	2.08	122.70	0.12
7	min169	0.5%tween80	0hr	polyp	3	2.04	82.75	0.08
9	CD2(2)	0.5%tween80	0hr	polyp	4	2.10	336.25	0.34
10	CD2(2)	0.5%tween80	0hr	polyp	3	2.20	76.50	0.08
11	CD2(2)	0.5%tween80	0hr	polyp	5	2.06	529.55	0.53
12	CD2(2)	0.5%tween80	0hr	polyp	5	2.10	346.05	0.35
13	CD2(2)	0.5%tween80	0hr	polyp	4	2.21	111.30	0.11
14	CD2(2)	0.5%tween80	0hr	polyp	3	2.02	78.40	0.08
15	CD2(2)	0.5%tween80	0hr	polyp	3	2.10	80.35	0.08
16	CD2(2)	0.5%tween80	0hr	polyp	4	2.14	75.00	0.08
17	CD2(2)	0.5%tween80	0hr	polyp	3	2.07	64.00	0.06
22	CD2(4)	0.5%tween80	0hr	polyp	5	2.08	289.55	0.29
23	CD2(4)	0.5%tween80	0hr	polyp	4	2.08	180.55	0.18
24	CD2(4)	0.5%tween80	0hr	polyp	3	2.07	85.85	0.09
25	CD2(4)	0.5%tween80	0hr	polyp	4	2.06	83.80	0.08
26	CD2(4)	0.5%tween80	0hr	polyp	4	2.10	231.20	0.23
27	CD2(4)	0.5%tween80	0hr	polyp	4	2.09	242.55	0.24

Filled colours represent polyps contributing to 3 RNA pools which were subsequently run on 3 separate Affymetrix GeneChips for data relating to time zero/vehicle treatment.

Appendix 2.1 Colon polyp RNA pooling for specific *Apc^{min/+}* treatment times.

Sample	Mouse	Injection	Timepoint	Tissue	Size (mm)	Abs 260/280	RNA (ng/ul)	RNA (ug/ul)
28	Min143	Gefitinib 75mg/kg	0hr	polyp	3	2.10	210.25	0.21
29	Min143	Gefitinib 75mg/kg	0hr	polyp	3	2.04	511.75	0.51
30	Min143	Gefitinib 75mg/kg	0hr	polyp	3	2.08	382.10	0.38
31	Min143	Gefitinib 75mg/kg	0hr	polyp	5	2.10	307.60	0.31
32	Min143	Gefitinib 75mg/kg	0hr	polyp	7	2.10	647.15	0.65
33	Min143	Gefitinib 75mg/kg	0hr	polyp	6	2.11	725.00	0.73
34	Min143	Gefitinib 75mg/kg	0hr	polyp	3	2.12	64.75	0.06
35	Min143	Gefitinib 75mg/kg	0hr	polyp	5	2.11	158.90	0.16
37	Min143	Gefitinib 75mg/kg	0hr	polyp	5	2.08	215.60	0.22
49	Min131	Gefitinib 75mg/kg	0hr	polyp	3	2.00	302.80	0.30
51	Min199	Gefitinib 75mg/kg	0hr	polyp	4	2.31	205.80	0.21
52	Min199	Gefitinib 75mg/kg	0hr	polyp	6	2.11	444.60	0.44
39	Min168	Gefitinib 75mg/kg	0hr	polyp	4	2.10	125.00	0.13
40	Min168	Gefitinib 75mg/kg	0hr	polyp	4	2.09	148.90	0.15
41	Min168	Gefitinib 75mg/kg	0hr	polyp	5	2.09	395.30	0.40
42	Min168	Gefitinib 75mg/kg	0hr	polyp	5	2.10	156.20	0.16
43	Min168	Gefitinib 75mg/kg	0hr	polyp	3	2.09	88.25	0.09
44	Min168	Gefitinib 75mg/kg	0hr	polyp	2	2.10	59.45	0.06

Filled colours represent polyps contributing to 3 RNA pools which were subsequently run on 3 separate Affymetrix GeneChips for data relating to time zero/gefitinib treatment.

Appendix 2.1 Colon polyp RNA pooling for specific *Apc^{min/+}* treatment times.

Sample	Mouse	Injection	Timepoint	Tissue	Size (mm)	Abs 260/280	RNA (ng/ul)	RNA (ug/ul)
60	Min140	Gefitinib 75mg/kg	4hr	polyp	4	2.15	101.90	0.10
61	Min140	Gefitinib 75mg/kg	4hr	polyp	6	2.1	1336.30	1.34
62	Min140	Gefitinib 75mg/kg	4hr	polyp	6	2.04	369.20	0.37
63	Min140	Gefitinib 75mg/kg	4hr	polyp	7	2.09	1680.70	1.68
64	Min140	Gefitinib 75mg/kg	4hr	polyp	6	2.09	1179.20	1.18
65	Min140	Gefitinib 75mg/kg	4hr	polyp	5	2.07	259.90	0.26
66	Min140	Gefitinib 75mg/kg	4hr	polyp	4	2.11	247.50	0.25
67	Min140	Gefitinib 75mg/kg	4hr	polyp	4	2.1	256.70	0.26
68	Min140	Gefitinib 75mg/kg	4hr	polyp	5	2.04	284.90	0.28
69	Min140	Gefitinib 75mg/kg	4hr	polyp	6	2.12	1032.60	1.03
70	Min140	Gefitinib 75mg/kg	4hr	polyp	6	2.09	1369.60	1.37
71	Min140	Gefitinib 75mg/kg	4hr	polyp	6	2.09	1708.50	1.71
84	Min159	Gefitinib 75mg/kg	4hr	polyp	3	2.05	505.40	0.51
87	Min159	Gefitinib 75mg/kg	4hr	polyp	5	2.08	247.60	0.25
88	Min159	Gefitinib 75mg/kg	4hr	polyp	6	2.03	427.60	0.43
89	Min159	Gefitinib 75mg/kg	4hr	polyp	5	2.06	370.60	0.37
90	Min159	Gefitinib 75mg/kg	4hr	polyp	7	2.04	390.20	0.39
91	Min159	Gefitinib 75mg/kg	4hr	polyp	7	2.09	1362.90	1.36
92	Min159	Gefitinib 75mg/kg	4hr	polyp	8	2.1	1481.20	1.48
73	Min167	Gefitinib 75mg/kg	4hr	polyp	8	2.06	2818.70	2.82
74	Min167	Gefitinib 75mg/kg	4hr	polyp	5	2.05	365.40	0.37
75	Min167	Gefitinib 75mg/kg	4hr	polyp	4	2.09	178.00	0.18
76	Min167	Gefitinib 75mg/kg	4hr	polyp	3	2.08	102.30	0.10
77	Min167	Gefitinib 75mg/kg	4hr	polyp	4	2.01	123.20	0.12
78	Min167	Gefitinib 75mg/kg	4hr	polyp	8	2.1	91.90	0.09
79	Min167	Gefitinib 75mg/kg	4hr	polyp	7	2.1	1508.30	1.51
80	Min167	Gefitinib 75mg/kg	4hr	polyp	7	2.09	1899.10	1.90
81	Min167	Gefitinib 75mg/kg	4hr	polyp	3	2.08	96.20	0.10

Filled colours represent polyps contributing to 3 RNA pools which were subsequently run on 3 separate Affymetrix GeneChips for data relating to time 4hours/gefitinib treatment.

Appendix 2.1 Colon polyp RNA pooling for specific *Apc*^{min/+} treatment times.

Sample	Mouse	Injection	Timepoint	Tissue	Size (mm)	Abs 260/280	RNA (ng/ul)	RNA (ug/ul)
94	Min251	0.5% tween 80	4	polyp	6	2.11	173.70	0.17
95	Min251	0.5% tween 80	4	polyp	5	2.06	103.30	0.10
96	Min251	0.5% tween 80	4	polyp	4	2.08	134.00	0.13
97	Min251	0.5% tween 80	4	polyp	5	2.13	80.60	0.08
98	Min251	0.5% tween 80	4	polyp	5	2.06	348.50	0.35
99	Min251	0.5% tween 80	4	polyp	5	2.13	178.90	0.18
100	Min251	0.5% tween 80	4	polyp	4	2.1	189.90	0.19
101	Min251	0.5% tween 80	4	polyp	4	2.1	115.00	0.12
102	Min251	0.5% tween 80	4	polyp	6	2.06	312.00	0.31
103	Min251	0.5% tween 80	4	polyp	6	2.03	547.00	0.55
104	Min251	0.5% tween 80	4	polyp	5	1.06	421.50	0.42
106	Min204	0.5% tween 80	4	polyp	7	2.03	398.10	0.40
107	Min204	0.5% tween 80	4	polyp	6	2.1	1380.00	1.38
108	Min204	0.5% tween 80	4	polyp	7	2.05	235.60	0.24
109	Min204	0.5% tween 80	4	polyp	4	2.07	101.50	0.10
110	Min204	0.5% tween 80	4	polyp	5	2.09	1156.40	1.16
111	Min204	0.5% tween 80	4	polyp	5	2	459.10	0.46
112	Min204	0.5% tween 80	4	polyp	5	2.09	249.10	0.25
113	Min204	0.5% tween 80	4	polyp	5	2.12	1179.80	1.18
115	Min247	0.5% tween 80	4	polyp	6	2.04	298.70	0.30
116	Min247	0.5% tween 80	4	polyp	10	2.01	3281.20	3.28
117	Min247	0.5% tween 80	4	polyp	10	1.97	3461.40	3.46
118	Min247	0.5% tween 80	4	polyp	8	2.08	1403.00	1.40
120	Min242	0.5% tween 80	4	polyp	5	2.13	99.20	0.10
121	Min242	0.5% tween 80	4	polyp	6	2.07	335.50	0.34
122	Min242	0.5% tween 80	4	polyp	3	2.09	53.00	0.05
123	Min242	0.5% tween 80	4	polyp	3	2.15	104.50	0.10
124	Min242	0.5% tween 80	4	polyp	3	2.04	91.50	0.09
125	Min242	0.5% tween 80	4	polyp	5	2.08	230.10	0.23
126	Min242	0.5% tween 80	4	polyp	3	2	66.30	0.07
127	Min242	0.5% tween 80	4	polyp	4	2.07	158.30	0.16

Filled colours represent polyps contributing to 3 RNA pools which were subsequently run on 3 separate Affymetrix GeneChips for data relating to time 4hour/vehicle treatment.

Appendix 2.1 Colon polyp RNA pooling for specific *Apc^{min/+}* treatment times.

Sample	Mouse	Injection	Timepoint	Tissue	Size (mm)	Abs 260/280	RNA (ng/ul)	RNA (ug/ul)
200	Min255	0.5% tween80	8hr	Polyp	8	2.11	1702.50	1.70
201	Min255	0.5% tween80	8hr	Polyp	8	2.07	2670.30	2.67
202	Min255	0.5% tween80	8hr	Polyp	3	2.03	43.60	0.04
203	Min255	0.5% tween80	8hr	Polyp	3	2.06	90.20	0.09
204	Min255	0.5% tween80	8hr	Polyp	4	2.04	508.60	0.51
205	Min300	0.5% tween80	8hr	Polyp	4	2.08	338.40	0.34
206	Min300	0.5% tween80	8hr	Polyp	4	2.07	80.3	0.08
207	Min300	0.5% tween80	8hr	Polyp	4	2.07	333.60	0.33
208	Min300	0.5% tween80	8hr	Polyp	4	2.07	257.00	0.26
209	Min300	0.5% tween80	8hr	Polyp	5	2.07	205.30	0.21
210	Min300	0.5% tween80	8hr	Polyp	3	2.12	123.70	0.12
212	Min300	0.5% tween80	8hr	Polyp	3	2.03	90.60	0.09
213	Min300	0.5% tween80	8hr	Polyp	3	2.13	88.70	0.09
214	Min302	0.5% tween80	8hr	Polyp	4	2.06	124.30	0.12
215	Min302	0.5% tween80	8hr	Polyp	6	2.09	1307.70	1.31
216	Min302	0.5% tween80	8hr	Polyp	6	2.12	1126.00	1.13
217	Min302	0.5% tween80	8hr	Polyp	3	2.11	203.40	0.20
218	Min302	0.5% tween80	8hr	Polyp	4	2.18	90.00	0.09
220	Min302	0.5% tween80	8hr	Polyp	3	1.96	44.40	0.04
221	Min302	0.5% tween80	8hr	Polyp	4	2.07	182.30	0.18
222	Min333	0.5% tween80	8hr	Polyp	6	2.11	1132.80	1.13
223	Min333	0.5% tween80	8hr	Polyp	4	2.11	118.10	0.12
224	Min336	0.5% tween80	8hr	Polyp	6	2.11	941.80	0.94
225	Min336	0.5% tween80	8hr	Polyp	4	2.07	135.30	0.14
226	Min336	0.5% tween80	8hr	Polyp	4	2.10	124.70	0.12
229	Min351	0.5% tween80	8hr	Polyp	5	2.06	197.00	0.20
230	Min351	0.5% tween80	8hr	Polyp	4	2.07	133.30	0.13
231	Min351	0.5% tween80	8hr	Polyp	5	2.06	342.80	0.34
232	Min351	0.5% tween80	8hr	Polyp	4	2.06	214.70	0.21
233	Min351	0.5% tween80	8hr	Polyp	4	2.10	125.30	0.13

Filled colours represent polyps contributing to 3 RNA pools which were subsequently run on 3 separate Affymetrix GeneChips for data relating to time 8hours/vehicle treatment.

Appendix 2.1 Colon polyp RNA pooling for specific *Apc^{min/+}* treatment times.

Sample	Mouse	Injection	Timepoint	Tissue	Size (mm)	Abs 260/280	RNA (ng/ul)	RNA (ug/ul)
236	Min248	Gefitinib 75mg/kg	8hr	Polyp	5	2.07	108.4	0.1
237	Min248	Gefitinib 75mg/kg	8hr	Polyp	4	2.07	100.1	0.1
238	Min248	Gefitinib 75mg/kg	8hr	Polyp	4	2.18	86.2	0.09
243	Min342	Gefitinib 75mg/kg	8hr	Polyp	7	2.01	436.5	0.44
244	Min342	Gefitinib 75mg/kg	8hr	Polyp	7	2.09	268.1	0.27
245	Min342	Gefitinib 75mg/kg	8hr	Polyp	4	2.07	180.7	0.18
246	Min342	Gefitinib 75mg/kg	8hr	Polyp	4	2.08	75.6	0.07
247	Min342	Gefitinib 75mg/kg	8hr	Polyp	5	2.08	217.5	0.22
249	Min342	Gefitinib 75mg/kg	8hr	Polyp	4	2.11	427	0.43
250	Min259	Gefitinib 75mg/kg	8hr	Polyp	5	2.07	302.6	0.3
251	Min259	Gefitinib 75mg/kg	8hr	Polyp	8	1.85	948.6	0.95
252	Min259	Gefitinib 75mg/kg	8hr	Polyp	5	2.06	177.7	0.18
253	Min259	Gefitinib 75mg/kg	8hr	Polyp	5	2.09	224	0.22
254	Min259	Gefitinib 75mg/kg	8hr	Polyp	4	2.23	55.2	0.06
255	Min259	Gefitinib 75mg/kg	8hr	Polyp	4	2.08	119.2	0.12
257	Min259	Gefitinib 75mg/kg	8hr	Polyp	3	2.11	105.8	0.11
258	Min174	Gefitinib 75mg/kg	8hr	Polyp	3	2.11	87.5	0.09
259	Min174	Gefitinib 75mg/kg	8hr	Polyp	3	2.07	219.4	0.22
260	Min174	Gefitinib 75mg/kg	8hr	Polyp	7	2.1	439.8	0.44
261	Min174	Gefitinib 75mg/kg	8hr	Polyp	6	2.06	184.8	0.14
262	Min174	Gefitinib 75mg/kg	8hr	Polyp	6	2.04	436.9	0.44
263	Min174	Gefitinib 75mg/kg	8hr	Polyp	5	2.08	315.8	0.32
264	Min174	Gefitinib 75mg/kg	8hr	Polyp	6	2.06	178.5	0.18
265	Min174	Gefitinib 75mg/kg	8hr	Polyp	5	2.02	313.6	0.31
266	Min174	Gefitinib 75mg/kg	8hr	Polyp	5	2.06	158.6	0.16
267	Min174	Gefitinib 75mg/kg	8hr	Polyp	5	2.03	56.6	0.05
268	Min233	Gefitinib 75mg/kg	8hr	Polyp	5	2.04	256.4	0.26
269	Min233	Gefitinib 75mg/kg	8hr	Polyp	5	2.02	130.7	0.13
270	Min233	Gefitinib 75mg/kg	8hr	Polyp	5	2.07	215.5	0.22

Filled colours represent polyps contributing to 3 RNA pools which were subsequently run on 3 separate Affymetrix GeneChips for data relating to time 8hour/gefitinib treatment.

Appendix 2.1 Colon polyp RNA pooling for specific *Apc^{min/+}* treatment times.

Sample	Mouse	Injection	Timepoint	Tissue	Size (mm)	Abs 260/280	RNA (ng/ul)	RNA (ug/ul)
273	Min272	Gefitinib 75mg/kg	12hr	polyp	7	2.04	230.80	0.23
274	Min272	Gefitinib 75mg/kg	12hr	polyp	4	2.01	119.60	0.12
275	Min272	Gefitinib 75mg/kg	12hr	polyp	4	1.98	126.30	0.13
276	Min272	Gefitinib 75mg/kg	12hr	polyp	7	2.04	1067.00	1.07
277	Min272	Gefitinib 75mg/kg	12hr	polyp	5	2.04	219.40	0.22
278	Min272	Gefitinib 75mg/kg	12hr	polyp	5	2.05	242.50	0.24
280	Min272	Gefitinib 75mg/kg	12hr	polyp	3	2.03	82.30	0.08
282	Min237	Gefitinib 75mg/kg	12hr	polyp	4	2.09	161.10	0.16
283	Min237	Gefitinib 75mg/kg	12hr	polyp	3	2.33	28.60	0.03
284	Min237	Gefitinib 75mg/kg	12hr	polyp	4	2.1	124.90	0.12
285	Min237	Gefitinib 75mg/kg	12hr	polyp	5	2.08	169.80	0.17
286	Min237	Gefitinib 75mg/kg	12hr	polyp	5	2.11	217.30	0.22
287	Min237	Gefitinib 75mg/kg	12hr	polyp	4	2.11	64.90	0.06
289	Min237	Gefitinib 75mg/kg	12hr	polyp	4	2.04	43.10	0.04
290	Min245	Gefitinib 75mg/kg	12hr	polyp	5	2.1	129.80	0.13
291	Min245	Gefitinib 75mg/kg	12hr	polyp	4	2.05	148.80	0.15
292	Min229	Gefitinib 75mg/kg	12hr	polyp	5	2.06	335.10	0.34
293	Min229	Gefitinib 75mg/kg	12hr	polyp	6	2.11	1285.40	1.29
294	Min229	Gefitinib 75mg/kg	12hr	polyp	7	2.1	1388.10	1.39
295	Min229	Gefitinib 75mg/kg	12hr	polyp	6	2.1	256.90	0.26
297	Min222	Gefitinib 75mg/kg	12hr	polyp	4	2	59.70	0.06
298	Min222	Gefitinib 75mg/kg	12hr	polyp	4	2.05	52.80	0.05
300	Min222	Gefitinib 75mg/kg	12hr	polyp	4	2.05	73.10	0.07
303	Min243	Gefitinib 75mg/kg	12hr	polyp	5	2.07	131.80	0.13
304	Min243	Gefitinib 75mg/kg	12hr	polyp	5	2.07	197.70	0.20
434	Min525	Gefitinib 75mg/kg	12hr	polyp	3	2.11	88.40	0.09
436	Min525	Gefitinib 75mg/kg	12hr	polyp	6	2.09	1002.80	1.00
437	Min525	Gefitinib 75mg/kg	12hr	polyp	6	2.07	164.30	0.17
438	Min525	Gefitinib 75mg/kg	12hr	polyp	8	2.1	1458.10	1.46
439	Min525	Gefitinib 75mg/kg	12hr	polyp	7	2.11	663.90	0.66

Filled colours represent polyps contributing to 3 RNA pools which were subsequently run on 3 separate Affymetrix GeneChips for data relating to time 12hour/gefitinib treatment.

Appendix 2.1 Colon polyp RNA pooling for specific *Apc*^{min/+} treatment times.

Sample	Mouse	Injection	Timepoint	Tissue	Size (mm)	Abs 260/280	RNA (ng/ul)	RNA (ug/ul)
306	Min466	0.5% tween80	12hr	polyp	6	2.1	1110.80	1.11
307	Min466	0.5% tween80	12hr	polyp	7	2.09	2260.40	2.26
308	Min466	0.5% tween80	12hr	polyp	6	2.11	1418.50	1.42
309	Min466	0.5% tween80	12hr	polyp	6	2.11	1043.30	1.04
310	Min466	0.5% tween80	12hr	polyp	4	2.12	112.65	0.11
312	Min466	0.5% tween80	12hr	polyp	3	2.12	131.00	0.13
313	Min466	0.5% tween80	12hr	polyp	3	2.07	216.70	0.22
314	Min466	0.5% tween80	12hr	polyp	3	2.05	246.20	0.25
315	Min466	0.5% tween80	12hr	polyp	4	2.06	273.70	0.27
316	Min400	0.5% tween80	12hr	polyp	2	1.96	53.40	0.05
317	Min400	0.5% tween80	12hr	polyp	5	2.07	217.90	0.22
318	Min400	0.5% tween80	12hr	polyp	6	1.98	515.70	0.52
319	Min400	0.5% tween80	12hr	polyp	5	2.09	596.40	0.60
320	Min400	0.5% tween80	12hr	polyp	5	2.08	160.80	0.16
321	Min400	0.5% tween80	12hr	polyp	6	1.99	483.60	0.48
322	Min400	0.5% tween80	12hr	polyp	7	2.09	1510.70	1.51
323	Min400	0.5% tween80	12hr	polyp	5	2.04	392.00	0.39
324	Min400	0.5% tween80	12hr	polyp	6	2.05	440.60	0.44
325	Min400	0.5% tween80	12hr	polyp	5	2.03	181.30	0.18
328	Min496	0.5% tween80	12hr	polyp	4	2.08	186.20	0.19
329	Min496	0.5% tween80	12hr	polyp	5	2.09	1477.20	1.48
330	Min496	0.5% tween80	12hr	polyp	5	2.07	334.50	0.33
331	Min496	0.5% tween80	12hr	polyp	4	2.14	60.90	0.06
332	Min496	0.5% tween80	12hr	polyp	5	2.1	188.10	0.19
333	Min496	0.5% tween80	12hr	polyp	4	2.04	334.20	0.33
334	Min441	0.5% tween80	12hr	polyp	5	2.09	613.10	0.61
335	Min441	0.5% tween80	12hr	polyp	5	2.1	769.10	0.77
336	Min441	0.5% tween80	12hr	polyp	6	2.09	2020.60	2.02
337	Min441	0.5% tween80	12hr	polyp	5	2.1	896.50	0.90

Filled colours represent polyps contributing to 3 RNA pools which were subsequently run on 3 separate Affymetrix GeneChips for data relating to time 12hour/vehicle treatment.

Appendix 2.1 Colon polyp RNA pooling for specific *Apc^{min/+}* treatment times.

Sample	Mouse	Injection	Timepoint	Tissue	Size (mm)	Abs 260/280	RNA (ng/ul)	RNA (ug/ul)
341	Min386	0.5%tween80	24hr	polyp	8	2.08	2651.70	2.65
342	Min386	0.5%tween80	24hr	polyp	7	2.10	1147.10	1.15
343	Min386	0.5%tween80	24hr	polyp	7	2.09	2214.40	2.21
353	Min386	0.5%tween80	24hr	polyp	3	2.00	79.60	0.08
354	Min386	0.5%tween80	24hr	polyp	4	2.06	299.40	0.30
355	Min386	0.5%tween80	24hr	polyp	3	2.16	52.15	0.05
356	Min364	0.5%tween80	24hr	polyp	6	2.09	1702.60	1.70
357	Min364	0.5%tween80	24hr	polyp	6	2.07	358.35	0.36
358	Min364	0.5%tween80	24hr	polyp	7	2.09	1977.60	1.98
359	Min364	0.5%tween80	24hr	polyp	5	2.07	313.40	0.31
360	Min364	0.5%tween80	24hr	polyp	5	2.10	1262.90	1.26
361	Min364	0.5%tween80	24hr	polyp	4	2.08	199.50	0.20
362	Min364	0.5%tween80	24hr	polyp	3	2.06	90.80	0.09
364	Min368	0.5%tween80	24hr	polyp	4	2.10	249.30	0.25
365	Min393	0.5%tween80	24hr	polyp	5	1.99	496.30	0.50
366	Min393	0.5%tween80	24hr	polyp	5	2.06	570.50	0.57
367	Min393	0.5%tween80	24hr	polyp	4	2.07	179.20	0.18
368	Min393	0.5%tween80	24hr	polyp	4	2.06	325.40	0.33
369	Min393	0.5%tween80	24hr	polyp	3	2.12	72.50	0.07
370	Min405	0.5%tween80	24hr	polyp	5	2.05	414.80	0.41
371	Min405	0.5%tween80	24hr	polyp	4	2.06	159.40	0.16
408	Min470	0.5%tween80	24hr	polyp	6	2.10	1263.00	1.26
409	Min470	0.5%tween80	24hr	polyp	6	2.10	1163.80	1.16
410	Min470	0.5%tween80	24hr	polyp	6	2.11	1053.20	1.05
411	Min470	0.5%tween80	24hr	polyp	5	2.07	407.80	0.41
412	Min470	0.5%tween80	24hr	polyp	5	2.10	621.10	0.62
413	Min470	0.5%tween80	24hr	polyp	4	2.04	337.40	0.34
414	Min470	0.5%tween80	24hr	polyp	4	1.98	350.60	0.35
415	Min470	0.5%tween80	24hr	polyp	3	1.99	357.00	0.36
417	Min470	0.5%tween80	24hr	polyp	4	2.03	325.00	0.33

Filled colours represent polyps contributing to 3 RNA pools which were subsequently run on 3 separate Affymetrix GeneChips for data relating to time 24hour/vehicle treatment.

Appendix 2.1 Colon polyp RNA pooling for specific *Apc^{min/+}* treatment times.

Sample	Mouse	Injection	Timepoint	Tissue	Size (mm)	Abs 260/280	RNA (ng/ul)	RNA (ug/ul)
373	Min279	Gefitinib 75mg/kg	24hr	polyp	5	2.08	203.50	0.20
374	Min279	Gefitinib 75mg/kg	24hr	polyp	4	2.05	184.90	0.18
375	Min279	Gefitinib 75mg/kg	24hr	polyp	3	2.18	53.70	0.05
376	Min279	Gefitinib 75mg/kg	24hr	polyp	5	2.07	322.00	0.32
377	Min279	Gefitinib 75mg/kg	24hr	polyp	5	2.04	438.60	0.44
378	Min279	Gefitinib 75mg/kg	24hr	polyp	3	2.03	46.15	0.05
379	Min279	Gefitinib 75mg/kg	24hr	polyp	2	2.02	50.00	0.05
380	Min279	Gefitinib 75mg/kg	24hr	polyp	4	2.06	622.80	0.62
382	Min279	Gefitinib 75mg/kg	24hr	polyp	4	2.05	255.20	0.26
384	Min380	Gefitinib 75mg/kg	24hr	polyp	6	2.05	1442.30	1.44
385	Min380	Gefitinib 75mg/kg	24hr	polyp	5	2.06	183.80	0.18
387	Min380	Gefitinib 75mg/kg	24hr	polyp	3	2.02	202.90	0.20
388	Min380	Gefitinib 75mg/kg	24hr	polyp	3	2.03	125.10	0.13
389	Min241	Gefitinib 75mg/kg	24hr	polyp	4	2.03	653.20	0.65
390	Min241	Gefitinib 75mg/kg	24hr	polyp	3	2.07	250.90	0.25
391	Min241	Gefitinib 75mg/kg	24hr	polyp	3	2.10	53.40	0.05
392	Min241	Gefitinib 75mg/kg	24hr	polyp	5	2.05	256.50	0.26
394	Min328	Gefitinib 75mg/kg	24hr	polyp	5	2.03	899.90	0.90
395	Min328	Gefitinib 75mg/kg	24hr	polyp	3	2.00	115.20	0.12
396	Min328	Gefitinib 75mg/kg	24hr	polyp	3	2.02	138.30	0.14
397	Min309	Gefitinib 75mg/kg	24hr	polyp	3	2.02	248.60	0.25
399	Min348	Gefitinib 75mg/kg	24hr	polyp	3	2.00	516.80	0.52
400	Min348	Gefitinib 75mg/kg	24hr	polyp	4	2.05	701.70	0.70
401	Min348	Gefitinib 75mg/kg	24hr	polyp	3	2.08	130.00	0.13
402	Min348	Gefitinib 75mg/kg	24hr	polyp	5	2.03	746.70	0.75
403	Min457	Gefitinib 75mg/kg	24hr	polyp	5	2.04	991.10	0.99
404	Min457	Gefitinib 75mg/kg	24hr	polyp	5	2.11	1540.80	1.54
405	Min457	Gefitinib 75mg/kg	24hr	polyp	6	2.11	976.30	0.98
406	Min457	Gefitinib 75mg/kg	24hr	polyp	3	2.06	188.50	0.19
407	Min457	Gefitinib 75mg/kg	24hr	polyp	4	2.08	308.20	0.31

Filled colours represent polyps contributing to 3 RNA pools which were subsequently run on 3 separate Affymetrix GeneChips for data relating to time 24hour/gefitinib treatment.

Appendix 2.2 Colon polyp RNA pools for biological replicate experiments of *Apc^{min/+}* mice treated with 0.5% tween80, gefitinib, 1x PBS or ME1 for 4 hours.

Sample	Mouse	IP Injection	Polyp size (mm)	Abs 260 _{nm} /280 _{nm}	RNA (ng/ug) DNasd RNA.	RNA ug/ul
640	Min799	0.5% tween 80	10	2.04	1898.90	1.90
641	Min799	0.5% tween 80	6	2.03	186.20	0.19
642	Min799	0.5% tween 80	5	2.06	1059.10	1.06
643	Min799	0.5% tween 80	5	2.07	145.20	0.15
644	Min799	0.5% tween 80	5	2.05	181.70	0.18
645	Min799	0.5% tween 80	7	2.02	288.80	0.29
646	Min799	0.5% tween 80	4	1.95	106.30	0.11
647	Min799	0.5% tween 80	4	2.00	382.60	0.38
648	Min572	0.5% tween 80	4	2.01	92.80	0.09
649	Min572	0.5% tween 80	5	2.12	136.00	0.14
650	Min572	0.5% tween 80	8	2.04	1908.10	1.91
651	Min572	0.5% tween 80	5	2.02	227.80	0.23
652	Min802	0.5% tween 80	8	1.98	399.40	0.40
653	Min802	0.5% tween 80	5	2.03	172.30	0.17
654	Min552	0.5% tween 80	4	2.02	315.50	0.32
655	Min552	0.5% tween 80	4	2.04	336.80	0.34
657	Min610	0.5% tween 80	6	2.07	223.70	0.22
658	Min610	0.5% tween 80	5	2.08	1313.80	1.31
659	Min610	0.5% tween 80	5	2.07	78.00	0.08
660	Min610	0.5% tween 80	4	2.10	259.20	0.26
661	Min610	0.5% tween 80	5	2.07	466.00	0.47
662	Min610	0.5% tween 80	5	2.11	158.00	0.16
663	Min610	0.5% tween 80	8	2.07	368.70	0.37
664	Min610	0.5% tween 80	5	2.02	561.30	0.56

Appendix 2.2 Colon polyp RNA pools for biological replicate experiments of *Apc^{min/+}* mice treated with 0.5% tween80, gefitinib, 1x PBS or ME1 for 4 hours.

Sample	Mouse	IP Injection	Polyp size (mm)	Abs 260 _{nm} /280 _{nm}	RNA (ng/ug) DNasd RNA.	RNA ug/ul
501	Min 581	Gefitinib 75mg/kg	5	2.03	205.60	0.21
502	Min 581	Gefitinib 75mg/kg	4	2.06	191.40	0.19
503	Min 581	Gefitinib 75mg/kg	5	2.03	243.10	0.24
504	Min 581	Gefitinib 75mg/kg	3	2.06	108.10	0.11
505	Min 581	Gefitinib 75mg/kg	6	2.05	1535.30	1.54
506	Min 581	Gefitinib 75mg/kg	4	2.05	98.80	0.10
507	Min 581	Gefitinib 75mg/kg	4	2.08	179.40	0.18
508	Min 581	Gefitinib 75mg/kg	5	2.06	122.50	0.12
509	Min 581	Gefitinib 75mg/kg	5	2.06	906.00	0.91
510	Min 581	Gefitinib 75mg/kg	4	2.07	131.70	0.13
511	Min 581	Gefitinib 75mg/kg	5	2.06	195.10	0.20
512	Min 581	Gefitinib 75mg/kg	4	2.03	188.60	0.19
513	Min 580	Gefitinib 75mg/kg	8	2.02	336.00	0.34
514	Min 580	Gefitinib 75mg/kg	6	2.00	390.60	0.39
517	Min 580	Gefitinib 75mg/kg	6	2.04	358.20	0.36
518	Min 580	Gefitinib 75mg/kg	4	2.01	309.40	0.31
519	Min 580	Gefitinib 75mg/kg	6	2.05	1649.30	1.65
520	Min 580	Gefitinib 75mg/kg	4	2.05	232.10	0.23
521	Min 580	Gefitinib 75mg/kg	7	2.06	1514.00	1.51
522	Min 580	Gefitinib 75mg/kg	5	2.08	273.80	0.27
523	Min 580	Gefitinib 75mg/kg	5	2.07	117.40	0.12
524	Min 580	Gefitinib 75mg/kg	6	2.04	1088.60	1.09
525	Min582	Gefitinib 75mg/kg	8	2.05	1528.00	1.53
526	Min582	Gefitinib 75mg/kg	6	2.05	1097.80	1.10
527	Min582	Gefitinib 75mg/kg	8	2.03	2121.80	2.12
528	Min582	Gefitinib 75mg/kg	6	2.04	1325.70	1.33
529	Min582	Gefitinib 75mg/kg	5	2.03	261.70	0.26
530	Min582	Gefitinib 75mg/kg	4	2.00	171.80	0.17
531	Min582	Gefitinib 75mg/kg	6	2.03	1508.20	1.51
532	Min582	Gefitinib 75mg/kg	6	2.04	756.70	0.76

Appendix 2.2 Colon polyp RNA pools for biological replicate experiments of *Apc^{min/+}* mice treated with 0.5% tween80, gefitinib , 1XPBS or ME1 for 4 hours.

Sample	Mouse	IP Injection	Polyp size (mm)	Abs 260 _{nm} /280 _{nm}	RNA (ng/ug) DNAsd RNA.	RNA ug/ul
775	Min951	1xPBS	4	20.60	184.40	0.18
776	Min951	1xPBS	6	2.10	1356.10	1.36
777	Min951	1xPBS	4	2.03	424.80	0.42
778	Min951	1xPBS	5	2.07	1022.60	1.02
779	Min951	1xPBS	5	1.98	340.40	0.34
780	Min951	1xPBS	4	2.00	85.90	0.09
781	Min951	1xPBS	10	2.08	2037.00	2.04
782	Min951	1xPBS	5	2.10	1371.60	1.37
783	Min951	1xPBS	3	2.06	100.00	0.10
784	Min951	1xPBS	4	2.11	638.20	0.64
785	Min1012	1xPBS	4	2.10	1036.20	1.04
786	Min1012	1xPBS	3	2.08	278.00	0.28
787	Min1012	1xPBS	4	2.04	365.90	0.37
788	Min1012	1xPBS	5	2.09	1446.00	1.45
789	Min1012	1xPBS	4	2.10	1055.80	1.06
791	Min1015	1xPBS	2	2.05	163.70	0.16
793	Min1170	1xPBS	3	2.05	133.60	0.13
794	Min1170	1xPBS	2	1.93	52.70	0.05
795	Min1170	1xPBS	2	1.98	167.30	0.17
796	Min794	1xPBS	3	2.08	256.10	0.26
797	Min780	1xPBS	5	2.10	1568.00	1.57
798	Min780	1xPBS	3	2.04	103.20	0.10
799	Min780	1xPBS	6	2.14	1835.40	1.84
800	Min780	1xPBS	5	2.05	359.20	0.36
801	Min780	1xPBS	4	2.06	217.30	0.22
802	Min780	1xPBS	4	2.08	269.00	0.27
803	Min780	1xPBS	7	2.03	398.70	0.40
804	Min780	1xPBS	3	2.05	79.80	0.08
805	Min1178	1xPBS	6	2.09	1191.60	1.19
806	Min1178	1xPBS	6	1.96	476.70	0.48

Appendix 2.2 Colon polyp RNA pools for biological replicate experiments of *Apc^{min/+}* mice treated with 0.5% tween80, gefitinib , 1XPBS or ME1 for 4 hours.

Sample	Mouse	IP injection	Polyp size (mm)	Abs 260 _{nm} /280 _{nm}	RNA (ng/ug) DNasd RNA.	RNA ug/ul
740	Min1172	ME1 1mg	5	2.02	449.80	0.45
741	Min1172	ME1 1mg	7	2.09	1525.00	1.53
742	Min1172	ME1 1mg	8	2.06	2673.70	2.67
743	Min1172	ME1 1mg	4	2.05	159.70	0.16
744	Min1172	ME1 1mg	5	1.99	463.00	0.46
745	Min1172	ME1 1mg	4	2.01	396.30	0.40
746	Min1172	ME1 1mg	3	2.10	175.20	0.18
747	Min1172	ME1 1mg	3	2.08	300.60	0.30
748	Min1172	ME1 1mg	4	2.04	379.80	0.38
749	Min848B	ME1 1mg	3	2.05	335.80	0.34
750	Min848B	ME1 1mg	4	2.10	129.50	0.13
751	Min848B	ME1 1mg	4	2.05	367.00	0.37
752	Min848B	ME1 1mg	5	2.06	260.80	0.26
753	Min848B	ME1 1mg	2	2.09	77.60	0.08
755	Min756	ME1 1mg	3	2.09	92.60	0.09
756	Min756	ME1 1mg	6	2.05	315.20	0.32
757	Min756	ME1 1mg	5	2.05	311.80	0.31
758	Min756	ME1 1mg	6	2.09	1832.30	1.83
759	Min756	ME1 1mg	5	2.10	1175.70	1.18
760	Min756	ME1 1mg	5	1.97	472.90	0.47
761	Min756	ME1 1mg	7	2.04	2807.50	2.81
762	Min756	ME1 1mg	3	2.06	158.80	0.16
763	Min902	ME1 1mg	4	2.05	328.90	0.33
764	Min902	ME1 1mg	4	2.03	382.50	0.38
765	Min902	ME1 1mg	3	2.06	180.70	0.18
766	Min902	ME1 1mg	7	2.09	2116.30	2.12
767	Min755	ME1 1mg	8	2.09	2142.00	2.14
768	Min755	ME1 1mg	9	2.07	2479.60	2.48
769	Min755	ME1 1mg	7	2.06	214.20	0.21
770	Min755	ME1 1mg	6	2.08	1833.00	1.83

Appendix 2.3 Colon polyp RNA pools for *Apc^{min/+}* mice exposed to chronic vehicle or gefitinib until survival endpoint reached

sample	mouse	IP injection	size polyp (mm)	Abs 260 _{nm} /280 _{nm}	RNA (ng/ul)	RNA (ug/ul)
1C	Min920	1% tween80 daily	3	1.83	91.90	0.09
2C	Min920	1% tween80 daily	4	1.86	126.80	0.13
3C	Min920	1% tween80 daily	2	1.96	20.40	0.02
4C	Min920	1% tween80 daily	4	1.87	86.40	0.09
5C	Min920	1% tween80 daily	4	1.84	101.10	0.10
6C	Min920	1% tween80 daily	5	1.83	84.90	0.08
7C	Min972	1% tween80 daily	3	1.87	43.20	0.04
8C	Min972	1% tween80 daily	5	1.85	156.20	0.16
10C	Min972	1% tween80 daily	2	1.99	38.20	0.04
11C	Min972	1% tween80 daily	3	2.12	48.20	0.05
13C	Min738	Gefitinib 75mg/kg daily	5	1.91	41.00	0.04
14C	Min738	Gefitinib 75mg/kg daily	2	1.90	25.80	0.03
15C	Min738	Gefitinib 75mg/kg daily	2	2.08	33.90	0.03
16C	Min738	Gefitinib 75mg/kg daily	2	1.91	38.30	0.04
17C	Min751	Gefitinib 75mg/kg daily	6	1.80	81.40	0.08
19C	Min751	Gefitinib 75mg/kg daily	4	1.94	52.00	0.05
20C	Min751	Gefitinib 75mg/kg daily	4	1.82	248.00	0.25
21C	Min751	Gefitinib 75mg/kg daily	5	1.85	163.70	0.16
23C	Min729	Gefitinib 75mg/kg daily	5	1.86	98.90	0.10
24C	Min729	Gefitinib 75mg/kg daily	5	2.04	110.60	0.11

NB. RNA was extracted using the illustra triplePrep kit.

Appendix 2.4 Colon polyp RNA pool from *AhCre^{T/+} Apc^{+/-} Kras^{+/+}* polyps exposed to a single dose of gefitinib

sample	mouse	IP injection	polyp size (mm)	Abs 260 _{nm} /280 _{nm}	RNA (ng/ug) DNasd RNA.	RNA ug/ul
159D	AKA455	Gefitinib 75mg/kg (4hrs)	3	1.79	17.50	0.02
160D	AKA455	Gefitinib 75mg/kg (4hrs)	6	1.97	272.10	0.27
161D	AKA431	Gefitinib 75mg/kg (4hrs)	6	1.87	174.40	0.17
162D	AKA431	Gefitinib 75mg/kg (4hrs)	4	2.08	90.90	0.09
163D	AKA431	Gefitinib 75mg/kg (4hrs)	5	1.44	131.60	0.13
164D	AKA431	Gefitinib 75mg/kg (4hrs)	3	2.00	36.80	0.04
165D	AKA431	Gefitinib 75mg/kg (4hrs)	2	2.10	46.00	0.05
166D	AKA431	Gefitinib 75mg/kg (4hrs)	3	2.07	64.60	0.06
167D	AKA431	Gefitinib 75mg/kg (4hrs)	3	1.84	70.90	0.07
168D	AKA431	Gefitinib 75mg/kg (4hrs)	2	1.80	22.10	0.02

Appendix 2.4 Colon polyp RNA pool from *AhCre^{T/+} Apc^{+/-} Kras^{v12/+}* polyps exposed to a single dose of gefitinib

sample	mouse	IP injection	polyp size (mm)	Abs 260 _{nm} /280 _{nm}	RNA (ng/ug) DNAsd RNA.	RNA (ug/ul)
170D	AKA1078	Gefitinib 75mg/kg (4hrs)	4	2.00	165.30	0.17
171D	AKA1078	Gefitinib 75mg/kg (4hrs)	3	2.10	77.50	0.08
172D	AKA1078	Gefitinib 75mg/kg (4hrs)	5	1.83	193.50	0.19
173D	AKA1078	Gefitinib 75mg/kg (4hrs)	3	2.08	129.20	0.13
174D	AKA1078	Gefitinib 75mg/kg (4hrs)	2	2.02	185.90	0.19
175D	AKA1078	Gefitinib 75mg/kg (4hrs)	2	2.07	46.00	0.05
176D	AKA1125	Gefitinib 75mg/kg (4hrs)	5	1.87	57.80	0.06
177D	AKA1125	Gefitinib 75mg/kg (4hrs)	5	1.92	75.00	0.08
178D	AKA1125	Gefitinib 75mg/kg (4hrs)	5	1.93	95.80	0.10
179D	AKA1125	Gefitinib 75mg/kg (4hrs)	3	2.10	177.70	0.18

Appendix 2.5 RNA extraction from human rectal cancer specimens

sample ID	Details	abs 260 _{nm} /280 _{nm}	RNA (ng/ul)	RNA (ug/ul)
1XE	XE007/001/01 baseline	1.86	181.25	0.18
2XE	XE007/001/02 4hrs post cetuximab	1.90	30.00	0.03
6XE	XE007/003/01 baseline	1.80	314.00	0.31
7XE	XE007/003/02 4hrs post cetuximab	1.69	92.90	0.09

NB RNA extracted using illustra triplePrep kit. On column DNase performed.

Appendix 2.6 Colon polyp protein determination from *Apc^{min/+}* mice exposed to 1X PBS for 4 hours

Sample	Mouse	Polyp size (mm)	Abs 480nm	Protein ug/5ul	Protein ug/ul
1	Min1315	5	0.614	27.9	5.6
2	Min1315	3	0.771	5.2	1.0
3	Min1315	5	0.621	26.9	5.4
4	Min1315	2	0.741	9.5	1.9
5	Min 1148	3	0.765	6.0	1.2
6	Min 1148	4	0.69	16.9	3.4
7	Min 1148	4	0.751	8.0	1.6
8	Min 1148	4	0.691	16.7	3.3
9	Min1188	2	0.746	8.8	1.8
10	Min1188	3	0.687	17.3	3.5
11	Min1188	4	0.637	24.5	4.9
12	Min1188	2	0.724	12.0	2.4
13	Min1188	4	0.615	27.7	5.5
14	Min1188	4	0.61	28.4	5.7
15	Min1188	3	0.691	16.7	3.3
17	Min1095	4	0.687	17.3	3.5
18	Min1095	5	0.641	24.0	4.8
19	Min1095	6	0.611	26.4	5.3
20	Min1095	3	0.69	14.7	2.9
21	Min1095	3	0.65	20.6	4.1

Appendix 2.6 Colon polyp protein determination from *Apc^{min/+}* mice exposed to ME1 for 4 hours

Sample	Mouse	Polyp size (mm)	Abs 480nm	Protein ug/5ul	Protein ug/ul
22	Min 1177	5	0.574	31.9	6.4
23	Min 1177	3	0.648	20.9	4.2
24	Min 1177	4	0.692	14.4	2.9
25	Min 1177	3	0.677	16.6	3.3
26	Min 1177	2	0.742	7.0	1.4
27	Min 1177	2	0.758	4.6	0.9
28	Min 1177	3	0.595	28.8	5.8
31	Min 1177	2	0.695	14.0	2.8
32	Min1186	2	0.666	18.3	3.7
33	Min1186	3	0.637	22.6	4.5
34	Min1186	2	0.718	10.6	2.1
35	Min1186	3	0.685	15.5	3.1
36	Min1186	2	0.583	30.6	6.1
37	Min1186	4	0.658	16.0	3.2
38	Min1186	6	0.652	17.1	3.4
39	Min1186	2	0.711	6.3	1.3
40	Min1186	2	0.698	8.7	1.7
41	Min1186	3	0.659	15.8	3.2
42	Min1186	3	0.7	8.3	1.7
43	Min1186	3	0.693	9.6	1.9

Appendix 2.6 Colon polyp protein determination from *Apc^{min/+}* mice exposed to AZ12553801 for 4 hours

Sample	Mouse	Polyp size (mm)	Abs 480nm	Protein ug/5ul	Protein ug/ul
1D	Min 1032	2	0.723	4.1	0.8
2D	Min 1032	2	0.728	3.2	0.6
3D	Min 1032	2	0.725	3.8	0.8
4D	Min 1032	3	0.643	18.7	3.7
5D	Min 992	2	0.706	7.2	1.4
6D	Min 992	3	0.709	6.7	1.3
7D	Min 992	4	0.63	21.1	4.2
8D	Min 992	3	0.698	8.7	1.7
9D	Min 992	3	0.683	11.4	2.3

Colon polyp protein determination from *Apc^{min/+}* mice exposed to 1% Tween80 vehicle for 4 hours

Sample	Mouse	Polyp size (mm)	Abs 480nm	Protein ug/5ul	Protein ug/ul
94D	Min1122	3	0.603	24.52	4.90
95D	Min1122	2	0.728	4.50	0.90
96D	Min1122	3	0.622	22.83	4.57
97D	Min1122	3	0.726	4.84	0.97
98D	Min1122	4	0.579	30.26	6.05
99D	Min1122	4	0.544	36.31	7.26
100D	Min1122	2	0.705	8.47	1.69
101D	Min1122	3	0.681	12.62	2.52
106D	Min1245	3	0.664	15.56	3.11
107D	Min1245	3	0.648	18.33	3.67
108D	Min1245	3	0.671	14.35	2.87
109D	Min1245	2	0.679	12.97	2.59
110D	Min1245	2	0.735	3.29	0.66
111D	Min1029	3	0.7	9.34	1.87
112D	Min1029	3	0.738	2.77	0.55
113D	Min1029	3	0.599	24.06	4.81
114D	Min1029	3	0.69	10.58	2.12
115D	Min1029	4	0.565	29.10	5.82
116D	Min1029	4	0.596	24.51	4.90

Appendix 2.6 Colon polyp protein determination from *Apc^{min/+}* mice exposed to gefitinib for 4 hours

Sample	Mouse	Polyp size (mm)	Abs 480nm	Protein ug/5ul	Protein ug/ul
50d	Min1187	3	0.68	17.1	3.4
51d	Min1187	3	0.557	40.1	8.0
52d	Min1187	4	0.644	23.9	4.8
53d	Min1187	5	0.564	38.8	7.8
54d	Min1187	4	0.656	21.6	4.3
55d	Min1187	4	0.578	36.2	7.2
56d	Min1187	3	0.71	11.5	2.3
57d	Min1187	5	0.57	37.7	7.5
58d	Min1187	6	0.511	48.7	9.7
59d	Min1187	6	0.548	41.8	8.4
60d	Min1262	2	0.701	13.2	2.6
61d	Min1262	4	0.596	32.8	6.6
62d	Min1262	6	0.374	61.4	12.3
63d	Min1262	6	0.573	29.4	5.9
64d	Min1262	4	0.584	27.6	5.5
65d	Min1262	3	0.679	12.3	2.5
66d	Min1262	3	0.702	8.6	1.7
67d	Min1262	5	0.58	28.2	5.6
68d	Min1216	4	0.565	30.6	6.1
69d	Min1216	3	0.605	24.2	4.8
70d	Min1216	3	0.596	25.6	5.1
71d	Min1216	2	0.686	11.2	2.2
72d	Min1216	2	0.69	10.5	2.1
73d	Min1216	3	0.648	17.3	3.5
74d	Min1216	3	0.701	8.7	1.7
75d	Min1216	3	0.695	9.7	1.9

Appendix 2.6 Colon polyp protein determination from *Apc^{min/+}* mice exposed to gefitinib and AZ12253801 for 4 hours

Sample	Mouse	Polyp size (mm)	Abs 480nm	Protein ug/5ul	Protein ug/ul
76d	Min1311	3	0.701	8.7	1.7
77d	Min1311	3	0.694	9.9	2.0
78d	Min1311	3	0.659	15.5	3.1
79d	Min1311	3	0.699	9.1	1.8
80d	Min1311	3	0.651	16.8	3.4
81d	Min1311	4	0.585	27.4	5.5
82d	Min1311	3	0.65	17.0	3.4
83d	Min1311	3	0.712	7.0	1.4
85d	Min1317	3	0.724	5.0	1.0
86d	Min1317	6	0.448	49.5	9.9
87d	Min1255	2	0.714	6.7	1.3
88d	Min1255	5	0.703	8.4	1.7
89d	Min1255	3	0.714	6.7	1.3
90d	Min1255	3	0.64	18.6	3.7
91d	Min1255	3	0.61	23.4	4.7
92d	Min1255	3	0.611	23.2	4.6
93d	Min1255	5	0.499	41.3	8.3

Appendix 2.6 Colon polyp protein determination from *Apc^{min/+}* mice exposed to gefitinib for 8 hours

Sample	Mouse	Polyp size (mm)	Abs 480nm	Protein ug/5ul	Protein ug/ul
117d	Min468	4	0.634	18.9	3.8
118d	Min468	3	0.631	19.3	3.9
120d	Min468	3	0.649	16.7	3.3
121d	Min468	4	0.609	22.6	4.5
122d	Min468	4	0.547	31.8	6.4
123d	Min468	2	0.723	5.7	1.1
124d	Min468	3	0.689	10.7	2.1
125d	Min468	3	0.624	20.4	4.1
126d	Min468	2	0.702	8.8	1.8
127d	Min468	2	0.666	14.1	2.8
129d	Min468	2	0.739	3.3	0.7
130d	Min468	2	0.744	2.6	0.5
131d	Min514	4	0.454	54.3	10.9
132d	Min514	2	0.704	11.1	2.2
133d	Min514	3	0.689	13.7	2.7
134d	Min514	4	0.618	26.0	5.2
135d	Min514	4	0.647	20.9	4.2
136d	Min1220	5	0.589	31.0	6.2
137d	Min1220	4	0.648	20.8	4.2
138d	Min1220	4	0.664	18.0	3.6
139d	Min1220	3	0.708	10.4	2.1
140d	Min1220	5	0.614	26.6	5.3

Colon polyp protein determination from *Apc^{min/+}* mice exposed to 0.5% Tween 80 vehicle for 8 hours

Sample	Mouse	Polyp size(mm)	Abs 480nm	Protein ug/5ul	Protein ug/ul
141d	Min1206	2	0.748	3.5	0.7
142d	Min1206	5	0.566	34.9	7.0
143d	Min495	6	0.47	51.5	10.3
144d	Min495	7	0.524	42.2	8.4
145d	Min495	6	0.502	46.0	9.2
146d	Min495	6	0.524	42.2	8.4
147d	Min495	5	0.602	28.7	5.7
148d	Min499	4	0.625	21.0	4.2
149d	Min499	3	0.677	12.6	2.5
150d	Min499	5	0.564	30.8	6.2
151d	Min499	5	0.507	45.1	9.0
152d	Min499	3	0.539	34.8	7.0
153d	Min499	4	0.509	39.7	7.9
154d	Min499	3	0.672	13.4	2.7
155d	Min499	4	0.667	14.2	2.8
157d	Min499	2	0.706	7.9	1.6

Appendix 2.6 Colon polyp protein determination from *Apc^{min/+}* mice treated with chronic 1% Tween 80 vehicle

Sample	Mouse	Polyp size (mm)	Abs 480nm	Protein ug/5ul	Protein ug/ul
1C	Min920	3	0.611	24.6	4.9
2C	Min920	4	0.636	20.3	4.1
4C	Min920	4	0.486	46.5	9.3
5C	Min920	4	0.556	34.2	6.8
6C	Min920	5	0.449	53.0	10.6
8C	Min972	5	0.498	44.4	8.9
9C	Min972	3	0.739	2.2	0.4

Colon polyp protein determination from *Apc^{min/+}* mice treated with chronic gefitinib

Sample	Mouse	Polyp size (mm)	Abs 480nm	Protein ug/5ul	Protein ug/ul
13C	Min738	5	0.581	29.9	6.0
17C	Min751	6	0.483	47.0	9.4
18C	Min751	4	0.656	16.8	3.4
19C	Min751	4	0.682	12.2	2.4
20C	Min751	4	0.548	35.6	7.1
21C	Min751	5	0.544	36.3	7.3
23C	Min729	5	0.511	42.1	8.4
24C	Min729	5	0.517	41.1	8.2

Colon polyp protein determination from *Apc^{min/+}* mice treated with chronic AZ12253801

Sample	Mouse	Polyp size (mm)	Abs 480nm	Protein ug/5ul	Protein ug/ul
25C	Min1003	4	0.59	28.7	5.7
26C	Min1003	3	0.548	34.7	6.9
27C	Min1003	4	0.607	26.2	5.2
28C	Min1003	3	0.741	7.0	1.4
29C	Min1003	2	0.77	2.9	0.6
30C	Min1003	2	0.66	18.6	3.7
31C	Min1050	4	0.66	18.6	3.7
32C	Min1050	4	0.655	19.4	3.9
33C	Min1050	3	0.65	20.1	4.0
34C	Min1050	4	0.606	26.4	5.3
35C	Min1050	4	0.662	18.4	3.7
36C	Min1058	3	0.692	14.1	2.8
37C	Min1058	4	0.679	15.9	3.2
38C	Min1058	4	0.594	28.1	5.6

Appendix 2.7 Protocol for Haematoxylin and Eosin staining

Step	Reagent	Time
1	Xylene	2min
2	Xylene	2min
3	Xylene	2min
4	100% Ethanol	2min
5	100% Ethanol	2min
6	100% Ethanol	2min
7	95% Ethanol	1min
8	70% Ethanol	1min
9	Water	3min
10	Gills II Haematoxylin	5min
11	Water	3min
12	1% Acid alcohol	10sec
13	Water	5min
14	1% Eosin	5min
15	Water	30sec
16	70% Ethanol	30sec
17	95% Ethanol	1min
18	100% Ethanol	1min
19	100% Ethanol	2min
20	100% Ethanol	2min
21	Xylene	1min
22	Xylene	2min
23	Xylene	2min

Sections mounted under cover glass using DPX mountant. All reagents and consumables obtained from Thermo Fisher Scientific

